



University
of Glasgow

Lee, Pearl (2015) The regulation of TIGAR. PhD thesis, University of Glasgow.

<http://theses.gla.ac.uk/7026/>

Copyright and moral rights for this thesis are retained by the author

A copy can be downloaded for personal non-commercial research or study, without prior permission or charge

This thesis cannot be reproduced or quoted extensively from without first obtaining permission in writing from the Author

The content must not be changed in any way or sold commercially in any format or medium without the formal permission of the Author

When referring to this work, full bibliographic details including the author, title, awarding institution and date of the thesis must be given

The Regulation of TIGAR

Pearl Lee

Submitted to the University of Glasgow in fulfilment of the requirements for the
degree of Doctor of Philosophy

Institute of Cancer Sciences
College of Medicine, Veterinary and Life Sciences
University of Glasgow

September 2015

Abstract

TIGAR (*TP53*-induced glycolysis and apoptosis regulator) functions to promote antioxidant defence, with a loss of TIGAR associated with a defect in a cell's ability to control reactive oxygen species (ROS) and resultant oxidative damage. TIGAR can function as a fructose-2,6-bisphosphatase, lowering the levels of fructose-2,6-bisphosphate, which is an activator of phosphofruktokinase-1. As a consequence, TIGAR activity results in a dampening of the glycolytic pathway and, by enhancing the pentose phosphate pathway, increases cellular antioxidant capacity by promoting the generation of NADPH and GSH.

Although TIGAR is clearly a transcriptional target of the tumour suppressor p53 in human cells, the activation of TIGAR expression in mouse cells *in vitro* and in a mouse model of intestinal regeneration was not dependent on p53 or its family member TAp73. However, TIGAR expression was strongly induced in the mouse intestine during proliferation following damage or APC loss, suggesting a role for the Wnt signalling pathway. The increase in TIGAR expression seen in response to APC loss was lost after simultaneous deletion of c-Myc, suggesting that TIGAR responds to c-Myc activation downstream of the Wnt signalling pathway. While TIGAR may be a direct Myc target, Myc was shown to induce ROS, which were also found to regulate the expression of TIGAR.

In order to further understand the function of TIGAR, a TIGAR-deficient mouse was generated and TIGAR was found to play a role in supporting intestinal regeneration by lowering oxidative stress in the small intestinal crypts following tissue damage by irradiation or cisplatin treatment. Moreover, TIGAR-null mice showed decreased tumour development in a model of intestinal adenoma. In particular, it was found that TIGAR acts to lower the damaging pool of ROS during oxidative stress. Through this, TIGAR can function to promote tumourigenesis and elevated TIGAR expression has been observed in various cancer types, independently of p53 status. This suggests that a deregulated expression of TIGAR may play a role in supporting rather than inhibiting cancer development.

This study reveals p53-independent mechanisms by which TIGAR is regulated and how TIGAR can contribute to promote cell growth and tumourigenesis.

Table of Contents

Abstract	2
Table of Contents	3
List of Figures	6
List of Tables	9
Accompanying Materials	10
Acknowledgements	11
Author's Declaration	12
List of Abbreviations	13
Chapter 1 Introduction	19
1.1 The Hallmarks of Cancer	19
1.2 Cancer Cell Metabolism	22
1.2.1 Nutrient Catabolism and the Warburg Effect	22
1.2.2 Oncogenes and Tumour Suppressors in Metabolic Networks	27
1.2.3 Redox Homeostasis and Cancer	34
1.3 The p53 Family in Metabolic Regulation	44
1.3.1 p53 and Cancer Metabolism	44
1.3.2 p63 and Cancer Metabolism	60
1.3.3 p73 and Cancer Metabolism	64
1.4 The Wnt Signalling Pathway and Cancer Metabolism	67
1.4.1 Components of the Wnt Signalling Pathway	67
1.4.2 Activation of the Wnt Signalling Cascade	70
1.4.3 Wnt Signalling in Diseases and Cancer	73
1.4.4 Links Between Wnt Signalling and Cell Metabolism	74
1.5 TIGAR: a Fructose-2,6-bisphosphatase	78
1.5.1 The Structure of TIGAR	78
1.5.2 The Phosphofructokinase-2/Fructose-2,6-bisphosphatase Family	78
1.5.3 The Activities of TIGAR	80
1.5.4 The Role of TIGAR under Stress	82
1.5.5 The Role of TIGAR in Cancer	84
1.5.6 The Regulation of TIGAR	87
1.5.7 Therapeutic Insights in Targeting PFK-2/FBPase-2 Enzymes	89
1.6 Aims and Objectives	90
Chapter 2 Materials and Methods	92
2.1 Materials	92

2.1.1 General Reagents and Kits	92
2.1.2 Solutions and Buffers	94
2.1.3 ChIP Solutions.....	96
2.2 Methods.....	98
2.2.1 Cells	98
2.2.2 Culturing Mouse Embryonic Fibroblasts.....	98
2.2.3 Small Intestinal Crypt Culture	98
2.2.4 Adenoma Crypt Culture	99
2.2.5 Animals.....	100
2.2.6 Irradiation Treatment in Mice.....	100
2.2.7 Immunohistochemistry	100
2.2.8 RNAscope Assay	102
2.2.9 Bradford Protein Determination Assay	103
2.2.10 SDS-PAGE and Western Blotting.....	103
2.2.11 iRFP Reporter Construct Generation	105
2.2.12 DNA Preparation	106
2.2.13 Plasmids.....	107
2.2.14 Transfections.....	108
2.2.15 iRFP Reporter Assays.....	108
2.2.16 DNA Sequencing.....	108
2.2.17 RNA Extraction and Quantitative Real-Time PCR.....	109
2.2.18 Chromatin-Immunoprecipitation (ChIP).....	110
2.2.19 Statistical Analyses	113
Chapter 3 Mechanisms of Control of TIGAR Expression.....	114
3.1 Basal Expression of TIGAR in Mouse Tissues.....	115
3.2 Basal Expression of TIGAR in Human Tissues.....	117
3.3 Induction of TIGAR Expression by p53	118
3.3.1 Comparison of Human and Mouse TIGAR p53 Binding Sites.....	118
3.3.2 Activation of TIGAR by p53 <i>in vitro</i>	121
3.3.3 Activation of TIGAR <i>in vivo</i>	128
3.4 Summary and Discussion.....	130
Chapter 4 Regulation of TIGAR by p53 Family Members.....	131
4.1 Loss of p53 does not Affect TIGAR <i>in vivo</i>	132
4.2 Activation of TIGAR by Other p53 Family Members <i>in vitro</i>	138
4.3 Loss of TAp73 does not Affect TIGAR <i>in vivo</i>	143
4.4 Loss of Both p53 and TAp73 does not Affect TIGAR <i>in vivo</i>	148

4.5	Summary and Discussion.....	153
Chapter 5	TIGAR as a Wnt-Myc Signalling Target Gene.....	155
5.1	Activation of TIGAR expression by Wnt signalling	155
5.1.1	Induction of TIGAR Expression by Wnt Signalling <i>in vitro</i>	155
5.1.2	Induction of TIGAR Expression by Wnt Signalling <i>in vivo</i>	162
5.2	Activation of TIGAR by c-Myc Downstream of the Wnt Pathway	164
5.2.1	Induction of TIGAR by c-Myc <i>in vitro</i>	164
5.2.2	Induction of TIGAR by c-Myc <i>in vivo</i>	165
5.3	Activation of TIGAR Expression by ROS.....	168
5.3.1	Myc Promotes ROS upon APC Loss.....	168
5.3.2	The Response of TIGAR to Qualitative Differences in ROS	169
5.3.3	The Regulation of TIGAR by ROS in Human Cells	175
5.4	Summary & Discussion	180
Chapter 6	The Role of TIGAR <i>in vivo</i>	183
6.1	Confirmation of Efficient TIGAR Deletion in Mice	184
6.2	TIGAR Expression is required for Small Intestine Proliferation after Acute Damage	185
6.3	Loss of TIGAR Leads to Increased Oxidative Stress After Irradiation.....	189
6.4	TIGAR is Important in Tumour Development in an Intestinal Adenoma Model	190
6.5	TIGAR Modulates Damaging ROS.....	192
6.6	TIGAR Expression in Human Cancers	199
6.7	Summary and Discussion.....	202
Chapter 7	Final Summary and Discussion.....	204
	Bibliography	213

List of Figures

Figure 1-1 Metabolic pathways of cell growth and proliferation.....	24
Figure 1-2 Signalling pathways driving the Warburg effect	30
Figure 1-3 Cellular redox homeostasis	36
Figure 1-4 Structure of full-length p53	45
Figure 1-5 p53 in metabolism	58
Figure 1-6 The Wnt Signalling Pathway	72
Figure 3-1 Basal TIGAR expression in mouse tissues	116
Figure 3-2 Basal TIGAR expression in human tissues	117
Figure 3-3 The human and mouse TIGAR gene promoter	118
Figure 3-4 Comparison of human and mouse TIGAR p53-binding sites	120
Figure 3-5 TIGAR expression in response to p53 activation in human TIFs	122
Figure 3-6 TIGAR expression in response to p53 activation in mouse 3T3s.....	123
Figure 3-7 TIGAR expression in response to p53 activation in intestinal crypt organoids.....	124
Figure 3-8 p53 does not bind to the <i>Tigar</i> promoter after cisplatin treatment.....	125
Figure 3-9 Organization of the dog <i>TIGAR</i> gene	126
Figure 3-10 TIGAR expression in response to p53 activation in MDCK cells.....	127
Figure 3-11 TIGAR expression in the small intestine after acute tissue damage	129
Figure 4-1 Basal TIGAR expression in p53-null animals	133
Figure 4-2 Ki67 expression in <i>p53</i> ^{-/-} small intestine after irradiation.....	134
Figure 4-3 p53 expression in <i>p53</i> ^{-/-} small intestine after irradiation	134
Figure 4-4 p21 expression in <i>p53</i> ^{-/-} small intestine after irradiation	135
Figure 4-5 TIGAR expression in <i>p53</i> ^{-/-} small intestine after irradiation	135
Figure 4-6 p53 expression in <i>AhCre</i> ⁺ <i>Mdm2</i> ^{fl/fl} small intestine.....	137
Figure 4-7 p21 expression in <i>AhCre</i> ⁺ <i>Mdm2</i> ^{fl/fl} small intestine.....	137
Figure 4-8 TIGAR expression in <i>AhCre</i> ⁺ <i>Mdm2</i> ^{fl/fl} small intestine.....	137
Figure 4-9 TAp63α and TAp73α can activate the TIGAR-hBS2 reporter	140
Figure 4-10 p73 isoforms can activate the TIGAR-hBS2 reporter	141
Figure 4-11 TIGAR expression in inducible Saos-2 cells	142
Figure 4-12 TIGAR expression in TAp73-null animals	143
Figure 4-13 Ki67 expression in <i>TAp73</i> ^{-/-} small intestine after irradiation	145
Figure 4-14 p53 expression in <i>TAp73</i> ^{-/-} small intestine after irradiation	145
Figure 4-15 p73 expression in <i>TAp73</i> ^{-/-} small intestine after irradiation	146
Figure 4-16 p21 expression in <i>TAp73</i> ^{-/-} small intestine after irradiation	146
Figure 4-17 TIGAR expression in <i>TAp73</i> ^{-/-} small intestine after irradiation	147
Figure 4-18 TIGAR expression in p53- and TAp73-null animals	148

Figure 4-19 Ki67 expression in $p53^{-/-}TAp73^{-/-}$ small intestine after irradiation	149
Figure 4-20 p53 expression in $p53^{-/-}TAp73^{-/-}$ small intestine after irradiation	150
Figure 4-21 p73 expression in $p53^{-/-}TAp73^{-/-}$ small intestine after irradiation	150
Figure 4-22 p21 expression in $p53^{-/-}TAp73^{-/-}$ small intestine after irradiation	151
Figure 4-23 TIGAR expression in $p53^{-/-}TAp73^{-/-}$ small intestine after irradiation .	151
Figure 4-24 TIGAR expression in $p53^{-/-}TAp73^{-/-}$ small intestine after irradiation .	152
Figure 5-1 TIGAR expression in response to increasing doses of rWnt3a.....	156
Figure 5-2 TIGAR expression in response to rWnt3a.....	157
Figure 5-3 TIGAR in response to rWnt3a in intestinal crypt organoids.....	158
Figure 5-4 Increased TIGAR expression in $Apc^{min/+}$ organoids	160
Figure 5-5 Increased TIGAR expression upon acute Apc loss.....	161
Figure 5-6 Increased TIGAR expression <i>in vivo</i> upon Apc loss	163
Figure 5-7 Induction of TIGAR by c-Myc <i>in vitro</i>	164
Figure 5-8 Loss of Myc attenuates Wnt-mediated proliferation	166
Figure 5-9 Loss of APC and Myc does not alter β -catenin levels.....	166
Figure 5-10 Loss of APC promotes TIGAR expression in a Myc-dependent manner	166
Figure 5-11 TIGAR expression in tissues of E μ -Myc mice.....	167
Figure 5-12 Loss of APC promotes oxidative stress in a Myc-dependent manner	168
Figure 5-13 TIGAR expression in response to oxidants in WT intestinal organoids	170
Figure 5-14 TIGAR expression in response to oxidants in $Apc^{min/+}$ organoids	171
Figure 5-15 TIGAR expression upon NAC treatment in $Apc^{min/+}$ organoids	173
Figure 5-16 TIGAR expression in response to antioxidants in $Apc^{min/+}$ organoids	174
Figure 5-17 TIGAR expression in response to hydrogen peroxide.....	176
Figure 5-18 TIGAR expression in response to tert-butyl hydroperoxide.....	177
Figure 5-19 TIGAR expression in response to rotenone	179
Figure 6-1 Confirmation of TIGAR-deficient mice.....	184
Figure 6-2 Increased TIGAR in the small intestine after cisplatin treatment.....	186
Figure 6-3 TIGAR expression increases in the small intestine after irradiation ...	186
Figure 6-4 TIGAR expression increases in the small intestine after irradiation ...	187
Figure 6-5 TIGAR RNA expression in the small intestine after irradiation.....	187
Figure 6-6 TIGAR-deficiency reduces regenerative capacity in intestinal crypts.	188
Figure 6-7 Loss of TIGAR leads to increased oxidative stress after irradiation...	189
Figure 6-8 TIGAR loss reduces tumour burden in an intestinal adenoma model	191
Figure 6-9 Loss of TIGAR and RAC1 reduces proliferation in an APC intestinal model.....	194

Figure 6-10 Loss of TIGAR and RAC1 lowers but does not completely abrogate Wnt signalling	195
Figure 6-11 Loss of TIGAR, but not RAC1, results in increased damaging ROS in <i>Apc</i> -deficient intestinal crypts	196
Figure 6-12 TIGAR expression upon APC and RAC1 loss.....	197
Figure 6-13 TIGAR expression upon APC and RAC1 loss in the liver	198
Figure 6-14 Proposed role of ROS after Wnt signalling activation	198
Figure 6-15 Basal TIGAR expression in human cancer cell lines.....	199
Figure 6-16 Increased TIGAR expression in primary human colon cancer and associated metastases	200
Figure 6-17 TIGAR is overexpressed in a number of human cancer types.....	201

List of Tables

Table 2-1 List of reagents.....	93
Table 2-2: Antibodies used for immunohistochemistry.....	102
Table 2-3: Primary antibodies used for Western blotting.....	104
Table 2-4: Secondary antibodies used for Western blotting.....	105
Table 2-5: Primers for iRFP construct inserts.....	106
Table 2-6: Plasmids.....	107
Table 2-7 Sequencing primer for iRFP reporters.....	108
Table 2-8 Primer sequences for qPCR.....	110
Table 2-9 ChIP set up conditions	111
Table 2-10 Primer sequences for ChIP qPCR.....	113

Accompanying Materials

Parts of this work have contributed to the publications that are enclosed at the back of the thesis:

Lee, P., Vousden, K.H., Cheung, E.C. p53- and p73-independent activation of TIGAR expression *in vivo*. Cell Death & Disease 2015; 10.1038/cddis.2015.205

Cheung, E.C., Athineos, D., Lee, P., Ridgway, R.A., Lambie, W., Nixon, C., Strathdee, D., Blyth, K., Sansom, O.J., Vousden, K.H. TIGAR is required for efficient intestinal regeneration and tumorigenesis. Developmental Cell 2013; 10.1016/j.devcel.2013.05.001

Acknowledgements

I am very grateful to my supervisor Karen Vousden for giving me the opportunity to carry out my PhD project in her lab and for the great support and guidance she has given me as my supervisor. I would also like to thank my advisor Sara Zanivan for useful discussions and input of new ideas.

From the lab I want to thank everyone, past and present, for an amazing work environment, the invaluable help offered in developing my technical skills, for all their advice, great laughs, fun lab outings and for happily eating all the cakes from my baking experiments. I would particularly like to thank Eric for all his help with getting started on the TIGAR project as well as with the immunohistochemistry and animal work, and Andreas for all the help with the iRFP reporter assays. It has been a real pleasure to work and learn from all of you.

I thank Cancer Research UK and the Medical Research Council for funding this research, and the Cancer Research UK Beatson Institute Histology Services, Biological Services Unit, and Molecular Technology Services for all their excellent support for the work carried out in this project.

And finally, I am very thankful to all my family and friends for their love and support from across the world during my time here.

Author's Declaration

I declare that I am the sole author of this thesis and the work presented here is entirely my own unless stated otherwise. This thesis does not include work that has been submitted for consideration for any other degree or qualification.

List of Abbreviations

2HG	2-hydroxyglutarate
3-PO	3-(3-pyridinyl)-1-(4-pyridinyl)-2-propen-1-one
3PG	3-phosphoglycerate
8-oxo-dG	8-oxo-deoxyguanosine
α -KG	α -ketoglutarate
ACLY	ATP citrate lyase
ALDH4	Aldehyde dehydrogenase 4
AMP	Adenosine monophosphate
AMPK	AMP-activated protein kinase
AP-1	Activator protein-1
APAF1	Apoptotic protease activating factor 1
APC	Adenomatous polyposis coli
ATM	Ataxia telangiectasia mutated
ATP	Adenosine 5'-triphosphate
β -TrCP	β -Transducin Repeat Containing E3 Ubiquitin Protein Ligase
BAX	Bcl-2-associated X protein
Bcl-2	B-cell lymphoma 2
BH3	Bcl-2 homology domain 3
BPAG1	Bullous pemphigoid antigen 1
Brf-1	Transcription factor IIIB 90 kDa subunit
CBP	CREB binding protein
CDK	Cyclin-dependent kinase
Cis	Cisplatin
CK1	Casein kinase 1
COX (2)	Cytochrome c oxidase (2)
Cox4il	Cytochrome c oxidase subunit 4
CPT-I	Carnitine-palmitoyl transferase I
CRC	Colorectal cancer
CREB	cAMP response-element binding protein
DKK	Dickkopf

DRAM1	DNA-damage regulated autophagy modulator 1
Dsh	Dishevelled
ECM	Extracellular matrix
EEC	Ectrodactyly Ectodermal dysplasia-Clefting
EGFR	Epidermal growth factor receptor
EMT	Epithelial-mesenchymal transition
ENTPD5	Ectonucleoside triphosphate diphosphohydrolase
ER	Endoplasmic reticulum
ERK	Extracellular signal-regulated kinase
ETC	Electron transport chain
F-1,6-P ₂	Fructose-1,6-bisphosphate
F-2,6-P ₂	Fructose-2,6-bisphosphate
F-6-P	Fructose-6-phosphate
FADH ₂	Flavin adenine dinucleotide
FBP1	Fructose-1,6-bisphosphatase
FBPase-2	Fructose-2,6-bisphosphatase
FBS	Foetal bovine serum
Fz	Frizzled
G3P	Glyceraldehyde-3-phosphate
G6P	Glucose-6-phosphate
G6PDH	Glucose-6-phosphate dehydrogenase
GAPDH	Glyceraldehyde-3-phosphate dehydrogenase
GDP	Guanosine diphosphate
GLS	Glutaminase
GMP	Guanosine monophosphate
GPX	Glutathione peroxidase
GRB2	Growth factor receptor-bound protein 2
GSH	Glutathione
GSK3	Glycogen synthase kinase 3
GSSG	Glutathione disulphide
GST-α1	Glutathione S-transferase
GTP	Guanosine triphosphate

H ₂ O ₂	Hydrogen peroxide
HIF-1/2	Hypoxia-inducible factor-1/2
HK2	Hexokinase 2
HMGB1	High mobility group protein 1
HO [•]	Hydroxyl radical
HO-1	Haem oxygenase-1
Hr	Hour(s)
IDH1/2	Isocitrate dehydrogenase 1/2
IGF	Insulin-like growth factor
IMP	Inosine monophosphate
Int-1	Integration 1
IR	Irradiation
KEAP1	Kelch-like ECH-associated protein 1
Krm	Kremens
LDH-A	Lactate dehydrogenase
LGR5	Leucine-rich repeat-containing G-protein coupled receptor 5
LKB1	Liver kinase B1
LRP	Lipoprotein receptor-related protein
MAP	Mitogen activating protein
MCT1	Monocarboxylate transporter 1
MDA	Malondialdehyde
MDM2	Mouse double minute 2 homolog
ME	Malic enzyme
MEK	Mitogen-activated protein kinase kinase
Mieap	Mitochondria-eating protein
Min	Minute(s)
MnSOD	Manganese superoxide dismutase
mtDNA	Mitochondrial DNA
mTOR	Mammalian target of rapamycin
mTORC 1/2	mTOR Complex 1/2
NAD ⁺	Nicotinamide adenine dinucleotide (oxidized)
NAC	N-acetyl cysteine

NADH	Nicotinamide adenine dinucleotide (reduced)
NADPH	Nicotinamide adenine dinucleotide phosphate
NDUFA4L2	NADH dehydrogenase (ubiquinone) 1 alpha subcomplex, 4-like 2
NF- κ B	Nuclear factor- κ B
NRF2	Nuclear factor (erythroid-derived 2)-like 2
NO $^{\bullet}$	Nitric oxide
NOS	Nitric oxide synthase
NOX	NADPH oxidase
NQO1	NAD(P)H:quinone oxidoreductase 1
O $_2^{\bullet -}$	Superoxide
O $_3$	Ozone
OAA	Oxaloacetate
OH $^-$	Hydroxide
ONOO $^-$	Peroxynitrite
OXPHOS	Oxidative phosphorylation
p53RE	p53 response element
PanIN	Pancreatic intraepithelial neoplasia
PCR	Polymerase chain reaction
PDAC	Pancreatic ductal adenocarcinomas
PDC	Pyruvate decarboxylase complex
PDK1	Pyruvate dehydrogenase kinase 1
PEP	Phosphoenolpyruvate
PFK-1/2	Phosphofructokinase-1/2
PGD	Phosphogluconate dehydrogenase
PI3K	Phosphoinositide 3-kinase
PIG3	p53 inducible gene 3
PIP $_2$	Phosphatidylinositol (4,5)-bisphosphate
PIP $_3$	Phosphatidylinositol (3,4,5)-triphosphate
PK	Pyruvate kinase
Porc	Porcupine
PP2A	Protein phosphatase 2A
PPP	Pentose phosphate pathway

PRX	Peroxiredoxin
PTEN	Phosphatase and tensin homolog
PTP	Permeability transition pore
PTP1B	Protein tyrosine phosphatase 1B
PUMA	p53-upregulated mediator of apoptosis
qPCR	Quantitative real-time PCR
R5P	Ribose-5-phosphate
RB	Retinoblastoma-associated
RISP	Rieske-Fe-S protein
ROR2	Receptor tyrosine kinase-like orphan receptor 2
ROS	Reactive oxygen species
RT-PCR	Reverse transcription PCR
RTK	Receptor tyrosine kinase
RYK	Receptor-like tyrosine kinase
SAM	Sterile α motif
SCO2	Synthesis of cytochrome c oxidase 2
SESN1	Sestrin 1
sFRPs	Secreted Frizzled related proteins
SIRT	Sirtuin
SLC1A5	Solute carrier family 1 member 5
SNP	Single nucleotide polymorphism
SOD	Superoxide dismutase
SOS	Son of sevenless
SOST	Sclerostin
SP1	Specificity protein 1
SREBP1	Sterol regulatory element-binding protein 1
SSP	Serine synthesis pathway
TAD	Transactivation domain
TAG	Triacylglycerol
TCA	Tricarboxylic acid
TCF	T-cell factor
TET	Ten-eleven translocation methylcytosine dioxygenase

TFAM A	Mitochondrial transcription factor A
TIGAR	<i>TP53</i> -induced glycolysis and apoptosis regulator
TP53INP1	Tumour protein p53-induced nuclear protein 1
TRX	Thioredoxin
TSC1/2	Tuberous sclerosis 1/2
VEGF-A	Vascular endothelial growth factor-A
VHL	von Hippel-Lindau
Wg	Wingless
WIF	Wnt inhibitor protein
Wls	Wntless
Wnt	Wingless/Int-1
WT	Wild-type
WTX	Wilms tumour gene on X chromosome
XMP	Xanthosine monophosphate

Chapter 1 Introduction

1.1 The Hallmarks of Cancer

Under normal healthy circumstances, the majority of cells are restricted to specific tissues, and cell growth and proliferation are tightly regulated processes. Cancer arises when the regulation of these processes is lost, resulting in the uncontrolled proliferation of cells, which can form primary tumours and acquire the ability to migrate from their primary sites to invade other tissue boundaries and form malignant tumours (Preston-Martin et al. 1990). Uncontrolled proliferation of cells is often observed when errors in DNA become incorporated following DNA damage, which can result in the alteration of genes that would regulate normal cell processes and thus drive the transformation of cells. Altogether, the key differences between normal cells and tumour cells are highlighted by the “hallmarks of cancer” (Hanahan and Weinberg 2000; Hanahan and Weinberg 2011).

Transformation of a normal cell into a cancer cell can arise through the acquisition of mutant genotypes, which confer a selective advantage to cells and allow them to outgrow and dominate the local microenvironment. The majority of these advantages arise from genomic instability, which can be caused by DNA damage from mutagens such as ultraviolet light, ionising radiation and tobacco smoke. In particular, genomic instability can result in single amino acid mutations as well as amplifications and deletions of chromosomal regions (Negrini et al. 2010). Normally, genomic maintenance systems support genomic integrity and resolve changes in the DNA by activating repair mechanisms, directly repairing the damaged DNA and/or inactivating mutagenic compounds before they can damage DNA (Ciccia and Elledge 2010; Negrini et al. 2010). Altogether, this ensures that genomic mutations are kept to a minimum and also forces cells with damaged DNA to undergo senescence or be removed through a form of programmed cell death known as apoptosis. By losing genome maintenance and repair mechanisms, potentially through genomic instability, cancer cells accumulate mutant genotypes that are favourable to their growth that would normally be detrimental for a normal cell environment. Furthermore, by acquiring mutations

that allow them to evade apoptosis, cancer cells with high levels of genomic instability that would normally be removed, continue to grow and proliferate.

Programmed cell death via the intrinsic and extrinsic pathways of apoptosis is one of the means to regulate cell number. The intrinsic pathway is triggered through internal defects such as substantial levels of DNA damage or chromosomal abnormalities, while the extrinsic pathway receives and processes extracellular death-inducing signals, for example, through the Fas ligand and Fas receptor (Adams and Cory 2007). Both pathways initiate a cascade of proteolysis of effector caspases, which are responsible for the execution phase of the apoptotic process during which the cell is disassembled and removed by phagocytic cells. Through this, apoptosis provides a barrier to cancer cell transformation. However, by acquiring mutations in the apoptotic pathway, cancer cells possess mechanisms to limit or interrupt the apoptotic pathway and thus maintain their survival. Tumour suppressor proteins such as TP53 (p53) and nuclear factor- κ B (NF- κ B) are able to initiate apoptosis and often during cancer progression, these proteins as well as their functions are lost. Furthermore, many cancer cells show an increased expression of anti-apoptotic regulators such as B-cell lymphoma 2 (Bcl-2) or the decreased expression of pro-apoptotic factors such as Bcl-2-associated X protein (BAX) and p53-upregulated modulator of apoptosis (PUMA) (Korsmeyer 1992; Lowe and Lin 2000).

In addition to avoiding cell death, cancer cells acquire mutations that allow for or promote sustained cell proliferation. Normal cells are usually only driven to proliferate under suitable conditions such as favourable levels of nutrients or appropriate signalling by external growth factor stimulation. Cancer cells overcome these constraints by generating their own growth factors, promoting the secretion of growth factors by surrounding fibroblasts as well as having elevated expression of receptor proteins on the cell surface to respond to external growth factor stimulation (Cheng et al. 2008). Moreover, cancer cells can develop independence from growth factor signalling through the constitutive activation of mitogenic signalling pathways as observed in the mitogen activating protein (MAP)-kinase (MAPK) pathway (Chen and Thorner 2007), which incorporates extracellular signalling through receptor tyrosine kinases (RTKs) such as epidermal growth

factor receptor (EGFR), which can be activated by a number of extracellular ligands including growth factors, hormones and cytokines (Shaul and Seger 2007). Upon ligand binding, a conformational change in the receptor results in the activation of the receptor's intrinsic tyrosine kinase activity, leading to the autophosphorylation of its intracellular domain. Through this, docking proteins such as growth factor receptor-bound protein 2 (GRB2) are recruited to the receptor, enabling the translocation of the guanine nucleotide exchange factor Son of Sevenless (SOS). The GRB2-SOS complex in turn activates Ras, a small GTPase, by facilitating the exchange of guanosine diphosphate (GDP) for guanosine triphosphate (GTP) (Brown and Sacks 2009). Once activated, Ras initiates the downstream induction of protein kinases including Raf, which in turn phosphorylates mitogen-activated protein kinase kinase (MEK) (Zheng and Guan 1994). MEK can go on to phosphorylate and activate extracellular signal-regulated kinase 1 (ERK1) and ERK2 (Payne et al. 1991), both of which can phosphorylate an array of target proteins (Ramos 2008). Mutations in Ras often result in constitutive activation of the protein, thus promoting high MAPK pathway activity, resulting in uncontrolled pro-growth signalling and can also drive proliferative independence from external growth factors (Dhillon et al. 2007).

Alongside sustaining pro-growth signalling and cell proliferation, cancer cells have developed methods to evade programmes that would normally suppress cell proliferation, many of which rely on the activity of tumour suppressor proteins. One such tumour suppressor is the retinoblastoma-associated (RB) protein, which can regulate cell cycle progression. When RB is in its hypophosphorylated state, it forms a complex with the transcription factor E2F and acts to restrict progression from G1 to S phase in the cell cycle. However, upon phosphorylation by cyclin-dependent kinases (CDKs), RB is unable to form a complex with E2F and E2F is released, which in turn can drive the transcription of DNA synthesis genes such as DNA polymerase α (Leone et al. 1998). Furthermore, E2F can direct the synthesis of cyclin E and CDK2, which form a complex together to activate the process of cell replication (Nevins 2001; Burkhardt and Sage 2008). Cancer cells possessing defects in the RB pathway lack the ability to regulate cell cycle progression, which results in persistent cell proliferation. Another important tumour suppressor protein

involved in regulating cell growth and proliferation is p53, which will be discussed in greater detail further on.

Much like normal tissues, tumours also require nutrients and oxygen in order to grow and proliferate at maximum capacity. However, in order to sustain uncontrolled cell proliferation, there is a requirement for an adjustment in energy metabolism to allow for an increased need in nutrients for energy as well as biosynthetic molecules to support cell growth. This metabolic need can be maintained through multiple ways such as the activation of oncogenic pathways, the loss of tumour suppressor signalling as well as the acquisition of mutations in metabolic proteins, all of which will be discussed in further detail below.

1.2 Cancer Cell Metabolism

1.2.1 Nutrient Catabolism and the Warburg Effect

All cells are dependent on a source of nutrients from their environments, which can be taken up and directed into metabolic pathways in order to maintain cellular homeostasis as well as used to create more biomass for cell growth. This includes the maintenance of ion gradients across cell membranes, the transport of materials between intracellular compartments as well as other housekeeping functions such as protein turnover, many of which are highly energetic processes and rely on the hydrolysis of adenosine 5'-triphosphate (ATP) as a source of free energy. In particular, cell division is a highly bioenergetic process and in order to support this, there are various metabolic pathways to generate ATP. Importantly, these metabolic pathways are tightly regulated through various control systems and altered depending on nutrient availability or the energetic demands of the cell. When nutrient availability is scarce, cells halt their proliferation and adapt their metabolism to conserve energy and assist in cell survival in order to survive a period of starvation. In contrast, when nutrients as well as growth factors are readily available, cell division is promoted as well as the production of biosynthetic compounds necessary for growth and proliferation (Vander Heiden et al. 2009).

Most cells use glucose as a primary substrate for ATP generation and a source of carbon for the biosynthesis of macromolecules (Dang 2012). Following its uptake

into cells, glucose is metabolised through various steps within glycolysis to eventually form pyruvate (Figure 1-1). Under aerobic conditions, where oxygen is readily available, pyruvate is shuttled into the mitochondrion where it is converted to acetyl-CoA through pyruvate decarboxylation by the pyruvate dehydrogenase (PDH) and fed into the tricarboxylic acid (TCA) cycle. This generates reduced nicotinamide adenine dinucleotide (NADH), which fuels oxidative phosphorylation (OXPHOS) at the mitochondrial electron transport chain (ETC) to maximize ATP production. Furthermore, shunting of pyruvate into the TCA cycle generates acetyl-CoA for the biosynthesis of lipids and amino acids. However, under anaerobic conditions, where oxygen levels are low or unavailable and cannot drive the ETC to generate ATP, high levels of lactate are generated from pyruvate by lactate dehydrogenase (LDH), which is secreted into the extracellular environment. By doing so, LDH recovers the oxidized nicotinamide adenine dinucleotide (NAD⁺) needed to maintain glycolysis. While ATP generation through glycolysis is less efficient, when there is an excess of glucose and the flux of the glycolytic pathway is high, glycolysis does possess the capability to generate high quantities of ATP to fuel biosynthetic processes (DeBerardinis et al. 2008; Aguilar and Fajas 2010; Ward and Thompson 2012) (Figure 1-1).

It was noted by Otto Warburg that cancer cells shift their metabolism to preferentially use glucose to generate lactate even under conditions where oxygen is readily available to support mitochondrial oxidative phosphorylation (Warburg et al. 1927). Therefore, their metabolism is also known as “aerobic glycolysis.” This preference for glycolysis allows the diversion of metabolic intermediates into anabolic pathways as well as adaptation to challenging microenvironments such as limiting the production of reactive oxygen species (ROS), which are a normal byproduct of cellular metabolism and elevated in cancer cells. If not limited, high levels of ROS can damage cellular structures (Vander Heiden et al. 2009). As a whole, this increase in aerobic glycolysis is also known as the Warburg effect.

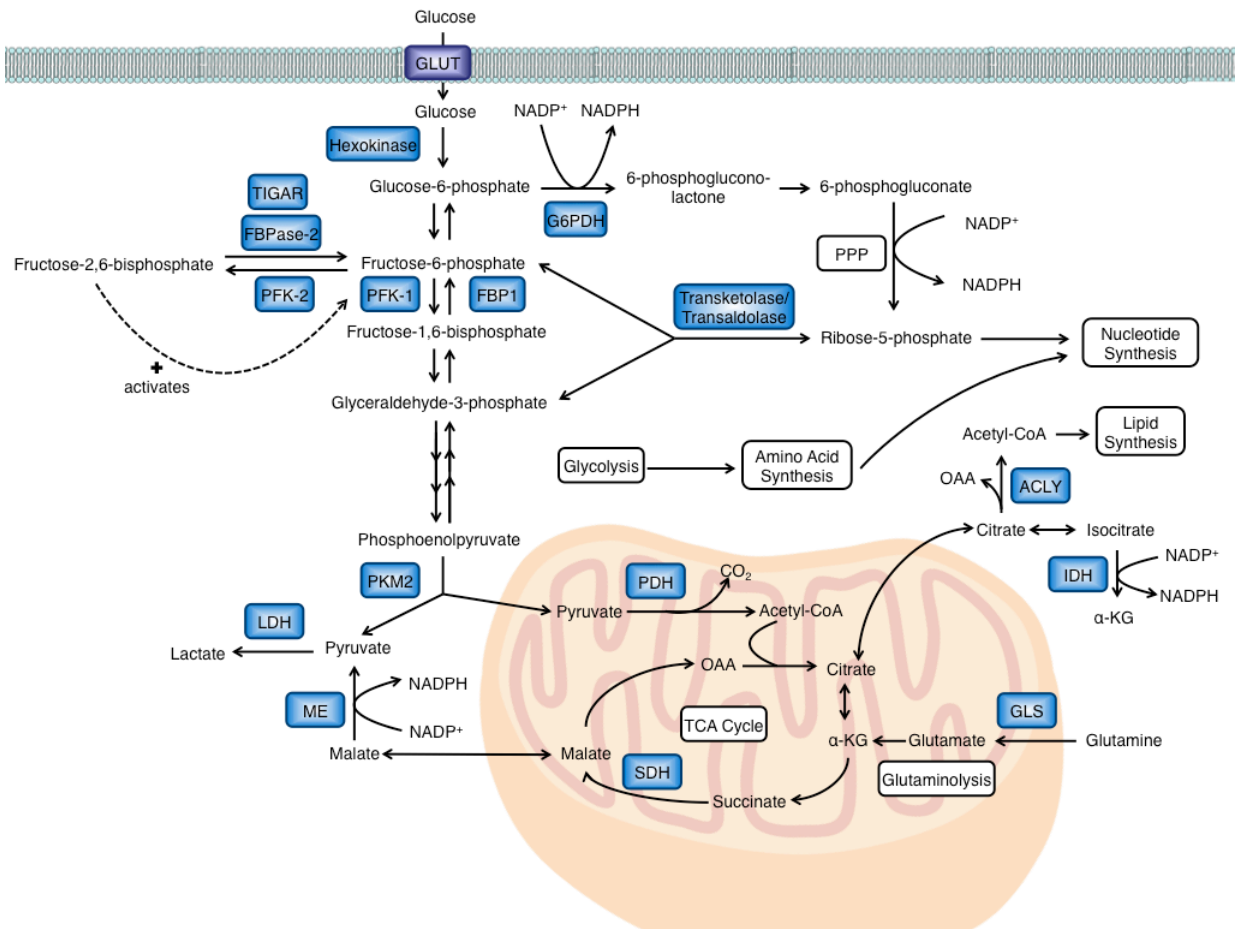


Figure 1-1 Metabolic pathways of cell growth and proliferation

Schematic showing the interplay between glycolysis, the pentose phosphate pathway (PPP), tricarboxylic acid (TCA) cycle and glutamine metabolism, all of which promote biosynthetic processes such as nucleotide, amino acid and lipid synthesis. Key enzymes controlling various steps in these pathways are highlighted in blue. α -KG, α -ketoglutarate; ACLY, ATP citrate lyase; FBP1, fructose-1,6-bisphosphatase; FBPase-2, fructose-2,6-bisphosphatase; G6PDH, glucose-6-phosphate dehydrogenase; GLS, glutaminase; IDH, isocitrate dehydrogenase; LDH, lactate dehydrogenase; ME, malic enzyme; OAA, oxaloacetate; PDH, pyruvate dehydrogenase; PFK-1, phosphofructokinase-1; PFK-2, phosphofructokinase-2; PKM2, pyruvate kinase M2; SDH, succinate dehydrogenase; TIGAR, *TP53*-induced glycolysis and apoptosis regulator.

Furthermore, cell division requires the abundance of other biosynthetic molecules for the production of nucleotides, amino acids and lipids. Therefore, glucose cannot only be used to generate free energy but also acts as part of central carbon metabolism that is linked with several other metabolic pathways. One such branch that is particularly important in cell growth is the pentose phosphate pathway (PPP) (Figure 1-1). During glycolysis, glucose is phosphorylated to form glucose-6-phosphate (G6P), which can enter the oxidative branch of the PPP where it is oxidized by glucose-6-phosphate dehydrogenase (G6PDH) to generate 6-phosphoglucono-lactone and reduced nicotinamide adenine dinucleotide phosphate (NADPH), which can contribute to the biosynthesis of fatty acids, cholesterol and reduced glutathione (GSH) (Figure 1-1). Subsequently, 6-phosphoglucono-lactone is hydrolysed by lactonase and 6-phosphogluconate dehydrogenase to produce ribulose-5-phosphate, which in turn is converted to ribose-5-phosphate (R5P), which plays a key role in nucleotide synthesis, along with another molecule of NADPH. On top of this, ribulose-5-phosphate can also be converted to xylulose-5-phosphate, which enters the reversible non-oxidative branch of the PPP and can feed back into glycolysis. Other products of glycolysis, fructose-6-phosphate (F-6-P) and glyceraldehyde-3-phosphate (G3P), can both also be shunted into the non-oxidative branch of the PPP to generate R5P (Patra and Hay 2014) (Figure 1-1).

Other glycolytic intermediates, such as 3-phosphoglycerate (3PG), can be used to provide the carbon backbone for non-essential amino acids through their flux into the serine synthesis pathway (SSP), which can also feed into phospholipid production. Glucose-derived pyruvate can also enter the TCA cycle downstream of glycolysis and contribute to the production of citrate, which under conditions of high ATP/ADP (adenosine 5'-diphosphate) and NADH/NAD⁺ can be shunted back into the cytosol, converted back to acetyl-CoA by ATP citrate lyase (ACLY) and used as a carbon source for growing acyl chains during *de novo* fatty acid biosynthesis (Vander Heiden et al. 2009).

In addition to glucose, central carbon metabolism can utilize amino acids as a carbon source. Glutamine is the most abundant free amino acid found in human serum and proliferating cells utilize glutamine to replenish intermediates in the

TCA cycle (a process also known as anaplerosis) through the deamidation of glutamine to glutamate as well as the conversion of glutamine to α -ketoglutarate (α -KG), which can feed into the TCA cycle (DeBerardinis and Cheng 2010). Glutamine-derived carbons can also contribute to the mitochondrial production of citrate and subsequent fatty acid synthesis as described above. In addition to this, when citrate is converted back to acetyl-CoA by ACLY, oxaloacetate (OAA) is generated, which can be further utilized in a variety of ways. OAA can be metabolized to malate by cytosolic malate dehydrogenase with the production of NAD^+ . Subsequently, this malate can be converted to pyruvate by malic enzyme (ME) with the generation of NADPH (Figure 1-1). OAA can also be converted to phosphoenolpyruvate (PEP) and feed into glycolysis. In addition, glutamine itself plays an important role in nucleotide metabolism by donating nitrogen atoms to purine rings as well as participating in the amination of xanthosine monophosphate (XMP) to form guanosine monophosphate (GMP). Glutamine can also be used in protein synthesis as well as the biosynthesis of non-essential amino acids and hexosamines (Cantor and Sabatini 2012; Boroughs and DeBerardinis 2015).

In addition to using glucose and glutamine to generate ATP, cells can utilize fatty acids. Fatty acids are normally esterified with glycerol to form triacylglycerol (TAG), which is stored in adipose tissue. When energy is required, hormones, such as adrenaline, stimulate TAG mobilization by activating hormone-sensitive lipases within adipose tissue. This liberates fatty acids, which are bound by serum albumin and transported in the blood towards tissues such as the muscle, which can utilize fatty acid β -oxidation. While fatty acids are able to diffuse into the cytosol, the enzymes responsible for β -oxidation are located within the mitochondria. Therefore, fatty acids are transported across the outer mitochondrial membrane by carnitine acyl transferases such as carnitine-palmitoyl transferase I (CPT-I) and carried across the inner mitochondrial membrane via carnitine. Once inside the mitochondrial matrix, fatty acyl-carnitine reacts with coenzyme A to release the fatty acid and produce acetyl-CoA. The fatty acids subsequently undergo β -oxidation, during which two carbon molecules of acetyl-CoA are repeatedly cleaved, which can enter the TCA cycle to eventually generate ATP through the ETC. In addition to generating acetyl-CoA, β -oxidation also produces reduced forms of flavin adenine dinucleotide (FADH_2) and NADH, both of which can directly

be used by the ETC to generate ATP. Therefore, β -oxidation is capable of generating a greater yield of ATP than most other pathways (Santos and Schulze 2012).

As previously noted, glycolysis is the favoured method by which cancer cells produce energy even though it is less efficient in generating ATP than other metabolic pathways such as OXPHOS or β -oxidation. This metabolic switch may provide a growth advantage and/or resistance to apoptosis in order to allow cancer cells to maintain mitochondrial bioenergetics during cell growth and proliferation. However, as a growing tumour with increased metabolic demands consumes all of its nutrient supply, it must activate pathways to maintain cellular bioenergetics for continual survival as well as promote metabolic adaptation in order to survive periods of metabolic stress. This metabolic adaptation can be observed in cultured cancer cells, which are able to restructure their metabolic pathways to compensate for the loss of major energy sources such as glucose or glutamine (Le et al. 2012) as well as in studies where glucose deprivation elicits a selective pressure for cancer cells that are able to survive low glucose conditions (Yun et al. 2009).

1.2.2 Oncogenes and Tumour Suppressors in Metabolic Networks

The Warburg effect in cancer cells reflects a shift in cell metabolism during cancer cell transformation and mutations that alter oncogene and tumour suppressor networks are further able to support as well as influence changes in metabolic pathways. In addition, mutations and changes in the expression of metabolic enzymes are also able to contribute to metabolic transformation.

1.2.2.1 Signalling Pathways Influencing Cancer Metabolism

A central regulator of metabolism in both transformed and non-transformed cells is phosphoinositide 3-kinase (PI3K), a lipid kinase located at the plasma membrane. Following induction by growth factor-mediated activation of RTKs, PI3K acts to phosphorylate phosphatidylinositol (4,5)-bisphosphate (PIP₂) to phosphatidylinositol (3,4,5)-triphosphate (PIP₃), which in turn initiates a signal transduction cascade leading to the activation of downstream effectors such as Akt. The PI3K/Akt signalling cascade is one of the most commonly altered signalling pathways in human cancers (Shaw and Cantley 2006) through activating

mutations in PI3K (Samuels et al. 2004; Samuels et al. 2005; Jia et al. 2008) or the loss of its negative regulator phosphatase and tensin homolog (PTEN), which dephosphorylates PIP₃ and through this, acts as a potent tumour suppressor (Cairns et al. 1997) (Figure 1-2).

Enhanced PI3K/Akt signalling can promote metabolic transformation via various downstream alterations such as the increased expression and membrane translocation of nutrient transporters, which allow for the increased uptake of glucose, amino acids and other nutrients (Edinger and Thompson 2002; Robey and Hay 2009). In addition, the signalling cascade can result in the increased transcription of genes involved in glycolysis and lipogenesis (Khatri et al. 2010). Akt itself can also stimulate glucose utilization by promoting the activity of the glycolytic enzymes, hexokinase and phosphofructokinase (Elstrom et al. 2004; Fan et al. 2010) (Figure 1-2). Moreover, Akt can activate ectonucleoside triphosphate diphosphohydrolase (ENTPD5), which acts to increase protein glycosylation in the endoplasmic reticulum (ER) and through this, indirectly increases glycolysis (Fang et al. 2010). Finally, Akt plays an important role in cellular signalling through mammalian target of rapamycin (mTOR) by phosphorylating and inhibiting its negative regulator tuberous sclerosis 2 (TSC2), which in turn disrupts the function of the TSC1/TSC2 complex, and subsequently promotes mTOR activation and its downstream activities (Robey and Hay 2009).

mTOR is the catalytic subunit of two distinct complexes known as mTOR Complex 1 (mTORC1) and 2 (mTORC2), and plays a central role in the metabolic integration of nutrient availability and cell growth (Guertin and Sabatini 2007). Activation of mTOR promotes protein and lipid biosynthesis, increases mRNA translation and ribosome biogenesis as well as influences autophagy, the process by which cellular components are broken down through the lysosome during starvation in response to changes in cellular nutrient and energy homeostasis (Edinger and Thompson 2002; Mamane et al. 2004). High mTOR signalling is observed in familial cancer syndromes arising from mutations in tumour suppressors such as TSC1/TSC2 and PTEN, which each function to negatively regulate mTOR signalling (Inoki et al. 2005). Studies in liver-specific TSC1 knockout mice, which result in elevated mTORC1 signalling, showed defects in

glucose and lipid homeostasis and these animals subsequently develop hepatocellular carcinomas (Menon et al. 2012). In contrast, the bioenergetic sensor adenosine monophosphate (AMP)-activated protein kinase (AMPK) inhibits mTOR by phosphorylating and activating TSC (Inoki et al. 2003).

AMPK is a crucial sensor of energy status within cells and plays an important role in the cellular response to energy availability. During periods of energetic stress, AMPK becomes activated in response to an increased AMP/ATP ratio and promotes a shift in cell metabolism towards a more oxidative phenotype. Moreover, it couples the energy status of cells to extracellular growth signals such as those from the PI3K/Akt signalling pathway and can oppose such effects in order to halt proliferation when energy levels are low. Through this, AMPK functions as a metabolic checkpoint for cells by linking the response of growth signals to energy availability (Jones et al. 2005; Kuhajda 2008; Shackelford and Shaw 2009). Therefore, the activity of AMPK must be overcome in order to induce uncontrolled proliferation (as observed in cancer cells) and activate growth signalling pathways even in an unfavourable microenvironment of high energetic stress. Several oncogenic mutations and alterations in signalling pathways can suppress the activity of AMPK, and many cancer cells exhibit a loss or inappropriate AMPK signalling. Liver kinase B1 (LKB1), the upstream kinase responsible for the activation of AMPK (Figure 1-2), has been identified as a tumour suppressor gene, and LKB1 mutations have been observed in cases of non-small cell lung cancer and cervical carcinoma (Ji et al. 2007; Wingo et al. 2009). Mutations in LKB1 have also been identified in the hereditary Peutz-Jeghers syndrome, which is characterized by the development of benign gastrointestinal and oral lesions (Jenne et al. 1998). The loss of AMPK signalling allows for the activation of mTOR. Altogether, this promotes a shift in metabolism towards a more glycolytic phenotype as observed in cancer cells (Cairns et al. 2011).

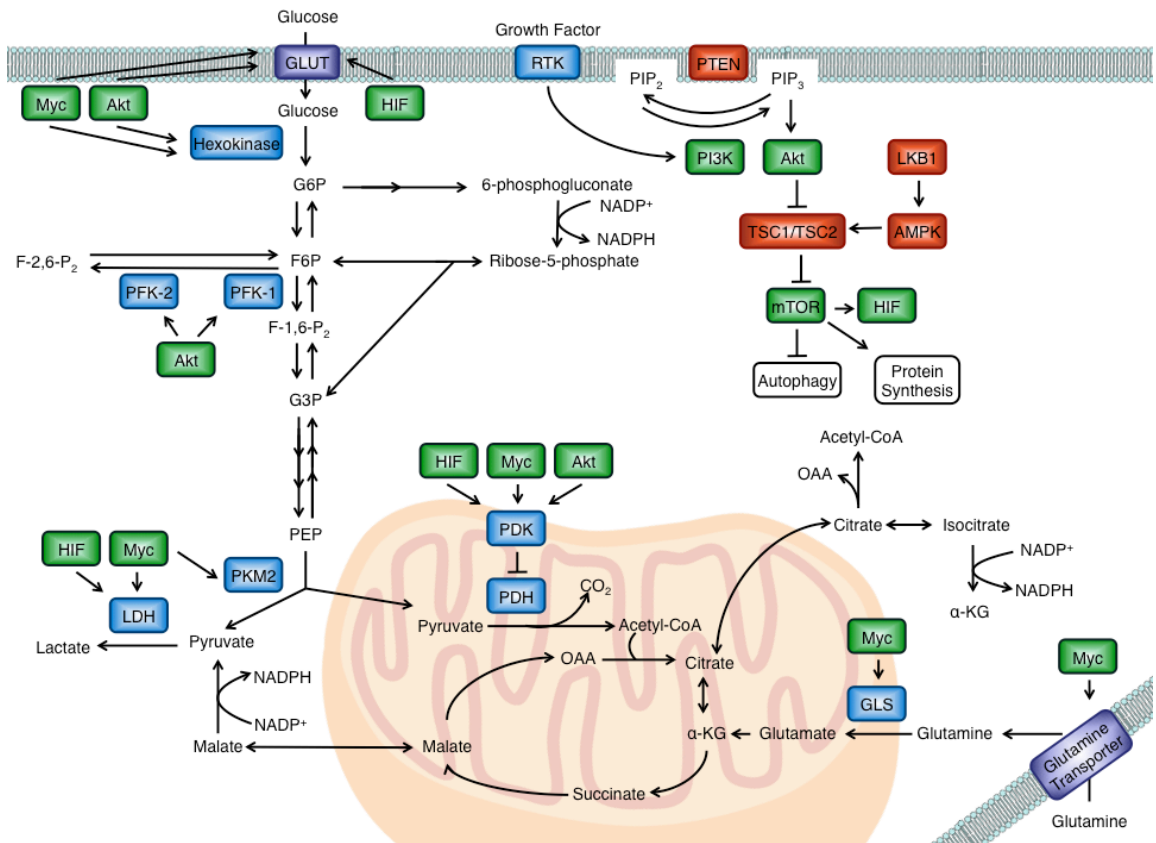


Figure 1-2 Signalling pathways driving the Warburg effect

Oncogenes and tumour suppressors can directly regulate key steps in metabolic pathways. Activation of receptor tyrosine kinase (RTK) activity by growth factors results in the activation of phosphoinositide 3-kinase (PI3K) and Akt. PI3K/Akt signalling can promote glucose uptake, glycolytic flux and mammalian target of rapamycin (mTOR) activity. While hypoxia-inducible factor (HIF) and Myc promote glycolytic flux, Myc can also promote glutamine metabolism. Liver kinase B1 (LKB1), phosphatase and tensin homolog (PTEN) and AMP-activated protein kinase (AMPK) signal to lower glycolytic activity during low nutrient availability. Oncogenes are marked in green while tumour suppressors are in red. Key enzymes controlling various steps in these pathways are highlighted in blue. α -KG, α -ketoglutarate; F-1,6-P₂, fructose-1,6-bisphosphate; F-2,6-P₂, fructose-2,6-bisphosphate; F6P, fructose-6-phosphate; G3P, glyceraldehyde-3-phosphate; G6P, glucose-6-phosphate; GLS, glutaminase; GLUT, glucose transporter; LDH, lactate dehydrogenase; OAA, oxaloacetate; PDH, pyruvate dehydrogenase; PDK, pyruvate dehydrogenase kinase; PEP, phosphoenolpyruvate; PFK-1, phosphofructokinase-1; PFK-2, phosphofructokinase-2; PIP₂, phosphatidylinositol (4,5)-bisphosphate; PIP₃, phosphatidylinositol (3,4,5)-triphosphate; PKM2, pyruvate kinase M2; TSC1/TSC2, tuberous sclerosis 1/tuberous sclerosis 2.

1.2.2.2 Transcription Factors in Metabolic Regulation

Transcription factors are also able to contribute to changes in cancer cell metabolism. For example, Myc is able to directly activate the expression of rate-limiting glycolytic enzymes such as hexokinase 2 (HK2), the enzyme responsible for the first step in glycolysis, glucose transporters, LDH, and pyruvate dehydrogenase kinase 1 (PDK1) (Dang 2009) (Figure 1-2). In addition to this, Myc is also able to stimulate genes involved in glutamine metabolism including glutamine transporters, SLC5A1 and SLC7A1, and glutaminase (GLS), the first enzyme involved in glutaminolysis (Gao et al. 2009) (Figure 1-2).

With respect to cell metabolism, oncogenic Myc has also been shown to interact with the hypoxia-inducible factor (HIF) family of transcription factors (Dang et al. 2008). HIF-1 and HIF-2 are the major transcription factors involved in regulating gene expression for the adaptation of cells to hypoxic conditions, where oxygen availability is low. While HIF-1 is ubiquitously expressed, HIF-2 is only found in endothelial cells and in the kidney, heart, lungs and small intestine. Each HIF complex functions as a heterodimer consisting of an oxygen-dependent α -subunit and a constitutively expressed β -subunit, which are rapidly stabilized under hypoxic conditions (Semenza 2002). Under normoxic conditions, the α -subunits of HIF undergo oxygen-dependent hydroxylation by prolyl hydroxylases (PHDs) on conserved proline residues, which result in their recognition and ubiquitination by von Hippel-Lindau tumour suppressor (VHL), an E3 ubiquitin ligase. This subsequently results in their degradation by the proteasome. In addition to its activation under hypoxia, HIF-1 can also be activated under normoxic conditions in response to oncogenic signalling pathways, such as the PI3K/Akt signalling cascade (Bertout et al. 2008) as well as mutations in tumour suppressor proteins such as VHL (Kaelin and Ratcliffe 2008). Loss of TCA cycle enzymes succinate dehydrogenase (SDH) or fumarate hydratase (FH) can induce pseudohypoxia, where HIF-1 is activated under normoxic conditions as a consequence of PHD inhibition by excess succinate or fumarate levels, respectively (King et al. 2006). Once activated, HIF-1 can induce the transcription of genes encoding glucose transporters and a majority of glycolytic enzymes, thereby increasing the glycolytic capabilities of the cell (Semenza 2010). HIF-1 can also increase the expression of pyruvate dehydrogenase kinase (PDK), which inactivates mitochondrial PDH and

decreases the flux of glucose-derived pyruvate into the TCA cycle (Kim et al. 2006; Papandreou et al. 2006; Lu et al. 2008). This decrease in TCA cycle activity lowers the rate of OXPHOS and oxygen consumption, thereby contributing to the glycolytic phenotype observed in cancer cells as well as sparing oxygen under harsh hypoxic conditions.

1.2.2.3 Metabolic Enzymes as Tumour Suppressors

In addition to metabolic changes as a consequence of altered growth signalling pathways, direct alterations in metabolic enzymes and their activity can also contribute to tumourigenesis.

One such glycolytic enzyme is pyruvate kinase (PK), which catalyses the rate-limiting, ATP-generating step of glycolysis in which phosphoenolpyruvate (PEP) is converted to pyruvate. Mammalian PK exists in four isoforms: the L and R isoforms are expressed in the liver and erythrocytes, respectively. All other tissues express either the M1 isoform or its splice variant, M2 (Noguchi et al. 1986). PKM1 expression is found predominantly in differentiated adult tissues with high ATP requirements such as the heart and muscle, and forms a stable, constitutively active tetramer (Imamura and Tanaka 1972; Clower et al. 2010; Mazurek 2011). PKM2 is expressed during development as well as in other adult tissues including the spleen and lung, and its activity is regulated by posttranslational modifications (Lv et al. 2011; Anastasiou et al. 2012) and allosteric effectors such as FBP (Christofk et al. 2008b; Anastasiou et al. 2012) and serine (Chaneton et al. 2012).

Interestingly, PKM2 is found expressed in all cancers and cancer cell lines studied to date (Imamura and Tanaka 1972; Clower et al. 2010; Mazurek 2011), suggesting PKM2 expression provides a selective advantage to cancer cells. However, while a selection for PKM2 has been observed in xenograft tumour models (Christofk et al. 2008a), various studies have found the ability of PKM2 to be inactivated to be important for cancer cell proliferation (Christofk et al. 2008a; Hitosugi et al. 2009; Varghese et al. 2010; Anastasiou et al. 2012), implying that low PK activity is favoured by proliferating cancer cells despite a selection for PKM2 expression. One such reasoning for this is that the inactive form of PK also possesses non-metabolic roles, which may contribute to tumourigenesis and

multiple abilities have been proposed including functioning as a protein kinase as well as a co-activator for transcription factors (Luo et al. 2011; Yang et al. 2011; Gao et al. 2012). Furthermore, although decreased PKM2 activity is associated with increased cell proliferation, it is possible that reactivation of PKM2 activity is important for non-proliferating cancer cells within the tumour and to allow for metabolic adaptation. Isoform specific loss of PKM2 in a model of breast cancer was found to accelerate tumour formation and PKM2-deficient tumours showed PKM1 expression in non-proliferating tumour cells and no detectable pyruvate kinase expression in proliferating cells, illustrating that PKM2 is not necessary for tumour cell growth but is required in non-proliferating tumour cells (Israelsen et al. 2013). In line with this, variable PKM2 expression and heterozygous PKM2 mutations have been identified in human tumours (Luftner et al. 2000; Schneider et al. 2002; Israelsen et al. 2013). Furthermore, the oncogenic transcription factor Myc has also been found to preferentially promote the expression of PKM2 (David et al. 2010) (Figure 1-2).

A particular outcome of alterations in the activity of metabolic enzymes is the production of NADPH. As mentioned previously, NADPH is important in the biosynthesis of macromolecules but also as a reducing agent in the production of GSH, an important antioxidant, which prevents damage to cells caused by reactive oxygen species (ROS) (Boroughs and DeBerardinis 2015). In addition to the PPP and the activity of malic enzyme (ME), NADPH can also be produced to regulate cellular redox status through the conversion of isocitrate to α -ketoglutarate (α -KG) by the enzymes isocitrate dehydrogenase 1 (IDH1) and IDH2, which are found in the cytoplasm and mitochondria, respectively. Both enzymes have been observed to acquire mutations, which link them to tumorigenesis, and mutations in IDH1 have been identified in glioblastoma and acute myeloid leukaemia. IDH1 and IDH2 are mutated in approximately 80% of grade II and grade III gliomas and secondary glioblastomas as well as approximately 30% of cytogenetically normal cases of acute myeloid leukaemia (Yan et al. 2009; Gross et al. 2010). These mutant forms of IDH act to promote the conversion of α -KG into 2-hydroxyglutarate (2HG), a novel oncometabolite, in a NADPH-dependent manner.

2HG is structurally similar to α -KG and glutamate and thus, high levels can result in the competitive inhibition of α -KG-dependent dioxygenases, which utilize α -KG as a co-substrate and are involved in fatty acid metabolism, oxygen sensing as well as modulating the epigenome (Nowicki and Gottlieb 2015). In particular, alterations in the epigenome are due to the inhibition of the ten-eleven translocation methylcytosine dioxygenase (TET) family of α -KG-dependent dioxygenases, which hydroxylate 5-methylcytosine to 5-hydroxymethylcytosine (5-hmC), which allows for subsequent DNA demethylation. Notably, in human glioma tissues, 5-hmC levels are reduced in IDH mutant tumours (Xu et al. 2011) and mutant IDH1-overexpressing immortalized astrocytes show a distinct pattern of CpG hypermethylation (Duncan et al. 2012; Turcan et al. 2012). In addition, the jumunji-C histone demethylases initiate the removal of methyl groups on histones by hydroxylation, resulting in changes in gene transcription depending on the site of histone methylation. Increases in histone methylation for H3K9 and H3K27, both of which are gene repressive, have been observed in human glioma samples with IDH1 or IDH2 mutations (Xu et al. 2011; Lu et al. 2012).

In addition to IDH, mutations in SDH and FH, have also been identified. SDH loss was initially discovered in familial paraganglioma while FH was originally identified in hereditary leiomyomatosis and renal cell cancer (Nowicki and Gottlieb 2015). As previously described, loss of SDH or FH results in an accumulation of succinate or fumarate, respectively, and both are able to competitively inhibit α -KG-dependent dioxygenases much like 2HG (Xiao et al. 2012).

1.2.3 Redox Homeostasis and Cancer

1.2.3.1 Reactive Oxygen Species

Reactive oxygen species (ROS) make up a class of oxygen-containing reactive species that are produced in cells as a normal byproduct of metabolic processes. There are two types of ROS, free radical ROS, which have one or more unpaired electron(s) and non-radical ROS, which do not have unpaired electron(s) but are chemically reactive and can be converted to radical ROS. Common forms of radical ROS in cells are superoxide (O_2^-), nitric oxide (NO^*) and hydroxyl radicals (HO^*), while non-radical ROS include hydrogen peroxide (H_2O_2), ozone (O_3), and hydroxide (OH^-). ROS can be found in the environment, for example as tobacco

smoke and radiation, or generated intrinsically in cells. ROS have a variety of properties and downstream effects dependent on the concentration at which they are present as well as their source (Sullivan and Chandel 2014).

The largest contributors to cellular ROS are the mitochondria (Figure 1-3). Mitochondria have eight known sites that are capable of producing superoxide, with complex I, II and III generating ROS with effects on cellular signalling (Murphy 2009). Complex I and II release ROS into the mitochondrial matrix, while complex III can do so to both sides of the mitochondrial inner membrane (Muller et al. 2004). Through its release to the mitochondrial inner membrane, Complex III-derived ROS is able to interact with cytosolic targets and thereby influence biological processes such as oxygen sensing and cell differentiation (Sena and Chandel 2012). The superoxide released from the ETC in the mitochondria can also be converted to hydrogen peroxide and water by superoxide dismutases (SOD). Hydrogen peroxide can then in turn be reduced to water by a variety of antioxidant enzymes including glutaredoxin (GRX), glutathione peroxidase (GPX), thioredoxin (TRX) and catalase (Figure 1-3). ROS can also be produced by NADPH oxidases (NOX), which catalyse the production of superoxide from oxygen and NADPH (Figure 1-3). These enzymes were originally discovered in phagocytes where high levels of oxidative stress are generated to destroy engulfed pathogens (Bedard and Krause 2007). This illustrates that ROS production also serves as a biological function within cells as opposed to simply a toxic byproduct. Oncogenes can promote the activity of NOX-dependent ROS production to stimulate cell proliferation as observed in cancer cell lines and primary tissues (Tominaga et al. 2007).

Nitric oxide is produced from the amino acid arginine by nitric oxide synthase (NOS) and is able to react with superoxide to form peroxynitrite (ONOO^-) (Figure 1-3). These reactive nitrogen species likely have both overlapping and distinct mechanisms in mediating cell signalling changes as they are capable of altering the structure and function of proteins by oxidizing and nitrating intracellular amino acids. In addition, in the presence of transition metals such as free Fe^{2+} , the Fenton reaction converts hydrogen peroxide to hydroxyl radicals, which are highly

reactive and can cause damage to intracellular components such as DNA, proteins and lipids (Trachootham et al. 2009).

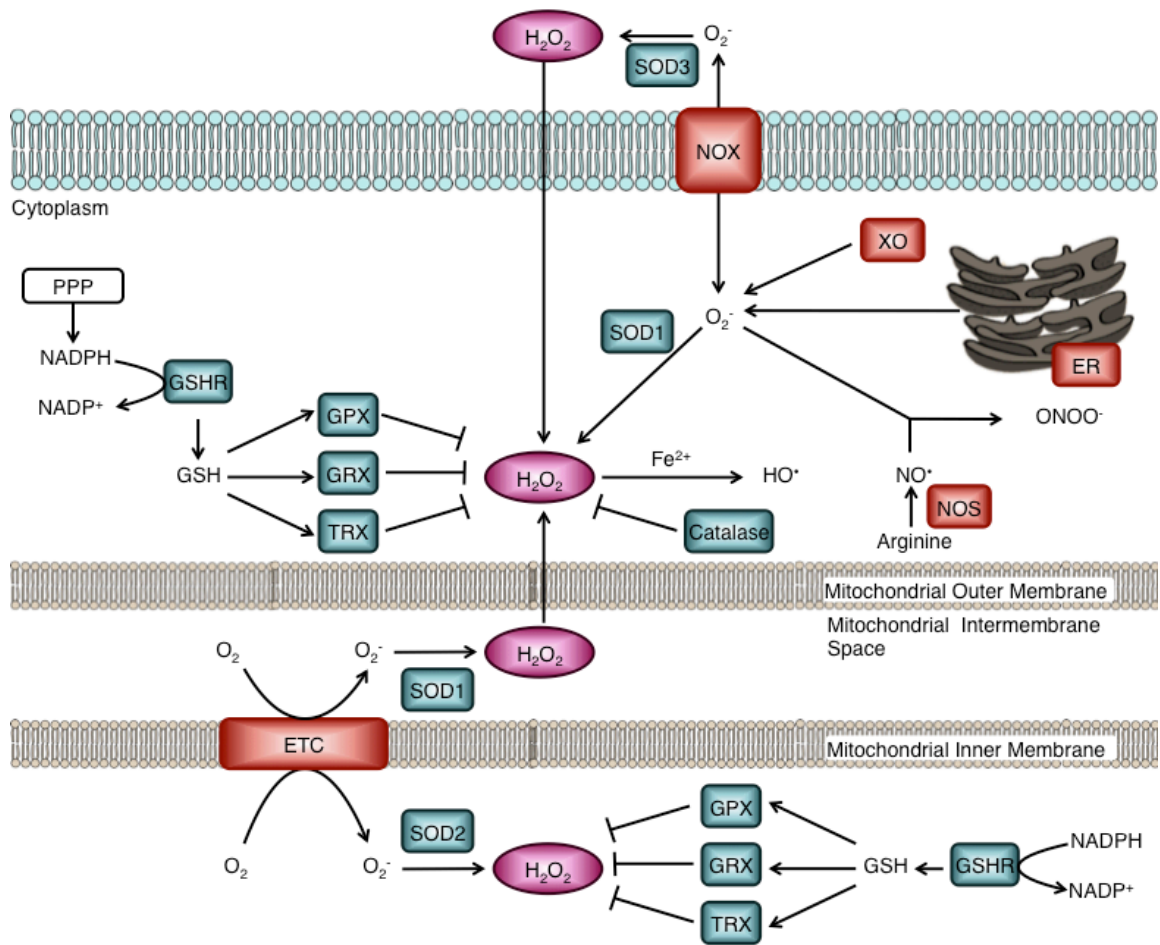


Figure 1-3 Cellular redox homeostasis

Major sites of reactive oxygen species (ROS) production include the endoplasmic reticulum (ER), NADPH oxidase (NOX) complex and the mitochondrial electron transport chain (ETC) where electrons are generated from the oxidation of metabolic intermediates. In the mitochondria, superoxide (O_2^-) is converted to hydrogen peroxide (H_2O_2) by superoxide dismutases (SOD), which can then be further converted to water by catalase. H_2O_2 can be degraded by glutathione peroxidases (GPX), glutaredoxin (GRX) and thioredoxin (TRX) using reducing equivalents obtained from the oxidative of reduced glutathione (GSH). Oxidized glutathione (GSSG) is reduced by glutathione reductase (GSXR), which obtains its equivalents from NADPH oxidation. In the presence of transition metals (Fe^{2+}), H_2O_2 is converted to hydroxyl radicals (HO^{\cdot}). Nitric oxide (NO^{\cdot}) is a reactive radical produced from arginine by nitric oxide synthase (NOS), which can also react with superoxide to peroxynitrite ($ONOO^-$). Major ROS scavenging enzymes are shown in green and ROS generating complexes are shown in red.

1.2.3.2 ROS as Signalling Molecules

Free radicals are highly reactive with biological molecules and can cause oxidative modifications. Through this, ROS can alter the function of various biomolecules and is essential for homeostatic signalling events depending on context, concentration and cell type.

It has been shown that the primary signalling ROS molecule is hydrogen peroxide, which at low concentrations can inactivate phosphatases through posttranslational modifications to allow for growth factor-dependent signalling (Sundaresan et al. 1995; Bae et al. 1997). As hydrogen peroxide is able to cross cell membranes and is more stable than radical ROS molecules, it is able to act on susceptible residues on target molecules and display functional selectivity. One mechanism of hydrogen peroxide signalling is via the oxidation of cysteine residues on proteins, which exist in equilibrium between the protonated thiol (Cys-SH) and the thiolate anion (Cys-S⁻) forms. Thiolate forms are inclined to oxidation by hydrogen peroxide to form sulfenic acid residues (Finkel 2012). When this occurs on the regulatory cysteine residues of proteins, it can result in allosteric modifications and alter activity or binding partners. The peroxidation of cysteine residues found in the active sites of proteins can also inhibit activity and thus, change the outcome of signalling transduction pathways (Finkel 2003).

ROS can enhance the PI3K/Akt signalling pathway and its downstream effects such as increased cell proliferation, promote survival and increased migration. Treatment of cells with exogenous hydrogen peroxide has been found to activate Akt activity through targeting a negative regulator of the PI3K/Akt pathway, PTEN (Nemoto and Finkel 2002). ROS acts to oxidize the cysteine found in the PTEN active site resulting in a disulphide bond formation to another cysteine within the protein. This modification results in the inactivation of PTEN activity and thereby, promotes the PI3K/Akt pathway (Lee et al. 2002; Leslie et al. 2003). In addition to extracellular sources of ROS, mitochondrial ROS has also been shown to inhibit PTEN (Connor et al. 2005; Pelicano et al. 2006). Through a similar mechanism, ROS can also inhibit other phosphatases that act on the PI3K/Akt pathway such as protein phosphatase 2A (PP2A) and protein tyrosine phosphatase 1B (PTP1B) (Ostman et al. 2011). PP2A and PTP1B normally dephosphorylate Akt, resulting in

its inactivation. However, this activity can be prevented by treatment with hydrogen peroxide (Rao and Clayton 2002; Salmeen et al. 2003; Lou et al. 2008). Thus, ROS can inhibit protein function, in particular, phosphatases involved in normal PI3K/Akt signalling pathway, thus resulting in a deregulation of this pro-growth and pro-survival signalling pathway.

ROS can also induce stress-responsive genes such as HIF-1, which can in turn activate the transcription of its target genes in order to drive cell survival during cell stress. Hypoxia leads to an increase in the levels of mitochondrial ROS and consequently, the stabilisation of HIF α -subunits. Cells depleted of their mitochondrial DNA are incapable of stabilizing HIF α -subunits under hypoxia, do not exhibit mitochondrial oxygen consumption and subsequently do not produce mitochondrial ROS (Chandel et al. 1998; Chandel et al. 2000). Moreover, hypoxia increases the release of superoxide from mitochondrial complex III to the mitochondrial intermembrane space (Waypa et al. 2010). Within complex III, electron transport is mediated by the Rieske-Fe-S protein (RISP), cytochrome b and cytochrome c1. Notably, while the loss of either RISP or cytochrome b results in the loss of mitochondrial oxygen consumption, only the loss of RISP eliminates mitochondrial ROS generation and cells deficient in RISP are unable to stabilize HIF α -subunits under hypoxia (Brunelle et al. 2005; Guzy et al. 2005). Altogether, this suggests that during hypoxia, the increased release of superoxide from complex III results in the inhibition of prolyl hydroxylases, leading to the subsequent stabilization of HIF α -subunits. While the complete mechanism by which this occurs is not fully known, one hypothesis is that ROS oxidizes intracellular Fe^{2+} , a co-factor required for prolyl hydroxylase function (Sullivan and Chandel 2014). Therefore, mitochondrial ROS is important for the hypoxic activation of HIF transcription factors.

In addition to affecting growth signalling pathways through the PI3K/Akt signalling cascade and hypoxic responses through HIF, ROS can also influence cellular metabolism. Metabolic processes generate ROS as a byproduct, particularly in the mitochondria through the ETC. Therefore, metabolic pathways also need to be appropriately regulated in order to maintain cellular redox homeostasis. ROS can directly influence the activity of proteins involved in glycolysis such as inhibiting

PKM2 activity by oxidizing important cysteine residues. This acts to divert glycolysis and results in increased PPP activity, increased glutathione levels and increased proliferation under hypoxia (Anastasiou et al. 2011). Moreover, ROS-mediated activation of HIF-1 can also result in the expression of glycolytic enzymes and transporters to increase glycolytic flux (Kim et al. 2006), including NADH dehydrogenase (ubiquinone) 1 alpha subcomplex, 4-like 2 (NDUFA4L2), which suppresses complex I activity and mitochondrial ROS (Tello et al. 2011).

1.2.3.3 Antioxidant Pathways Balance ROS

High levels of ROS can cause irreversible oxidative damage to macromolecules such as DNA, proteins and lipids, resulting in the activation of apoptosis. Therefore, it is important for cells to maintain ROS homeostasis for normal cell growth and survival. Protein folding and disulphide bond formation at the ER also generate ROS, which must be counteracted to avoid protein misfolding and ER stress (Malhotra and Kaufman 2007). Excessive levels of ROS are lowered through the regulation of ROS-generating proteins as well as utilizing ROS-scavenging systems.

As mentioned previously, the SOD proteins (SOD1-3) convert superoxide into hydrogen peroxide. Hydrogen peroxide can subsequently be further reduced by antioxidant enzymes such as TRX, GRX and GPX, which utilize reduced glutathione (GSH) generated by glutathione reductase (GSHR), which obtains its equivalents from NADPH oxidation. GPX1 activity can be increased by phosphorylation by c-Abl to protect against high levels of oxidative stress (Cao et al. 2003) and protein thiol oxidation as a consequence of high levels of hydrogen peroxide can be reversed by TRX and GRX in an NADPH-dependent manner (Sabharwal and Schumacker 2014). Both of these systems are expressed independently in the cytosol as well as in the mitochondria, allowing for independent regulatory mechanisms of the redox status in these subcellular compartments (Holmgren 1989) (Figure 1-3).

The major transcriptional response that increases the production of antioxidant and detoxifying proteins is through the activation of the transcription factor nuclear factor (erythroid-derived 2)-like 2 (NRF2). Under basal conditions when ROS

levels are low, NRF2 is kept transcriptionally inactive through binding to its negative regulator Kelch-like ECH-associated protein 1 (KEAP1), which targets NRF2 for proteasomal degradation. During conditions where ROS levels are high, oxidation of specific cysteine residues on KEAP1 results in a disruption in the NRF2-KEAP1 interaction, which leads to NRF2 stabilisation. NRF2 can then bind to antioxidant response elements (ARE) or electrophile response elements (EpRE) on DNA and drive the expression of antioxidant genes involved in the response to oxidative stress (Sporn and Liby 2012). For example, NRF2 can decrease ROS levels and oxidative stress by suppressing the expression of NOS as well as inducing the expression of catalase (Hayes et al. 2010).

Another protein that can contribute to the cellular antioxidant response is DJ-1 (also known as PARK7), which can also stabilize NRF2 and through this, promote the antioxidant response (Clements et al. 2006). Studies on DJ-1 have originally been focused on neurodegenerative disorders, in particular Parkinson's disease, where it is believed that a loss of function results in elevated oxidative stress in the brain and increased neuronal cell death (Kahle et al. 2009).

The distinction and interplay between not just the levels of ROS, but also the source, cytoplasmic or mitochondrial, as well as the type of ROS, whether it is pro-growth or detrimental to cell growth, is important in determining the cellular response to ROS.

1.2.3.4 Adaptation to Oxidative Stress in Cancer Cells

Pre-exposure of normal epithelial cells to low, but continuous levels of oxidants confers a resistance to subsequent exposures to higher levels of oxidative stress, suggesting that cells are able to adapt to oxidative stress (Choi et al. 1997). Similar to normal cells, high levels of oxidative stress are toxic to cancer cells. Due to the proliferative capacity and the altered metabolism of cancer cells, these cells are exposed to constant high levels of endogenous oxidants and elevated levels of oxidative stress have been observed in many cancer cell types (Zhou et al. 2003; Kamiguti et al. 2005). Moreover, increased oxidative stress is correlated with poor prognosis and the aggressiveness of tumours, and studies have shown an increase in oxidative damaged biomolecular compounds such as oxidized DNA

bases (8-oxo-deoxyguanosine) and lipid peroxidation products (Patel et al. 2007; Tsao et al. 2007; Kumar et al. 2008; DeNicola et al. 2011). Therefore, during oncogenic transformation, there is a selective advantage for cancer cells that are able to adjust their redox homeostasis and adapt to this increased oxidative stress (Ogasawara and Zhang 2009).

In cancer progression, several oncogenes have been shown to cause increased ROS production. HRas-transformed cells, which possess increased levels of ROS, also show an elevation in antioxidant proteins such as TRX compared to its non-tumourigenic parental cells (Young et al. 2004). This increased antioxidant capacity allows for the evasion of ROS-induced apoptosis. Furthermore, loss of this antioxidant capacity, such as through glutathione depletion, resulted in ROS accumulation and cell death (Trachootham et al. 2006), illustrating an important pro-survival role for antioxidants. Similarly, studies using inducible c-Myc in melanoma cells showed an increased expression of GSH synthesis enzymes, and downregulation of c-Myc resulted in apoptosis due to a depletion of GSH (Benassi et al. 2006). The ability to suppress ROS is also observed through the activity of sirtuin 3 (SIRT3), an NAD⁺-dependent protein and one of the three mitochondrial sirtuins, which modulates mitochondrial function via the deacetylation of proteins involved in the TCA cycle, the ETC as well as the antioxidant response (Bell and Guarente 2011; Roth and Chen 2014). Human tumours have shown a significant decrease in SIRT3 expression and loss of SIRT3 through genetic knockout resulted in increased levels of mitochondrial ROS, while an overexpression of SIRT3 led to a suppression of mitochondrial ROS (Bell and Guarente 2011; Finley et al. 2011). Furthermore, animal studies using knockout or transgenic overexpression of ROS-scavenging enzymes SOD and GPX have also suggested a potential for these proteins as tumour suppressors (Lu et al. 1997; Egler et al. 2005; Elchuri et al. 2005). Thus, during malignant transformation, oncogenic signalling can promote both ROS generation as well as the systems by which cells use to adapt to and minimize oxidative stress.

In particular, the altered activity of redox-sensitive transcription factors such as NRF2 can also lead to an increased expression of ROS-scavenging proteins such as SOD and GPX, as well as increased levels of antioxidant molecules such as

TRX and GSH (Sporn and Liby 2012). Much like how normal cells activate NRF2 during oxidative stress, cancer cells also promote the NRF2 transcriptional response. This is supported by studies in mouse models of pancreatic cancer and in human pre-invasive pancreatic intraepithelial neoplasia (PanIN) and pancreatic ductal adenocarcinomas (PDAC), where elevated expression of the NRF2 target gene, NAD(P)H:quinone oxidoreductase 1 (*Nqo1*) and decreased markers of oxidative stress were noted in KRas-mutant murine and human PanIN and PDAC (DeNicola et al. 2011). In addition, gain-of-function mutations of NRF2 have also been identified in skin, lung and larynx squamous cell carcinomas (Kim et al. 2010b). These NRF2 mutations result in an inability for KEAP-1, the negative regulator of NRF2, to interact with NRF2 and prevent NRF2 degradation, therefore leading to increased levels of NRF2 protein and activity (Solis et al. 2010). Furthermore, loss of function mutations in KEAP-1 have also been identified in lung, gallbladder, ovary, breast, liver and stomach carcinomas (Singh et al. 2006; Nioi and Nguyen 2007; Ohta et al. 2008; Shibata et al. 2008a; Shibata et al. 2008b; Konstantinopoulos et al. 2011; Yoo et al. 2012), all of which result in constitutive NRF2 activity. While the frequency of mutations in NRF2 and KEAP1 are often low compared to oncogenes and tumour suppressors, increased expression of NRF2 and decreased expression of KEAP1 are correlated with poor prognosis (Solis et al. 2010).

However, it is not fully understood whether an elevation in NRF2 can directly promote tumourigenesis or that elevation in NRF2 activity is a consequence of increased stress induced by oncogenes. Evidence suggesting this is a direct consequence of oncogenic signalling arises from the transcriptional induction of NRF2 in mouse models of cancer with the activation of KRas, BRaf or Myc (DeNicola et al. 2011). DJ-1 has also been found to function as an oncogene. In addition to stimulating the PI3K/Akt pathway by regulating the function of PTEN (Kim et al. 2005), DJ-1 can also promote tumourigenesis by lowering oxidative stress caused by aberrant cell proliferation by stabilizing NRF2 and promoting its antioxidant activities (Clements et al. 2006). Furthermore, the high expression of DJ-1 found in cases of lung, ovarian and oesophageal cancers has been correlated with poor outcome (Kim et al. 2005; Davidson et al. 2008; Yuen et al. 2008). While these adaptive mechanisms keep ROS levels within a range that

allows cancer cells to escape severe oxidative damage and survive periods of stress, increased levels of mitochondrial ROS generated by cancer cells can also further promote cancer cell transformation by causing genomic instability (Sullivan and Chandel 2014).

By targeting mitochondrial DNA (mtDNA), mitochondrial ROS can lead to genomic instability and further mutations, which can subsequently lead to further metabolic malfunction, oxidative stress and cancer cell proliferation. As mtDNA is not protected by histones, the rate of mitochondrial mutations is much greater than nuclear DNA. When a mutation arises, it can be passed to daughter cells along with normal mtDNA, resulting in a state of heteroplasmy. Heteroplasmic mutations have been found particularly enriched in tumours compared to normal tissue and seem to confer a selective advantage during tumourigenesis (Larman et al. 2012). For example, heteroplasmic mutations in the complex I subunit NADH dehydrogenase subunit 6 increase the metastatic potential of cells through an increased production of mitochondrial ROS alongside an activation of HIF-1 (Ishikawa et al. 2008). This activity was inhibited following treatment with the antioxidant N-acetyl cysteine (NAC). Moreover, heterozygosity for mitochondrial transcription factor A (TFAM A) resulted in a mitochondrial ROS-dependent increase in intestinal tumourigenesis in an *Apc^{min/+}* mouse model of cancer (Woo et al. 2012). In addition, these animals were then bred with transgenic mice that overexpress catalase targeted to the mitochondrial matrix and showed fewer intestinal polyps alongside a decrease in mitochondrial ROS. However, in contrast to this study, a complete loss of TFAM A inhibited tumour formation in a mouse model of KRas-driven lung cancer (Weinberg et al. 2010). This shows that, while low levels of heteroplasmic mutations can promote cancer cell growth, increased levels of heteroplasmic or homoplasmic mutations in mtDNA can impair overall cell metabolism and therefore decrease tumour progression.

Mutations in mtDNA can also affect mtDNA-encoded TCA cycle enzymes such as SDH and FH, which have both been reported mutated in a variety of human tumours (Sudarshan et al. 2009; Dahia 2014). Loss of FH leads to an accumulation of fumarate, which succinates the thiol residue on intracellular glutathione resulting in the production of succinated glutathione (GSF). This

process consumes NADPH, and thus, GSF lowers overall NADPH levels leading to increased mitochondrial ROS levels and HIF-1 stabilization (Sullivan et al. 2013). Moreover, FH-deficient cells also show an elevated expression of NRF2 due to the succination and inactivation of KEAP1 as a consequence of increased levels of fumarate. This indicates that FH-deficient cells upregulate NRF2 in order to suppress fumarate-mediated ROS production and to maintain favourable conditions for cell proliferation (Adam et al. 2011; Ooi et al. 2011; Sullivan et al. 2013).

1.3 The p53 Family in Metabolic Regulation

1.3.1 p53 and Cancer Metabolism

1.3.1.1 The Structure and Regulation of p53

The p53 transcription factor is most well known for its role as a tumour suppressor protein through its ability to initiate various cellular responses, including cell cycle arrest, apoptosis and senescence in order to inhibit tumourigenesis. Through this genome guarding function, p53 prevents the accumulation of malignant cells and the maintenance of cell homeostasis (Zuckerman et al. 2009).

The human *p53* gene is located at chromosome 17p13.1 and spans 19,200 base pairs across 11 exons, while the mouse *p53* gene is composed of 12,000 base pairs spanning over 11 exons. p53 possesses two distinct N-terminal transactivation domains (TAD), TAD I and TAD II, both of which interact with the transcription machinery, as well as a proline rich domain, which is required for the transactivation of certain target genes (Venot et al. 1998; Venot et al. 1999) (Figure 1-4). The DNA-binding domain confers sequence-specific binding activity to promoters of p53 target genes possessing a p53 response element (p53RE) (el-Deiry et al. 1992). Furthermore, p53 contains five conserved boxes, which are regions of high conservation across species, and conserved box I is required for interaction with the ubiquitin ligase mouse double minute 2 (MDM2) that acts as a p53 regulator (Chen et al. 1993) (Figure 1-4). p53 also possesses a nuclear localization signal (NLS) and a nuclear export signal (NES), which allow the protein to shuttle in and out of the nucleus (Shaulsky et al. 1990), and forms a tetrameric complex out of two homodimers via its tetramerisation domain in order

to become a fully active transcription factor (Clore et al. 1995). Finally, the C-terminus of p53 contains regulatory domains, which are available for posttranslational modifications.

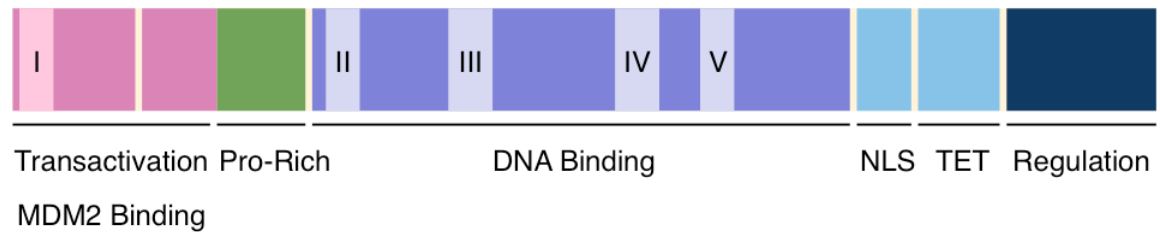


Figure 1-4 Structure of full-length p53

The domains of the full-length p53 protein include the transactivation domain, proline-rich domain, DNA binding domain, nuclear localization signal (NLS), tetramerisation domain (TET) and C-terminal regulatory domain. The MDM2 binding site is found in the transactivation domain and I-V indicate the conserved boxes.

While most studies have focused on the full-length p53 protein (FLp53), multiple other p53 isoforms have also been described. Originally, one promoter and three mRNA splice variants were discovered for p53, which encode for FLp53, p53 β (also known as p53i9) (Chow et al. 1993; Flaman et al. 1996) and Δ 40p53 (also known as Δ Np53) (Yin et al. 2002; Ghosh et al. 2004). The variant p53 β is encoded by alternative splicing of intron 9, leading to a p53 isoform deleted of the last 60 amino acids, consequently lacking the regulatory and tetramerisation domain and therefore, defective in transcriptional activity (Chow et al. 1993; Flaman et al. 1996). In contrast, as a consequence of alternative splicing in intron 2 or through an alternative initiation site of translation, Δ 40p53 is an amino-terminally truncated p53 isoform lacking the first 40 amino acids. The Δ 40p53 isoform retains TAD II and is therefore still able to activate gene expression. However, the activity of this isoform results in an inhibition of wild-type p53 transcription as well as apoptosis (Ghosh et al. 2002; Yin et al. 2002; Ghosh et al. 2004; Murray-Zmijewski et al. 2006). Moreover, this isoform lacks the MDM2-binding N-terminal and is therefore, not targeted by MDM2 for proteasomal degradation (Ghosh et al. 2004).

It is now understood that transcription of the *TP53* gene can also be initiated from two distinct sites upstream of exon 1 as well as from an internal promoter in intron 4 (Bourdon et al. 2005). Transcription from the alternative promoter leads to the expression of an N-terminally truncated p53 initiated at codon 133 ($\Delta 133p53$), which lacks both TADs as well as part of the DNA-binding domain and is therefore unable to induce p53 target genes. In contrast, $\Delta 133p53$ was found to inhibit wild-type p53 activity, particularly p53-mediated apoptosis (Bourdon et al. 2005). Furthermore, this isoform has been found to promote angiogenesis and tumourigenesis (Bernard et al. 2013). Translation of the $\Delta 133p53$ mRNA transcript can also be initiated at an alternative start site (ATG at codon 160) resulting in an even shorter $\Delta 160p53$, which lacks the first 160 amino acids (Marcel et al. 2010). Intron 9 can also be alternatively spliced to produce three isoforms, p53, p53 β and p53 γ , where p53 γ , much like p53 β , lacks the regulatory and oligomerisation domains. Finally, these C-terminal alternative splice events can occur concurrently with N-terminal deletions, giving rise to a further 12 potential p53 isoforms (Bourdon et al. 2005).

Amongst all these p53 isoforms there are various activities. While full-length p53 has a higher affinity towards the p21 and MDM2 promoters, p53 β binds preferentially to p53-responsive p21 and Bax promoters (Bourdon et al. 2005). Furthermore, p53 β can form a complex with full-length p53, specifically enhancing p53 transcriptional activity at the Bax promoter and increase p53-mediated apoptosis. In contrast, co-transfection of p53 with $\Delta 133p53$ strongly inhibits p53-mediated apoptosis (Bourdon et al. 2005). Altogether, this suggests a complex balance between the various p53 isoforms in order to regulate the cellular response to p53 activation.

In addition to the isoforms described above, the *p53* gene also contains a common single nucleotide polymorphism (SNP) within the proline-rich domain at codon 72, which can encode for a proline or an arginine residue. While both variants are common, this SNP influences the transcriptional output of p53 (Puente et al. 2006; Whibley et al. 2009). For example, peptidyl-prolyl cis-trans isomerase (PIN1) binds to the proline-rich domain of p53 and preferentially to the R72 variant (Mantovani et al. 2007). Moreover, the P72 variant shows increased binding to the anti-

apoptotic inhibitor of apoptosis-stimulating protein of p53 (iASPP) compared to R72, making the R72 variant of p53 a more potent inducer of apoptosis (Bergamaschi et al. 2006).

During unstressed conditions, p53 is regulated via protein turnover, mainly by the ubiquitin E3 ligase MDM2, which itself is a p53 target gene resulting in a negative feedback loop (Haupt et al. 1997; Honda et al. 1997; Kubbutat et al. 1999). MDM2 constantly ubiquitinates newly synthesized p53 protein under unstressed conditions, which targets it for proteasomal degradation, thereby keeping basal levels of p53 low. This is particularly notable in MDM2-deficient mice, which are embryonic lethal due to elevated levels of p53 leading to apoptosis (Jones et al. 1995; Montes de Oca Luna et al. 1995). Moreover, this phenotype can be rescued with a simultaneous loss of p53 in these animals. MDM2 modifies multiple lysine residues on p53 using the small protein ubiquitin through facilitating the formation of an isopeptide bond between the ϵ -group of the target lysine residue and the C-terminal glycine residue of ubiquitin downstream of the 3-enzyme cascade of protein ubiquitination (Rodriguez et al. 2000; Chan et al. 2006; Shloush et al. 2011).

MDM2 belongs to a family of RING finger ligases where the RING domain is crucial for the catalytic activity of MDM2 by directly contacting the ubiquitin-conjugating E2 enzyme (Budhidarmo et al. 2012). The MDM2 RING domain is located in the C-terminus and mutations disrupting the RING structure abrogate its ability to ubiquitinate p53 (Fang et al. 2000). Animals with a knock-in amino acid substitution in the RING domain are embryonic lethal due to elevated levels of p53 resulting in apoptosis, much like observed in animal models of a complete MDM2 knockout (Itahana et al. 2007). In addition to targeting p53 for degradation, MDM2 can also block p53 TADs and thereby inhibit the induction of p53 target genes (Momand et al. 1992; Oliner et al. 1993). The central domain of MDM2, while not involved in the catalytic activity of MDM2, can also serve as a secondary contact point with the core domain of p53 (Kulikov et al. 2006; Wallace et al. 2006) and also plays a role in p53 degradation (Kawai et al. 2003; Meulmeester et al. 2003). Furthermore, this central domain also functions as a platform for binding MDM2-interacting proteins such as p14^{ARF} and L11, which can inhibit the ubiquitin ligase

activity of MDM2 (Sdek et al. 2004). A stretch of amino acids in the extreme C-terminus of MDM2 is also important for MDM2 dimerisation (Poyurovsky et al. 2007; Uldrijan et al. 2007; Linke et al. 2008). RING finger ubiquitin ligases generally function as a dimer and MDM2 is only functional when present as a homodimer with itself or its closely related protein MDMX (also known as MDM4) through interactions between their RING domains (Tanimura et al. 1999). While MDMX possesses a RING finger and a similar p53-binding domain to MDM2, it possesses no ubiquitin ligase activity. Despite this, MDMX knockout mice are embryonic lethal, much like the MDM2 knockout mice, and can also be rescued with a simultaneous loss of p53 (Parant et al. 2001; Migliorini et al. 2002). Interestingly, the MDM2-MDMX heterodimer shows greater ubiquitin ligase activity towards p53 compared to the more stable MDM2 homodimer (Kawai et al. 2007), and it was later found that MDMX negatively regulates p53 by promoting MDM2 ubiquitin ligase activity (Badciong and Haas 2002; Linares et al. 2003; Wang et al. 2007b). MDM2 is also able to promote a negative feedback loop by ubiquitinating itself as well as its binding partner MDMX (Honda and Yasuda 2000; de Graaf et al. 2003; Pan and Chen 2003).

MDM2 targets p53 at all C-terminal lysine residues for modification by ubiquitin and mutations of all these residues to an arginine (6KR) results in a blockage of p53 degradation by MDM2 despite still being ubiquitinated *in vitro* (Rodriguez et al. 2000). Moreover, mice with this mutant p53 did not present a more stable p53 protein (Feng et al. 2005; Krummel et al. 2005), suggesting that ubiquitin modification of p53 is not limited to these C-terminal lysine residues. Lysine residues found in the DNA binding domain as well as the tetramerisation domain of p53 can also be ubiquitinated by MDM2 (Chan et al. 2006; Shloush et al. 2011).

These lysine residues can also be altered by other posttranslational modifications such as acetylation and methylation. Acetylation of p53 predominantly occurs at lysine residues, where acetyl groups can be conjugated to either the N-terminal amino groups or Σ -amino groups in the C-terminus and the main histone acetyltransferase that acts to acetylate p53 is cAMP response element-binding protein (CREB) binding protein/p300 (CBP/p300) (Tang et al. 2008). Acetylation of lysine residues 373 and 382 is induced upon DNA damage and results in an

overall enhanced sequence-specific DNA-binding of p53 to its target genes (Gu and Roeder 1997; Ito et al. 2001). Acetylation can also enhance p53 protein stability by blocking MDM2-mediated ubiquitination (Li et al. 2002). On the other hand, upon DNA damage, lysine 372 can also be methylated by the methyltransferase Set9, leading to increased activation of p21 (Chuikov et al. 2004). Three arginine residues in the tetramerisation domain of p53 can be methylated by protein arginine methyltransferase 5 (PRMT5) in response to DNA damage, which contributes to the activation of a number of p53 target genes including p21 and PUMA (Jansson et al. 2008).

1.3.1.2 Activation of the p53 Stress Response

As part of the cellular response to stress, p53 is activated by numerous intrinsic and extrinsic stress signals including DNA damage, proto-oncogene activation, and nutrient or oxygen deprivation, which result in a rapid stabilization of the p53 protein. In addition to acetylation and methylation, posttranslational modifications of both p53 and MDM2 by phosphorylation can regulate their interaction in order to influence the p53 response.

DNA damage activates stress-induced kinases, which phosphorylate the N-terminus of p53 at residues important for its interaction with MDM2 (Siliciano et al. 1997). One such kinase, ataxia telangiectasia mutated kinase (ATM), is activated in response chromatin alterations, which are a consequence of DNA strand breaks induced by ionizing radiation (Bakkenist and Kastan 2003). Serine residues can also be phosphorylated by ataxia telangiectasia and Rad3 related kinase (ATR) (Tibbetts et al. 1999), which is activated by replication blockage and stalled replication forks. Both ATM and ATR can activate kinases further downstream involved in p53 phosphorylation. ATM phosphorylates and activates checkpoint kinase 2 (Chk2) (Matsuoka et al. 2000), which in turn can phosphorylate p53 (Chehab et al. 2000; Hirao et al. 2000), while ATR can phosphorylate and activate checkpoint kinase 1 (Chk1), and consequently also result in p53 phosphorylation and MDM2 dissociation (Shieh et al. 2000). While phosphorylation of MDM2 does not affect its interaction with p53, ATM- and ATR-induced phosphorylation of MDM2 results in an inhibition of MDM2-driven nuclear export of p53 (Khosravi et al. 1999; Maya et al. 2001; Shinozaki et al. 2003). Moreover, MDM2

phosphorylation by ATM can also disrupt the dimerisation of MDM2 RING domains (Cheng et al. 2009).

In addition to DNA damage, activation of proto-oncogenes such as Myc and Ras also triggers p53 activation, through an upregulation in p14^{ARF} expression, which serves as an inhibitor of MDM2 activity (Palmero et al. 1998; Pomerantz et al. 1998; Zindy et al. 1998). Moreover, ribosomal stress releases ribosomal proteins such as L11 (Lohrum et al. 2003; Zhang et al. 2003) and L23 (Dai et al. 2004; Jin et al. 2004), which can inhibit the ubiquitin ligase activity of MDM2. Furthermore, metabolic stress such as glucose starvation can also activate p53 through phosphorylation by AMPK (Imamura et al. 2001). This is also observed under hypoxia, where p53 expression is elevated potentially through a downregulation of MDM2 (Alarcon et al. 1999) or phosphorylation by ATR (Hammond et al. 2002).

Clearly, p53 can be activated via many mechanisms. However, the outcome of the p53 transcriptional response is highly dependent on the context of the cellular situation as well as the extent and duration of the stress. During periods of transient or mild-stress, which cells are able to resolve, p53 activation promotes the necessary pathways to induce cell repair as opposed to apoptosis. It can do so by inducing as well as repressing genes involved in cell cycle checkpoints as observed when the DNA template replicate contains errors or when chromosomes are damaged. Cell cycle arrest allows for DNA repair to occur in order to prevent an accumulation of damaged cells. While there are many p53-target genes which induce cell cycle arrest, the most prominent p53-target gene contributing to cell cycle arrest is the cyclin-dependent kinase (CDK) inhibitor p21 (also known as CIP1 and WAF1) (el-Deiry et al. 1993; Harper et al. 1993), which functions by inhibiting the G1/S specific kinases CDK2, 3, 4, and 6 (Harper et al. 1995). This prevents the hyperphosphorylation of RB and thus, cell cycle progression to S-phase.

In contrast, prolonged or severe stress, which cells are unable to resolve, leads to the activation of p53 and its target genes that initiate cell death programmes in order to eliminate cells from transformation due to proto-oncogene activation or DNA damage. Such apoptosis eliciting p53 target genes include the pro-apoptotic Bcl-2 family member Bcl-2 associated X protein (BAX), which locates to the outer

mitochondrial membrane where it triggers the collapse of the mitochondrial membrane potential and the release of cytochrome c into the cytoplasm (Miyashita and Reed 1995). Cytochrome c then forms the apoptosome together with apoptotic protease activating factor 1 (APAF1), inducing the apoptotic initiator caspase 9, which cleaves and activates effector caspases. p53 can also induce the transcription of the Bcl-2 homology domain 3 (BH3)-only proteins PUMA (Nakano and Vousden 2001) and Noxa (Oda et al. 2000), which also causes the release of cytochrome c by binding to anti-apoptotic Bcl-2 and activating BAX and Bak (Gallenne et al. 2009; Dai et al. 2011). Alongside this, ROS can also contribute to p53-induced apoptosis through an upregulation of p53 inducible gene 3 (PIG3), which encodes an NADPH-dependent reductase that generates ROS as part of the mitochondrial disassembly in apoptosis (Contente et al. 2002). PIG6 encodes a proline oxidase, which also produces a pro-apoptotic ROS (Rivera and Maxwell 2005), and p53 is also able to repress NRF2-induced antioxidant genes such as Glutathione S-transferase (GST- α 1) and NQO1 (Faraonio et al. 2006).

Along side, cell cycle arrest and apoptosis, p53 can also trigger senescence an irreversible G1 cell cycle arrest that halts the growth of damaged cells. To induce senescence following DNA damage, proto-oncogene activation or telomere shortening, p16^{INK4A} and p21 inhibit CDKs to prevent the hyperphosphorylation of RB, thereby inhibiting the activity of E2F transcription factors and cell cycle progression (Serrano et al. 1997). In addition to these tumour suppressive functions, p53 contributes to the suppression of angiogenesis by mediating the production of anti-angiogenic factors such as thrombospondin 1 (Dameron et al. 1994) and can induce the expression of prolyl hydroxylases, which cleave collagen and leads to the release of anti-angiogenic collagen 4 and 18 fragments (Teodoro et al. 2006). p53 can also repress the invasive phenotype observed in cancer cells. The expression of CD82 (also known as KAI-1), a cell surface glycoprotein involved in cell-to-cell and cell-to-ECM interactions is increased by p53 (Mashimo et al. 1998), as well as the expression of macrophage inhibitory cytokine (MIC-1), which can also inhibit cell movement (Cheng et al. 2011).

Another one of the hallmarks of cancer that p53 is able to influence is cellular metabolism. In particular, p53 is able to counter the metabolic changes, which drive the Warburg effect, and this will be discussed in greater detail below.

As p53 poses a major barrier during cancer cell transformation, p53-deficient mice can show normal development but are prone to the development of spontaneous neoplasms (Donehower et al. 1992). Somatic mutations in the *p53* gene are frequent in most human cancers, ranging from 5 to 80% depending on the type, stage, and aetiology of tumours, with the majority of cases (50%) showing inactivating mutations in the coding sequence of p53 (Petitjean et al. 2007). Whilst most cancer patients harbour somatic p53 mutations, patients who carry germline p53 mutations present an increased risk of tumour development, particularly sarcomas and leukaemia, in a syndrome known as Li-Fraumeni (Malkin et al. 1990). Most p53 mutations are missense mutations resulting in the expression of a full-length p53 with a single amino acid exchange, predominantly in the DNA binding domain (Soussi and Lozano 2005; Petitjean et al. 2007). These mutants can be separated as amino acids directly contacting the DNA (such as R248 and R273) and amino acids important in p53 conformation (such as R175, G245 and R282) (Cho et al. 1994). This disrupts p53-specific binding to DNA resulting in a loss of wild-type p53 transcriptional activity and can also lead to pro-tumorigenic gain of function. Furthermore, mutant forms of p53 are often overexpressed in tumours (Iggo et al. 1990), suggesting that mutant p53 is a far more stable protein than wild-type p53. While the mechanism for this is not fully understood, it is hypothesized that much like wild-type p53, mutant p53 can be stabilized during cell stress, which is highly prevalent in tumour cells and their microenvironment (Lang et al. 2004).

1.3.1.3 The Role of p53 in Metabolism

While the various tumour suppressive activities of p53 play an important role in protecting against tumourigenesis, there is now interest in the activities of p53 in regulating metabolism and providing cells the means to survive modest or transient periods of metabolic stress (Li et al. 2012a; Jiang et al. 2015). In particular, transient metabolic stresses can trigger a p53-mediated adaptive

response to induce metabolic remodeling as well as a decrease in proliferation and cell growth.

p53 plays a complex but important role in the regulation of several metabolic pathways. Like other cellular stress signals, metabolic stress can activate p53 through cellular metabolic sensors. In line with responding to conditions of limited nutrient availability, p53 is able to modulate growth signalling pathways such as the IGF-1/Akt/mTOR pathway, which results in limiting cell growth and division as well as energy consumption under conditions where this is detrimental. As mentioned previously, the upstream activation of AMPK during low energy levels can lead to p53 activation (Imamura et al. 2001; Jones et al. 2005) (Figure 1-5). In addition, p53 can activate AMPK by driving the expression of sestrins (Sestrin 1 and 2), which can activate AMPK and inhibit mTORC1 (Budanov and Karin 2008). Other negative regulators of mTORC1 signalling that p53 can influence include IGF-binding protein 3 (IGF-BP3), PTEN and TSC2 (Feng et al. 2007; Matthew et al. 2009). IGF-BP3 is able to bind to IGF-1 and prevent it from binding to its receptor, thereby inhibiting the IGF-1/Akt/mTOR signalling pathway, while PTEN inactivates Akt, thus resulting in decreased activation of PDK1 and mTORC2. Moreover, loss of Akt activity also promotes the activity of the mTORC1 negative regulators, TSC1/TSC2, which can also be directly induced by p53 (Figure 1-5). In order to modulate cellular homeostasis, mTOR itself can also influence p53 activity when cell growth and proliferation is viable. Survival signalling via the Notch1 receptor, which activates mTORC1 via the PI3K/Akt signalling cascade, promotes eIF4a-mediated inhibition of p53 (Mungamuri et al. 2006). In contrast, mTORC1 can also drive p53 expression by increasing the expression of p14^{ARF}, which inhibits MDM2, thus stabilizing p53 protein levels (Miceli et al. 2012).

The mTOR pathway is also a major contributor to the regulation of autophagy, a catabolic process where autophagosomes form around cytoplasmic cellular components that have been targeted for degradation. Once enclosed, autophagosomes fuse with lysosomes resulting in autolysosomes and are able to catabolize their contents. This process promotes normal cell homeostasis by removing aged or dysfunctional organelles and proteins as well as the release of nutrients from these degraded biomolecules. Autophagy is particularly upregulated

during cell stress such as nutrient deprivation (Mordier et al. 2000) but has also been implicated in various diseases including cancer (Rubinsztein et al. 2012).

p53 is able to both promote and inhibit autophagy depending on the circumstances (Morselli et al. 2009; Maiuri et al. 2010). By negatively regulating mTORC1, p53 is able to activate autophagy and many direct p53 target genes are able to promote autophagy independent of mTORC1 such as the lysosomal DNA-damage regulated autophagy modulator 1 (DRAM-1) (Crighton et al. 2006). While autophagy can promote cell survival by recycling non-essential cell components during nutrient deprivation, DRAM-mediated autophagy was found to contribute to the p53-mediated apoptosis (Crighton et al. 2007). Moreover, the p53 target PUMA can induce mitochondrial autophagy (mitophagy) in a Bax-dependent manner (Yee et al. 2009) and p53-mediated expression of etoposide-induced protein 2.4 homolog (Ei24) was found essential in the basal autophagic response in neurons and hepatocytes for the clearance of aggregate-prone proteins, and its regulation by p53 under normal conditions, suggests a homeostatic role for p53 in promoting autophagy (Zhao et al. 2012). Autophagic proteins can also promote p53 activity. Autophagy-related protein 7 (ATG7) can increase p53-dependent transcription of p21, and through this, promote cell cycle arrest and survival during periods of nutrient deprivation. While basal levels of autophagy have a tumour suppressive function, stress-induced autophagy can provide a pro-survival role for tumour cells during metabolic stress (Morselli et al. 2009), as observed in Myc-driven lymphomas where inhibition of p53-induced autophagy resulted in tumour regression (Amaravadi et al. 2007; Maclean et al. 2008).

Alongside the modulation of growth signalling pathways during metabolic stress, p53 is also able to influence proteins directly involved in metabolic pathways. Several studies have shown that p53 can regulate glycolysis, oxidative phosphorylation as well as the pentose phosphate pathway (PPP). ATP and ADP can directly alter p53 activity, with ADP promoting and ATP inhibiting the ability of p53 to bind DNA (Okorokov and Milner 1999). p53 can also exert its tumour suppressive function by counteracting the increase of glycolytic flux observed in cancer cells by influencing the expression of nutrient transporters such as decreasing the expression of glucose transporters, GLUT1 and GLUT4, in order to

lower glucose uptake (Schwartzberg-Bar-Yoseph et al. 2004). p53 is also able to repress the expression of monocarboxylate transporter 1 (MCT1) to prevent the efflux of lactate under hypoxic conditions, resulting in the lowering of glycolytic rates (Boidot et al. 2012) (Figure 1-5).

Moreover, p53 can influence the expression of metabolic enzymes involved in central carbon metabolism. In fibroblasts, p53 can repress the expression of phosphoglycerate mutase (PGAM), the enzyme responsible for the conversion of 3-phosphoglycerate to 2-phosphoglycerate during glycolysis (Kondoh et al. 2005). p53 is also able to negatively regulate the expression of pyruvate dehydrogenase kinase 2 (PDK2), which inactivates pyruvate dehydrogenase (PDH) (Contractor and Harris 2012) (Figure 1-5). Through this mechanism, p53 promotes the production of acetyl-CoA rather than lactate from pyruvate. While it seems that p53 lowers glycolysis, some activities of p53 seem to contradict this, suggesting tissue- and context-dependent manners of regulation. A muscle specific isoform of PGAM is transcriptionally activated by p53 in cardiomyocytes (Ruiz-Lozano et al. 1999). Greater complexities in p53-mediated regulation of cell metabolism can be observed in the PPP where p53's activities vary dependent on the type of stress. While p53 can inhibit the diversion of glycolytic intermediates into the PPP by binding and inhibiting G6PDH (Jiang et al. 2011), *TP53*-induced glycolysis and apoptosis regulator (TIGAR) acts to promote the PPP by indirectly altering the activity of PFK-1 (Bensaad et al. 2006). The role of TIGAR, particularly during oxidative stress, will be further discussed in detail in the following chapters.

The inhibition of glycolytic flux is paralleled by the ability of p53 to promote OXPHOS and the maintenance of mitochondrial health. The ability to increase the rate of TCA cycle activity is reflected in p53's ability to promote glutamine utilization by transcriptionally activating glutaminase 2 (GLS2) (Hu et al. 2010; Suzuki et al. 2010), which catalyzes the hydrolysis of glutamine to glutamate and consequently be converted to α -KG, which can feed into the TCA cycle. p53 can repress the expression of malic enzymes, ME1 and ME2, which recycle malate to pyruvate and consequently direct TCA metabolites into biosynthetic pathways (Jiang et al. 2013) (Figure 1-5). p53 can also induce the expression of synthesis of cytochrome c oxidase 2 (SCO2), a key component for the assembly of the

cytochrome c oxidase (COX) complex, making up complex IV in the mitochondrial ETC in the mitochondria (Matoba et al. 2006). Furthermore, p53 can promote mitochondrial health and maintenance such as through the expression of ribonucleotide reductase subunit p53R2 whose activity is required for the stability of mitochondrial DNA (Bourdon et al. 2007; Kulawiec et al. 2009). Moreover, p53 can promote the clearance of damaged mitochondria through mitophagy by promoting the expression of mitochondria-eating protein (Mieap) (Kitamura et al. 2011).

Amino acids can also support cell survival and cell growth, and p53 can function to help cells survive serine and glutamine starvation by inducing p21-mediated cell cycle arrest (Maddocks et al. 2013; Reid et al. 2013). Rapidly proliferating cells possess a high requirement for serine, which can be synthesized *de novo* or taken up extracellularly for protein synthesis as well as the production of anabolic intermediates including nucleotides, NADPH and GSH (Locasale et al. 2011; Labuschagne et al. 2014). Upon serine starvation, PKM2 activity is decreased which facilitates the diversion of glycolytic intermediates into the *de novo* serine synthesis pathway (SSP) (Chaneton et al. 2012). In order to balance the subsequent decrease in energy production as a consequence of this diversion in glycolytic flux, there is an increased rate of OXPHOS, which in turn generates higher levels of ROS. In order to ensure cellular adaptation to serine deprivation, the p21-mediated cell cycle arrest induced by p53 as well as the inhibition of nucleotide synthesis allow for a sustained generation of GSH to combat this increased oxidative stress (Maddocks et al. 2013). Normally, these adaptations are reversed when the synthesis of *de novo* serine has restored the levels of intracellular serine. However, cells lacking p53 continue to support nucleotide synthesis, undergo oxidative stress and eventually cell death. In this context, p53 can be beneficial for cancer cells by supporting their survival under serine-deficient conditions. p53 can also inhibit cystine uptake and sensitize cells to ROS-induced ferroptosis, a non-apoptotic form of cell death, by repressing expression of *SLC7A11*, a key component of the cystine/glutamate antiporter (Jiang et al. 2015).

Alongside carbon metabolism, p53 can also function as a regulator of lipid metabolism. As a tumour suppressor protein, p53 generally functions as a

negative regulator of lipid synthesis by promoting fatty acid oxidation and animals deficient in p53 show enhanced lipid accumulation (Wang et al. 2013). Moreover, activated p53 inhibits the induction of adipocyte differentiation in mouse embryonic fibroblasts (Molchadsky et al. 2008). Lipid metabolism itself is associated with glycolysis and the PPP, both of which supply the necessary components needed for lipid synthesis and is therefore also regulated by mTOR. Therefore, by influencing mTOR activity, p53 is able to affect lipid metabolism. In addition, p53 is able to directly induce the expression of proteins involved in lipid metabolism such as carnitine acetyltransferases, which act to transport fatty acids into the mitochondria for fatty acid oxidation (Zaugg et al. 2011) as well as transcription factors involved in lipid homeostasis such as sterol regulatory element-binding protein 1 (SREBP), an important transcription factor involved in fatty acid synthesis. By suppressing the expression of the SREBP1c isoform in mouse adipose tissue, p53 is able to repress the expression of fatty acid synthase (FASN), acetyl-CoA carboxylase (ACC) and ATP citrate lyase (ACLY) (Yahagi et al. 2003; Yahagi et al. 2004). Following glucose starvation, p53 is able to induce the expression of guanidinoacetate methyltransferase (GAMT), an enzyme involved in creatine synthesis, which promotes fatty acid oxidation (Ide et al. 2009).

By regulating carbohydrate and lipid metabolism, p53 is also able to regulate ROS levels in order to either promote the removal of damaged cells that have suffered sustained oxidative stress, or limit levels of ROS in order to lower oxidative stress and consequently, potential cell damage. By driving the expression of TIGAR and promoting PPP activity, p53 can increase the production of NADPH, which can be used to generate the cellular antioxidant GSH (Bensaad et al. 2006). Moreover, at the expense of nucleotide synthesis, p53 can also promote GSH synthesis following serine starvation, thereby lowering ROS levels during metabolic stress (Maddocks et al. 2013). As previously mentioned, mitochondria are major generators of ROS. Therefore, by maintaining mitochondrial integrity, p53 can also limit ROS production. In addition, p53 can promote the transcription of antioxidant genes such as the sestrin family of proteins (Budanov and Karin 2008), aldehyde dehydrogenase 4 (ALDH4) (Yoon et al. 2004) and tumour protein p53-induced nuclear protein 1 (TP53INP1) (Cano et al. 2009). Moreover, p53 can repress the expression of pro-oxidant genes such as nitric oxide synthase 2 (NOS2) (Ambs et al. 1998) and cyclooxygenase 2 (COX2) (Subbaramaiah et al. 1999).

However, if the damage caused by oxidative stress is too prevalent, p53 must induce apoptosis in order to eliminate these cells. To achieve this, p53 promotes a pro-oxidant state by inducing the expression of pro-oxidant genes such as PIG6 as well as ferredoxin reductase (Liu and Chen 2002; Rivera and Maxwell 2005). Under these conditions, p53 can inhibit antioxidant functions such as directly inhibiting the activity of G6PDH (Jiang et al. 2011) and repressing the expression of malic enzymes (Jiang et al. 2013) and manganese superoxide dismutase (MnSOD) (Zhao et al. 2005). Moreover, p53 can activate necrosis in response to oxidative stress by accumulating in the mitochondrial matrix and triggering the opening of the mitochondrial permeability transition pore (PTP) through interaction with the PTP regulator cyclophilin D, resulting in mitochondrial rupture (Vaseva et al. 2012).

The interaction between p53 and NRF2, a regulator of the cellular oxidative stress response, can also influence the outcome of the response to ROS levels. p53 can both enhance and repress NRF2 activity depending on the context. Low levels of p53 enhance NRF2 protein levels by promoting the expression of p21, which acts

to stabilize NRF2 by binding to its negative regulator KEAP and thus, promote cell survival (Chen et al. 2009). In contrast, scenarios of high stress result in the inhibition of NRF2 by p53 to promote ROS-induced apoptosis (Chen et al. 2012).

Taken together, p53 acts to balance cell metabolism to allow for homeostatic cell growth by allowing efficient energy production while maintaining basal anabolic pathways. Through this regulation, p53 can also play a tumour suppressive role as loss of p53 has been implicated in contributing to the acquisition of the Warburg phenotype observed in cancer cells.

1.3.2 p63 and Cancer Metabolism

The p53 family of transcription factors also includes two p53-related proteins called p63 and p73, which are homologues of p53 consisting of high structural and functional similarities (Kaghad et al. 1997; Yang et al. 1998) and both are capable of inducing certain p53 targets but also possess specific targets in unique roles such as development.

1.3.2.1 The Structure and Function of p63

The human *p63* gene is composed of 15 exons, located on chromosome 3q27, while mouse *p63* gene is composed similarly of 15 exons located on chromosome 16 (Schmale and Bamberger 1997; Yang et al. 1998). Transcription of the *p63* gene generates a protein much like p53 possessing an N-terminal transactivation domain, a central DNA-binding domain and a tetramerisation domain with the DNA-binding domain being highly homologous to p53. Both human and mouse *p63* genes can express at least three alternatively spliced C-terminal isoforms (α , β and γ), all of which can be transcribed from an alternative promoter in intron 3. The full-length TAp63 isoforms are generated through a promoter upstream of exon 1, while an alternative promoter results in the expression of N-terminal truncated isoforms lacking the transactivating domain, Δ Np63 (Yang et al. 1998). Altogether, the *p63* gene expresses at least six mRNA variants, encoding for six different p63 protein isoforms (TAp63 α , TAp63 β , TAp63 γ , Δ Np63 α , Δ Np63 β and Δ Np63 γ) (Murray-Zmijewski et al. 2006).

While TAp63 α represents the full-length protein, TAp63 β lacks exon 13, which encodes for the sterile α motif (SAM) domain. TAp63 γ is a smaller isoform as it lacks exons 11, 12, 13 and 14. Furthermore, as the TAp63 α isoform possesses a transcription inhibitory domain, which can fold back and interact with the N-terminal transactivation domain, TAp63 α is less transcriptionally active than TAp63 β or TAp63 γ (Serber et al. 2002). Interestingly, this inhibitory domain can be cleaved by caspases during the cellular stress response (Sayan et al. 2007). TAp63 isoforms are capable of binding to p53 response elements and able to induce p53 targets such as p21 and induce cell cycle arrest (Osada et al. 1998). However, as the TAp63 response element differs slightly from that of p53, TAp63 also possesses its own preferred response element (Osada et al. 2005b; Sasaki et al. 2005). Thus p63-specific target genes were discovered, such as bullous pemphigoid antigen 1 (BPAG1), that are not responsive to p53 (Osada et al. 2005a). While the Δ Np63 isoforms are also able to bind to DNA via p53 response elements, they also possess a distinct set of target genes that are not induced by TAp63 isoforms (Dohn et al. 2001; Wu et al. 2003). Furthermore, Δ Np63 isoforms can lower p53, p63 and p73 activities by competing for DNA binding sites or through direct protein interaction (Benard et al. 2003).

While p63 can exert functions similar to p53 with regard to cell cycle arrest and apoptosis, studies on transgenic mice have shown that p63 plays an essential role in epidermal morphogenesis and limb development (Armstrong et al. 1995; Mills et al. 1999). Animals deficient in p63 only survive a few days after birth and present craniofacial malformations, limb truncations and a failure to develop skin and other epithelial tissues (Yang et al. 1998; Mills et al. 1999). In particular, Δ Np63 is the predominant isoform found in the skin and is crucial for the maintenance of the epidermal stem cell niche as well as the proliferation of committed precursors (Parsa et al. 1999; Senoo et al. 2007). Further transgenic mouse studies have allowed a greater understanding for isoform-specific functions. Animals with an inducible loss of Δ Np63 were viable but showed skin fragility (Koster et al. 2009), while epidermis-specific loss of TAp63 did not result in any abnormalities (Su et al. 2009). Furthermore, isoform-specific reconstitution studies found that Δ Np63 could restore epidermis formation in p63-null animals while the reconstitution of TAp73 was unable to do so (Romano et al. 2009). Whilst most tissues express higher

levels of $\Delta Np63$, oocytes have been shown to highly express TAp63, which protects the female germline by inducing apoptosis following DNA damage (Suh et al. 2006; Livera et al. 2008).

While less severe than the phenotype observed in knockout animals, germ-line mutations in p63 have also been identified in humans and result in rare autosomal dominant developmental diseases, such as ectrodactyly ectodermal dysplasia-clefting (EEC) syndrome which results in hand and feet anomalies and developmental defects of ectodermal-derived structures such as hair, and facial clefts. Notably, EEC syndrome is a result from heterozygous germline missense mutations in the DNA-binding domain of p63, therefore affecting all p63 isoforms (Celli et al. 1999).

In contrast to p53, p63 is rarely mutated in cancer. However, its expression is frequently deregulated (Hagiwara et al. 1999). While some p63 heterozygous mice were cancer prone, mostly squamous cell carcinomas and histiocystic sarcomas (Flores et al. 2005), others have shown p63 heterozygous mice on a different genetic background presented premature ageing but no development of cancer (Keyes et al. 2005). In humans, the p63 gene is often amplified in squamous cells in lung and cervical carcinomas (Wang et al. 2001; Massion et al. 2003), and a number of squamous cell carcinomas of the head and neck express high levels of $\Delta Np63$ (Hibi et al. 2000). Despite this, $\Delta Np63$ amplification has been correlated with good treatment response (Massion et al. 2003). However, it should also be noted that most tumours lose the wild-type p63 allele and loss of p63 is associated with a more invasive phenotype (Barbieri et al. 2006).

1.3.2.2 The Role of p63 in Metabolism

Alongside its ability to regulate known p53 responses, a role for p63 in regulating different aspects of metabolism has also been discovered, particularly with lipid metabolism.

Activation of the mTOR signalling pathway is able to induce the expression of TAp63 and $\Delta Np63$, which signals downstream to activate the Notch signalling pathway in order to influence cell differentiation (Ma et al. 2010). TAp63-deficient

mice develop defects in lipid utilisation, fatty acid oxidation and show insulin resistance and glucose intolerance (Su et al. 2012). Moreover, TAp63 can regulate fat and glucose metabolism by responding to metabolic stress and induce the expression of activate silent information regulator T1 (SIRT1) and AMPK α 2, and LKB1 resulting in increased fatty acid synthesis and decreased fatty acid oxidation (Su et al. 2012). In addition, TAp63 γ levels were elevated in response to metformin and can act to lower blood glucose levels following metformin-induced activation of AMPK α (Su et al. 2012). The induced expression of TAp63 α in Saos-2 cells promoted glycolysis and lowered the channelling of glucose-derived metabolites into the TCA cycle. By doing so, TAp63 α can promote the PPP, which was found uncoupled from nucleotide synthesis, but retained its ability to increase antioxidant defence through the generation of GSH. In addition to this, a link between patient survival rate and the co-expression of p63, G6PDH and phosphogluconate dehydrogenase was observed (D'Alessandro et al. 2014). TAp63 is also able to induce the expression of GLS2 during the *in vitro* differentiation of primary human keratinocytes, and both proteins could be induced in cancer cells upon exposure to oxidative stresses. Furthermore, loss of GLS2 inhibited skin differentiation and sensitized these cells to ROS-induced apoptosis (Giacobbe et al. 2013).

Work on Δ Np63 α using transformed and immortalized epithelial cells showed a transcriptional activation of FASN as well as the maintenance of fatty acid synthesis and fatty acid oxidation (Sabbisetti et al. 2009). Moreover, the expression of both p63 and FASN was positively correlated in clinical squamous cell carcinoma samples (Sabbisetti et al. 2009). In squamous cell carcinoma, Δ Np63 α plays a role in stress-induced autophagy by inducing the expression of several *ATG* family genes as well as miRNAs, which in turn modulate the activity of ATG proteins (Huang et al. 2012). Alongside this, deletion of Δ Np63 can also lead to metabolic reprogramming and regression of p53-deficient tumours via the increased expression of *IAPP*, the gene that encodes amylin, a peptide co-secreted with insulin by pancreatic β -cells. Amylin functions through the calcitonin receptor and receptor activity modifying protein 3 (RAMP3) and lowers glycolysis as well as increases levels of ROS and apoptosis. In addition, the *CYBG* gene, encoding for cytoglobin, a scavenger for nitric oxide as well as other forms of ROS,

was also found to be a transcriptional target of Δ Np63 and in proliferating keratinocytes, Δ Np63 acts to protect against oxidative stress-induced apoptosis through the induction of *CYBG* (Latina et al. 2015). A recent study has also found that Δ Np63 can support aerobic respiration by regulating HK2 expression in epithelial cells (Viticchie et al. 2015).

1.3.3 p73 and Cancer Metabolism

1.3.3.1 The Structure and Function of p73

The mouse and human *p73* genes are both made up of 15 exons located on chromosome 4 and chromosome 1p36.3, respectively. Much like *p63*, the *p73* gene generates a transcription factor highly homologous to p53, particularly in the DNA-binding domain (Melino et al. 2003). Similar to other p53 family members, p73 is subjected to multiple alternative splice events, which give rise to at least seven alternatively spliced C-terminal isoforms (α , β , γ , δ , ϵ , ζ and η) and at least four alternatively spliced N-terminal isoforms.

A promoter upstream of exon 1 generates the transactivating isoforms (TAp73), of which include a full-length TAp73 α isoform and shorter variants lacking various exons (TAp73 β , TAp73 γ , TAp73 δ , TAp73 ϵ and TAp73 ζ) (Kaghad et al. 1997; De Laurenzi et al. 2000; Melino et al. 2002). Alongside this, an alternative promoter found in intron 3 generates the amino-truncated isoforms (Δ Np73 α , Δ Np73 β , Δ Np73 γ , Δ Np73 δ , Δ Np73 ϵ , Δ Np73 ζ and Δ Np73 η), which lack the transactivation domain (Ishimoto et al. 2002). Altogether, the p73 gene expresses at least 35 mRNA variants, which can theoretically encode for 29 different p73 isoforms of which 14 have been described (Murray-Zmijewski et al. 2006).

Similar to p63, full-length p73 also contains a SAM domain, which is only found in the α and ζ isoforms. TAp73 α is less transcriptionally potent than TAp73 β . While the C-terminal of TAp63 α was shown to directly interact with the N-terminal transactivation domain, both the SAM domain and a following inhibitory domain are required to suppress the activity of TAp73 α . However, TAp73 α is still much more efficient at inducing its target genes than TAp63 α , potentially due to differences in their C-terminal inhibitory domains as the inhibitory sequence found

in the C-terminus of TAp63 α is not present in TAp73 α (Liu and Chen 2005; Straub et al. 2010).

The TAp73 isoforms can bind specifically to DNA through p53 response elements and activate the transcription of known p53-target genes such as p21 and PIG3 (Jost et al. 1997; Zhu et al. 1998; Lee and La Thangue 1999) to induce cell cycle arrest, senescence and apoptosis. The Δ Np73 isoforms bind DNA through p53 response elements to exert inhibitory effects over p53, p63 and p73 activities, and are also able to directly activate the expression of genes not induced by TAp73 isoforms (Liu et al. 2004; Liu and Chen 2005). Much like Δ Np63, Δ Np73 isoforms do this by competing for DNA binding or through direct protein interactions and thereby can show anti-apoptotic activities. Moreover, p73 proteins can bind to specific response elements different from p53 suggesting a distinct set of target genes (Sasaki et al. 2005).

p73 activity can be induced in response to DNA damage by oncogenes such as Myc, phenocopying a p53 response (Zaika et al. 2001). However, p73 also possesses a role unlike p53 in neuronal development. The importance of p73 in the brain was illustrated in studies using p73-null animals, which show hippocampal dysgenesis, hydrocephalus, chronic infections, and abnormalities in pheromone sensory pathways as well as abnormal reproductive and social behaviour (Yang et al. 2000). This was due to a defect in both the embryonic and adult vomeronasal organ, a structure involved in pheromone detection where Δ Np73 is highly expressed. While these animals were first reported to show no increase in cancer susceptibility (Yang et al. 2000), some heterozygous animals for p73 did present lung adenocarcinomas, haemangiosarcomas and thymic lymphomas (Flores et al. 2005). Further isoform-specific studies showed that Δ Np73 is highly expressed in the developing mouse brain where it acts to counteract p53-induced neuronal apoptosis. This was further demonstrated where increasing levels of Δ Np73 alone were able to rescue neuronal cell death (Pozniak et al. 2000) and Δ Np73-null neurons were more sensitive to DNA damage (Wilhelm et al. 2010). In contrast, TAp73-specific knockout animals presented infertility, genomic instability and the development of spontaneous tumours (Tomasini et al. 2008). Furthermore, a switch in p73 isoforms from Δ Np73 to

TAp73 is also observed in kidney organogenesis in the developing nephron suggesting a role in p73 isoform regulation during the terminal differentiation programme (Saifudeen et al. 2005). Recently, TAp73 was found to also play a role in spermatogenesis as TAp73-null mice exhibited increased DNA damage and cell death in spermatogonia, resulting in male infertility, all of which were not observed in p53-deficient animals (Inoue et al. 2014).

While no human genetic disorders have been associated with germline mutations in the *p73* gene, there is a significant loss of heterozygosity of *p73* in a number of cancers (Moll and Slade 2004). Moreover, the *p73* promoter has been found to be hypermethylated, which inhibits p73 transcription in lymphomas and leukaemias (Corn et al. 1999; Kawano et al. 1999). In contrast, ovarian cancers have shown overexpression of p73 (Chen et al. 2000; Ng et al. 2000) and an overexpression of Δ Np73 was found to be a marker for poor prognosis in neuroblastoma patients (Casciano et al. 2002).

1.3.3.2 The Role of p73 in Metabolism

Similar to p53, p73 is a major regulatory of autophagy (Crighton et al. 2007). mTORC1 negatively regulates the expression of p73. Therefore, when mTORC1 signalling is inhibited, p73 is activated in order to induce the expression of autophagosome- and lysosome-associated genes to promote autophagy (Rosenbluth et al. 2008; Rosenbluth and Pietsenpol 2009). While p73, like p53, is also able to induce the expression of DRAM-1, p73-mediated autophagy does not rely on DRAM-1 activity (Crighton et al. 2007). In addition, suppression of p73 by mTORC1 can also regulate insulin response genes (Rosenbluth et al. 2008) as well as genes involved in mesenchymal differentiation and tumourigenesis (Rosenbluth et al. 2011). AMPK can also negatively regulate p73 activity through direct interaction with AMPK α (Lee 2009).

Transgenic TAp73-deficient mice have allowed for a further understanding of TAp73's role in autophagy, particularly through its regulation of ATG5. Through this, TAp73 can contribute to lipid metabolism in liver hepatocellular carcinoma models (He et al. 2013). Furthermore, cytochrome c oxidase subunit 4 (Cox4il) is a TAp73 target, and TAp73-null mice showed decreased activity of mitochondrial

complex IV, oxygen consumption and ATP production, as well as increased levels of ROS and sensitivity to oxidative stress. In addition, these animals also showed signs of premature ageing associated with elevated levels of oxidative stress (Rufini et al. 2012).

TAp73 can also activate serine biosynthesis, resulting in increased intracellular levels of serine and glycine. However, TAp73 does not directly regulate the expression of metabolic enzymes involved in the SSP but rather, transcriptionally upregulates GLS2, which drives serine biosynthesis by converting glutamine to glutamate, which then feeds into the SSP. Serine and glutamate can then be utilised for GSH synthesis, thus promoting an oxidative stress response (Amelio et al. 2014; Velletri et al. 2015). Much like p53 and TAp63, TAp73 can also promote the PPP, NADPH generation and antioxidant defence by directly activating G6PDH and increasing flux into the PPP (Du et al. 2013). However, rather than supporting proliferation, it is thought that TAp73 promotes anabolism in order to counteract cellular senescence (Agostini et al. 2014).

1.4 The Wnt Signalling Pathway and Cancer Metabolism

Another major growth signalling pathway that is often deregulated in cancer cells is the Wnt signalling cascade. The Wnt gene, originally named Integration-1 (Int-1), was identified through its activation via the integration of mouse mammary tumour virus proviral DNA in virally-induced breast tumours (Nusse and Varmus 1982). It was later found that Int-1 shared homology with a known *Drosophila* gene, *Wingless* (Wg), which plays a role in segment polarity during larval development (Nusslein-Volhard and Wieschaus 1980; Rijsewijk et al. 1987). Therefore, nomenclature of the gene was changed to Wnt (Wingless/Int-1).

1.4.1 Components of the Wnt Signalling Pathway

Cell signalling by the Wnt family of glycoproteins is one of the main mechanisms driving cell proliferation, polarity as well as cell fate during embryonic development and tissue homeostasis (Logan and Nusse 2004). Consequently, mutations in the Wnt signalling pathway are often linked to human diseases including cancer (Clevers 2006). The canonical Wnt signalling pathway acts to regulate the protein

levels of the transcriptional co-activator β -catenin, which controls the expression of key developmental target genes. In addition, Wnt signalling can go through a number of non-canonical pathways, independent of β -catenin, which can result in changes in cell polarity as well as changes in intracellular calcium levels (Seifert and Mlodzik 2007).

Upstream of the Wnt signalling cascade, complexity and specificity of the pathway is first conferred through the synthesis of the Wnt ligands. There are 19 known Wnt ligands, all of which have a high number of conserved cysteine residues, contain an N-terminal signal peptide for secretion and are ~40 kDa in size (Tanaka et al. 2002). Furthermore, Wnt ligands are N-linked glycosylated, which is important for their secretion (Komekado et al. 2007) as well as lipid modified (Hausmann et al. 2007), which is important for effective signalling (Willert et al. 2003; Galli et al. 2007; Komekado et al. 2007) and secretion from the ER (Takada et al. 2006). In particular, cysteine palmitoylation by the multipass transmembrane O-acetyltransferase Porcupine (Porc) in the ER is essential for Wnt maturation (Hofmann 2000; Hausmann et al. 2007), and loss of Porc results in an accumulation of Wnt ligand at the ER (Takada et al. 2006). In addition, Wntless (Wls), a seven transmembrane protein found in endosomes, the Golgi and the plasma membrane, bind to Wnt proteins and is also required for the secretion of Wnt proteins (Banziger et al. 2006). Moreover, studies in nematodes have shown that the retromer, a multiprotein trafficking complex, is also necessary for Wnt signalling by retrieving endosomal Wls, which is otherwise degraded, and trafficking it to the Golgi network (Coudreuse et al. 2006; Port et al. 2008; Yang et al. 2008).

Once secreted, Wnt proteins bind to a heterodimeric receptor complex, consisting of a frizzled (Fz) and a lipoprotein receptor-related protein 5/6 (LRP5/6) on target cells (Pinson et al. 2000; He et al. 2004; Tamai et al. 2004). Mammalian Fz proteins are seven transmembrane receptors and possess large extracellular N-terminal cysteine-rich domains (Bhanot et al. 1996). These provide a platform for Wnt ligand interaction at multiple surfaces (Dann et al. 2001), including with the lipid modifications on Wnt ligands (Janda et al. 2012). Moreover, a single Wnt ligand can bind to multiple Fz proteins and vice versa (Bhanot et al. 1996; Janda et

al. 2012). Other Wnt receptors also exist such as receptor-like tyrosine kinase (RYK) and receptor tyrosine kinase-like orphan receptor 2 (ROR2), both of which are transmembrane tyrosine kinase receptors (van Amerongen et al. 2008).

Much like many signalling transduction pathways, signalling via Wnt receptors involves ligand-induced conformational changes followed by the phosphorylation of key target proteins. In particular, binding of the protein Axin to the cytoplasmic tail of LRP6 is a crucial step (Mao et al. 2001) and is regulated by the phosphorylation of the LRP6 tail by at least two different protein kinases, glycogen synthase kinase 3 (GSK3) and casein kinase (CK1) (He et al. 2004; Tamai et al. 2004). GSK3 phosphorylates the serine in PPPSP motifs found in multiple Wnt signalling components (Zeng et al. 2005), while CK1 is anchored in the plasma membrane and phosphorylates the same proteins adjacent to the motifs targeted by GSK3 (Davidson et al. 2005). The interaction between the LRP tail and Axin is further facilitated by the interaction between the cytoplasmic part of Fz receptor and another protein, Dishevelled (Dsh) (Chen et al. 2003).

Alongside Wnt proteins, norrin and R-spondin are also capable of promoting the signalling pathway. Norrin is a specific ligand for the Fz4 and functions through the Fz4 and LRP5/6 complex during retinal vascularisation to promote Wnt signalling (Xu et al. 2004), while R-spondin proteins function alongside Wnt, Fz and LRP6 (Kazanskaya et al. 2004; Wei et al. 2007), and are often co-expressed with Wnt (Kazanskaya et al. 2004). Recently, it was found that the leucine-rich repeat containing G protein-coupled receptor (LGR) family of seven transmembrane domain receptors act to bind to and mediate R-spondin signalling in the canonical Wnt pathway, particularly to enhance signalling by low doses of Wnt protein (Carmon et al. 2011; de Lau et al. 2011; Glinka et al. 2011). These receptors possess a large N-terminal extracellular leucine-rich repeat domain that allows binding to glycoprotein hormones. While LGR receptors bind R-spondin through this N-terminal domain, there is no evidence suggesting the use of G proteins (Carmon et al. 2011; de Lau et al. 2011). Moreover, LGR5 was found to be a Wnt target gene in colon cancer as well as a marker for adult stem cells in actively self-renewing organs such as the intestinal tract (Jaks et al. 2008; Barker et al. 2009; Barker et al. 2010).

Alongside agonists, several secreted proteins are able to antagonize the Wnt signalling pathway. Secreted Frizzled related proteins (sFRPs) and Wnt inhibitory factor (WIF) bind to Wnt proteins and in the case of sFRPs, also to Fz. By doing so, they are able to inhibit both canonical and non-canonical Wnt pathways (Bovolenta et al. 2008). sFRPs resemble the ligand-binding cysteine-rich domain of Fz (Hoang et al. 1996), while WIF proteins are secreted molecules sharing similarities with the extracellular domain of RYK Wnt receptors (Hsieh et al. 1999). These Wnt binding properties suggests that these proteins can regulate Wnt protein stability, diffusion and extracellular distribution. Furthermore, two further classes of Wnt inhibitors are the Dickkopf (DKK) family and the WISE/Sclerostin (SOST) family of proteins. DKK proteins are LRP5/6 antagonists and are considered specific inhibitors of the Wnt signalling cascade. Although various different models for this inhibition have been proposed (Semenov et al. 2001; Mao et al. 2002), the most likely model suggests a disruption by DKK of the Wnt-induced Fz-LRP6 receptor complex. Similarly, the WISE/SOST family of proteins also disrupts the Wnt-induced Fz-LRP6 complex (Semenov et al. 2005). In addition, Shisa proteins act to trap Fz proteins in the ER and thus, inhibit the Wnt signalling pathway by preventing Fz receptors from reaching the plasma membrane (Yamamoto et al. 2005).

1.4.2 Activation of the Wnt Signalling Cascade

The central player in the canonical Wnt cascade is β -catenin, a cytoplasmic protein whose stability is regulated by the destruction complex. Axin functions as a scaffold for the destruction complex by interacting with β -catenin, adenomatous polyposis coli (APC), Wilms tumor gene on X chromosome (WTX), GSK3 and CK1. APC consists of three Axin-binding motifs interspersed between series of amino acid repeats with which β -catenin interacts. Importantly, APC is essential for the function of the destruction complex. Moreover, WTX, another protein that interacts with the destruction complex, also promotes the degradation of β -catenin (Major et al. 2007), although the mechanism of this is not yet known (Clevers and Nusse 2012).

Following recent studies on the destruction complex, a new model for Wnt activation has been identified. When the Wnt receptors Fz/LRP are not activated,

the destruction complex interacts with a component of an E3 ubiquitin ligase complex, F-box/WD repeat-containing protein 1A (better known as β TrCP). Here, β -catenin is phosphorylated by CK1 and GSK3 at highly conserved serine/threonine residues, as well as ubiquitinated by β TrCP (Li et al. 2012b) (Figure 1-6). Consequently, β -catenin is targeted for degradation by the proteasome, preventing its translocation to the nucleus and downstream induction of its target genes (Aberle et al. 1997) (Figure 1-6). Upon Wnt activation, the intact destruction complex is recruited to the phosphorylated tail of LRP. Thus, the destruction complex is still able to phosphorylate β -catenin but ubiquitination of β -catenin by β TrCP is blocked. Subsequently, the destruction complex becomes saturated with phosphorylated β -catenin leading to the accumulation of newly synthesised β -catenin, which can translocate to the nucleus (Li et al. 2012b) (Figure 1-6).

Following on from its translocation to the nucleus, β -catenin interacts with the DNA-bound T-cell factor (TCF) and lymphoid enhancer factor (LEF) (Behrens et al. 1996; Molenaar et al. 1998). When the Wnt signalling pathway is inactive, TCF/LEF interacts with the transcriptional repressor Groucho, which prevents the transcription of Wnt pathway target genes (Cavallo et al. 1998; Roose et al. 1998). However, when Wnt signalling is active, β -catenin interaction converts TCF/LEF into a transcriptional activator of its target genes such as *Axin2* (Lustig et al. 2002), *Myc* (He et al. 1998) and *cyclin D1* (Tetsu and McCormick 1999) (Figure 1-6). Furthermore, β -catenin itself can also function as a transcriptional activator by binding to histone modifiers such as CBP and Transcription factor IIIB 90 kDa subunit (Brf-1) (Stadeli et al. 2006).

Alongside its role in the Wnt signalling pathway, β -catenin can bind to various cadherins such as E-cadherin found in cellular adhesion junctions (Peifer et al. 1992). This illustrates two different pools of β -catenin, as the half-life of β -catenin involved in the signalling pathway is rather short while adhesion junction pool of β -catenin is very stable (Korswagen et al. 2000).

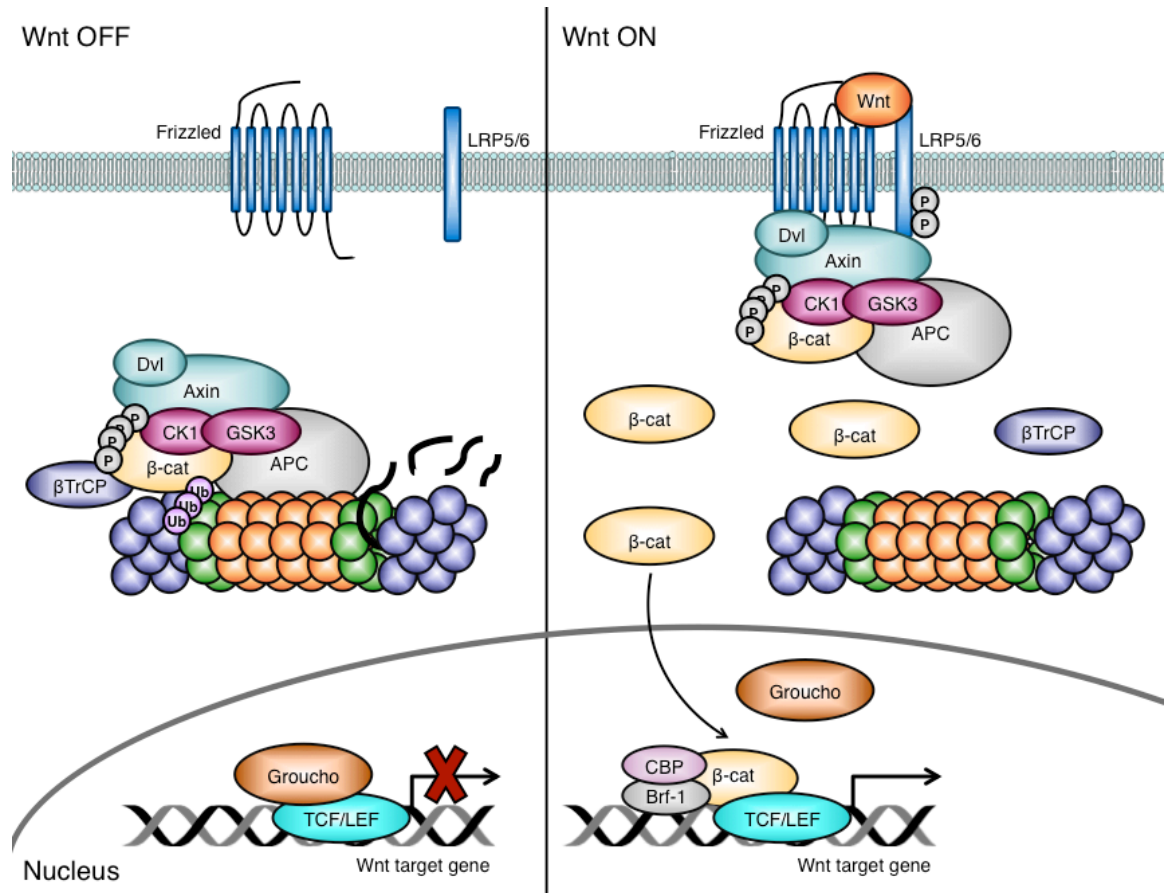


Figure 1-6 The Wnt Signalling Pathway

The new model of Wnt signalling at the receptor and destruction complex level. In the absence of Wnt ligands, the destruction complex resides in the cytoplasm, where it binds, phosphorylates, and ubiquitinates β -catenin (β -cat) by β TrCP. The proteasome recycles the complex by degrading β -catenin. T-cell factor/Lymphoid enhancer factor (TCF/LEF) occupies and represses Wnt target genes, helped by the transcriptional co-repressors such as Groucho. In the presence of Wnt ligands, a receptor complex forms between Frizzled and LRP5/6, and induces the association of an intact destruction complex to the phosphorylated tail of LRP5/6. After binding to LRP5/6, the destruction complex is still able to bind and phosphorylate β -catenin but is unable to promote its ubiquitination by β TrCP. This allows for the accumulation of newly synthesized β -catenin and nuclear translocation of β -catenin where it displaces Groucho from TCF and recruits transcriptional co-activators such as CREB binding protein (CBP) and Transcription factor IIIB 90 kDa subunit (Brf-1) to drive target gene expression.

1.4.3 Wnt Signalling in Diseases and Cancer

Various components of the Wnt signalling pathway such as Wnt receptors, agonists, antagonists and signalling proteins have all been implicated in a variety of diseases.

Mutations in *Porc* result in a rare genetic disorder, which is characterized by skin abnormalities and other developmental defects (Wang et al. 2007a), while mutations in *R-spondin* lead to XX sex reversal (Parma et al. 2006). Furthermore, mutations in *Fz4* and *LRP5* are associated with familial exudative vitreoretinopathy (Toomes et al. 2004), which is marked by defective retinal vascularisation. This is also observed in Norrie disease, which arises from mutations in the Wnt agonist *Norrin* (Xu et al. 2004).

Notably, mutations in Wnt pathway components have also been linked to bone diseases as Wnt signalling activates osteoblasts and can influence bone mass. Loss-of-function mutations in *LRP5* have been identified in patients with osteoporosis pseudoglioma syndrome, which is characterized by abnormal eye vasculature as well as low bone mass (Gong et al. 2001). In contrast, gain-of-function mutations in *LRP5*, which render it resistant to its inhibition by *SOST*, have been identified in patients with high bone mass diseases (Boyden et al. 2002; Little et al. 2002). Mutations in *SOST* itself result in sclerosteosis, which resemble high bone mass disorders (MacDonald et al. 2009).

Notably, the Wnt signalling pathway also contributes to the maintenance of stem cell homeostasis. Early studies in mice found that mutations in *TCF4* led to animals lacking intestinal stem cells and the subsequent loss of the tissue (Korinek et al. 1998). In the hair follicle, Wnt signalling also plays various roles in the stem cell niche and the biology of stem cell progenitors (DasGupta and Fuchs 1999). Blocking Wnt signalling eliminates hair follicles and other skin appendages such as the mammary gland (Andl et al. 2002), while activation of the Wnt pathway using mutant forms of β -catenin results in an expansion of haematopoietic and hair follicle stem cells (Gat et al. 1998).

As the Wnt pathway plays an important role in adult stem cell biology, mutations in the various components of the Wnt signalling pathway also contribute to cancer, particularly in tissues where Wnt signalling plays an important role in cell renewal or regeneration. Germline mutations in APC, resulting in a deregulated stabilisation of β -catenin and an increase in Wnt pathway activity, result in a hereditary cancer syndrome known as familial adenomatous polyposis, which is characterized by colon adenomas and polyps (Kinzler and Vogelstein 1996). Further mutations in KRas, p53 and mothers against decapentaplegic homolog 4 (SMAD4) can result in the progression of the polyps to malignant cancers. Global exome-sequencing found that the majority of colorectal cancers possess inactivating APC mutations (Wood et al. 2007). In particular, the β -catenin target gene c-Myc is essential for the oncogenic potential of canonical Wnt signalling in colorectal cancer (Sansom et al. 2007). However, in cases where wild-type APC is present, *Axin2* is often mutated (Liu et al. 2000). Hereditary loss of *Axin2* leads to a predisposition to colon cancer and tooth agenesis (Lammi et al. 2004), while loss-of-function mutations in *Axin2* have been linked to hepatocellular carcinomas (Rubinfeld et al. 1997). Mutations in β -catenin were first identified in colon cancer and melanomas (Morin et al. 1997; Rubinfeld et al. 1997), but have now also been found in a variety of cancers (Reya and Clevers 2005).

Interestingly, a link between Wnt signalling and metabolism has been emerging where an increased risk for type II diabetes has been associated to specific SNPs in *Wnt5b* (Kanazawa et al. 2004), *Wnt10b* (Christodoulides et al. 2006) and *TCF7L2* (Grant et al. 2006). While the mechanisms of this are still unclear, animals deficient in *TCF7L2* show enhanced glucose tolerance, lowered insulin levels and protection against type II diabetes (Savic et al. 2011).

1.4.4 Links Between Wnt Signalling and Cell Metabolism

Much like many other growth signalling pathways, Wnt signalling has now also been implicated in influencing cellular metabolism and whole-body energy homeostasis in normal cells.

Various animal studies have revealed a role for Wnt signalling in regulating metabolism in adult livers by contributing to hepatic carbohydrate and glutamine

metabolism (Cadoret et al. 2002; Tan et al. 2005; Chafey et al. 2009). While Wnt signalling can promote the expression of peroxisome proliferator-activated receptor δ (PPAR δ), which is associated with mitochondrial biogenesis and lipid oxidation (Jeong et al. 2009), Wnt signalling can also suppress the adipogenic isoform PPAR γ . This interplay is particularly important during adipocyte differentiation (Liu et al. 2006), breast cancer (Jiang et al. 2009) and in steatotic tissues (Tsukamoto et al. 2008).

Furthermore, the Wnt pathway is linked to cellular mechanisms of nutrient sensing. Murine models of nutrient surplus have shown an altered expression of Wnt ligands and Wnt antagonists in adipose tissue (Lagathu et al. 2009). Similarly, following refeeding in fasted rats, β -catenin levels were increased in the liver, muscle as well as adipose tissue (Anagnostou and Shepherd 2008). In macrophages, alterations in glucose availability can also induce autocrine activation of the Wnt signalling pathway (Anagnostou and Shepherd 2008). The biosynthesis of mature Wnt ligands is also dependent on posttranslational lipid modifications. This implies that lowered levels of non-esterified fatty acids may lead to decreased Wnt ligand biosynthesis as well as the converse, where excessive lipid availability may lead to inappropriate Wnt signalling activation (Sethi and Vidal-Puig 2010). However, this is not yet fully understood.

When considering the role of the Wnt pathway in adult tissue remodelling in response to injury, liver regeneration and cancer, the Wnt pathway also plays an important role in coordinating the required metabolic alterations. Particularly in the liver, the Wnt pathway contributes to carbohydrate and glutamine metabolism (Cadoret et al. 2002; Tan et al. 2005; Apte et al. 2009; Chafey et al. 2009). The Wnt pathway can also decrease oxidative stress through the induction of cytochrome P450s and glutathione transferase (Braeuning 2009). In contrast, loss of liver-specific APC suggests a role in fat deposition and the development of fatty liver under conditions of high nutrient uptake (Chafey et al. 2009). In the pancreas, the Wnt pathway contributes to the development of both the exocrine and endocrine pancreas, and recent studies have found that the Wnt signalling pathway can modulate mature β -cell biology including glucose-stimulated insulin secretion (Schinner et al. 2008; Shu et al. 2008), survival (Liu and Habener 2009)

and proliferation (Rulifson et al. 2007). Brown adipose tissue (BAT) is another organ that is highly important in whole-body energy homeostasis. Brown adipocytes function in energy dissipation through oxidative metabolism and a number of Wnt-related genes show inverse correlation with brown adipogenic potential while Wnt antagonists such as sFRP2 correlate with BAT differentiation (Tseng et al. 2005). Early Wnt pathway activation blocks BAT differentiation, while activation of the Wnt signalling pathway in mature brown adipocytes activates their conversion into white adipocytes (Longo et al. 2004). In contrast, white adipose tissue (WAT) functions as a major storage site for nutrient reserves and activation of the Wnt pathway here inhibits adipogenesis *in vitro* as well as *in vivo* (Prestwich and Macdougald 2007). Most likely, the mechanism by which this occurs is through the inhibition of adipogenic transcription factors PPAR γ and CCAAT-enhancer-binding proteins (C/EBP) (Freytag and Geddes 1992; Fu et al. 2005).

While normal Wnt signalling can modulate normal cell metabolism, deregulation of the pathway can also result in altered metabolism as observed in cancer cells. This was first observed in ovarian cancer where a large number of metabolic genes were found to be β -catenin/TCF/LEF target genes, particularly those involved in glutamine and fatty acid metabolism (Menendez and Lupu 2007). In breast cancer, canonical Wnt signalling was found to increase glycolytic rate by suppressing mitochondrial respiration through the repression of COX (Lee et al. 2012). Similarly in colorectal cancer, Wnt signalling can promote glycolysis through an upregulation of PDK1, which decreases the activity of PDH and thus results in decreased pyruvate oxidation (Pate et al. 2014). Furthermore, the lactate transporter MCT1 is also upregulated, which facilitates lactate secretion (Pate et al. 2014).

As mentioned previously, the oncogene c-Myc is a well-established target of the canonical Wnt signalling pathway. Therefore, β -catenin mediated c-Myc expression can also result in an upregulation of glycolytic genes such as GLUT1, LDH and PKM2 (Wu et al. 2014). Moreover, c-Myc can also promote glutaminolysis through the induction of the solute carrier family 1 member 5 (SLC1A5) glutamine transporter and mitochondrial GLS (Gao et al. 2009). Furthermore, this increase in glycolysis and glutaminolysis also promotes the *de*

novo synthesis of nucleotides and fatty acids (Thompson 2014). Glycolytic enzymes themselves can also further contribute to the Wnt signalling pathway as observed in the nuclear translocation of PKM2. This allows PKM2 to interact with β -catenin downstream of EGF signalling in a variety of cancer cell types to induce the expression of c-Myc and subsequently increase the expression of glycolytic genes including GLUT and LDH (Yang et al. 2011; Yang et al. 2012b; Yu et al. 2013).

ROS levels in cancer cells can also alter the activity of β -catenin as ROS can interrupt the interaction between β -catenin and TCF4 to facilitate the interaction between β -catenin and another transcription factor, FOXO3a (Dong et al. 2013). In breast cancer, this change in interaction shifts cancer stem cells to a more differentiated state and reduces tumorigenesis (Dong et al. 2013). Oxidative stress can also activate the Wnt pathway upstream of β -catenin through Dsh, where interaction between nucleoredoxin and Dsh inhibits Dsh activity. This interaction can be augmented through treatment with hydrogen peroxide, thus activating the Wnt pathway independent of the presence of extracellular Wnt ligands (Funato et al. 2006). Along with regulation by various proteins, the Wnt signalling pathway can also be altered by nutrients themselves. Glucose can promote β -catenin acetylation and nuclear accumulation in order to activate the transcription of Wnt target genes (Chocarro-Calvo et al. 2013). Furthermore, AMPK can inhibit the Wnt signalling pathway by reducing the activity of Dsh as observed in cervical cancer cells (Zoncu et al. 2011).

In addition to canonical β -catenin signalling, β -catenin independent Wnt signalling (non-canonical) mechanisms can also alter cancer cell metabolism. This is particularly observed through alterations in mTOR signalling. Murine hyperplastic mammary tissues with an overexpression of Wnt1 show elevated mTOR activity via an inhibition of GSK3, which would normally phosphorylate and activate the mTOR negative regulator TSC2 (Inoki et al. 2006). In line with this, independent of β -catenin, the LRP6 receptor can promote aerobic glycolysis by activating Akt in prostate cancer cells (Tahir et al. 2013), and Akt itself can also influence β -catenin signalling to promote glycolytic activity, potentially through Akt-mediated inhibition

of GSK3 (Kim et al. 2010a). This suggests a further link between Wnt signalling and the Akt/mTOR pathway in order to regulate cancer cell metabolism.

1.5 TIGAR: a Fructose-2,6-bisphosphatase

1.5.1 The Structure of TIGAR

TIGAR (*TP53*-induced glycolysis and apoptosis regulator) was discovered through a microarray analysis of ionizing radiation-responsive genes directly regulated by p53 (Jen and Cheung 2005). The human *TIGAR* (also known as *C12orf5*) gene is located on chromosome 12p13-3 and contains six coding exons and two p53-binding sites, one upstream of the first exon, termed BS1, and one within the first intron, named BS2. Of the two sites, BS2 is much more efficient in binding p53. In the mouse, *Tigar* is found on chromosome 6 and shows a similar genomic organisation (Bensaad et al. 2006).

Comparison of the amino acid sequence of TIGAR protein revealed a high level of conservation amongst vertebrate species from human to zebrafish (Bensaad et al. 2006) and in particular, high level of similarities with the bisphosphatase domain of the glycolytic enzyme phosphofructokinase-2/fructose-2,6-bisphosphatase (PFK-2/FBPase-2). Structural and biochemical studies using TIGAR from zebrafish found that the overall structure of TIGAR forms a histidine phosphatase fold with a phosphate molecule coordinated to the catalytic histidine residue as well as a second phosphate molecule in a position not observed in other phosphatases (Li and Jogl 2009). Furthermore, the TIGAR active site is open and positively charged, similar to other bisphosphatases. TIGAR is also structurally related to the bacterial broad specificity phosphatase PhoE and further structural comparisons revealed that TIGAR combines the accessible active site found in PhoE with a charged substrate-binding pocket as observed in the bisphosphatase domain of PFK-2/FBPase-2 (Li and Jogl 2009).

1.5.2 The Phosphofructokinase-2/Fructose-2,6-bisphosphatase Family

The PFK-2/FBPase-2 family of enzymes are bifunctional proteins, which possess both a kinase domain within the N-terminus as well as a bisphosphatase domain

at the C-terminus of the protein. The activity of these enzymes is regulated through the formation of a dimer stabilized by interactions at the kinase domain of the protein (Rider et al. 2004).

These enzymes catalyze the synthesis of fructose-2,6-bisphosphate (F-2,6-P₂) from fructose-6-phosphate (F-6-P) and ATP, at the N-terminal kinase domain, while the C-terminal bisphosphatase domain catalyses the reverse reaction through the hydrolysis of F-2,6-P₂ into F-6-P and inorganic phosphate. F-2,6-P₂ acts as a powerful allosteric activator phosphofructokinase-1 (PFK-1) and therefore, promotes glycolysis. Notably, PFK-1 can be inhibited by citrate, fatty acids as well as ATP through a negative feedback loop, which limits glycolysis during aerobic conditions (also known as the Pasteur effect). Allosteric activation of PFK-1 by F-2,6-P₂ removes this inhibition. Through this, high levels of F-2,6-P₂ allows cancer cells to maintain high glycolytic rates despite the generation of ATP. In contrast, PFK-2 is not affected by ATP levels and can be stimulated by inorganic orthophosphate, while PEP and citrate can inhibit PFK-2 activity. Furthermore, PFK-2 activity can be inhibited by sn-glycerol-3-phosphate, which competes with F-6-P for the PFK-2 catalytic binding site. Alongside this, sn-glycerol-3-phosphate can stimulate the activity of FBPase-2 (Frenzel et al. 1988). Similarly, GTP can promote FBPase-2 activity (van Schaftingen et al. 1982). In addition to promoting PFK-1 activity, F-2,6-P₂ also functions as an inhibitor of fructose-1,6-bisphosphatase (FBP1), which acts to oppose the activity of PFK-1 by catalysing the conversion of fructose-1,6-bisphosphate (F-1,6-P₂) to fructose-6-phosphate (van Schaftingen et al. 1982).

Four different genes encode the PFK-2/FBPase-2 enzymes, *PFKFB1* to *PFKFB4*, all of which are located on different chromosomes. Despite high conservation within the catalytic domains of the isoforms, differences can be found in tissue specificity, regulatory mechanisms and preferential catalytic activity of the isoforms. Co-expression of different PFK-2/FBPase-2 isoforms has also been observed in cells, suggesting distinct isoform functions (Minchenko et al. 2005; Ros and Schulze 2013).

The *PFKFB1* gene contains 17 exons, which from different promoters encode for three mRNAs (L, M, and F) that only differ in their first exon (Darville et al. 1992;

Dupriez et al. 1993). The first exon of the L isoform (L-PFK-2) generates a protein with a serine residue that can be phosphorylated and is expressed in the liver, skeletal muscle and white adipose tissue (WAT). In contrast, the M isoform (M-PFK-2) does not possess any residues that can be targeted for phosphorylation and is expressed in the skeletal muscle and WAT, while the promoter of the F isoform (F-PFK-2) is expressed in fibroblasts as well as foetal tissue. The *PFKFB2* gene encodes for the heart isoform (H-PFK-2) and through different promoters, can generate four different mRNAs that only vary in the 5' non-coding sequences (Chikri and Rousseau 1995; Heine-Suner et al. 1998). The *PFKFB3* gene contains 19 exons and can generate at least six different transcripts through alternative splicing. The resulting polypeptides differ by variable C-terminal regions, and the two main isoforms are the ubiquitous PFK-2 (u-PFK-2) and the inducible PFK-2 (i-PFK-2) (Navarro-Sabate et al. 2001). Lastly, the *PFKFB4* gene possesses at least 14 exons and encodes the testes isoenzyme (T-PFK-2) (Sakata et al. 1991). However, several splice variants of the *PFKFB4* mRNA have also been identified in different rat tissues (Minchenko et al. 2008).

While the structural organisation and the sequence of the catalytic core between the various PFK-2/FBPase-2 isoenzymes are highly conserved, differences between the proteins can be noted at the extreme N- and C-terminal regions where enzymatic activity can be modulated (Ros and Schulze 2013). *PFKFB1* and *PFKFB2* share similar relative kinase and bisphosphatase activities, while *PFKFB3* possesses greater kinase activity. In contrast, *PFKFB4* presents slightly greater bisphosphatase activity (Okar et al. 2001). However, as the different isoenzymes can be regulated by posttranslational modifications, their kinase and bisphosphatase can also be further altered.

Interestingly, TIGAR only shares similarities with the bisphosphatase domain of PFK-2/FBPase-2, with clear structural similarities despite limited amino acid conservation (Bensaad et al. 2006; Li and Jogl 2009).

1.5.3 The Activities of TIGAR

TIGAR as well as the bisphosphatase activities of PFK-2/FBPase-2, decreases the activity of PFK-1 by lowering the levels of F-2,6-P₂ and subsequently reduces the

downstream glycolytic flux. Studies have found that a decrease in TIGAR expression results in an elevation in F-2,6-P₂ levels and increased glycolytic flux (Bensaad et al. 2006; Kimata et al. 2010; Pena-Rico et al. 2011). This is consistent with a model where rather than inhibiting glycolysis, TIGAR acts to dampen the pathway. Through this, the consequences of TIGAR activity can be predicted, including the diversion of glycolytic metabolites to other metabolic branches including the hexosamine biosynthesis pathway as well as the oxidative and non-oxidative branches of the pentose phosphate pathway (PPP). The PPP plays an important role in cells by generating ribose-5-phosphate, which is utilized for nucleotide synthesis. Moreover, the oxidative arm of the PPP can generate NADPH, which provides a cellular antioxidant function and is also required in several anabolic pathways including fatty acid synthesis.

A lowering of glycolytic flux through the regulation of F-2,6-P₂ levels (Ros et al. 2012), the glycosylation of PFK-1 (Yi et al. 2012) or via ROS-mediated inhibition of PKM2 (Anastasiou et al. 2011) results in an elevation in NADPH and antioxidant activity, which could be due to an increase in PPP activity. Similarly, the bisphosphatase activity of TIGAR results in a comparable response and studies have shown that a downregulation of TIGAR expression is accompanied with decreased levels of NADPH (Lui et al. 2010; Lui et al. 2011; Yin et al. 2012), lower levels of GSH (Bensaad et al. 2006; Bensaad et al. 2009; Wanka et al. 2012; Yin et al. 2012) and consequently an increase in ROS (Bensaad et al. 2009; Cheung et al. 2013).

However, TIGAR appears to possess more than just its FBPase-2 activity as observed during hypoxia where a fraction of TIGAR relocalises to the mitochondria and associates with HK2. This results in increased HK2 activity, a lowering of mitochondrial membrane potential and decreased ROS levels (Cheung et al. 2012). This activity can also be seen in PFK-2/FBPase-2, where the FBPase-2 domain can bind and activate glucokinase (or hexokinase 4) (Baltrusch et al. 2001; Massa et al. 2004). In line with this non-enzymatic role, the C-terminal domain of the PFKFB4 variant 5 allows for nuclear translocation of the enzyme where F-2,6-P₂ can promote the expression and activity of cyclin-dependent kinase 1 (CDK1) and through this, promote cell proliferation (Yalcin et al. 2009). Recent studies

have also found that TIGAR can regulate the nuclear translocation of thioredoxin-1, where it activates AP-1 and redox sensitive systems following DNA damage in glioma cells (Zhang et al. 2014). This was also observed in liver cancer cells following treatment with epirubicin or hypoxia and TIGAR also showed nuclear localisation under these conditions. In the nucleus, TIGAR can promote the phosphorylation of ATM by CDK5 to mediate DNA-damage response signalling (Yu et al. 2015).

As discussed previously, hypoxia can influence many cellular responses associated with tumour development, including cancer cell metabolism via HIF-1 activation. HIF-1 is able to induce the expression of *PFKFB3* and *PFKFB4*, which both possess hypoxia response elements within their promoters (Minchenko et al. 2003; Minchenko et al. 2004; Obach et al. 2004). Interestingly, mutant TIGAR protein lacking the enzymatic FBPase-2 activity retains the ability to bind and enhance HK2 activity. Furthermore, the antioxidant function of TIGAR during hypoxia depends on both HK2 binding and catalytic activity (Cheung et al. 2012; Cheung et al. 2013). A recent study also identified a novel enzymatic activity for TIGAR as a 2,3-bisphosphoglycerate phosphatase, which acts to convert 2,3-bisphosphoglycerate to 3-phosphosphoglycerate (Gerin et al. 2014). However, the physiological function of this ability is not yet understood.

1.5.4 The Role of TIGAR under Stress

The effect of TIGAR expression on glycolysis and the regulation of ROS is cell type and context dependent. TIGAR expression in cytokine-dependent lymphoid cells resulted in decreased growth, potentially due to decreased glycolysis (Bensaad et al. 2006) and in a similar manner, TIGAR was found to also contribute to cell death in cardiac myocytes (Kimata et al. 2010). However, in the majority of cases, the ability of TIGAR to limit ROS levels is closely associated with cellular protection against ROS-induced cell death (Bensaad et al. 2006; Bensaad et al. 2009; Lui et al. 2011; Wanka et al. 2012; Yin et al. 2012; Cheung et al. 2013; Ye et al. 2013). Furthermore, by modulating ROS levels, TIGAR can also function to influence autophagy in response to cell stress (Bensaad et al. 2009; Ye et al. 2013). The role of TIGAR is associated with senescence, where decrease in TIGAR expression can induce senescence in glioblastoma cells (Pena-Rico et al.

2011), however, TIGAR can also inhibit senescence in adult T-cell leukaemia cells (Hasegawa et al. 2009).

A clearer understanding of TIGAR's physiological roles has been provided through *in vivo* studies. Unlike many other metabolic enzymes, which are essential for normal development (Piruat et al. 2004; Yang et al. 2010), TIGAR-deficient mice showed no profound developmental defects (Cheung et al. 2013). However, the loss of TIGAR in these animals has elucidated the role of TIGAR in response to various forms of cell stress including ischaemia/reperfusion injury (as seen in heart failure and stroke) and cancer.

Following ischaemia/reperfusion injury, cardiac myocytes undergo cell death due to the oxidative stress and subsequent tissue damage after the return of oxygenated blood following ischaemia. Studies have shown that p53 and TIGAR are induced in mouse models of myocardial infarction, and both have been linked to an elevation in cell death due to decreased glycolytic flux (Kimata et al. 2010). In addition, the role of p53 and TIGAR in this scenario was also associated with their ability to inhibit autophagy, particularly mitophagy. Animals lacking p53 or TIGAR were able to promote mitophagy following cardiac injury in order to clear damaged mitochondria and therefore showed better recovery following tissue damage. In this case, an elevation in ROS levels as a result of TIGAR deficiency acts as a signal to increase BCL2/adenovirus E1B 19 kDa protein-interacting protein 3 (BNIP3) expression and thus, an increase in mitophagy (Hoshino et al. 2012).

This rescue upon TIGAR loss was also observed in zebrafish models of PTEN-induced putative kinase 1 (PINK1) loss. Loss-of-function mutations in PINK1 typically result in early onset Parkinson's disease due to a lack of PINK1-mediated recruitment of parkin to damaged mitochondria and subsequent mitophagy (Narendra et al. 2010). Loss of PINK-1 in zebrafish resulted in an early impairment of mitochondrial function and these animals showed high levels of TigarB (the zebrafish orthologue). Loss of TigarB in PINK1-deficient larvae resulted in the complete normalisation of mitochondrial function, again suggesting a damaging role for TIGAR when mitophagy is important in clearing damaged mitochondria (Flinn et al. 2013).

The role of TIGAR during ischaemia/reperfusion injury has also been investigated in kidney proximal tubules. TIGAR is selectively induced in the renal outermedullary proximal straight tubules following ischaemia/reperfusion injury (Kim et al. 2015) and results in the inhibition of PFK-1, ATP depletion and an increase in oxidative stress, autophagy and apoptosis. Much like observed in the heart following ischaemia/reperfusion injury, loss of TIGAR attenuated the damage observed in ischaemic kidneys and interestingly, lowered oxidative stress (Kim et al. 2015).

In contrast, the functions of TIGAR during ischaemia/reperfusion injury are converse during brain ischaemia, where cerebral reperfusion injury exacerbates ischaemic brain damage due to the marked increase in ROS levels (Crack and Taylor 2005). In this scenario, TIGAR plays a neuroprotective role. In animal models and cultured primary neurons, oxygen and glucose deprivation (OGD)/reoxygenation injury induces TIGAR expression and loss of TIGAR aggravates ischaemic injury. Notably, overexpression of TIGAR was able to decrease ROS levels and increase GSH following OGD/reoxygenation and supplementation of NADPH to these systems was able to alleviate the further increase in tissue damage upon TIGAR loss. Furthermore, similar to what was observed during hypoxia (Cheung et al. 2012), OGD/reoxygenation injury increased the mitochondrial localisation of TIGAR in order to lower mitochondrial ROS levels (Li et al. 2014b). Furthermore, studies in primary cortical neurons treated with hydrogen peroxide showed an increase in TIGAR expression, which was dampened upon pre-treatment with NADPH (Sun et al. 2015) illustrating the role of TIGAR in lowering oxidative stress.

1.5.5 The Role of TIGAR in Cancer

The remodelling of metabolic pathways to assist in the regulation of redox homeostasis in order to support continuous proliferation is particularly important in tumour development. Despite the tumour suppressive functions of TIGAR as part of the p53 stress response, the activities of TIGAR in lowering ROS levels and promoting anabolic pathway also suggest potential pro-tumourigenic roles.

Firstly, high levels of F-2,6-P₂ have been noted in various cancer cell lines (Mojena et al. 1985; Miralpeix et al. 1990; Nissler et al. 1995) and while this elevation can help maintain the high glycolytic flux necessary in cancer cells, the bisphosphatase activities of PFK-2/FBPase-2 can provide an accumulation of glycolytic intermediates to be used in anabolic processes and redox control. Several studies on PFK-2/FBPase-2 isoforms have identified various roles for these enzymes during tumorigenesis.

All *PFKFB* mRNAs have been reported overexpressed in human lung cancers and while the role of *PFKFB1* has not been characterized in cancer, it observed elevated in proliferating cells to support increased glycolysis (Darville et al. 1992).

PFKFB2 has shown to be induced in prostate cancer cells following direct recruitment of the ligand-activated androgen receptor to the *PFKFB2* promoter. Loss of *PFKFB2* leads to lowered glucose uptake and lipogenesis suggesting that the androgen-mediated activation of *de novo* lipid synthesis requires the transcriptional upregulation of *PFKFB2* in these cells (Moon et al. 2011). Furthermore, *PFKFB3*, which predominantly possesses kinase activity, has been suggested to promote tumorigenesis by increasing PFK-1 activity and glycolytic flux. In particular, i-PFK-2 is reported overexpressed in several human cancer cell lines and required for tumour cell growth *in vitro* and *in vivo* (Chesney et al. 1999). Moreover, HIF-1-mediated induction of *PFKFB3* mRNA was found in various cancer cell lines including glioblastoma, gastric and pancreatic cells (Bobarykina et al. 2006), and *PFKFB3* is also highly phosphorylated in colon and breast carcinomas suggesting increased PFK-2 activity in these cancers (Bando et al. 2005). *PFKFB4* has also been reported induced in breast, colon, lung, gastric and pancreatic cell lines (Minchenko et al. 2005; Bobarykina et al. 2006; Minchenko et al. 2008), and shown to promote the survival of glioma stem-like cells. Loss of *PFKFB4* induced apoptosis in these cells (Goidts et al. 2012). Similarly, loss of *PFKFB4* in prostate cancer cells decreased cell viability (Ros et al. 2012). As *PFKFB4* predominantly presents bisphosphatase activity, this suggests that these cancer cells rely on *PFKFB4* to lower glycolysis, upregulate the PPP and regulate ROS levels, similar to the activities of TIGAR. However, this response to *PFKFB4*

expression may be more complicated than simply an inhibition of the PFK-1 step in glycolysis.

In contrast, loss of FBP1, whose activity opposes PFK-1, has been observed in liver, colon, gastric and breast cancer (Bigl et al. 2008; Chen et al. 2011). A role for FBP1 has also been found in clear cell renal cell carcinoma (ccRCC), a form of kidney cancer characterized by increased glycogen levels, fat deposition and elevated HIF activity. FBP1 is lost in the majority of ccRCC tumours and acts to inhibit ccRCC progression by lowering glycolytic flux. In addition, FBP1 can restrain cell proliferation, glycolysis as well as the PPP in a catalytic-independent mechanism by inhibiting the function of nuclear HIF via interacting directly with the HIF inhibitory domain (Li et al. 2014a). In these contexts, FBP1 expression is linked with decreased glycolysis and enhanced TCA cycle flux, but also a decreased PPP flux, and thereby an increase in ROS levels.

As TIGAR is able to lower ROS levels and promote anabolic pathways, this suggests a potential oncogenic role for TIGAR. Indeed, overexpression of TIGAR has been noted in many tumour types including nasopharyngeal carcinoma (Wong et al. 2015), invasive breast cancer (Won et al. 2012) and glioblastoma (Wanka et al. 2012; Sinha et al. 2013). Knockdown of TIGAR in glioma cells resulted in radiosensitisation due to an accumulation of ROS levels, leading to DNA damage and subsequent cellular senescence (Pena-Rico et al. 2011). Inhibition of the PPP enzyme transketolase-1 was able to reverse the benefits of TIGAR expression, supporting the role of the PPP and NADPH in sustaining cancer cell proliferation (Wanka et al. 2012). Moreover, treatment of neuroblastoma cells with D-galactose induces oxidative stress and results in an upregulation of TIGAR expression (Li et al. 2011).

TIGAR has also been shown to balance the redox state of multiple myeloma cells, where inhibition of the oncoprotein MUC1-C resulted in a decrease in TIGAR expression, decreased levels of NADPH and subsequently, increased ROS levels and apoptosis (Yin et al. 2012). Following studies from this group showed that targeting MUC1-C is synergistic with the proteasome inhibitor bortezomib in suppressing TIGAR-mediated regulation of ROS to induce multiple myeloma cell death (Hasegawa et al. 2009; Yin et al. 2012).

In nasopharyngeal cancer cells, inhibition of the tyrosine kinase c-Met, whose overexpression is linked with poor patient survival and metastasis, resulted in a reduction in TIGAR expression, decreased NADPH and increased cell death (Lui et al. 2011). Furthermore, it was found that TIGAR also promotes the invasiveness of nasopharyngeal carcinoma cells and loss of TIGAR also resulted in a decrease in the expression of two mesenchymal markers, fibronectin and vimentin (Wong et al. 2015). In liver cancer cell lines, loss of TIGAR resulted in an increase in apoptosis and autophagy (Ye et al. 2013; Xie et al. 2014), and exacerbated DNA damage caused by hypoxia or treatment with epirubicin (Yu et al. 2015).

While this role of TIGAR in promoting tumorigenesis appears to counteract the p53 tumour suppressor pathway, it should be noted that tumour cells with increased TIGAR expression often show an uncoupling from regulation by p53 and does not depend on the maintenance of wild-type p53 (Cheung et al. 2013). This pro-tumorigenic ability has also been observed in other p53-target genes such as CPT-1C (Zaugg et al. 2011).

1.5.6 The Regulation of TIGAR

While initial studies identified TIGAR as a p53 target gene (Bensaad et al. 2006; Hasegawa et al. 2009; Dai et al. 2013; Hamard et al. 2013; Agnoletto et al. 2014), its expression in human breast cancer was inversely correlated to the expression of p53 (Won et al. 2012).

The regulation, particularly p53-independent regulation, of TIGAR is not fully understood, which could be through transcriptional, translational, via protein stability or through other posttranslational modifications of the protein. In addition, other members of the p53 family, p63 and p73, can potentially influence the expression of TIGAR, as they are also capable of activating the promoters of various p53 target genes such as p21 and Bax (Yang et al. 1998; Lee and La Thangue 1999). Furthermore, TAp73 was recently found to promote PPP activity by activating G6PDH to support tumorigenesis (Du et al. 2013), suggesting a potential role for TAp73 in inducing TIGAR expression as well. Notably, while the expression of *PFKFB3* can be induced by HIF-1 (Minchenko et al. 2004; Obach et al. 2004; Bobarykina et al. 2006), TIGAR expression levels are not induced by

HIF-1 during hypoxia. However, the activity of TIGAR is clearly modulated under these conditions (Cheung et al. 2012). Other transcription factors, CREB and specificity protein-1 (SP-1) (Zou et al. 2012; Zou et al. 2013), have both been implicated in regulating the basal expression of TIGAR in liver cancer cells. Furthermore, SP-1 was found induced along with TIGAR following OGD/reoxygenation in mice and inhibition of SP-1 blocked the upregulation of TIGAR in primary neurons (Sun et al. 2015).

Various cell signalling pathways can influence the activity of PFK-2/FBPase-2 isoforms, and thus, levels of F-2,6-P₂, through posttranslational modifications at the catalytic domains of PFK-2/FBPase-2. As mentioned previously, the L-PFK-2 isoform can be phosphorylated at a serine residue in its C-terminal regulatory domain (Pilkis et al. 1995). In response to glucagon, cAMP-dependent protein kinase (also known as Protein Kinase A) phosphorylates this serine residue in L-PFK-2 resulting in the inactivation of its PFK-2 activity, while activating its FBPase-2 activity. This decreases glycolytic flux while promoting gluconeogenesis in the liver (Bartrons et al. 1983). In contrast, insulin promotes the activity of Akt, which in turn phosphorylates the heart isoform, H-PFK-2, resulting in increased kinase activity and subsequently an increase in glycolysis in the heart (Deprez et al. 1997). Furthermore, activation of AMPK during ischaemia results in the phosphorylation of H-PFK-2 and also results in an increase in glycolysis (Marsin et al. 2000). Interestingly the regulation of PFKFB3 isoforms can also occur through protein stability. PFKFB3 contains a KEN box motif, which is recognized by the anaphase-promoting complex/cyclosome (APC/C), an E3 ubiquitin ligase complex that acts to degrade several cell cycle proteins (Almeida et al. 2010). A decrease in APC/C activity results in an accumulation of PFKFB3 and enhances the glycolytic flux in malignant cells (Almeida et al. 2010), indicating that proliferation and increased glycolytic rate are both important components of cancer cell transformation. Interestingly, no posttranslational modifications have yet been identified for PFKFB4 or TIGAR. Nevertheless, it is likely that the activity of both these enzymes can be modulated by changes in substrate and product concentrations, or the presence of activators or inhibitors. Furthermore, animals injected with adrenalin, hydrocortisone or glucagon showed an increase in TIGAR

expression in the brain. This was also observed in neuronal cell lines treated in a similar manner (Sun et al. 2015).

Promoter DNA methylation has also been associated with the loss of FBP1 observed in various human cancers and breast cancer cell lines, suggesting a role for epigenetic regulation in altering cancer cell metabolism (Bigl et al. 2008; Chen et al. 2011; Dong et al. 2013). In addition, microRNAs (miRNAs) are noncoding RNAs that act as post-transcriptional negative regulators of gene expression, and in lung cancer cells, miR-144 can function to decrease cell proliferation as well as induce apoptosis and autophagy by targeting TIGAR (Chen et al. 2015).

1.5.7 Therapeutic Insights in Targeting PFK-2/FBPase-2 Enzymes

By better understanding the functions of TIGAR under normal as well as disease conditions, predictions concerning the benefits of modulating TIGAR for therapeutic intervention can be made.

Current studies have focused on targeting the PFK-2/FBPase-2 class of enzymes, in particular the kinase activity of PFKFB3 as multiple oncogenes as well as hypoxia can induce its expression. Initially, N-bromoacetylalanine phosphate was developed as a synthetic substrate analogue for fructose biphosphate aldolase, the enzyme which converts F-1,6-P₂ into dihydroxyacetone phosphate and glyceraldehyde 3-phosphate. However, it was later found to be an irreversible PFK-2 inhibitor (Hirata et al. 2000). Following this, the small molecule inhibitor 3-(3-pyridinyl)-1-(4-pyridinyl)-2-propen-1-one (3-PO) was identified, which was able to lower glucose uptake and F-2,6-P₂ levels *in vivo* and suppress the growth of breast, leukaemia and lung adenocarcinoma cells (Clem et al. 2008). Structure-based approaches allowed for the development of two more PFKFB3 inhibitors, N4A and YB1, which may possess increased specificity as they target the F-6-P binding site as opposed to the ATP binding pocket (Seo et al. 2011). However, as there is strong homology between all PFKFB isoforms in their PFK domain, it is possible that the anti-proliferative effects observed in cancer cells may not be solely attributed to the inhibition of PFKFB3.

In contrast, the FBPase-2 activity of PFBFK4 has also been implicated in promoting tumour growth as observed in prostate cancer cells (Ros and Schulze 2013). While PFKFB4 has the potential to be a therapeutic target, no selective strategy for its inhibition has yet been developed. Alongside this, overexpression of TIGAR is found in a number of tumour types and the loss of TIGAR following the establishment of tumours showed beneficial consequences, suggesting that TIGAR may be a potential therapeutic target (Wanka et al. 2012; Won et al. 2012; Cheung et al. 2013). However, further investigation into the role of TIGAR, particularly its regulation, localisation and potential posttranslational modification are necessary to fully understand how TIGAR can contribute to cell metabolism and its function in response to cell stress.

1.6 Aims and Objectives

Here we will focus on one aspect of the p53 stress response: the induction of TIGAR. While the ability to lower oxidative stress through the activity of TIGAR in healthy cells is beneficial (Bensaad et al. 2006; Lui et al. 2010; Lui et al. 2011; Wanka et al. 2012; Yin et al. 2012), the expression of TIGAR in cancers seems to provide tumours the ability to cope with elevated levels of oxidative stress (Wanka et al. 2012; Won et al. 2012; Cheung et al. 2013; Wong et al. 2015). Therefore, the role of TIGAR in healthy tissues as well as tumour models was investigated along with the consequences of TIGAR loss in these models. Furthermore, the role of TIGAR in cells cultured in conditions of oxidative stress were also investigated to better understand the method by which TIGAR can promote survival.

Interestingly, it has recently become clear that the expression and activity of TIGAR can be uncoupled from the p53 response (Won et al. 2012; Cheung et al. 2013) and that the contribution of TIGAR to cancer development may depend on the manner by which it is regulated. Therefore, this study is also aimed at determining the mechanisms by which TIGAR expression is promoted, particularly assessing the role of p53 family members (p53, p63 and p73) and the role of the Wnt/c-Myc signalling pathway using *in vitro* as well as *in vivo* models.

In brief, the main goals of this work were to:

- Understand the mechanism of control of TIGAR expression in mouse and human cells (Chapter 3).
- Assess the regulation of TIGAR *in vivo* by p53 family members (Chapter 4).
- Assess the regulation of TIGAR by the Wnt/c-Myc signalling pathway (Chapter 5).
- Analyse the role of TIGAR *in vivo* (Chapter 6).

Chapter 2 Materials and Methods

2.1 Materials

2.1.1 General Reagents and Kits

Reagent	Source
AccuGel 29:1 (40% w/v)	Geneflow
Advanced DMEM F/12	Life Technologies
Agarose	Sigma-Aldrich
AlbuMAX I Lipid-Rich BSA	Life Technologies
Alkaline Phosphatase Substrate Kit II	Vector Laboratories
Ampicillin	Sigma-Aldrich
Ammonium Persulfate (APS)	Sigma-Aldrich
Avidin/Biotin Blocking Kit	Vector Laboratories
B27	Life Technologies
Bio-Rad Protein Assay Dye Reagent Concentrate	Bio-Rad
Bovine Serum Albumin (BSA)	Sigma-Aldrich
Citrate Buffer (10x)	Life Technologies
Complete mini protease inhibitor	Roche
DAB Peroxidase (HRP) Substrate kit	Vector Laboratories
Deoxycholate	Sigma-Aldrich
Dimethyl Sulfoxide (DMSO)	Sigma-Aldrich
Dulbecco's Modified Eagle Medium (DMEM)	Life Technologies
EDTA	Sigma-Aldrich
Epidermal Growth Factor (EGF)	Peptotech
Ethanol	VWR
Ethidium Bromide (EtBr)	Sigma-Aldrich
Foetal Bovine Serum (FBS)	Life Technologies
Formaldehyde (37%)	Sigma-Aldrich
GeneJuice	Merck
Glucose	Sigma-Aldrich
Glutamine	Life Technologies
Glycine	Sigma-Aldrich
Glycogen	Ambion
HEPES	Life Technologies
Homogenous protein G-agarose suspension	Sigma-Aldrich

Hydrogen Peroxide	Sigma-Aldrich
Igepal	Sigma-Aldrich
Kanamycin	Sigma-Aldrich
Leupeptin	Sigma-Aldrich
Lithium Chloride	Sigma-Aldrich
Matrigel (Growth Factor Reduced)	BD
Methanol	VWR
Milk Powder	Marvel
mR-Spondin	R&D Systems
rWnt3a	R&D Systems
NEBuffer 2	New England Biolabs
Noggin	Peprtech
OptiMEM	Life Technologies
Penicillin-Streptomycin	Life Technologies
Phenol-chloroform-isoamylalcohol (PCI)	Sigma-Aldrich
Phenylmethylsulfonyl Fluoride (PMSF)	Life Technologies
Pierce ECL Western Blotting Substrate	Life Technologies
Proteinase K	Sigma-Aldrich
4x Protogel Resolving Buffer	Geneflow
RNase A	Sigma-Aldrich
Rotenone	Sigma-Aldrich
Sodium Bicarbonate (NaHCO ₃)	Sigma-Aldrich
Sodium Butyrate (NaBu)	Sigma-Aldrich
Sodium Chloride (NaCl)	Sigma-Aldrich
Sodium Dodecyl Sulphate (SDS)	Sigma-Aldrich
Spectra Multicolor Broad Range Protein Ladder	Life Technologies
Tetramethylethylenediamine (TEMED)	Sigma-Aldrich
Tert-butyl hydroperoxide (tBHP)	Sigma-Aldrich
Triton X-1000	Sigma-Aldrich
Trypsin 2.5%	Life Technologies
VECTASTAIN ABC Alkaline Phosphatase Kit	Vector Laboratories
VECTASTAIN ABC Peroxidase Kit	Vector Laboratories
Xylene	VWR

Table 2-1 List of reagents

2.1.2 Solutions and Buffers

Electroblotting Buffer

192 mM Glycine

25 mM Tris-HCl pH 8.3

20% Methanol

Lysogeny Broth (LB)

1% Bacto-Trypone

86 mM NaCl

0.5% Yeast extract

LB Agar

1% Bacto-Tryptone

86 mM NaCl

0.5% Yeast extract

1.5% Agar

Phosphate Buffered Saline (PBS)

170 mM NaCl

3.3 mM KCl

1.8 mM Na₂HPO₄

10.6 mM KH₂PO₄

pH 7.4

Resolving Gel

8-12% Acrylamide

375 mM Tris-HCl pH 8.8

0.1% SDS

0.1% APS

50 mM TEMED

RIPA

1% NP-40

0.5% NaDeoxycholate

0.1% SDS

In TBS, pH 7.8

SDS-PAGE Running Buffer

0.1% SDS

192 mM Glycine

25 mM Tris-HCl pH 8.3

SDS Sample Buffer (3x)

15% β -Mercaptoethanol

30% Glycerol

9% SDS

188 mM Tris pH 6.8

0.1% Orange G

Stacking Gel

5% Acrylamide

0.4% SDS

500 mM Tris pH 6.8

Tris-Buffered-Saline (TBS)

25 mM Tris-HCl pH 7.4

147 mM NaCl

5 mM KCl

TBS-Tween (TBST)

25 mM Tris-HCl pH 7.4

147 mM NaCl

5 mM KCl

0.1% Tween 20

Tris-EDTA (TE)

10 mM Tris-HCl pH 8.0

1 mM EDTA

2.1.3 ChIP SolutionsChIP Cell Lysis Buffer (CLB)

10 mM Tris pH 8.0

10 mM NaCl

0.2% Igepal

10 mM NaBu

50 µg/ml PMSF

1 µg/ml Leupeptin

Top up with H₂OChIP Nuclear Lysis Buffer (NLB)

50 mM Tris pH 8.0

10 mM EDTA

1% SDS

10 mM NaBu

50 µg/ml PMSF

1 µg/ml Leupeptin

Top up with H₂OChIP Dilution Buffer (IPDB)

20 mM Tris pH 8.0

150 mM NaCl

2 mM EDTA

1% Triton X-100

0.01% SDS

10 mM NaBu

50 µg/ml PMSF

1 µg/ml Leupeptin

Top up with H₂O

ChIP Wash Buffer 1 (IPWB1)

20 mM Tris pH 8.0

50 mM NaCl

2 mM EDTA

1% Triton X-100

0.01% SDS

Top up with H₂O

ChIP Wash Buffer 2 (IPWB2)

10 mM Tris pH 8.0

250 mM LiCl

1 mM EDTA

1% Igepal

1% Deoxycholate

Top up with H₂O

ChIP Elution Buffer (IPEB)

100 mM NaHCO₃

1% SDS

Top up with H₂O

2.2 Methods

2.2.1 Cells

A431, A549, A2780, H1299, HCT116 (p53 wild-type, p53-null), HepG2, HT29, MCF7 (p53 wild-type, p53-null), RKO (p53 wild-type, p53-null), Saos-2 p53, Saos-2 TAp73 α , Saos-2 TAp73 β , Saos-2 TAp73 γ , SW480, TIF, U2OS and U2OS-MycER were the human cell lines used. 3T3s, L-cells, MEFs were the murine cells and MDCK was a canine cell line that was used. All cells were cultured in DMEM supplemented with 10% FBS, 2 mM glutamine and antibiotics and grown in a 37 °C incubator at 5% CO₂.

2.2.2 Culturing Mouse Embryonic Fibroblasts

Pregnant females were culled 13 – 14 days after plugging was noticed. Fur was sprayed with 70% ethanol and the intact uterus containing embryos was extracted and transferred to a sterile dish. The uterus was then sectioned between each embryo, placed on individual dishes and washed with sterile PBS. The membranes and umbilical cord were removed and using a scalpel, the abdominal wall was incised and haematopoietic tissue and tubular intestine were removed. The bulk of the central nervous system was trimmed by dissecting the head above the oral cavity. Work was then transferred to a tissue culture hood. The embryo body was minced in 5 ml of 1x trypsin for up to 3 min and the dish was placed for 15 min in a 37 °C incubator. Cells were then transferred to a 15 ml tube and mechanically pipetted to further dissociate tissue. 5 ml of complete DMEM was added and cells were spun at 1,000 rpm for 5 min. The supernatant was aspirated and the embryonic cell pellet was resuspended in 10 ml of fresh DMEM and transferred to a clean dish.

2.2.3 Small Intestinal Crypt Culture

The small intestine of mice was washed in ice cold PBS, villi were scraped off using a glass coverslip and tissue material was transferred to a tissue culture hood. The small intestine was then cut into small pieces and further washed in ice cold PBS. PBS was aspirated and intestinal pieces were further washed in ice cold PBS. This was repeated for approximately 10 times. The intestinal pieces were

then transferred into PBS with 2 mM EDTA and incubated on a roller for 30 min at 4 °C. The crypts were collected in a fresh tube by pipetting mechanically to form a crypt enriched supernatant and pelleted via centrifugation at 1,200 rpm for 5 min before being suspended in ADF media (Advanced DMEM F/12, 1% of glutamine, 1% of penicillin/streptomycin, 0.1% of AlbuMAX I BSA, 10 mM HEPES). The fraction was then washed and spun at 600 rpm for up to 3 min. The final crypt pellet was resuspended with growth factor reduced matrigel and 20 µl was plated per well in a 12-well plate. Matrigel was allowed to solidify for 30 min in a 37 °C incubator before ADF was added supplemented with 0.05 µg/ml EGF, 0.1 µg/ml noggin and 0.5 µg/ml mR-spondin. New growth factors were supplemented every other day, while media was changed after every 5 days.

Crypts were passaged once a week depending on growth. Crypt cultures were harvested in ice cold PBS using mechanical pipetting and collected in a tube. Crypts were then spun down at 700 rpm for 3 min. Supernatant was aspirated slowly and the crypt pellet was dissociated with 100 µl ice cold PBS using mechanical pipetting. The tube was then topped up to 15 ml with ice cold PBS and crypts were spun down at 700 rpm for up to 5 min. This procedure was repeated for up to 5 times to ensure crypts were fully dissociated. The final crypt pellet was resuspended with growth factor reduced matrigel and 20 µl was plated per well in a 12-well plate. Matrigel was allowed to solidify for 30 min in a 37 °C incubator before ADF was added supplemented with 0.05 µg/ml EGF, 0.1 µg/ml noggin and 0.5 µg/ml mR-spondin.

2.2.4 Adenoma Crypt Culture

Adenomas were removed from the intestines of *Apc^{min/+}* mice using scissors and work was transferred to a tissue culture hood. The adenomas were then cut into smaller pieces and washed up to 5 times with ice cold PBS to remove debris, and incubated in 5 mM EDTA for 10 min at 4 °C on a roller. The crypts were then washed two times with ice cold PBS to remove EDTA and incubated in 10x trypsin for 30 min at 37 °C. The crypt-enriched supernatant was collected and washed approximately 5 times with 5 ml ADF through mechanical pipetting. This was then filled to 50 ml with ADF and passed through a 70 µm cell strainer and again topped up to 50 ml with ADF. The crypts were pelleted via centrifugation at 1,200

rpm for 5 min. This was resuspended in growth factor reduced matrigel and 20 μ l was plated per well in a 12-well plate. Matrigel was allowed to solidify for 30 min in a 37 °C incubator before ADF was added supplemented with 0.05 μ g/ml EGF and 0.1 μ g/ml noggin. New growth factors were supplemented every other day, while media was changed after every 5 days.

Crypts were passaged once a week depending on growth in a similar manner as performed for normal small intestinal crypts cultures (2.2.3).

2.2.5 Animals

All animal work was carried out under the UK Home Office guidelines in line with Animal (Scientific Procedures) Act 1986 and the EU Directive 2010. Experimental cohorts and breeding stocks were maintained for defined periods of time and the health of animals was checked at least two times weekly. Animals were euthanized by carbon dioxide (CO₂) asphyxiation. Mouse ear notching and general husbandry (food, water and housing) were carried out by the Cancer Research UK Beatson Institute Biological Services Unit. Genotyping was carried out by Transnetyx, Inc. (Cordova, TN, US).

The *TIGAR*^{-/-} (Cheung et al. 2013), *AhCre*⁺ *TIGAR*^{fl/fl} (Cheung et al. 2013), *p53*^{-/-} (Donehower et al. 1992), *TAp73*^{-/-} (Tomasini et al. 2008), *AhCre*⁺ *Apc*^{fl/fl} (Sansom et al. 2004), *AhCre*⁺ *Apc*^{fl/fl} *Rac1*^{fl/fl} (Myant et al. 2013), *AhCre*⁺ *Apc*^{fl/fl} *TIGAR*^{fl/fl} (Cheung et al. 2013) and E μ -Myc (Harris et al. 1988) animals have been previously described.

2.2.6 Irradiation Treatment in Mice

Mice were exposed to gamma irradiation from ¹³⁷Cs sources to induce intestinal damage, which delivered gamma-irradiation at 0.423 Gy/min.

2.2.7 Immunohistochemistry

Slides were dewaxed by washing two times in xylene for 10 min each, two times in 100% ethanol for 3 min each, once in 70% ethanol for 3 min and rinsed in running tap water for 1 min. Antigen retrieval was then performed by immersing slides in

10 mM citrate buffer using a SBB Aqua 5 Plus water bath (Grant) for 1 hr at 99 °C and then left to cool for 30 min at room temperature (RT). Slides were washed three times in TBST for 3 min each. Endogenous staining was blocked using 2% BSA/TBS for 1 hr at RT, followed by three washes in TBST for 3 min each. Slides were blocked with Avidin solution (Vector Laboratories) for 15 min at RT followed by three washes of TBST for 3 min each. After which they were blocked with Biotin solution (Vector Laboratories) for 15 min at RT, followed by three washes of TBST for 3 min each. Slides were then incubated with designated primary antibodies overnight at 4 °C (Table 2-2).

After incubation with primary antibody, slides were washed three times with TBST for 3 min each. Endogenous peroxidase activity was blocked by incubating slides in 5% H₂O₂/TBS for 30 min at RT and washed three times with TBST for 3 min each. Slides were then incubated in biotinylated anti-rabbit secondary antibody in 2% BSA/TBS for 1 hr at RT followed by three washes in TBST for 3 min each. Signal amplification was performed using the VECTASTAIN ABC Peroxidase Kit (Vector Laboratories), which was applied for 30 min at RT. Slides were then washed again three times in TBST for 3 min each. Staining was visualised using the DAB Peroxidase (HRP) Substrate Kit (Vector Laboratory), which was applied on the slides for an appropriate time. Slides were then washed with tap water for 3 min.

For malondialdehyde (MDA) staining, a similar protocol was followed. However, slides were blocked with 5% BSA/TBS and incubation in H₂O₂/TBS was omitted. VECTASTAIN ABC Alkaline Phosphatase Kit (Vector Laboratories) was used for signal amplification and the Alkaline Phosphatase Substrate Kit II (Vector Laboratories) was used for visualisation.

Counterstaining, dehydration and mounting of slides with coverslips was performed by the Cancer Research UK Beatson Institute Histology Services. Images were taken using an Olympus BX51 microscope.

The following antibodies were used for immunohistochemistry (1:200 dilution):

Target	Antibody name and supplier
β -catenin	6B3; Cell Signaling Technology
Ki67	RM-9106; Thermo Scientific
MDA	ab6463; Abcam
p21	M-19; Santa Cruz Biotechnology
p53	CM-5; Vector Laboratories
p73	S-20; Santa Cruz Biotechnology
TIGAR	AB10545; Millipore
Biotinylated anti-rabbit IgG	BA-1000; Vector Laboratories

Table 2-2: Antibodies used for immunohistochemistry

2.2.8 RNAscope Assay

RNAscope assays were done on formalin-fixed paraffin-embedded slides and performed by the Cancer Research UK Beatson Institute Histology Services. All reagents and probes to detect murine TIGAR (Mm-Tigar targeting 619-1574 of NM_177003.5) were purchased from Advanced Cell Diagnostics.

Slides were dewaxed by washing two times in xylene for 5 min each, two times in 100% ethanol for 3 min each and air dried for 5 min. Pre-Treatment Solution 1 was then added to the slides for 10 min and slides were washed two times in distilled water. Sections were boiled in Pre-Treatment Solution 2 for 15 min at 100 °C and transferred into distilled water. Slides were rinsed two times in distilled water, three times in 100% ethanol and air dried for 5 min. Slides were incubated in Pre-Treatment Solution 3 for 30 min at 40 °C and washed two times in distilled water before being incubated in hybridize targeting probe for 2 hr at 40 °C. Sections were rinsed two times in RNAscope Wash Buffer for 2 min each between incubations with Hybridise Amp 1 for 30 min at 40 °C, Hybridise Amp 2 for 15 min at 40 °C, Hybridise Amp 3 for 30 min at 40 °C, Hybridise Amp 4 for 15 min at 40 °C, Hybridise Amp 5 for 30 min at RT, Hybridise Amp 6 for 15 min at RT, and DAB solution for 10 min at RT. Finally, sections were counterstained, dehydrated and mounted with coverslips. Images were taken using an Olympus BX51 microscope.

2.2.9 Bradford Protein Determination Assay

A standard curve was first established using Bradford values obtained from stock concentrations of BSA (0 – 1 mg/ml) in order to determine the concentration of unknown values. Bio-Rad Protein Assay Dye Reagent Concentrate (5x) was first diluted in water. Samples were prepared in cuvettes with 5 μ l of sample and 995 μ l of reagent. Absorbance of the samples was read using a BioSpectrometer (Eppendorf) at 595 nm. The concentration of the samples was then determined from the standard curve.

2.2.10 SDS-PAGE and Western Blotting

Cells were washed in PBS and directly lysed from the plates in RIPA on ice. Samples were left for 30 min on ice and then spun down at 13,000 rpm for 15 min at 4 °C. Intestinal crypts were harvested by aspirating the media and careful washing with ice cold PBS. Matrigel containing the crypts was dislodged, transferred to a tube and spun down at 600 rpm for 3 min to form an intestinal crypt pellet. The supernatant containing the matrigel was carefully aspirated and the pellet was again washed with cold PBS. Spinning and washing was repeated several times until supernatant was clear of matrigel. Crypts were lysed in RIPA and left for 30 min on ice before being spun down at 13,000 rpm for 15 min at 4 °C. Tissues were homogenized using an Argos Pellet Mixer with disposable pestles on ice in RIPA and left for 30 min on ice before being spun down at 13,000 rpm for 15 min at 4 °C.

Protein concentration was determined using a Bradford protein assay (2.2.9). Samples were boiled in sample buffer for 10 min at 99 °C and loaded on SDS-polyacrylamide gels with 12% acrylamide content. Electrophoresis was performed in SDS-PAGE buffer at 110 – 130 V on Hoefer Mighty Small Vertical Units SE250 (Amersham) and proteins were transferred to 0.2 μ M nitrocellulose membrane (Amersham) in electroblotting buffer by Western blotting using the Hoefer TE22 Mini Transfer Tank (Amersham) at 250 mA for up to 3 hr. Membranes were blocked in 5% milk powder in TBST for 30 min and incubated with primary antibodies overnight at 4 °C (Table 2-3).

For horseradish-peroxidase (HRP) visualization, membranes were first washed three times in TBST for 3 min each, followed by incubation with HRP-conjugated secondary antibodies at 1:10,000 for a minimum of 1 hr (Table 2-4). Proteins were visualised by Pierce ECL reagent, using Fuji Medical X-Ray Film Super RX 18x24 on an AGFA classic E.O.S film processor.

For infrared visualization, membranes were washed three times in TBST for 3 min each, followed by incubation with IRDye secondary antibodies at 1:10,000 for a minimum of 1 hr (Table 2-4). Membranes were then washed three times in TBST for 3 min each and rinsed in water before being scanned using a LI-COR Odyssey. Image Studio software (LI-COR, V2.1.10) was used to quantify the membranes.

The following primary antibodies were used for Western blotting (1:1000 dilution):

Target	Antibody name and supplier
Actin	I-19-R; Santa Cruz Biotechnology
β -catenin	6B3; Cell Signaling Technology
c-Myc	D84C12; Cell Signaling Technology
CDK4	DCS-35; Santa Cruz Biotechnology
Cyclin D1	DCS6; Cell Signaling Technology
HA.11	16B12; Covance
HO-1	H-105; Santa Cruz Biotechnology
HSP90	Cell Signaling Technology
NRF2	C-20; Santa Cruz Biotechnology
p21	C-19; Santa Cruz Biotechnology
p53 (human)	DO-1; Beatson Molecular Services
p53 (murine)	1C12; Cell Signaling Technology
TIGAR (human)	G-2; Santa Cruz Biotechnology
TIGAR (murine)	M-209; Santa Cruz Biotechnology

Table 2-3: Primary antibodies used for Western blotting

The following secondary antibodies were used for Western blotting (1:10,000 dilution):

Target	Supplier
Sheep anti-mouse IgG HRP-linked	GE Healthcare
Donkey anti-rabbit IgG HRP-linked	GE Healthcare
IRDye 800CW donkey anti-goat	LI-COR
IRDye 800CW donkey anti-mouse	LI-COR
IRDye 800CW donkey anti-rabbit	LI-COR

Table 2-4: Secondary antibodies used for Western blotting

2.2.11 iRFP Reporter Construct Generation

The iRFP reporter vector was obtained from A. Hock (Hock et al. 2014). iRFP reporter inserts were annealed in 80 μ l NE on a Thermomixer heat block (Eppendorf) for 10 min at 99 °C. The heat block was then turned off, and inserts were allowed to cool for 1 hr. The original vector was digested to remove previous insert by combining 5 μ l vector, 5 μ l 10x NEBuffer 2 (New England Biolabs), 1 μ l Spel (Roche), 1 μ l EcoRI (Life Technologies), 1 μ l BSA and 37 μ l diethyl pyrocarbonate (DEPC)-treated water in a tube and placed in a water bath for 2 hr at 37 °C. The digested vector was then run on an agarose gel at 40 mV and analysed under UV after which the correct band was cut out of the gel. The vector DNA was then purified using the NucleoSpin Gel and PCR Clean-Up kit (Machery-Nagel) according to manufacturer's instructions. Reporter inserts were ligated into the iRFP vector using the InFusion HD Eco Dry system (Clontech) according to manufacturer's instructions (Table 2-5).

The following insert primer sequences were used (synthesized and purified by Eurofins MWG Operon):

Name	Sequence (5' - 3')
TIGAR hBS1 for	CTG TGG ACT AGT CCA CAA AGC AAG TCT CTG TAA
TIGAR hBS1 rev	TTA CAG AGA CTT GCT TTG TGG ACT AGT CCA CAG
TIGAR hBS2 for	AGA CAT GTC CAC AGA CTT GTC TGG GTA C

TIGAR hBS2 rev	GTA CCC AGA CAA GTC TGT GGA CAT GTC T
TIGAR mBS1 for	GGA CCT AAC TTG TTC TTT ACT TGG AAC TTG CTT TGT CC
TIGAR mBS1 rev	GGA CAA AGC AAG TTC CAA GTA AAG AAC AAG TTA GGT CC
TIGAR mBS2 for	GAA GAC ATG ACC CGG CCT CTC GAC T
TIGAR mBS2 rev	AGT CGA GAG GCC GGG TCA TGT CTT C
p53RE for	GGA CAT GCC CGG GCA TGT CCC CAG AGA CAT GTC CAG ACA TGT CCC CAG GAA CAT GTC CCA ACA TGT TGT CCA GGA GAC ATG TCC AGA CAT GTC CCC AGG AAC ATG TCC CAA CAT GTT GT
p53RE rev	ACA ACA TGT TGG GAC ATG TTC CTG GGG ACA TGT CTG GAC ATG TCT CCT GGA CAA CAT GTT GGG ACA TGT TCC TGG GGA CAT GTC TGG ACA TGT CTC TGG GGA CAT GCC CGG GCA TGT CC
WAF1 for	GAA CAT GTC CCA ACA TGT TG Published (el-Deiry et al. 1993)
WAF1 rev	CAA CAT GTT GGG ACA TGT TC Published (el-Deiry et al. 1993)
BPAG1 for	CGC CAT GCA TGA ATT CCG CGT TCT GCC TGC TTT GTT CAT ACT TGT AGG CAC TAG TTA GGC GTG TA Published (Osada et al. 2005a)
BPAG1 rev	TAC ACG CCT AAC TAG TGC CTA CAA GTA TGA ACA AAG CAG GCA GAA CGC GGA ATT CAT GCA TGG CG Published (Osada et al. 2005a)

Table 2-5: Primers for iRFP construct inserts

2.2.12 DNA Preparation

Competent *E. coli* DH5 α bacteria (Cancer Research UK Beatson Institute Molecular Technology Services) were transformed with plasmid DNA by combining 2 μ g DNA with 100 μ l competent bacteria. Following incubation of 15 min on ice, the bacteria-DNA combination was heat-shocked for 45 sec at 42 °C and placed on ice for 2 min. 1 ml LB was added and incubated with shaking for 1 hr at 37 °C.

The bacteria suspension was then plated on LB agar plates containing 100 μ g/ml Ampicillin or 50 μ g/ml Kanamycin. Plates were placed for 1 hr in a 37 °C incubator before being inverted to grow colonies. Single colonies were picked and left

shaking in 4 ml LB for small scale DNA preparation (mini prep) or 250 ml LB for large scale DNA preparation (maxi prep) with 100 µg/ml Ampicillin or 50 µg/ml Kanamycin for overnight at 37 °C.

The Cancer Research UK Beatson Institute Molecular Technology Services performed all small-scale DNA preparations using a QIAGEN BioRobot 9600 according to the QIAprep 96 Plus Miniprep protocol, and large-scale DNA preparations using an Invitrogen Purelink plasmid filter purification kit according to the manufacturer's manual.

2.2.13 Plasmids

The following plasmids were used in this study:

Plasmid	Source
pCMV mouse p53	from K. Ryan
pcDNA3 empty	Life Technologies
pcDNA3 p53	from K. Ryan
pcDNA HA-TAp63α	from G. Melino (De Laurenzi et al. 2000)
pcDNA HA-TAp63β	from G. Melino
pcDNA HA-TAp63γ	from G. Melino
pcDNA HA-ΔNp63α	from G. Melino (Candi et al. 2006)
pcDNA HA-TAp73α	from G. Melino (De Laurenzi et al. 1998)
pcDNA HA-TAp73β	from G. Melino
pcDNA HA-TAp73γ	from G. Melino
pcDNA HA-ΔNp73α	from G. Melino
BPAG1	iRFP reporter construct
p53RE	iRFP reporter construct
TIGAR hBS1	iRFP reporter construct
TIGAR hBS2	iRFP reporter construct
TIGAR mBS1	iRFP reporter construct
TIGAR mBS2	iRFP reporter construct
WAF1	iRFP reporter construct

Table 2-6: Plasmids

2.2.14 Transfections

For iRFP reporter assay studies, p53/HA-tagged p63/HA-tagged p73 and iRFP reporters were transfected at a ratio of 1:1.

Cells were transfected using GeneJuice (Merck Biosciences). 3×10^5 cells per well were seeded in 6 well plates and cultured for 24 hr before. 100 μ l OptiMEM (Life Technologies) was mixed with 3 μ l GeneJuice, mixed thoroughly by vortexing and incubated for 5 min at RT. A total of 2 μ g of DNA was then added to the GeneJuice/OptiMEM combination and mixed through gentle pipetting. This was then incubated for 15 min at RT. The entire volume was then added to the cells in a drop-wise fashion and cells were incubated for 24 hr before harvesting for analysis. For iRFP reporter assay scans, transfections were performed in 96-well plates and volumes were scaled down to 3×10^4 cells per well, 6.3 μ l OptiMEM, 0.35 μ l GeneJuice and a total DNA content of 0.12 μ g.

2.2.15 iRFP Reporter Assays

24 hr post-transfection, 96-well plates were scanned using a LI-COR Odyssey infrared scanner at 169 μ M resolution, 3.5 mm offset and a low intensity setting. Image Studio software (LI-COR, V2.1.10) was used to quantify iRFP reporter readings from the plates.

2.2.16 DNA Sequencing

The correct insertion of response elements into iRFP constructs was confirmed through DNA sequencing by the Cancer Research UK Beatson Institute Molecular Technology Services on an Applied Biosystems 3130xl genetic analyser. The results were analysed using the ApE plasmid editor v1.17.

The following sequencing primer was used (synthesized and purified by Eurofins MWG Operon) to confirm insertion of response elements:

Name	Sequence
iRFP seq rev	GCG GTT GGA TGG CAC CGG GG

Table 2-7 Sequencing primer for iRFP reporters

2.2.17 RNA Extraction and Quantitative Real-Time PCR

RNA was extracted using the RNeasy kit (QIAGEN) following manufacturer's instructions from cells or mouse tissues. RNA concentration was determined using a Nanodrop 2000c (Thermo Scientific). cDNA was synthesised through reverse transcription polymerase chain reaction (RT-PCR) from 1 µg RNA using Oligo d(T) primers and using the DyNAmo SYBR Green two-step kit (Finnzymes) according to manufacturer's instructions using a PTC-200 Peltier Thermal Cycler (MJ Research). The quantitative real-time PCR (qPCR) reaction was performed with 5 µl cDNA, diluted 1:20, using the DyNAmo SYBR Green two-step kit (Finnzymes).

The amount of fluorescent PCR product accumulating during the PCR programme (15 min at 95 °C hot start, 40 cycles of 20 sec denaturing at 94 °C, 30 sec annealing at 60 °C and 30 sec elongation at 72 °C, final elongation 10 min 72 °C) was detected by a Chromo4 Reader (Bio-Rad) and analysed using the Opticon Monitor 3 software. Gene expression was quantified relative to the housekeeping gene ribosomal protein, large, P0 (RPLP0) or mouse glyceraldehyde-3-phosphate dehydrogenase (GAPDH) (Primer Design) according to the comparative $\Delta\Delta C_T$ -method.

The mouse TIGAR primer was purchased from QIAGEN. The following mRNA primers (5' → 3') were used (synthesized and purified by Eurofins MWG Operon):

Name	Sequence
Axin2 for	GCT CCA GAA GAT CAC AAA GAG C
Axin2 rev	AGC TTT GAG CCT TCA GCA TC
Hexokinase 2 for	TTC GCA CTG AGT TTG ACC AG
Hexokinase 2 rev	CCA TCC TTC TCC CCT TCA AT
HO-1 for	CAG GAG CTG CTG ACC CAT GA
HO-1 rev	AGC AAC TGT CGC CAC CAG AA
p21 (human) for	CTG GAG ACT CTC AGG GTC GAA A
p21 (human) rev	GAT TAG GGC TTC CTC TTG GAG AA
p21 (mouse) for	GGC CCG GAA CAT CTC AGG
p21 (mouse) rev	AAA TCT GTC AGG CTG GTC TGC
p53 (human) for	CCC TTC CCA GAA AAC CTA CC
p53 (human) rev	CTC CGT CAT GTG CTG TGA CT

p53 (mouse) for	CAC GTA CTC TCC TCC CCT CAA T
p53 (mouse) rev	AAC TGC ACA GGG CAC GTC TT
RPLP0 for	GCA ATG TTG CCA GTG TCT G
RPLP0 rev	GCC TTG ACC TTT TCA GCA A
TAp73 (mouse) for	GCA CCT ACT TTG ACC TCC CC
TAp73 (mouse) rev	GCA CTG CTG AGC AAA TTG AAC
TIGAR (human) for	CGG CAT GGA GAA AGA AGA TT
TIGAR (human) rev	TCC TTT CCC GAA GTC TTG AG

Table 2-8 Primer sequences for qPCR

2.2.18 Chromatin-Immunoprecipitation (ChIP)

Plates were set up for approximately 8×10^5 cells on 10 cm plates. 24 hr after plating, cells were treated with 50 μ M cisplatin for 24 hr. Plates were first washed with 4 ml PBS. Formaldehyde solution was prepared by combining 405 μ l 37% formaldehyde with 15 ml serum free DMEM, and 4 ml of this solution was added to each plate in a drop-wise manner. Plates were then incubated with gentle agitation for 10 min at RT. Cross-linking was stopped with the addition of 200 μ l 2.5 M glycine and incubated with gentle agitation for 5 min at RT.

Media was completely aspirated and plates were placed on ice. Ice cold PBS was used to wash the plates once. Cells were scraped in 5 ml ice cold PBS and transferred to 15 ml tubes. This was repeated to ensure all cells were harvested (final volume of 10 ml per sample). Cells were centrifuged at 1,200 rpm for 5 min at 4 °C and the final cell pellet was resuspended with 1.5 ml ice cold PBS and kept on ice. Cells were then centrifuged at 2,000 rpm for 5 min at 4 °C.

The cell pellet was gently resuspended in 1.5x pellet volume (approximately 200 μ l) of ChIP cell lysis buffer (CLB) with gentle pipetting and incubated for 10 min on ice. This was then centrifuged at 2,500 rpm for 5 min at 4 °C to collect cell nuclei. The supernatant was carefully discarded and nuclei were resuspended in 95 μ l of ChIP nuclear lysis buffer (NLB) and incubated for 10 min on ice. ChIP dilution buffer (IPDB) was added to top up sample to 400 μ l and samples were transferred to Eppendorf tubes. Volumes used for cell lysis and nuclei collection were based on 8×10^5 cell samples and were adjusted according to cell number.

Before sonication, 10 µl of each sample was taken for running on an agarose gel as “pre-sonication”. Samples were sonicated using the VCX130 Vibra-Cell sonicator (Sonics) at 100% amplitude, 30 sec on/30 sec off for a total of 10 min (two repeats of 5 min) in order to shear the DNA into approximately 200-500 bp fragments. Ice was replaced and the probe was washed in between each 5 min run. Following sonication, 10 µl of each sample was taken for running on an agarose as “post-sonication”. To ensure samples were appropriately fragmented, pre- and post-sonication samples were run on a 1.5% agarose gel at 40 mV and analysed under UV.

Samples were then centrifuged at 13,000 rpm for 5 min at 4 °C, and 600 µl IPDB was added to obtain a final volume of 1 ml. Chromatin was pre-cleared by adding 16.7 µl normal rabbit IgG (Santa Cruz Biotechnology) and incubated on a rotating wheel for 1 hr at 4 °C. Following this, 33.3 µl of homogenous protein G-agarose suspension (Sigma-Aldrich) was added and incubated on a rotating wheel for at least 3 hr (to overnight) at 4 °C.

Samples with beads were centrifuged at 3,000 rpm for 2 min at 4 °C. Modified IPDB (IPDBmod) was then made by combining 1:4 NLB:IPDB. The supernatant was transferred to new Eppendorf tubes and set up in the necessary conditions for CHIP with p53 and HA as a negative control (Table 2-9). 4 µl chromatin was set up as an input control and stored at -20 °C. Samples were incubated on a rotating wheel overnight at 4 °C.

CHIP Target	Conditions
p53	400 µl chromatin + 400 µl IPDBmod + 10 µg p53 antibody
HA	400 µl chromatin + 400 µl IPDBmod + 10 µg HA antibody

Table 2-9 CHIP set up conditions

Following incubation, samples were centrifuged at 13,000 rpm for 5 min at 4 °C and transferred to new Eppendorf tubes. 50 µl homogenous protein G-agarose suspension was added and samples were incubated on a rotating wheel for at least 4 hr at 4 °C. Samples were then centrifuged at 13,000 rpm for 30 sec at 4 °C. The supernatant was removed and pellets were washed twice with 750 µl CHIP

wash buffer 1 (IPWB1). Samples were vortexed briefly between each wash and centrifuged at 7,500 rpm for 2 min at 4 °C. Pellets were washed similarly with 750 µl ChIP wash buffer 2 (IPWB2) and twice with 750 µl TE.

To elute ChIP material, 200 µl ChIP elution buffer (IPEB) was added to the samples with 2 µl RNase A (Sigma-Aldrich) and 2 µl Proteinase K (Sigma-Aldrich), and heated on a Thermomixer heat block (Eppendorf) at 900 rpm overnight for 65 °C. Input samples were similarly processed.

Following this, samples were transferred to fresh Eppendorf tubes and 200 µl TE was added. Phase-lock tubes (5 Prime) were used for phenol-chloroform-isoamylalcohol (PCI, Sigma-Aldrich) isolation. Tubes were first spun at 14,000 rpm for 1 min at RT to pellet the solvent in the tubes. 400 µl PCI was added to samples and thoroughly mixed before being transferred to phase-lock tubes. This was then spun at 14,000 rpm for 5 min at RT. The upper phase was carefully transferred to new Eppendorf tubes.

16 µl of 5 M NaCl and 8 µl glycogen (Ambion) was added to the samples and then vortexed. 1 ml of ice cold 100% ethanol was added to each sample and then vortexed. Samples were then stored for a minimum of 30 min at -80 °C. Following this, samples were spun at 13,000 rpm for 15 min at 4 °C, and the supernatant was discarded. Pellets were washed with 1 ml ice cold 80% ethanol and spun at 13,000 rpm for 10 min at 4 °C. The supernatant was discarded and pellets were dried at RT with tube lids opened in a fume hood for approximately 10 min. DNA was eluted in 50 µl 10 mM Tris-HCl and heated on a Thermomixer heat block (Eppendorf) for 10 min at 50 °C in order to dissolve the pellet.

Samples were finally analysed via qPCR. Primers were first prepared for 100 pmol/µl (Table 2-10). For each sample, 15 µl of master mix was made up consisting 4 µl RNase free water, 1 µl primer mix and 10 µl Fast SYBR Green Master Mix (Applied Biosystems). This was added to 5 µl DNA per well on a MicroAmp fast optical 96-well reaction plate (Applied Biosystems). The PCR conditions were: 45 cycles of 95 °C for 5 sec, 94 °C for 20 sec, 60 °C for 30 sec, 72 °C for 30 sec, followed by 72 °C for 5 min and was detected on a 7500 Fast Real-Time System (Applied Biosystems). Values were calculated as % input.

The following primers (5' → 3') were used (synthesized and purified by Eurofins MWG Operon):

Name	Sequence
p21 (-2400 bp) for	CTG GAC TGG GCA CTC TTG TC
p21 (-2400 bp) rev	CCC CTT CCT CAC CTG AAA AC
p21 N/S (-50 bp) for	GGC ACT CAG AGG AGG TGA GA
p21 N/S (-50 bp) rev	ACC CGC GCA CTT AGA GAC AC
TIGAR mBS1 (-2062 bp) for	GGA AGA AGG TTG TCC ATT GT
TIGAR mBS1 (-2062 bp) rev	ACA AAG CAA GTT CCA AGT AAA G
TIGAR N/S (-992 bp) for	GTT CTC CAG AGG AGC AAA TAA
TIGAR N/S (-992 bp) rev	CAG GGA CAA AGG TTC TGT ATA A
TIGAR mBS2 (+263 bp) for	GAA GCC GGG TCT TAA ATG TC
TIGAR mBS2 (+263 bp) rev	GGT CAT GTC TTC TCG CAA TG

Table 2-10 Primer sequences for CHIP qPCR

2.2.19 Statistical Analyses

Statistical significance ($p < 0.05$, $p < 0.005$) of differential findings between experimental groups was determined by a Student's t-test using GraphPad software. Error bars represent the standard error of the mean (SEM) of three independent experiments unless otherwise indicated.

Chapter 3 Mechanisms of Control of TIGAR Expression

TIGAR was initially identified in human cells as a target of the tumour suppressor protein p53 (Jen and Cheung 2005; Bensaad et al. 2006). The human *TIGAR* gene possesses two p53-binding sites, hBS1 and hBS2, where hBS2 is the functional p53-binding site (Bensaad et al. 2006). In the mouse genome, *Tigar* also possesses two p53-binding sites, mBS1 and mBS2, arranged in a similar organisation to human *TIGAR*. Little is known about p53-independent expression of TIGAR, although other transcription factors such as SP1 (Zou et al. 2012) and CREB (Zou et al. 2013) have been implicated.

To understand the regulation of TIGAR by p53, the basal expression of TIGAR protein and RNA were first characterised in mouse as well as human tissues. These experiments were followed by an investigation of the induction of TIGAR expression by p53 *in vitro* using cancer cell lines and infrared fluorescent protein (iRFP) reporter assays as well as through the use of a mouse model of intestinal regeneration.

3.1 Basal Expression of TIGAR in Mouse Tissues

Although it has been previously shown that TIGAR is expressed in several mouse tissues (Cheung et al. 2013), the precise expression pattern is not well documented. As such, we undertook a more detailed examination of the relative levels of TIGAR expression across a variety of tissues from wild-type (WT) mice. In this analysis, TIGAR protein levels were detected in all the tissues tested with the highest expression found in muscle and brain (Figure 3-1A). To complement these data, the expression of TIGAR mRNA was assessed in the same tissues in order to compare the observed protein levels to transcriptional activity (Figure 3-1B).

Interestingly, the expression of TIGAR protein was not completely mirrored by mRNA expression. For example, although the expression of TIGAR protein in the liver and pancreas are similar, the mRNA expression of TIGAR was much lower in the pancreas than in the liver (Figure 3-1). This suggests the presence of additional mechanisms such as translational or posttranslational control that regulate TIGAR protein expression in certain tissues.

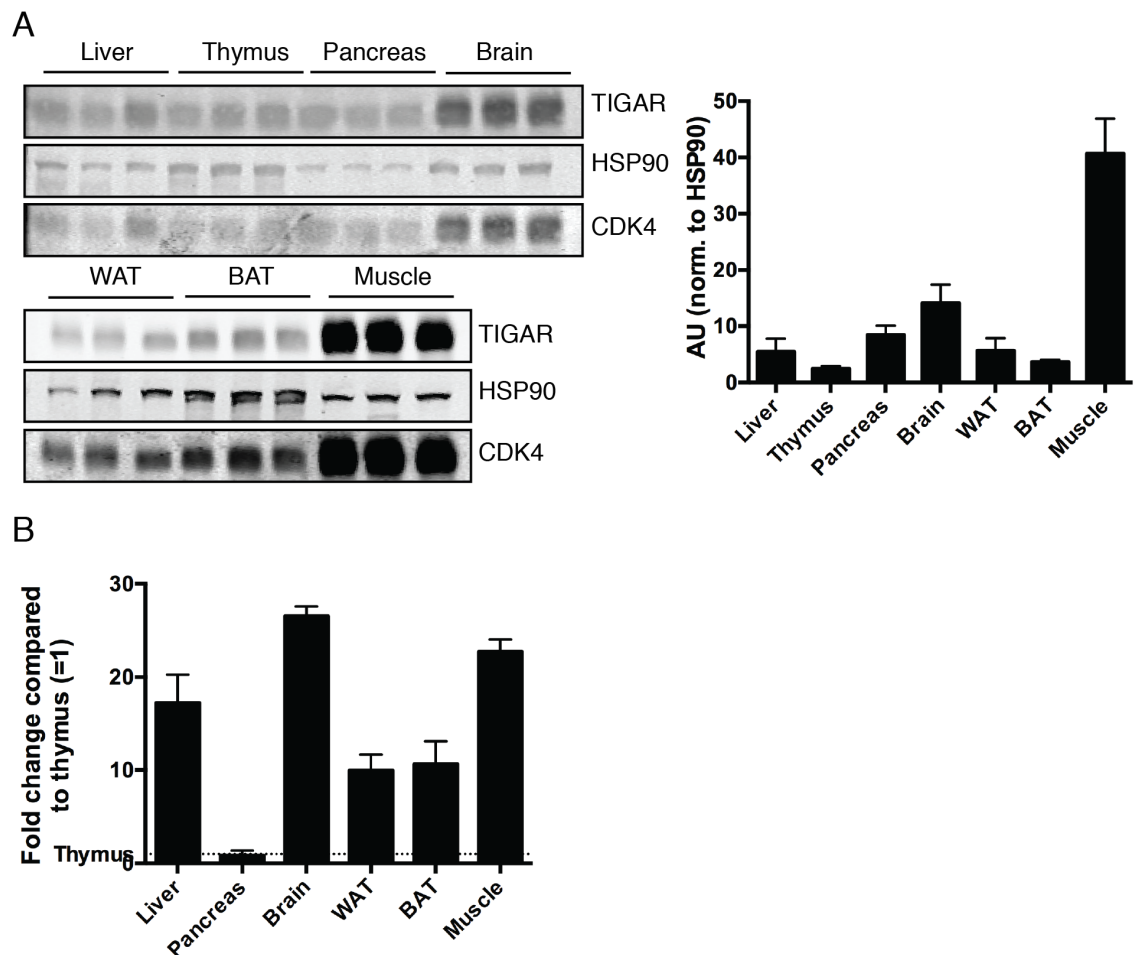


Figure 3-1 Basal TIGAR expression in mouse tissues

Left: Western blot analysis of indicated tissues from three different wild-type (WT) animals. Right: Graph represents quantification of Western blots. Values represent mean \pm SD. $n = 3$ mice. (B) mRNA expression of TIGAR in indicated tissues of WT animals. Values represent mean \pm SEM. $n = 3$ mice with 3 technical replicates.

3.2 Basal Expression of TIGAR in Human Tissues

As in the mouse, the basal expression of TIGAR protein and mRNA were further investigated in human tissues. Both protein and mRNA data sets were obtained from The Human Protein Atlas (<http://www.proteinatlas.org>) and compared with the expression data that we generated in mice (Figure 3-2). Interestingly, while mouse liver showed lower levels of expression in TIGAR compared to the muscle and brain, in human tissues, the liver showed high levels of TIGAR expression. In human tissues, TIGAR RNA did not completely correlate with protein expression. For example, while the protein expression of TIGAR in the spleen is low compared to other tissues, TIGAR RNA expression in the spleen is relatively high. However, for some tissues such as the ovary, TIGAR protein and RNA expression are at similar levels. Based on these observations, we conclude that TIGAR is expressed in all tissues to varying levels.

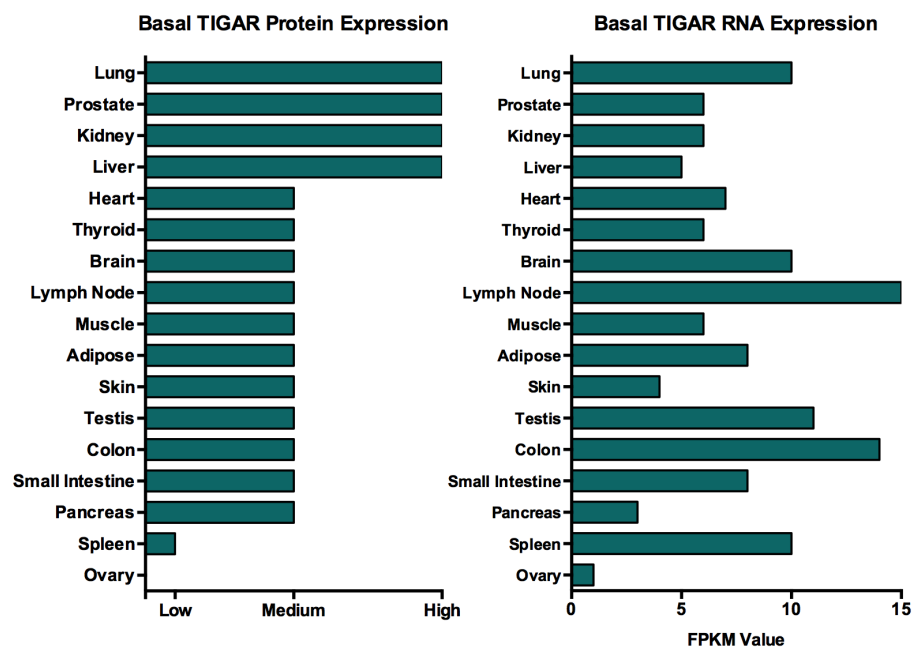


Figure 3-2 Basal TIGAR expression in human tissues

Left: Graph represents basal TIGAR protein expression in various tissues. Scores based on antibody intensity or protein expression in each tissue. Right: Graph represents basal TIGAR RNA expression in various tissues with values calculated as fragments per kilobase of exon per million fragments mapped (FPKM). Data obtained from The Human Protein Atlas.

3.3 Induction of TIGAR Expression by p53

3.3.1 Comparison of Human and Mouse TIGAR p53 Binding Sites

Both human and mouse p53 possess two p53-binding sites, one upstream of the transcriptional start site and one within the first intron (Figure 3-3) (Bensaad et al. 2006). Based on this, and as in human TIGAR, previous work has suggested that murine TIGAR is also a target of p53 (Kimata et al. 2010; Li et al. 2012a; Hamard et al. 2013).

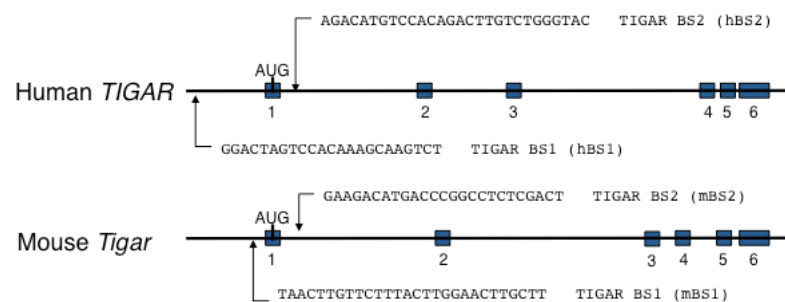


Figure 3-3 The human and mouse TIGAR gene promoter

To investigate the differences between the human (hBS1 and hBS2) and mouse (mBS1 and mBS2) p53-binding sites of TIGAR directly, the sequences corresponding to each of the p53-binding sites were cloned into infrared fluorescent protein (iRFP) reporter constructs (Hock et al. 2014). These constructs were then co-transfected into HCT116 p53-null (HCT116 p53^{-/-}) cells plated on 96-well plates along with increasing amounts of human or mouse p53 (0 – 60 µg). If the reporter is activated by the transcriptional activity of p53, iRFP will be synthesized from the reporter, which can subsequently be measured on an infrared scanner. 24 hours post-transfection, the plates were scanned using an infrared scanner (LI-COR Odyssey) and fluorescence from iRFP was quantified. The major advantage of iRFP fluorescence for reporter assays is the ability to process and quantify data on a high-throughput scale without the need to harvest cells, which reduces sample preparation error. Cells were also harvested 24 hours post-transfection to assess transfection efficiency by analysing the levels of human or mouse p53 protein via Western blot. This Western blot analysis confirmed increasing levels of human or mouse p53 transfection into the cell lines (Figure 3-4C)

Based on the iRFP reporter data (Figure 3-4A-B), we conclude that each of the p53-binding site reporters tested (TIGAR-hBS1, TIGAR-hBS2, TIGAR-mBS1 and TIGAR-mBS2) were activated by both human (hp53) and mouse p53 (mp53). Even so, the responsiveness of each to p53 was different. TIGAR-hBS2, the more efficient of the two human p53 binding sites, for example, was efficiently activated by either human or mouse p53. In contrast, TIGAR-mBS1 was more responsive to both human and mouse p53 than TIGAR-mBS2. It was also slightly more responsive to p53 than TIGAR-hBS1, although it was less active than TIGAR-hBS2. Interestingly, mouse p53 was slightly more effective in the induction of all the binding site reporters with the exception of TIGAR-mBS2 (Figure 3-4A-B). Taken together, the results suggest that the weaker p53-binding site (BS1), located upstream of the promoter, is structurally and functionally conserved between human and mouse but the stronger BS2 in humans is only very weakly active in the mouse.

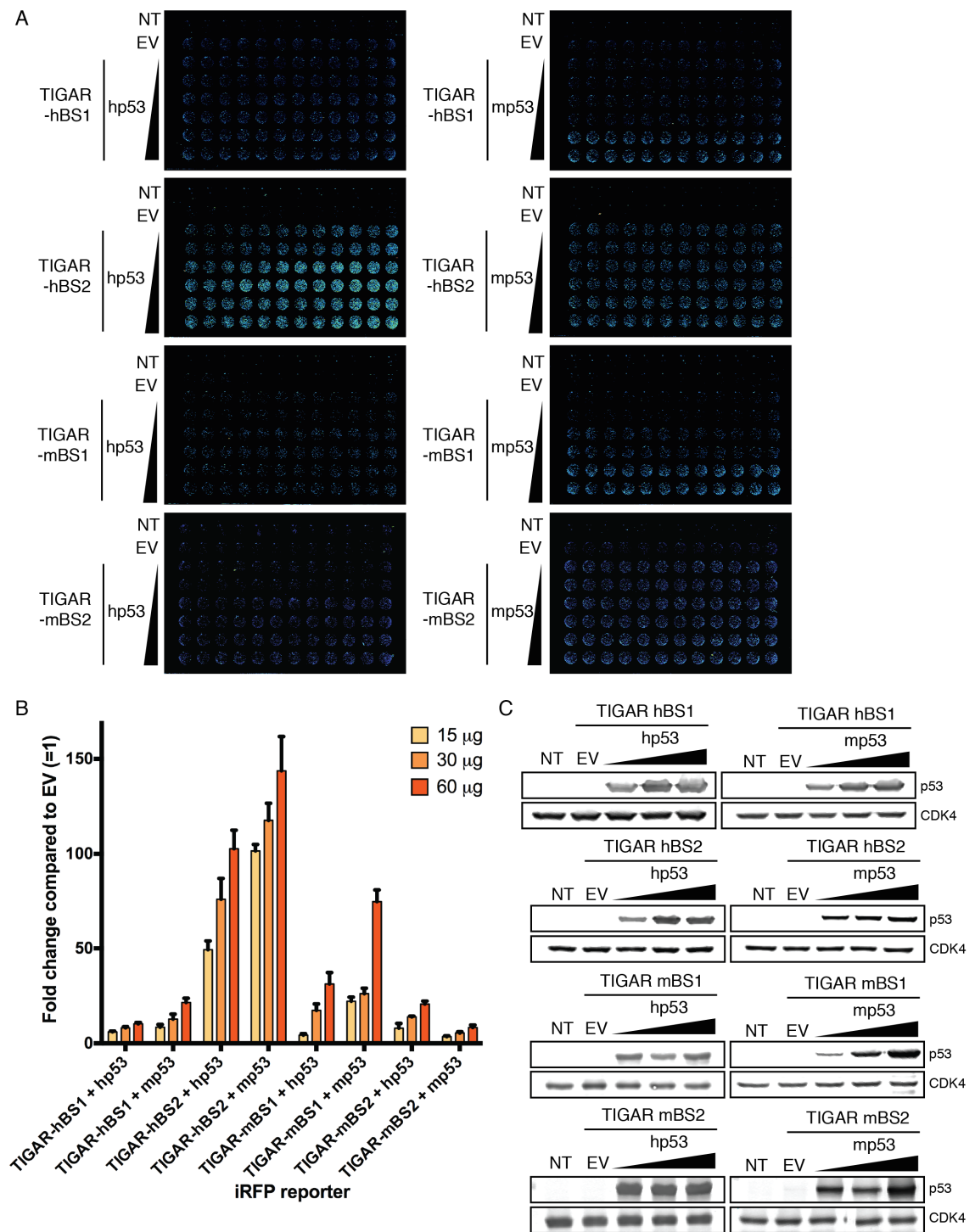


Figure 3-4 Comparison of human and mouse TIGAR p53-binding sites

(A) iRFP reporter assay scans of HCT116 p53^{-/-} cells 24 hr after co-transfection with TIGAR-hBS1, TIGAR-hBS2, TIGAR-mBS1 or TIGAR-mBS2 iRFP reporters and increasing amounts of human or mouse p53. (B) Quantification of iRFP reporter scans. Values represent mean \pm SEM. $n = 3$ independent experiments with at least 12 technical replicates. (C) Western blot analysis of HCT116 p53^{-/-} cells transfected with increasing amounts of human or mouse p53. $n = 2$ independent experiments. NT, non-transfected. EV, empty vector.

3.3.2 Activation of TIGAR by p53 *in vitro*

While the data from the iRFP reporter assays suggest that mouse TIGAR is not as strongly induced by p53 as human TIGAR, several published studies have shown that endogenous mouse TIGAR is responsive to the transcriptional activity of p53 (Li et al. 2012a; Hamard et al. 2013). In line with this model, p53-deficient mice lose the ability to induce TIGAR expression following myocardial injury (Kimata et al. 2010; Hoshino et al. 2012). However, it has also been shown that TIGAR can be induced in mouse primary neurons following oxygen and glucose deprivation/reoxygenation in a p53-independent manner (Li et al. 2014b).

To compare the induction of TIGAR in human and mouse cells by p53 activation, a panel of human and mouse fibroblasts were treated with the drug cisplatin. Cisplatin causes genotoxic stress by binding to and distorting the structure of the DNA complex, which results in the activation of p53 (Zamble et al. 1998). Subsequently, the induction of TIGAR protein and mRNA were assessed and compared to the response of the well-established p53 target gene, p21.

For this experiment, human tert-immortalized fibroblasts (TIFs) were treated with increasing concentrations of cisplatin. Low doses of cisplatin were used to induce genotoxic stress and cause p53-induced cell cycle arrest and DNA repair rather than apoptosis (Zamble et al. 1998; Offer et al. 2002).

TIFs showed an increase in p53 protein level, as expected when inducing genotoxic stress. Moreover, an increased expression of both p21 and TIGAR protein were observed after cisplatin treatment (Figure 3-5A). Furthermore, human TIFs showed a significant increase in p21 and TIGAR mRNA after cisplatin treatment, although the promotion of p21 mRNA was far greater than that for TIGAR (Figure 3-5B).

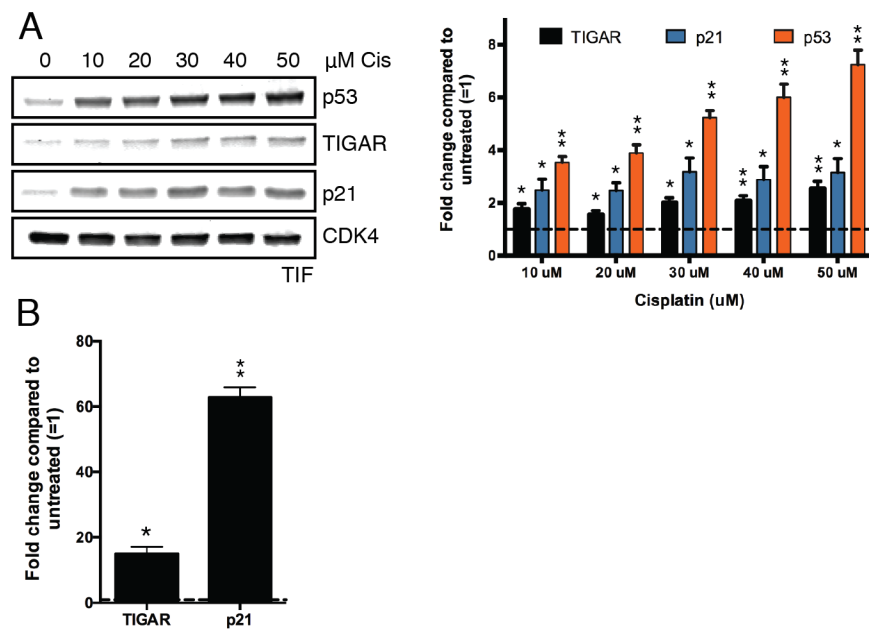


Figure 3-5 TIGAR expression in response to p53 activation in human TIFs

(A) Left: Western blot analysis of tert-immortalised fibroblasts (TIFs) treated with indicated concentrations of cisplatin (cis) for 24 hr. Right: Graph represents quantification of Western blots with fold change compared to untreated. Values represent mean \pm SEM. $n = 3$ independent experiments. (B) mRNA expression of TIGAR and p21 following 24 hr of cisplatin (cis) treatment (50 μM) in TIFs. Values represent mean \pm SEM. $n = 3$ independent experiments with 3 technical replicates. * $p < 0.05$, ** $p < 0.005$ compared to untreated.

For comparison, mouse 3T3s were similarly treated with cisplatin in order to induce genotoxic stress but not induce cell death. Following treatment with cisplatin, an elevation in both p53 and p21 protein were observed much like previously seen in the human TIFs. However, the expression of TIGAR protein was unaffected after treatment in these cells (Figure 3-6A). Mouse 3T3s also showed a significant increase in p21 mRNA expression but no significant increase in TIGAR mRNA after cisplatin treatment (Figure 3-6B). Combined, these observations suggest differences between the regulation of TIGAR in human and mouse cell lines in response to genotoxic stress.

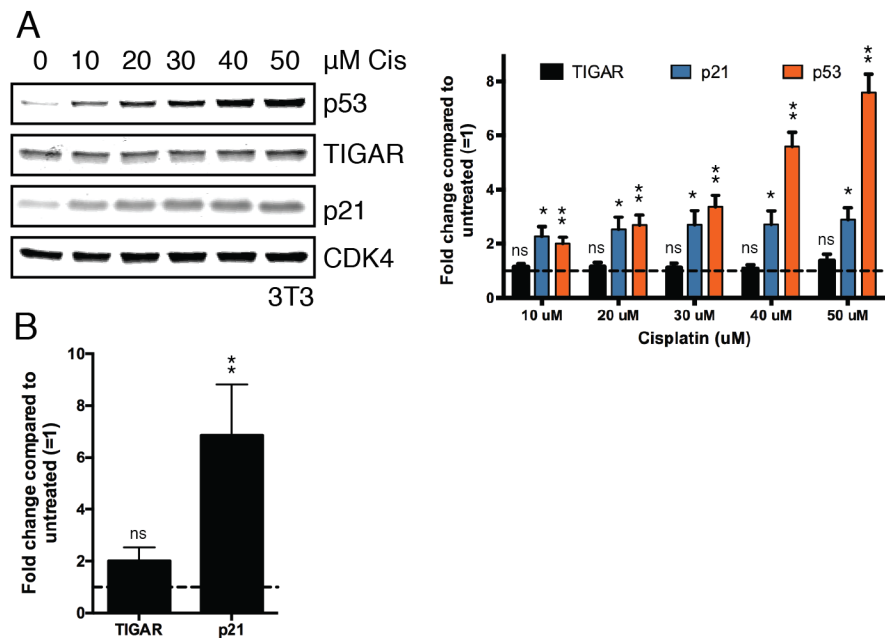


Figure 3-6 TIGAR expression in response to p53 activation in mouse 3T3s
 (A) Left: Western blot analysis of 3T3s treated with indicated concentrations of cisplatin (cis) for 24 hr. Right: Graph represents quantification of Western blots with fold change compared to untreated. Values represent mean \pm SEM. n = 3 independent experiments.
 (B) mRNA expression of TIGAR and p21 following 24 hr of cisplatin (cis) treatment (50 μM) in 3T3s. Values represent mean \pm SEM. n = 3 independent experiments with 3 technical replicates. *p < 0.05, **p < 0.005 compared to untreated. NS, not significant.

Most of the previous studies showing a p53-dependent induction of TIGAR expression in mouse cells were carried out *in vivo* (Li et al. 2012a; Hamard et al. 2013), possibly suggesting that this response could be limited to cells in a more physiologically normal environment. To further investigate p53-dependent activation of TIGAR in mouse cells, an *in vitro* intestinal crypt culture model using small intestinal crypts derived from wild-type mice was also tested for TIGAR expression in response to cisplatin. Intestinal crypts were treated with 50 μM cisplatin for 24 hours, a protocol that did not induce major cell death (Figure 3-7A). As seen in the 3T3s, cisplatin treatment on the intestinal crypts was able to induce the expression of p53 and p21, but no obvious induction of TIGAR protein was observed (Figure 3-7B). These results suggest that p53 activation in mouse cells in culture does not consistently induce TIGAR expression.

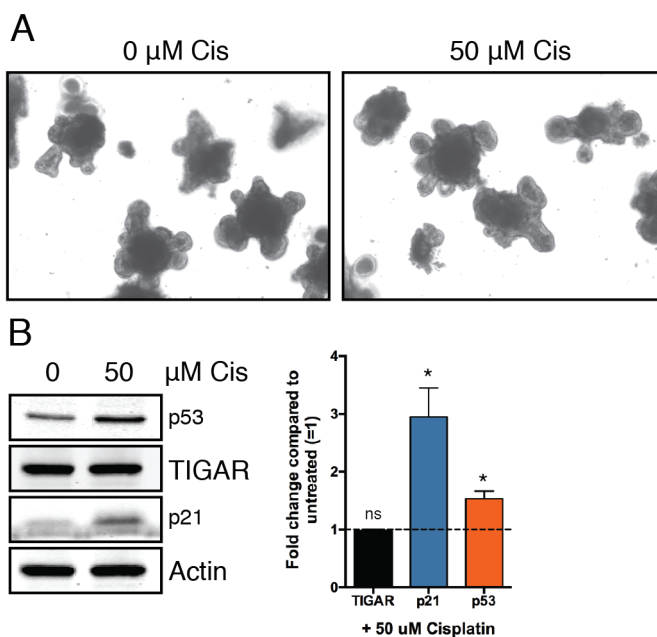


Figure 3-7 TIGAR expression in response to p53 activation in intestinal crypt organoids

(A) Brightfield images of small intestinal crypt organoids obtained from wild-type (WT) mice treated with 50 μM cisplatin (cis) for 24 hr. (B) Left: Western blot analysis of small intestinal crypt organoids treated with 50 μM cisplatin (cis) for 24 hr. Right: Graph represents quantification of Western blots with fold change compared to untreated. Values represent mean \pm SEM. $n = 3$ independent experiments. * $p < 0.05$, ** $p < 0.005$ compared to untreated. NS, not significant.

To determine whether p53 can bind to either of the two putative binding sites in the mouse *Tigar* promoter (mBS1 and mBS2), chromatin-immunoprecipitation (ChIP) was carried out in mouse 3T3 cells treated with cisplatin for 24 hours to activate p53. Quantitative PCR (qPCR) was then performed for mBS1 (-2062 bp) and mBS2 (+263 bp). A p53-responsive element on the *p21* promoter (-2400 bp) was used as a positive control while non-specific (N/S) binding regions on the *Tigar* (-992 bp) and *p21* promoter (-50 bp) were used as regions where no binding should occur (negative controls). While p53 was clearly recruited to the *p21* promoter following cisplatin treatment, no increased binding of p53 to either mBS1 or mBS2 could be detected in these cells (Figure 3-8). The failure to recruit p53 to the *Tigar* promoter explains the observed failure of p53 to activate the expression of mouse TIGAR seen in several cell types *in vitro*.

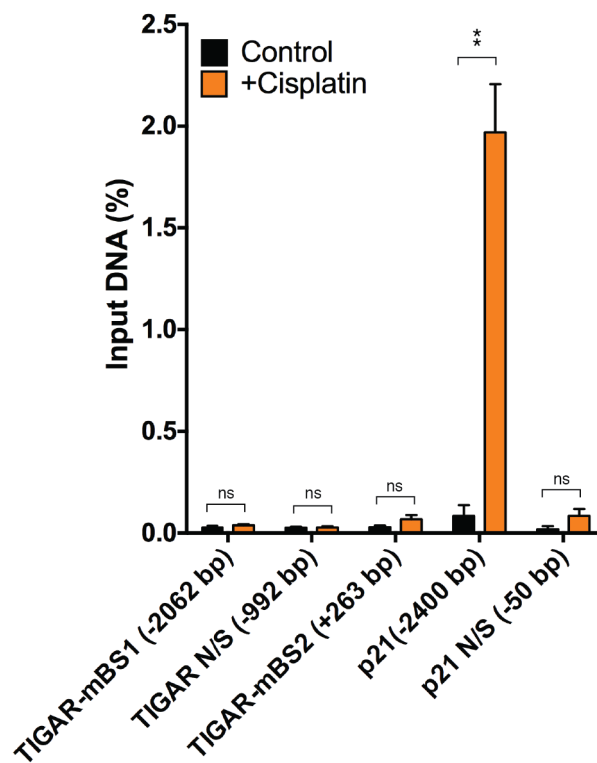


Figure 3-8 p53 does not bind to the *Tigar* promoter after cisplatin treatment
Chromatin-immunoprecipitation (ChIP) was performed for p53 along with qPCR for mBS1 (-2062 bp), mBS2 (+263 bp), a p53-response element on the *p21* promoter (-2400 bp) and non-specific (N/S) binding regions on the *Tigar* (-992 bp) and *p21* promoter (-50 bp), using 3T3s treated with 50 μ M cisplatin for 24 hr. Values represent mean \pm SEM. n = 3 independent experiments with 2 technical replicates. *p < 0.05, **p < 0.005 compared to control. NS, not significant.

To better understand the role of the second p53-binding site (hBS2 and mBS2) in modulating TIGAR expression, its conservation was investigated across additional mammalian species. Much like observed in human and mouse, canine *TIGAR* consists of six exons. Using the BioBase Match transcription factor programme (<http://www.gene-regulation.com/cgi-bin/pub/programs/match/bin/match.cgi>) and analysing the sequence upstream and downstream of the canine *TIGAR* promoter, one potential p53-binding site was found. Interestingly, this binding site was closer to the location of mBS1 in mouse *Tigar* than hBS1 in human *TIGAR* (Figure 3-9). However, no predicted second p53-binding site was found in an analogous position to the mouse or human BS2.

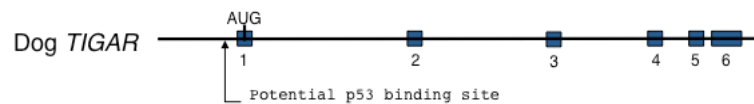


Figure 3-9 Organization of the dog *TIGAR* gene

We investigated the single predicted potential p53-binding site in canine TIGAR using Madin-Darby canine kidney (MDCK) cells. To test whether activation of dog TIGAR is reliant on p53, MDCK cells were treated with cisplatin for 24 hours to induce a p53 response without inducing cell death. MDCK cells showed an induction in p53 expression, although this was only weakly detected by Western blot, as well as a strong elevation in p21 expression. However, no increase in TIGAR protein levels were observed (Figure 3-10), suggesting that p53 does not obviously induce TIGAR expression in canine cells. Interestingly, these cells showed very high basal expression of TIGAR.

Taken together, our data suggest that the p53-binding site located within the first intron of human TIGAR (BS2) is particularly important in promoting p53-driven expression of TIGAR and that other species lack a strongly p53-responsive site in the TIGAR promoter.

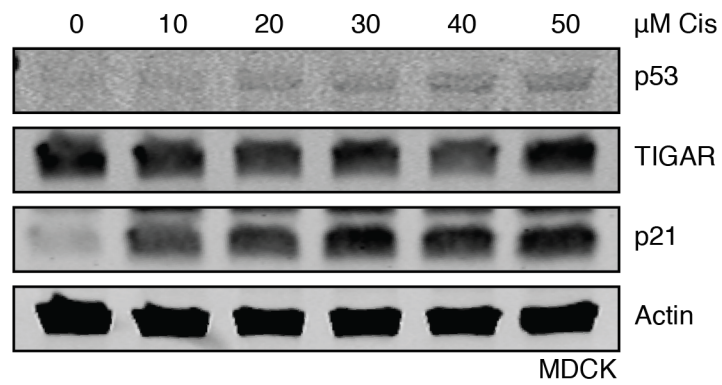


Figure 3-10 TIGAR expression in response to p53 activation in MDCK cells
Western blot analysis of MDCK cells treated with indicated concentrations of cisplatin (cis) for 24 hr. n = 3 independent experiments.

3.3.3 Activation of TIGAR *in vivo*

To examine the induction of TIGAR *in vivo*, tissue regeneration in the murine small intestine was analysed as a model organ system. In this model, damage caused by treatment with cisplatin or irradiation is sufficient to cause tissue ablation and to initiate regeneration. Following damage, a period of recovery ensues, during which rapid tissue regeneration occurs (Martin et al. 1998; Potten and Grant 1998; Metcalfe et al. 2014).

In wild-type (WT) mice, small intestinal regeneration is characterized by a rapid regrowth of intestinal crypts, which can be observed 72 hours following treatment with cisplatin or irradiation (IR) (Martin et al. 1998; Ashton et al. 2010; Cheung et al. 2013). TIGAR expression was found relatively low in the untreated small intestines and localised to the intestinal crypts where most proliferation occurs (Figure 3-11). Following cisplatin treatment or IR, we observed a marked increase in TIGAR expression within the intestinal crypts. This is in contrast to our *in vitro* data. It is not clear why the cisplatin-dependent induction of TIGAR was only seen *in vivo*, and not in cultured cells, although this may be due to differences in cell type or culture conditions (Figure 3-11).

Taken together, these results suggest that TIGAR expression is induced in the mouse in response to stress but that this may reflect a p53 independent response. This hypothesis was therefore investigated further in the next chapters.

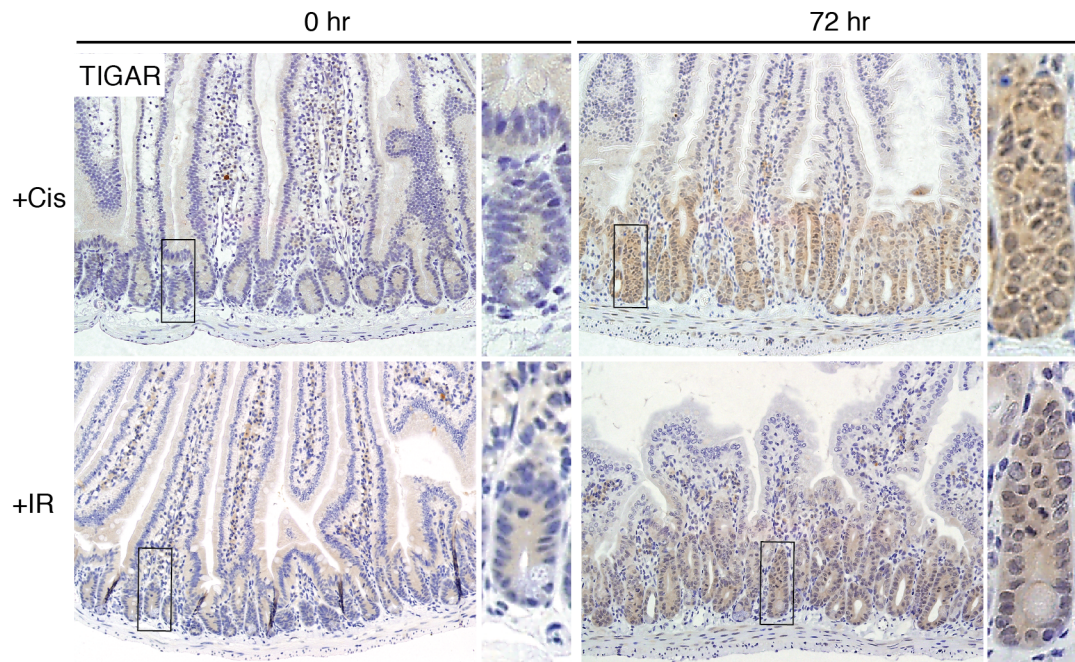


Figure 3-11 TIGAR expression in the small intestine after acute tissue damage

Immunohistochemistry for TIGAR on wild-type (WT) animals before and after 72 hr cisplatin (+Cis) or 14 Gy irradiation (+IR) treatment. Panels show more detailed crypt structures indicated in the box. $n = 3$ mice per genotype per condition, each stained 3 times.

3.4 Summary and Discussion

In humans, TIGAR is a p53 target gene that has been found to play a role in cell survival during conditions of mild stress (Bensaad et al. 2006; Bensaad et al. 2009; Lui et al. 2011; Cheung et al. 2012; Wanka et al. 2012; Lee et al. 2014). Here the mechanisms by which TIGAR is induced were investigated in human and mouse cells.

The basal expression of TIGAR protein and RNA were first investigated in various human and mouse tissues. While tissues such as the pancreas showed medium levels of TIGAR protein and RNA in both species compared to other tissues, the expression of TIGAR in human liver was high but low in mouse liver. Furthermore, the TIGAR RNA expression did not completely correlate with protein expression in both human and mouse tissues. For example, in the mouse liver and human spleen, TIGAR RNA levels were high compared to other tissues but TIGAR protein expression was relatively low. This suggests additional mechanisms by which TIGAR expression can be regulated, which may include protein degradation. To address this, the half-life of TIGAR was investigated in cultured cells by inhibiting proteasomal degradation using cycloheximide and assessing TIGAR levels over time. TIGAR was noted to be very stable in these experiments (data not shown).

The ability of p53 to induce TIGAR expression was then investigated in cultured human and mouse cells. These studies did not show a clear p53-dependent increase in TIGAR expression in mouse cells. Upon closer examination of the transcriptional control regions of human and mouse TIGAR, the principal p53-responsive element in human TIGAR was found to be not well conserved in mouse TIGAR and much less responsive to mouse p53. However, the second, weaker binding site in humans seems to be conserved and somewhat more responsive to p53 in the mouse. Even so, overall the p53-binding sites in the human TIGAR promoter appear to be more responsive than those found in the mouse. Despite the inability of p53 to induce TIGAR in mouse cells following cisplatin treatment, TIGAR expression was clearly induced in the small intestine following cisplatin treatment or irradiation *in vivo* using a model of intestinal regeneration. This suggests that TIGAR expression can be induced in the mouse in response to stress although this may through a p53-independent stress response.

Chapter 4 Regulation of TIGAR by p53 Family Members

While TIGAR was identified as a transcriptional target of p53 in human cells (Jen and Cheung 2005; Bensaad et al. 2006), my studies showed that in mouse cells, TIGAR is less responsive to p53 activation following cisplatin treatment. This observation was further supported by ChIP experiments in mouse cells following cisplatin treatment where p53 was not recruited to the *Tigar* promoter. Combined, these findings illustrate differences in the human and mouse TIGAR promoter *in vitro*.

Even so, following either cisplatin treatment or irradiation *in vivo*, TIGAR expression was clearly elevated in the mouse small intestine. These results suggest that the responsiveness of TIGAR to p53 may be limited to the *in vivo* situation, or that the expression of p53 in mouse cells and tissue is regulated through alternative mechanisms. Other members of the p53 family (p63 and p73) are able to activate promoters of p53 targets such as p21 (Yang et al. 1998; Lee and La Thangue 1999) and can contribute to the regulation of metabolic genes (Sabbisetti et al. 2009; Du et al. 2013; Giacobbe et al. 2013; Agostini et al. 2014; Amelio et al. 2014; D'Alessandro et al. 2014; Velletri et al. 2015). It is therefore possible that p63 and/or p73 could regulate TIGAR expression.

To understand the regulation of TIGAR by p53 *in vivo*, the induction of TIGAR was assessed in p53-deficient mice. At the same time, the induction of TIGAR expression by other p53 family members was investigated *in vitro* using cancer cell lines and iRFP reporter assays. The expression of TIGAR was also investigated in animals deficient in the p53 family member TAp73, as well as those lacking both p53 and TAp73.

4.1 Loss of p53 does not Affect TIGAR *in vivo*

As shown in Chapter 3, we found that TIGAR levels increased in the crypts of WT mice during intestinal regeneration following tissue ablation by irradiation (IR) or cisplatin treatment (Figure 3-11). Since others have shown an upregulation of p53 in the small intestine following IR (Merritt et al. 1994), the ability of TIGAR expression to be controlled by p53 *in vivo* was examined in this system. TIGAR protein levels were first assessed in various organs of WT and p53-deficient ($p53^{-/-}$) mice to see whether loss of p53 would affect basal TIGAR expression. No significant reduction in TIGAR expression was observed in response to p53 loss at either the protein or mRNA level, with a possible exception of a slight reduction in TIGAR mRNA in $p53^{-/-}$ muscle (Figure 4-1). By contrast, p21 showed a very clear decrease in mRNA expression in all the $p53^{-/-}$ organs examined.

To extend these characterization studies, we proceeded to test whether increased TIGAR expression in the regenerating intestinal system was p53-dependent (Figure 3-11). A comparison of WT and $p53^{-/-}$ mice showed normal crypt architecture and similar levels of proliferation in each cohort, as indicated by immunohistochemistry staining for the proliferative marker Ki67 under unstressed conditions (Figure 4-2). The basal expression of p53, p21 and TIGAR protein were also low in the crypts of both WT and $p53^{-/-}$ animals under unstressed conditions (Figure 4-3, Figure 4-4, Figure 4-5). Tissue ablation of the intestinal epithelium was then performed by IR, followed by 72 hours of recovery. As shown by others (Merritt et al. 1994), small intestines of both WT and $p53^{-/-}$ animals undergo rapid proliferation during their tissue regeneration as observed through increased Ki67 staining (Figure 4-2). The loss of p53 in the $p53^{-/-}$ animals was confirmed through immunohistochemistry where only WT animals showed an increase in p53 after IR (Figure 4-3). Furthermore, the induction of p21 after irradiation was clearly reduced in the $p53^{-/-}$ animals, again supporting the loss of p53 transcriptional activity in $p53^{-/-}$ mice (Figure 4-4). In contrast to p21, the expression of TIGAR was increased in the intestinal crypts of both WT and $p53^{-/-}$ animals (Figure 4-5). These data show that p53 is not necessary to maintain the basal expression of TIGAR or induce TIGAR levels following tissue damage in the small intestine such as through irradiation.

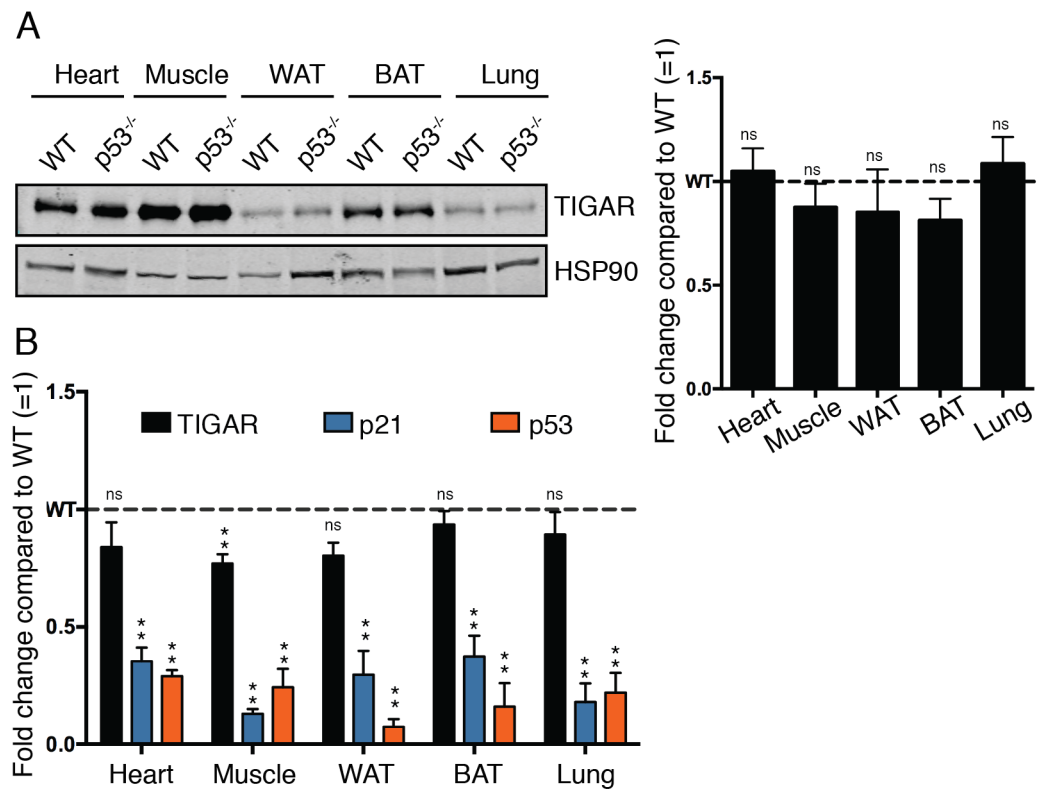


Figure 4-1 Basal TIGAR expression in $p53$ -null animals

(A) Left: Western blot analysis of TIGAR protein expression in organs of wild-type (WT) and $p53^{-/-}$ mice. Right: Graph represents quantification of Western blots with fold change compared to WT. Values represent mean \pm SEM. $n = 3$ mice per genotype. (B) mRNA expression of TIGAR, p21 and p53 in organs of WT and $p53^{-/-}$ mice. Values represent mean \pm SEM. $n = 3$ mice per genotype with 3 technical replicates. * $p < 0.05$, ** $p < 0.005$ compared to WT. NS, not significant. WAT, white adipose tissue. BAT, brown adipose tissue.

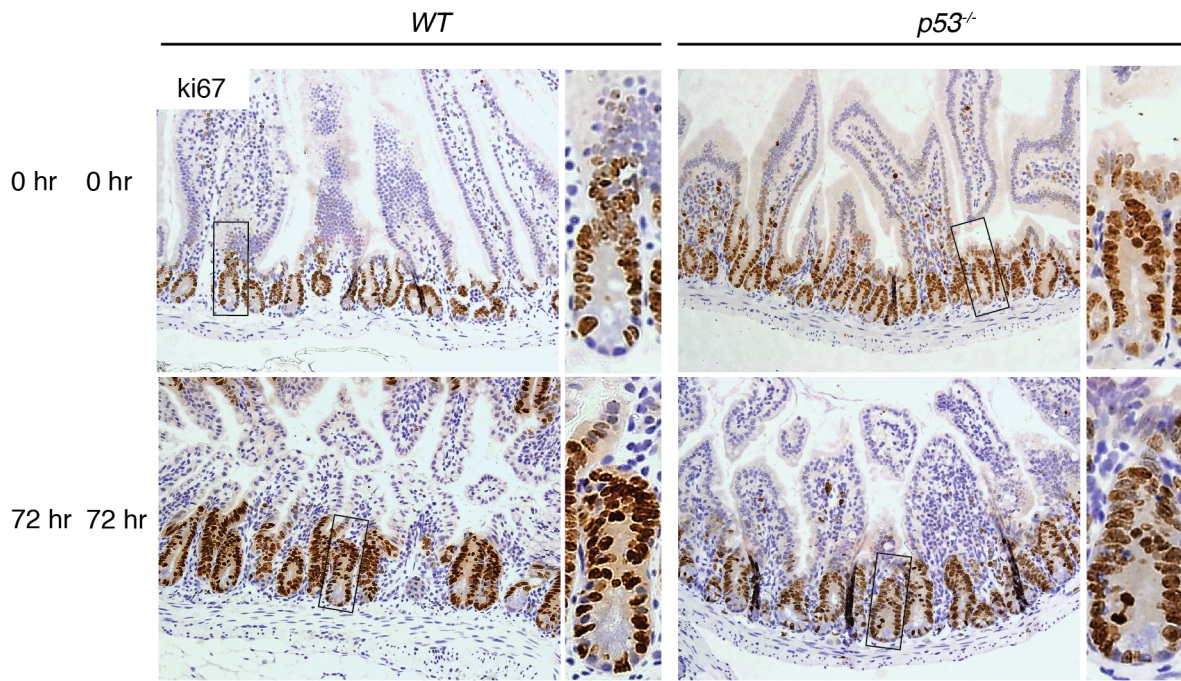


Figure 4-2 Ki67 expression in $p53^{-/-}$ small intestine after irradiation

Immunohistochemistry for Ki67 on small intestines from wild-type (WT) and $p53^{-/-}$ animals 72 hr after 10 Gy IR. Panels show more detailed crypt structures indicated in the box. $n = 3$ mice per genotype per condition.

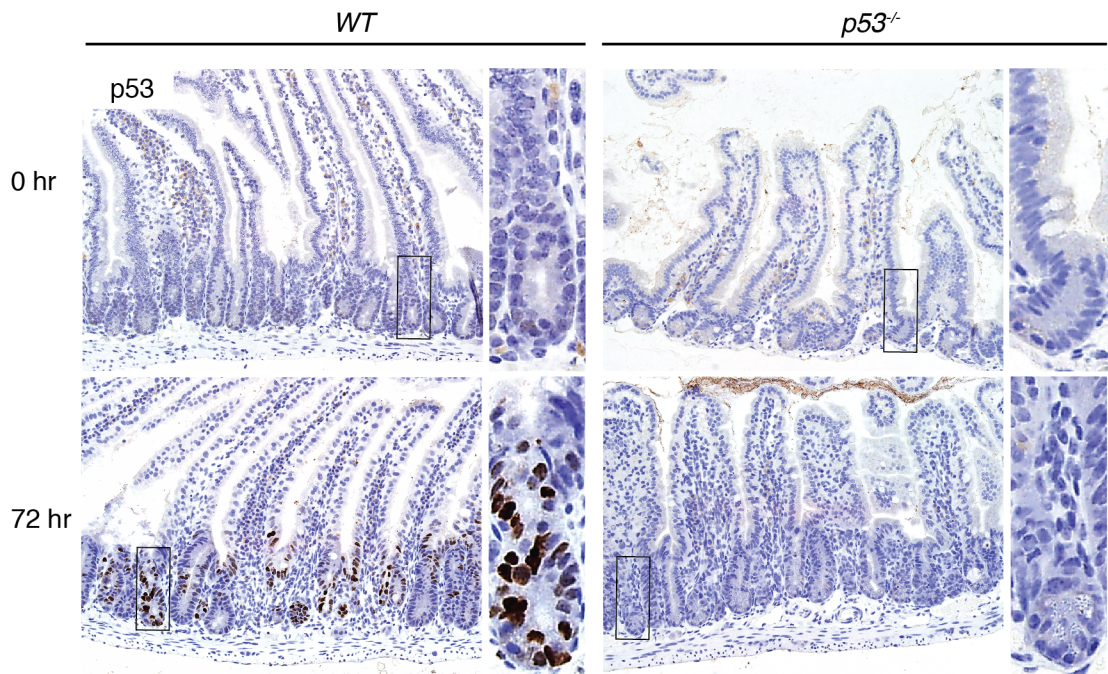


Figure 4-3 p53 expression in $p53^{-/-}$ small intestine after irradiation

Immunohistochemistry for p53 on small intestines from wild-type (WT) and $p53^{-/-}$ animals 72 hr after 10 Gy IR. Panels show more detailed crypt structures indicated in the box. $n = 3$ mice per genotype per condition.

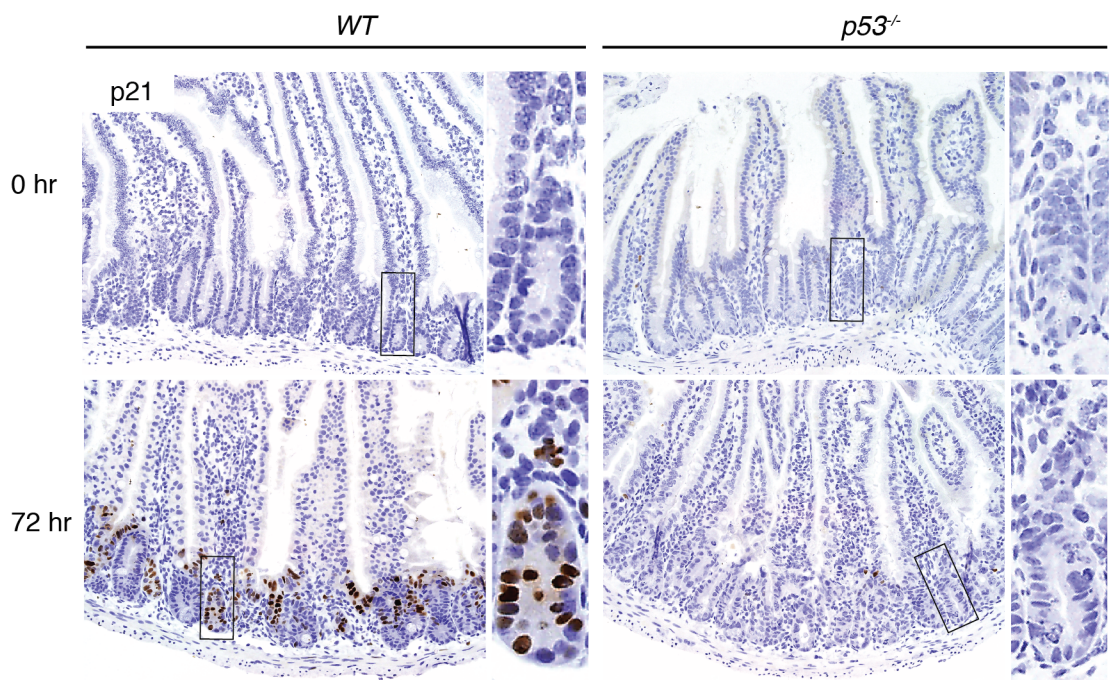


Figure 4-4 p21 expression in $p53^{-/-}$ small intestine after irradiation

Immunohistochemistry for p21 on small intestines from wild-type (WT) and $p53^{-/-}$ animals 72 hr after 10 Gy IR. Panels show more detailed crypt structures indicated in the box. $n = 3$ mice per genotype per condition.

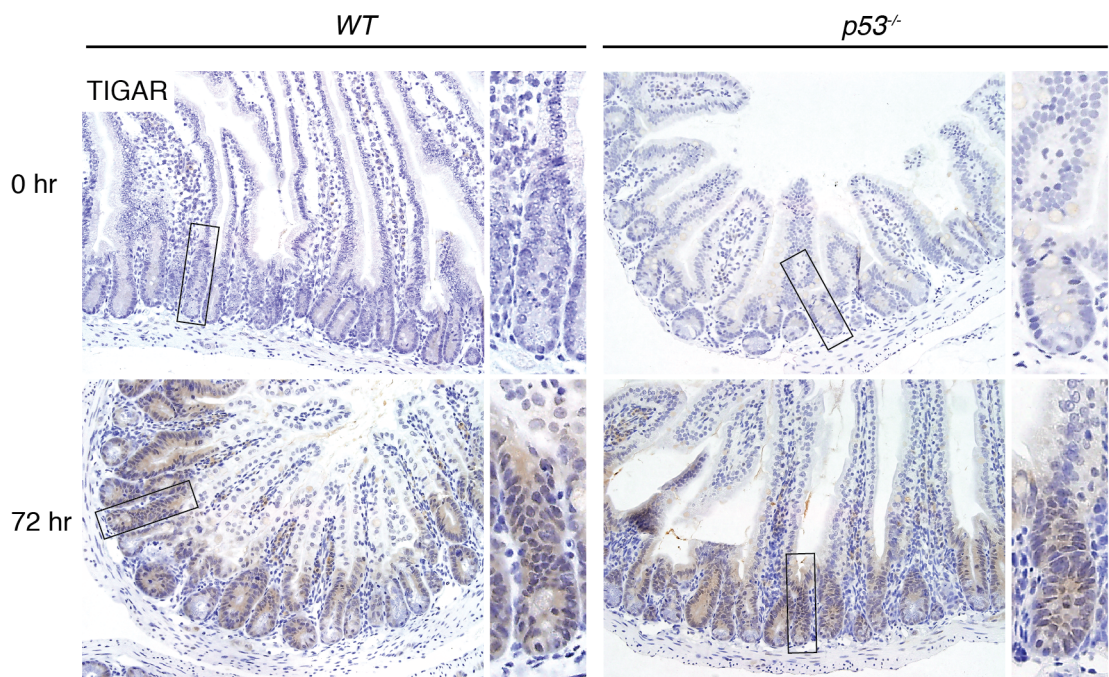


Figure 4-5 TIGAR expression in $p53^{-/-}$ small intestine after irradiation

Immunohistochemistry for TIGAR on small intestines from wild-type (WT) and $p53^{-/-}$ animals 72 hr after 10 Gy IR. Panels show more detailed crypt structures indicated in the box. $n = 3$ mice per genotype per condition, each stained 2 times.

The regulation of TIGAR by p53 *in vivo* was then further investigated through an independent method. This was achieved using a system where the Cre recombinase transgene is placed under the control of the *Cyp1A1* aryl hydrocarbon-responsive promoter (*AhCre*) (Ireland et al. 2004) with an *Mdm2*^{fl^{ox}} (Grier et al. 2006). Cre-mediated excision of *Mdm2* was induced by injection of β -naphthoflavone, which resulted in Cre expression within the small intestinal crypt as well as in hepatocytes (Ireland et al. 2004). MDM2 is a negative regulator of p53 and whole body loss of MDM2 is embryonic lethal due to high levels of p53 and subsequently, unregulated apoptosis (Jones et al. 1995; Montes de Oca Luna et al. 1995). As p53 levels are increased upon MDM2 deletion, the ability of p53 to upregulate TIGAR in the small intestine was assessed in this model.

Comparison of WT and *AhCre*⁺ *Mdm2*^{fl/fl} animals showed normal crypt architecture. While p53 expression was mildly elevated in the *AhCre*⁺ *Mdm2*^{fl/fl} (Figure 4-6), its target gene, p21, showed a significant increase in expression (Figure 4-7). As seen in the *p53*^{-/-} animals following irradiation, changes in p53 expression due to MDM2 loss did not alter the levels of TIGAR protein (Figure 4-8). These data further support the conclusion that p53 does not activate TIGAR in the mouse small intestine.

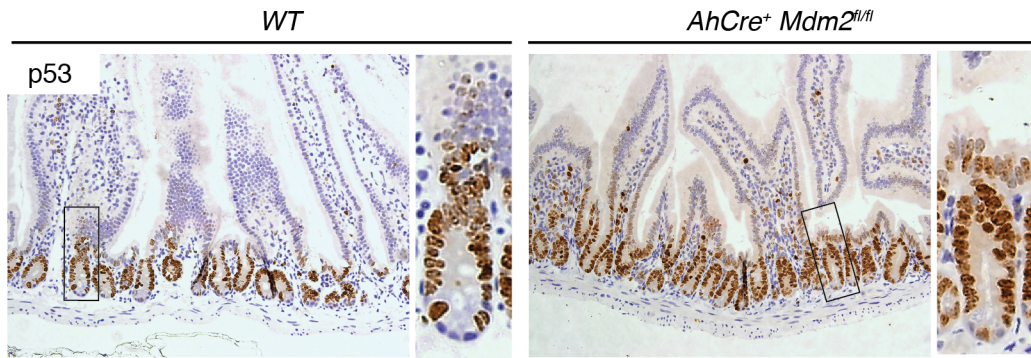


Figure 4-6 p53 expression in *AhCre⁺ Mdm2^{fl/fl}* small intestine

Immunohistochemistry for p53 on small intestines from wild-type (WT) and *AhCre⁺ Mdm2^{fl/fl}*. Panels show more detailed crypt structures indicated in the box. n = 3 mice per genotype.

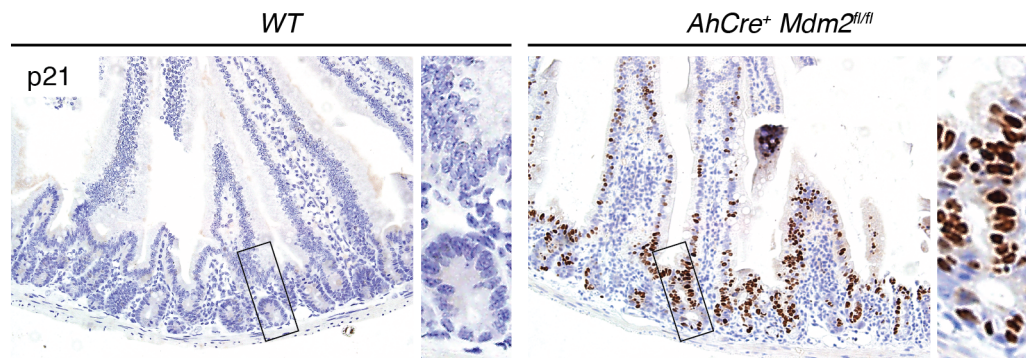


Figure 4-7 p21 expression in *AhCre⁺ Mdm2^{fl/fl}* small intestine

Immunohistochemistry for p21 on small intestines from wild-type (WT) and *AhCre⁺ Mdm2^{fl/fl}*. Panels show more detailed crypt structures indicated in the box. n = 3 mice per genotype.

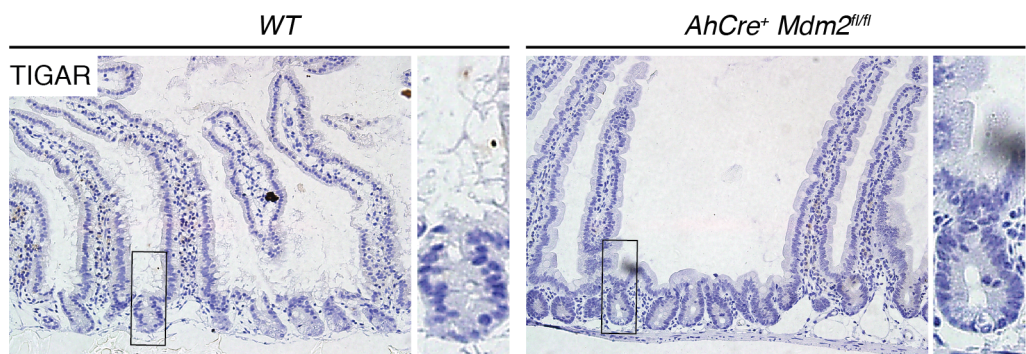


Figure 4-8 TIGAR expression in *AhCre⁺ Mdm2^{fl/fl}* small intestine

Immunohistochemistry for TIGAR on small intestines from wild-type (WT) and *AhCre⁺ Mdm2^{fl/fl}*. Panels show more detailed crypt structures indicated in the box. n = 3 mice per genotype, each stained 2 times.

4.2 Activation of TIGAR by Other p53 Family Members *in vitro*

As p53 did not seem to regulate the expression of TIGAR in mouse cells *in vitro* or *in vivo*, the potential role of other p53 family members in regulating TIGAR was examined. Firstly, the functional human p53-binding site iRFP reporter (TIGAR-hBS2) was co-transfected with p53, TAp63 α or TAp73 α into cells to assess transcriptional activity. As positive controls, iRFP expression constructs containing p53 response element encoding repeats of a known p53 binding sequence (p53RE), the p53-binding site of p21 (WAF1) (el-Deiry et al. 1993) and a p63 response element from the skin-specific promoter of bullous pemphigoid antigen 1 (BPAG1) (Osada et al. 2005a) were used. 24 hours post-transfection, plates were scanned using an infrared scanner (LI-COR Odyssey) and readings were quantified with the LI-COR software. Both TAp63 α and TAp73 α induced a response from the human TIGAR-hBS2 iRFP reporter construct, although the activity of TAp63 α was extremely weak (Figure 4-9A-B). The pattern of expression observed from the TIGAR-hBS2 iRFP reporter was similar to that seen with the p53RE or WAF1, where p53 was the most efficient, followed by TAp73 α , then TAp63 α . Strong activity for TAp63 α was only measured using the BPAG1 promoter, although even here TAp73 α was more active. As an additional control, transfection efficiency of each construct was assessed through Western blotting (Figure 4-9C).

In light of these results, p73 isoforms were further investigated as potential activators of TIGAR expression using both human TIGAR-hBS2 as well as mouse TIGAR-mBS1 and TIGAR-mBS2 iRFP reporters. The TAp73 α isoform has been shown to contain an inhibitory domain that limits its activity, making it less efficient than other p73 isoforms (Liu and Chen 2005). Therefore, the activity of p73 isoforms, TAp73 α , TAp73 β , TAp73 γ or Δ Np73 α , were examined in these assays. While full length TAp73 isoforms can induce p53 target genes (Zhu et al. 1998), Δ Np73 isoforms, which lack the N-terminal activation domain (Ishimoto et al. 2002), have been shown to inhibit TAp73 transcriptional activity along with regulating an additional set of target genes (Liu et al. 2004). As expected (Nozell et al. 2003; Moll and Slade 2004), TAp73 β was consistently more effective in driving iRFP expression from p53RE, WAF1 or BPAG1 promoters. In these

assays, TAp73 γ and Δ Np73 α did not show strong transcriptional activity. Turning to the reporter constructs containing TIGAR p53-binding sites (hBS2, mBS1 and mBS2), TAp73 α was more effective at inducing expression from TIGAR-hBS2, while both TAp73 α and TAp73 β modestly induced expression from TIGAR-mBS1 and TIGAR-mBS2 (Figure 4-10A-B). Again, transfection efficiency was assessed through Western blotting (Figure 4-10C). Taken together, these data suggest that TAp73 has the capability to drive the expression of both mouse and human TIGAR.

As the reporter assays suggested that TAp73 isoforms may drive the expression of human TIGAR, this was further assessed using p53-null Saos-2 inducible cell lines where treatment with doxycycline induced the expression of p53, HA-tagged TAp73 α , HA-tagged TAp73 β or HA-tagged TAp73 γ isoforms. Cells were treated for up to 24 hours with 0.2 μ g/ml doxycycline (Dox) and protein expression of inducible p53, TAp73 α , TAp73 β or TAp73 γ was observed. The expression of p21, a target gene of both p53 and p73, increased following Dox induction (Figure 4-11). However, while TAp73 α , TAp73 β and TAp73 γ were able to activate the TIGAR-hBS2 iRFP reporter in cells, following gene induction in the Saos-2 inducible cells, only p53 was able to promote the expression of TIGAR protein (Figure 4-11). This reflects previous observations in the iRFP reporter assays, where p53 allowed for a stronger activation of the TIGAR reporter than TAp73 α . Altogether, these findings suggest that p53 predominantly regulates the expression of TIGAR rather than its family members, p63 and p73, in human cells.

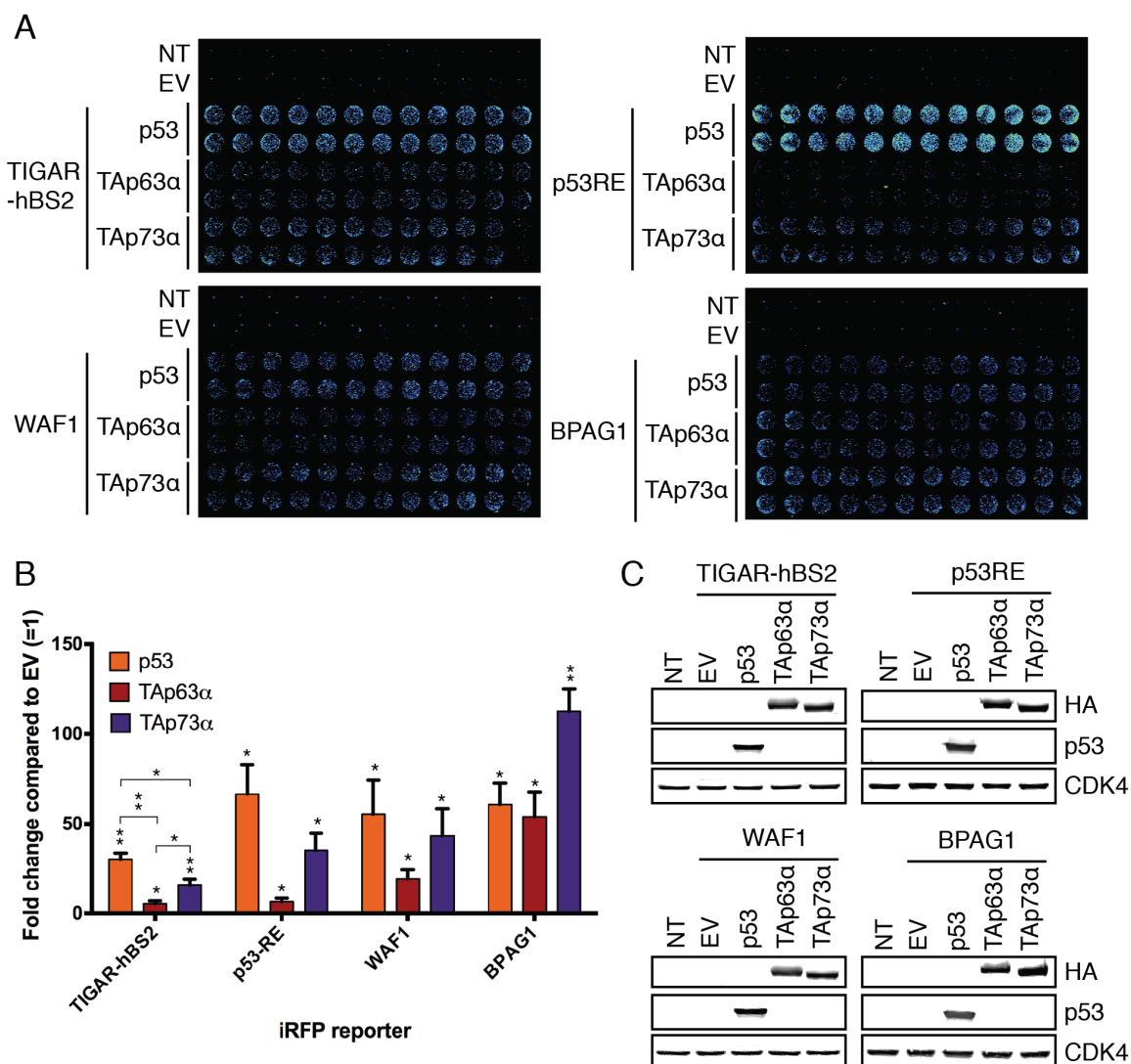


Figure 4-9 TAp63 α and TAp73 α can activate the TIGAR-hBS2 reporter

(A) iRFP reporter assay scans of HCT116 p53^{-/-} cells 24 hr after co-transfection with TIGAR-hBS2, p53RE, WAF1 or BPAG1 iRFP reporters along with human p53, HA-tagged TAp63 α or HA-tagged TAp73 α . (B) Quantification of iRFP reporter scans. Values represent mean \pm SEM. n = 3 independent experiments with at least 12 technical replicates. (C) Western blot analysis of HCT116 p53^{-/-} cells transfected with p53, HA-tagged TAp63 α or HA-tagged TAp73 α . n = 2 independent experiments. *p < 0.05, **p < 0.005 compared to EV unless otherwise indicated. NT, non-transfected. EV, empty vector.

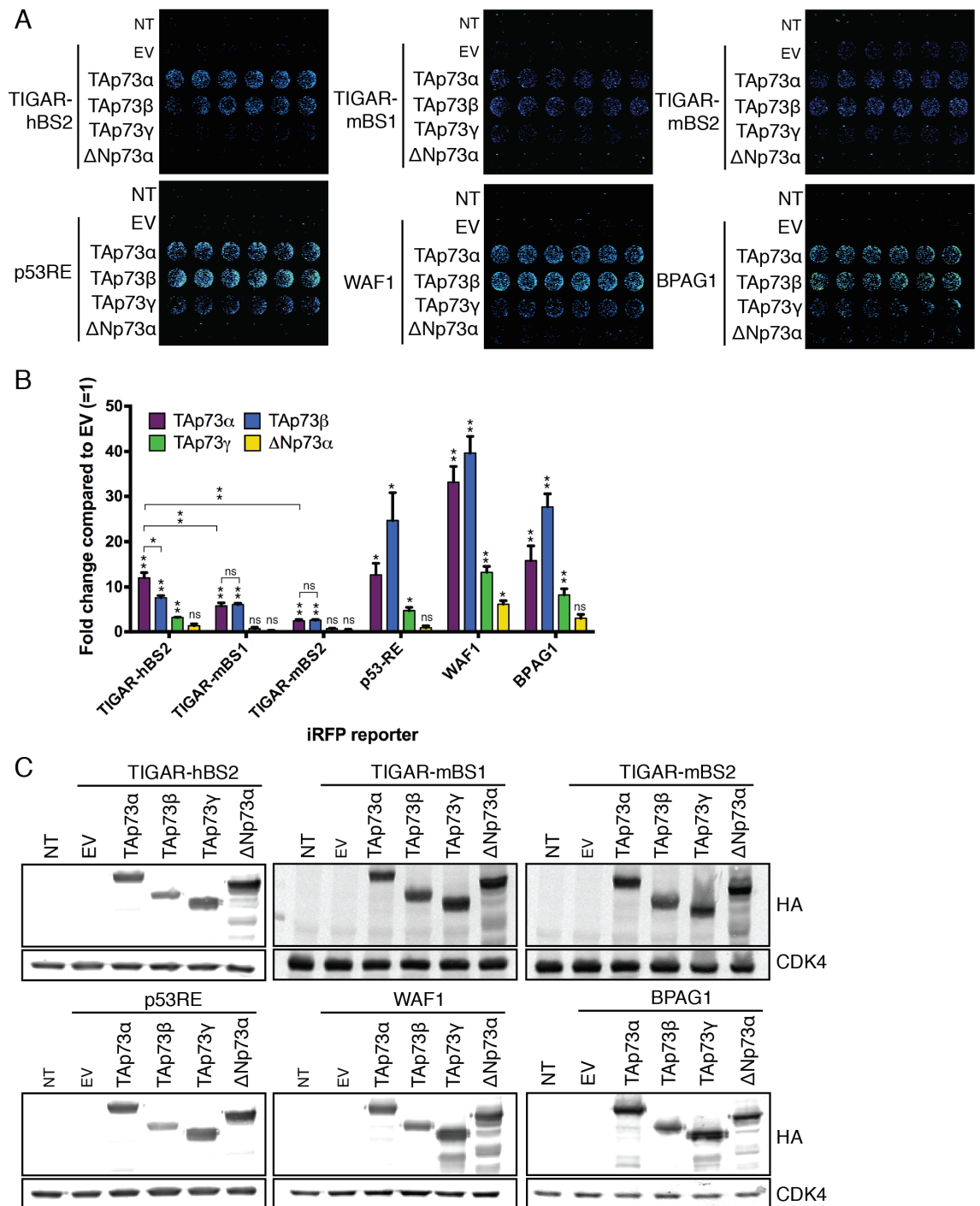
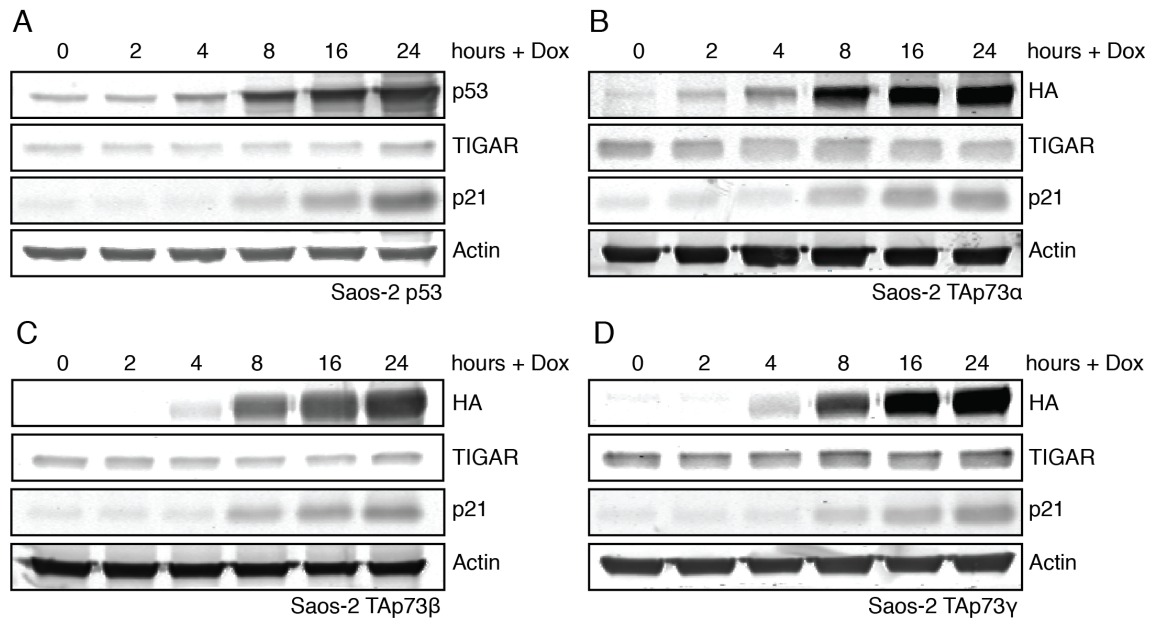


Figure 4-10 p73 isoforms can activate the TIGAR-hBS2 reporter

(A) iRFP reporter assay scans of HCT116 p53^{-/-} cells 24 hr after co-transfection with TIGAR-hBS2, TIGAR-mBS1, TIGAR-mBS2, p53RE, WAF1 or BPAG1 iRFP reporters along with TAp73α, TAp73β, TAp73γ or ΔNp73α. (B) Quantification of iRFP reporter scans. Values represent mean ± SEM. n = 3 independent experiments with 6 technical replicates. (C) Western blot analysis of HCT116 p53^{-/-} cells transfected with HA-tagged TAp73α, HA-tagged TAp73β, HA-tagged TAp73γ or HA-tagged ΔNp73α. n = 2 independent experiments. *p < 0.05, **p < 0.005 compared to EV unless otherwise indicated. NT, non-transfected. EV, empty vector. NS, not significant.

**Figure 4-11 TIGAR expression in inducible Saos-2 cells**

Western blot analysis of Saos-2 cells with doxycycline inducible expression of p53 (A), TAp73 α (B), TAp73 β (C) or TAp73 γ (D). Cell lines were treated with 0.2 μ g/ml doxycycline (Dox) for the indicated hours. n = 3 independent experiments.

4.3 Loss of TAp73 does not Affect TIGAR *in vivo*

Like p53, p73 can be activated by DNA damage (Agami et al. 1999; Gong et al. 1999; Yuan et al. 1999), potentially mediating the induction of TIGAR expression in response to irradiation (IR) independently of p53. To investigate whether the DNA damage-induced expression of TIGAR in mice was through TAp73, TIGAR induction in TAp73-deficient (*TAp73*^{-/-}) mice was examined. First, the basal expression of TIGAR was assessed in various organs of untreated WT and *TAp73*^{-/-} mice. As seen in the *p53*^{-/-} mice, no clear significant decrease in TIGAR expression in various tissues was observed in *TAp73*^{-/-} animals, with a possible small reduction in protein as well as mRNA levels in the muscle (Figure 4-12A-B).

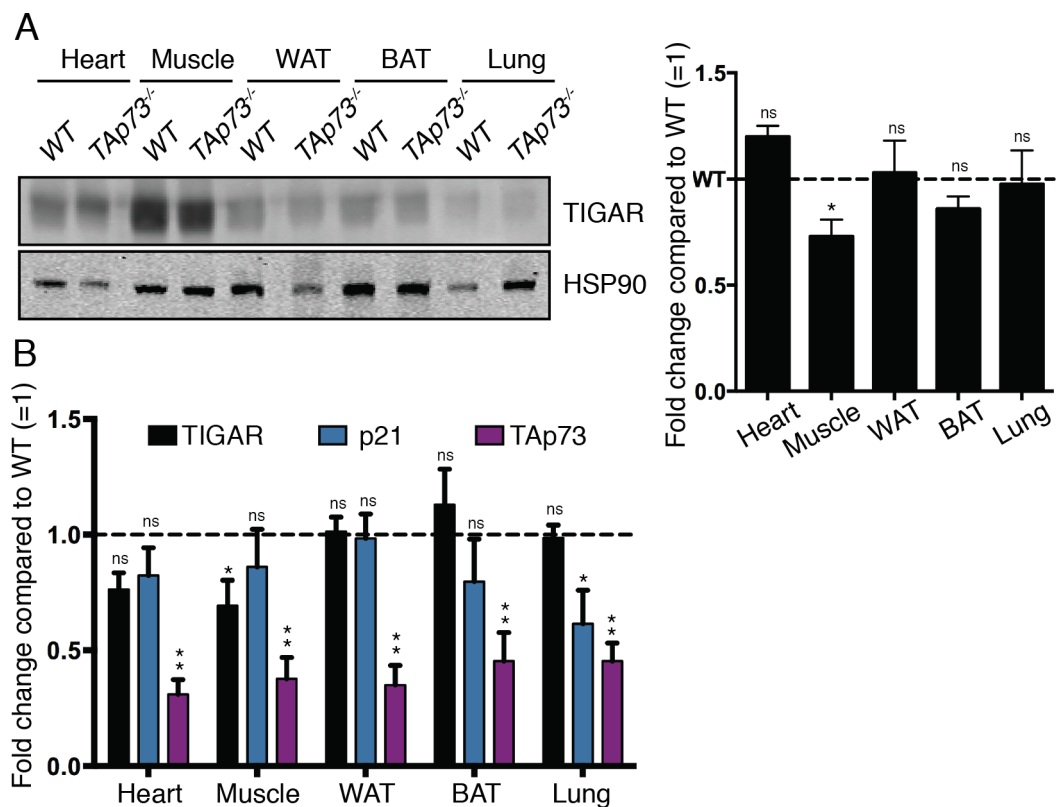


Figure 4-12 TIGAR expression in TAp73-null animals

(A) Left: Western blot analysis of TIGAR protein expression in organs of wild-type (WT) and *TAp73*^{-/-} mice. Right: Graph represents quantification of Western blots with fold change compared to WT. Values represent mean \pm SEM. $n = 3$ mice per genotype. (B) mRNA expression of TIGAR, p21 and p73 in organs of WT and *TAp73*^{-/-} mice. Values represent mean \pm SEM. $n = 3$ mice per genotype with 3 technical replicates. * $p < 0.05$, ** $p < 0.005$ compared to WT. NS, not significant. WAT, white adipose tissue. BAT, brown adipose tissue.

To extend these studies, the possibility of a TAp73-dependent increase in TIGAR expression *in vivo* after tissue damage was investigated, focusing on the intestinal system using irradiation, much like in the *p53*^{-/-} animals. Comparison of WT and *TAp73*^{-/-} mice showed normal crypt architecture and similar levels of proliferation, as indicated by Ki67 staining under unstressed conditions (Figure 4-13). The basal expression of p53, p73, p21 and TIGAR were also low in the crypts of both WT and *TAp73*^{-/-} animals under unstressed conditions (Figure 4-14, Figure 4-15, Figure 4-16, Figure 4-17). Tissue ablation of the intestinal epithelium was then performed by IR, which was followed by 72 hours of recovery.

As seen in the *p53*^{-/-} animals, the crypts in *TAp73*^{-/-} mice were able to undergo rapid proliferation during intestinal regeneration after IR, as shown by Ki67 staining (Figure 4-13). Confirmation of TAp73-deficiency was also performed by immunohistochemistry, where only WT animals showed an increase in p73 expression after IR (Figure 4-15). The increased expression of p53 was, however, retained in the *TAp73*^{-/-} animals (Figure 4-14), as well as the increased expression of p21, most likely through the induction of p53 (Figure 4-16). The expression of TIGAR remained increased in the intestinal crypts of both WT and *TAp73*^{-/-} animals (Figure 4-17). These data show that TAp73 is not necessary to maintain basal expression of TIGAR or to induce TIGAR levels following tissue damage in the small intestine. However, potential compensation could occur when either p53 or TAp73 is lost, which may result in no changes in TIGAR expression.

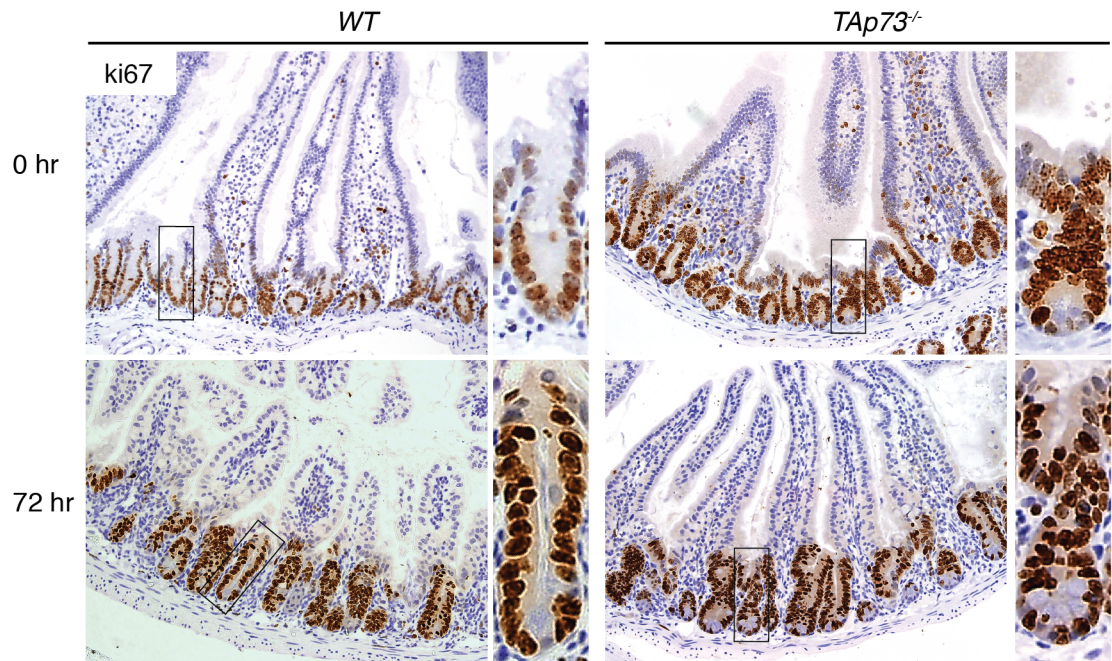


Figure 4-13 Ki67 expression in *TAp73^{-/-}* small intestine after irradiation

Immunohistochemistry for Ki67 on small intestines from wild-type (WT) and *TAp73^{-/-}* animals 72 hr after 10 Gy IR. Panels show more detailed crypt structures indicated in the box. n = 3 mice per genotype per condition.

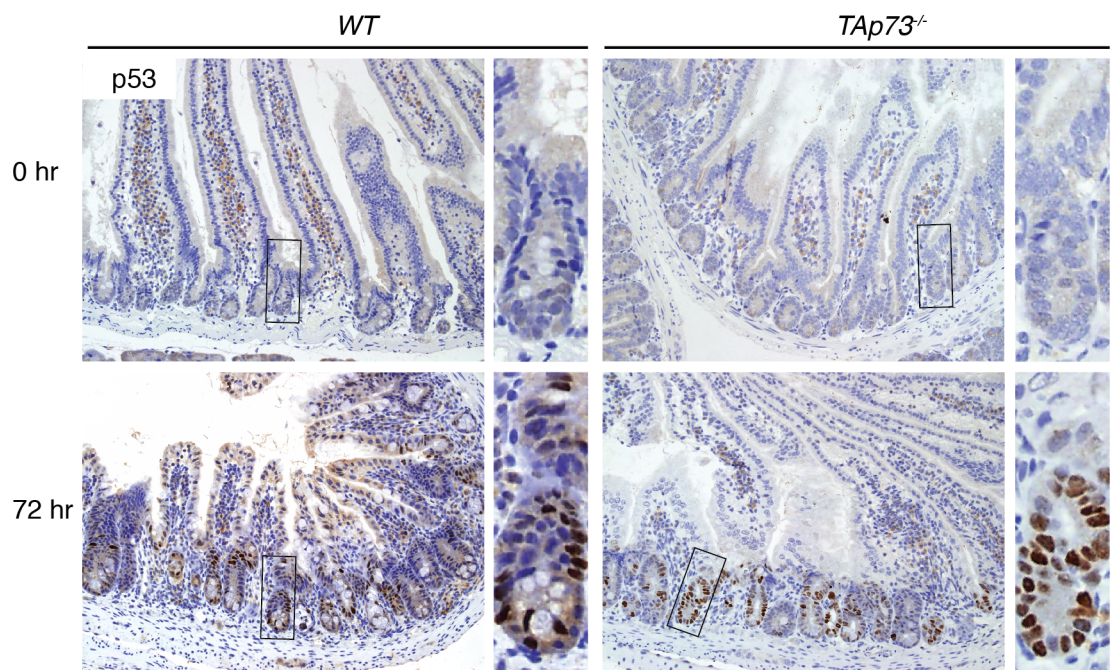


Figure 4-14 p53 expression in *TAp73^{-/-}* small intestine after irradiation

Immunohistochemistry for p53 on small intestines from wild-type (WT) and *TAp73^{-/-}* animals 72 hr after 10 Gy IR. Panels show more detailed crypt structures indicated in the box. n = 3 mice per genotype per condition.

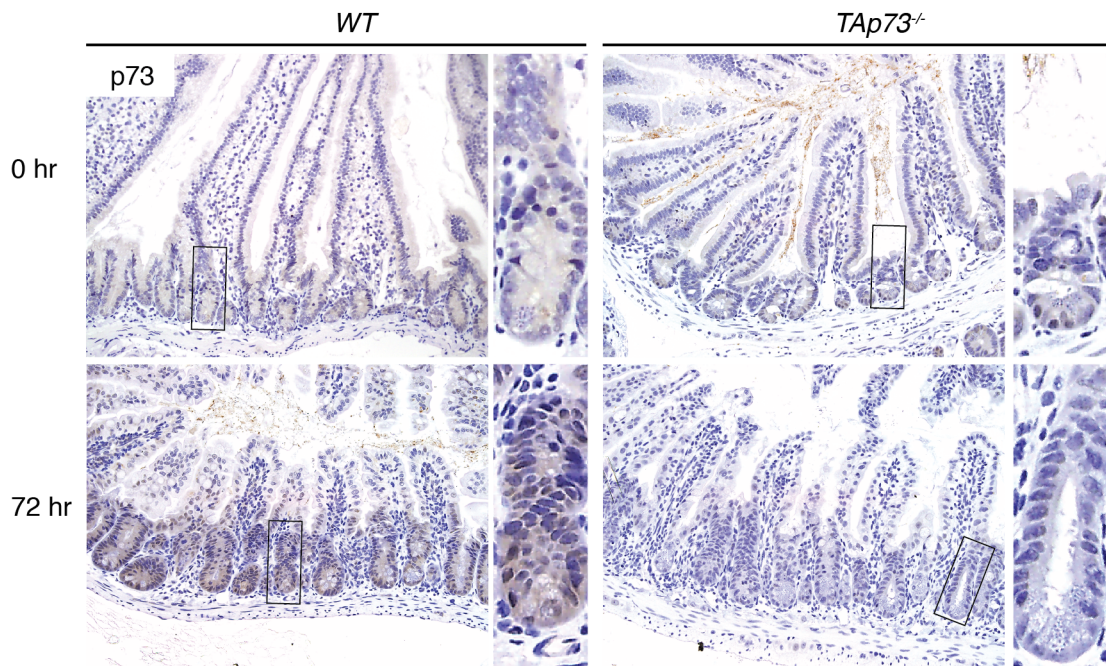


Figure 4-15 p73 expression in *TAp73^{-/-}* small intestine after irradiation

Immunohistochemistry for p73 on small intestines from wild-type (WT) and *TAp73^{-/-}* animals 72 hr after 10 Gy IR. Panels show more detailed crypt structures indicated in the box. n = 3 mice per genotype per condition, each stained 3 times.

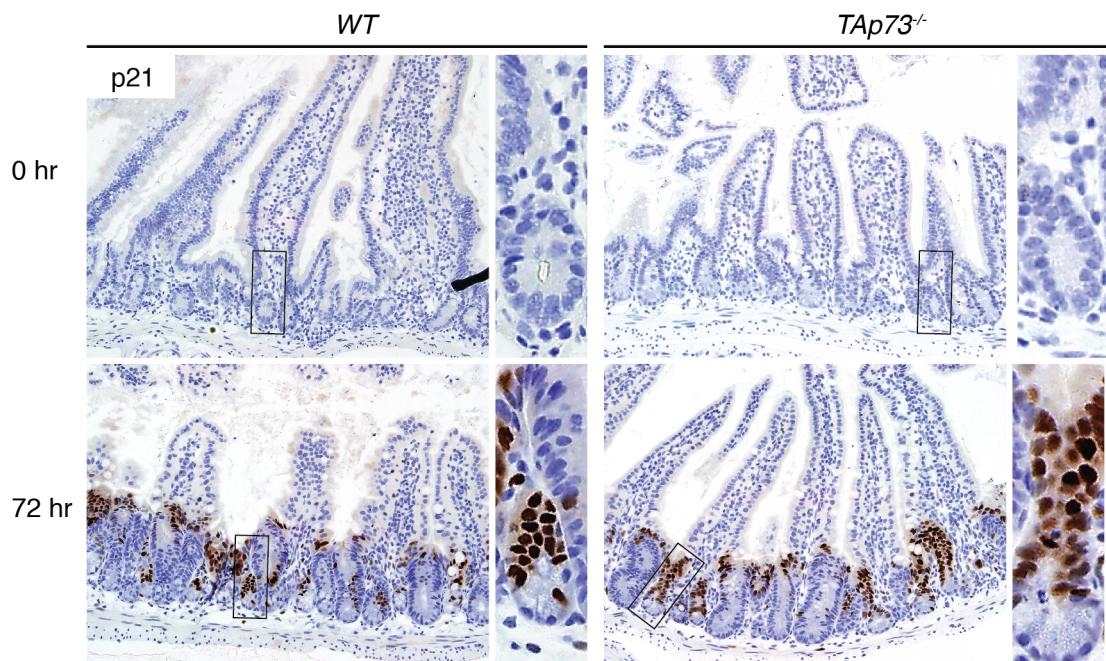


Figure 4-16 p21 expression in *TAp73^{-/-}* small intestine after irradiation

Immunohistochemistry for p21 on small intestines from wild-type (WT) and *TAp73^{-/-}* animals 72 hr after 10 Gy IR. Panels show more detailed crypt structures indicated in the box. n = 3 mice per genotype per condition.

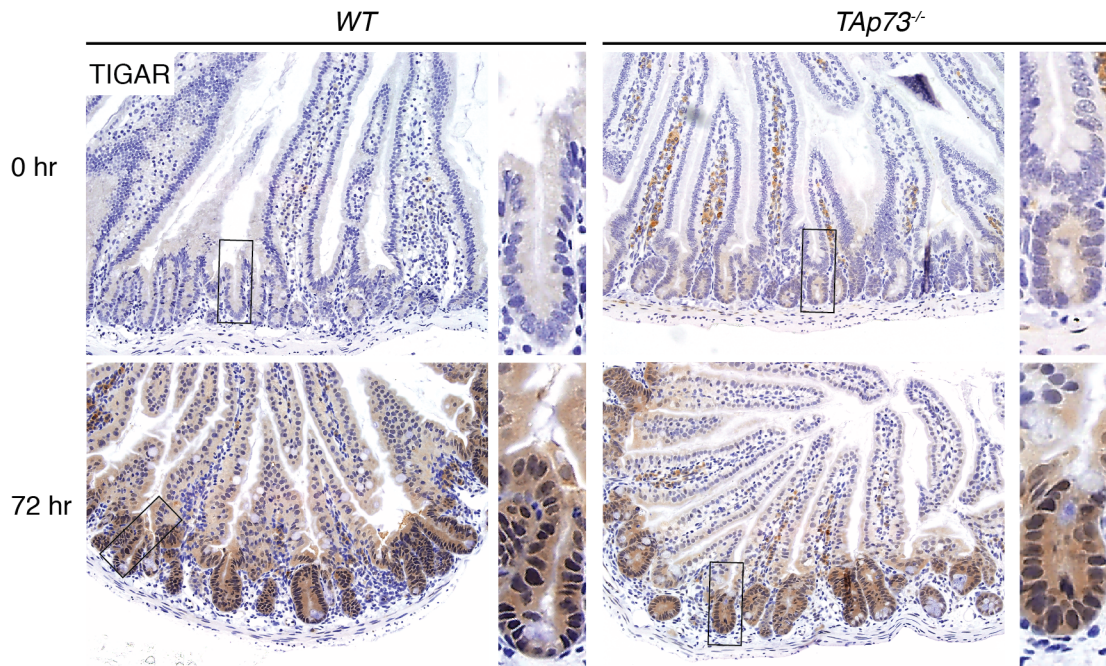


Figure 4-17 TIGAR expression in *TAp73^{-/-}* small intestine after irradiation
Immunohistochemistry for TIGAR on small intestines from wild-type (WT) and *TAp73^{-/-}* animals 72 hr after 10 Gy IR. Panels show more detailed crypt structures indicated in the box. n = 3 mice per genotype per condition.

4.4 Loss of Both p53 and TAp73 does not Affect TIGAR *in vivo*

In order to address the potential compensation that could occur when either p53 or TAp73 is lost, both transcriptional factors were simultaneously deleted *in vivo* ($p53^{-/-}TAp73^{-/-}$). Basal TIGAR protein expression was first assessed in various organs of untreated wild-type (WT) and $p53^{-/-}TAp73^{-/-}$ mice. As seen in $p53^{-/-}$ and $TAp73^{-/-}$ mice, no significant decrease in TIGAR expression was observed in $p53^{-/-}TAp73^{-/-}$ animals (Figure 4-18). Interestingly, the minor reduction in TIGAR expression in the muscle that was seen in $p53^{-/-}$ and $TAp73^{-/-}$ mice was lost in the $p53^{-/-}TAp73^{-/-}$ animals.

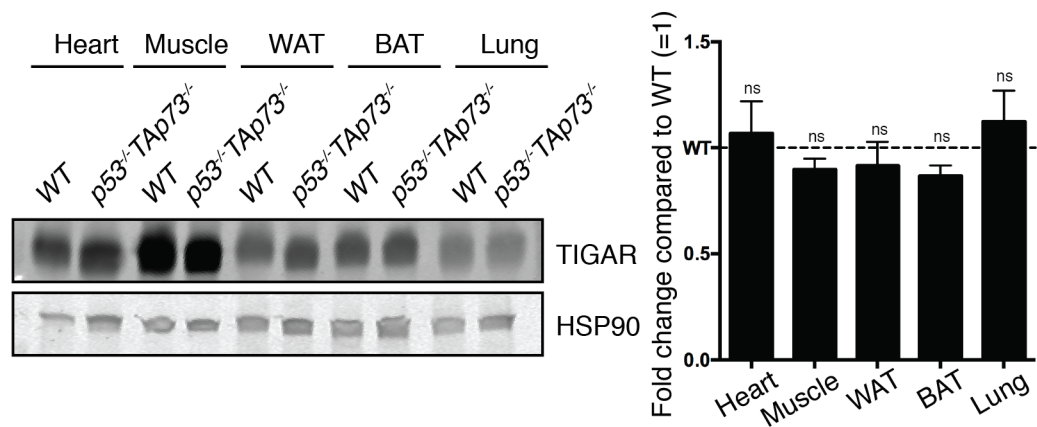


Figure 4-18 TIGAR expression in p53- and TAp73-null animals

(A) Left: Western blot analysis of TIGAR protein expression in organs of wild-type (WT) and $p53^{-/-}TAp73^{-/-}$ mice. Right: Graph represents quantification of Western blots with fold change compared to WT. Values represent mean \pm SEM. $n = 3$ mice per genotype. NS, not significant. WAT, white adipose tissue. BAT, brown adipose tissue.

As performed for the p53-null and TAp73-null animals, a model of intestinal tissue damage via irradiation was used to assess TIGAR protein induction in $p53^{-/-}TAp73^{-/-}$ mice. Comparison of WT and $p53^{-/-}TAp73^{-/-}$ mice showed normal crypt architecture and similar levels of proliferation as indicated by Ki67 staining under unstressed conditions (Figure 4-19). The basal expression of p53, p73, p21 and TIGAR were also low in the crypts of WT and $p53^{-/-}TAp73^{-/-}$ mice when unstressed (Figure 4-20, Figure 4-21, Figure 4-22, Figure 4-23).

Similar to previous studies in $p53^{-/-}$ and $TAp73^{-/-}$ mice, 72 hours following intestinal tissue ablation by IR, $p53^{-/-}TAp73^{-/-}$ mice were able to undergo rapid proliferation during intestinal regeneration, as observed by Ki67 staining (Figure 4-19). Loss of both p53 and TAp73 was confirmed as only p53, p73 and p21 were upregulated following IR in WT animals (Figure 4-20, Figure 4-21, Figure 4-22). In addition, the upregulation of TIGAR expression was similar in the intestinal crypts of both WT and $p53^{-/-}TAp73^{-/-}$ mice following IR (Figure 4-23).

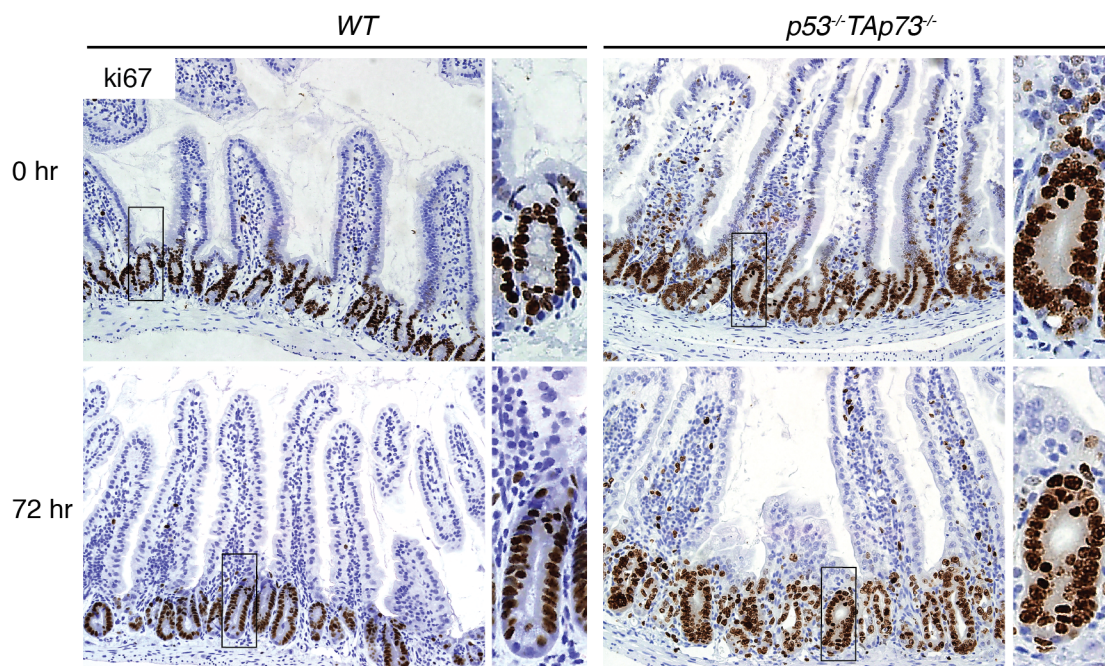


Figure 4-19 Ki67 expression in $p53^{-/-}TAp73^{-/-}$ small intestine after irradiation
Immunohistochemistry for Ki67 on small intestines from wild-type (WT) and $p53^{-/-}TAp73^{-/-}$ animals 72 hr after 10 Gy IR. Panels show more detailed crypt structures indicated in the box. n = 3 mice per genotype per condition.

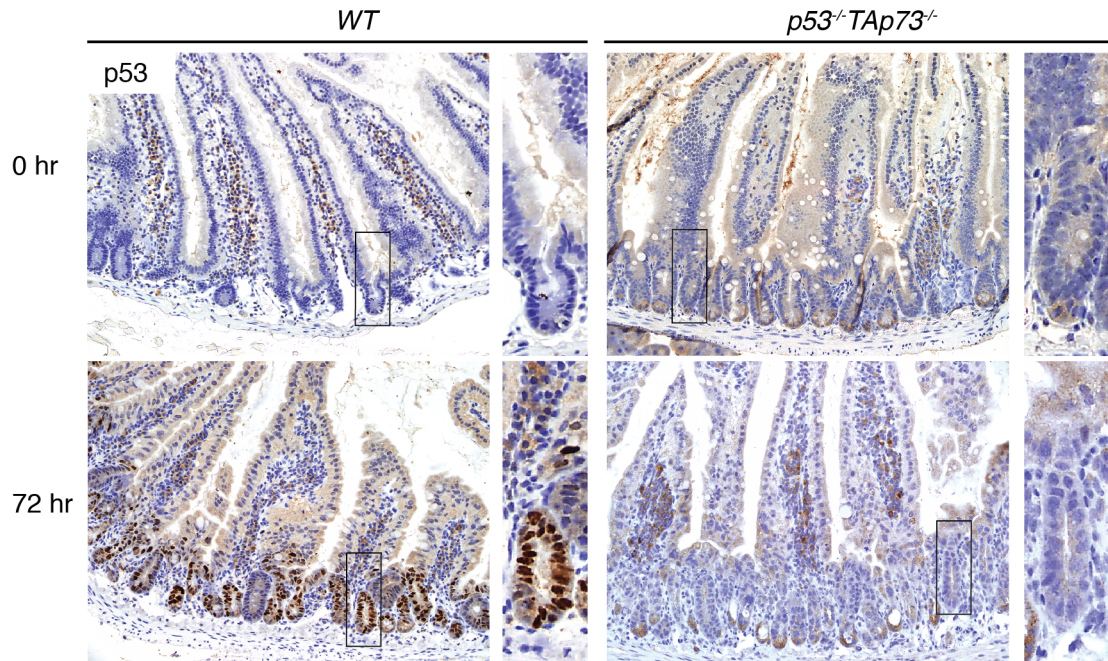


Figure 4-20 p53 expression in $p53^{-/-}TAp73^{-/-}$ small intestine after irradiation
 Immunohistochemistry for p53 on small intestines from wild-type (WT) and $p53^{-/-}TAp73^{-/-}$ animals 72 hr after 10 Gy IR. Panels show more detailed crypt structures indicated in the box. $n = 3$ mice per genotype per condition.

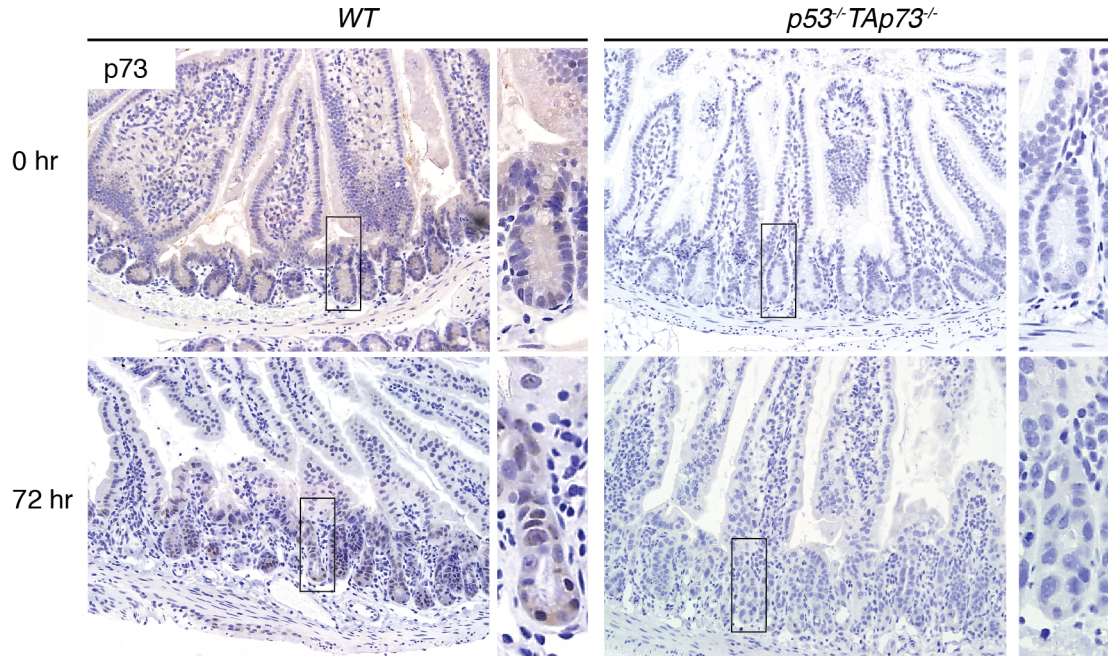


Figure 4-21 p73 expression in $p53^{-/-}TAp73^{-/-}$ small intestine after irradiation
 Immunohistochemistry for p53 on small intestines from wild-type (WT) and $p53^{-/-}TAp73^{-/-}$ animals 72 hr after 10 Gy IR. Panels show more detailed crypt structures indicated in the box. $n = 3$ mice per genotype per condition, each stained 3 times.

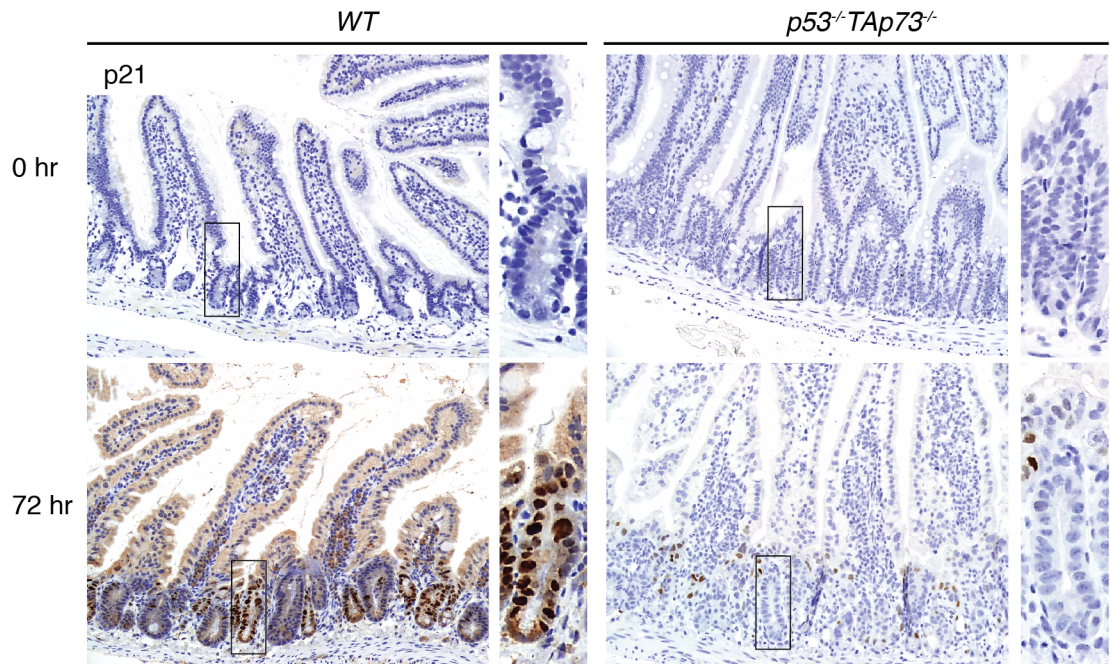


Figure 4-22 p21 expression in $p53^{-/-}TAp73^{-/-}$ small intestine after irradiation
 Immunohistochemistry for p21 on small intestines from wild-type (WT) and $p53^{-/-}TAp73^{-/-}$ animals 72 hr after 10 Gy IR. Panels show more detailed crypt structures indicated in the box. n = 3 mice per genotype per condition.

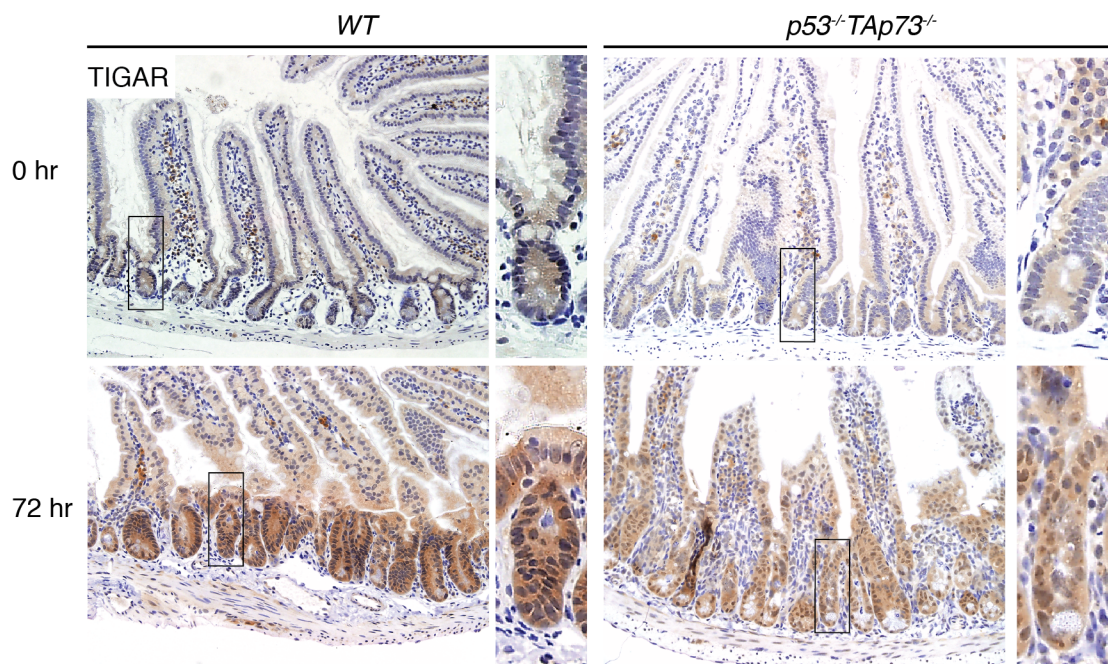


Figure 4-23 TIGAR expression in $p53^{-/-}TAp73^{-/-}$ small intestine after irradiation
 Immunohistochemistry for TIGAR on small intestines from wild-type (WT) and $p53^{-/-}TAp73^{-/-}$ animals 72 hr after 10 Gy IR. Panels show more detailed crypt structures indicated in the box. n = 3 mice per genotype per condition.

To further confirm p53- and TAp73-independent upregulation of TIGAR, small intestine tissue from both WT and $p53^{-/-}TAp73^{-/-}$ mice were harvested before and 72 hours after 10 Gy irradiation treatment to assess TIGAR protein expression via Western blot. As seen by immunohistochemistry, both WT and $p53^{-/-}TAp73^{-/-}$ animals showed increased levels of TIGAR following irradiation (Figure 4-24).

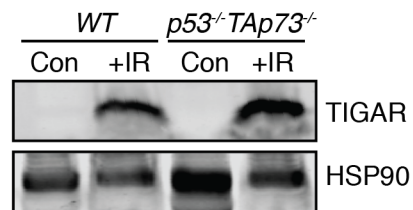


Figure 4-24 TIGAR expression in $p53^{-/-}TAp73^{-/-}$ small intestine after irradiation

Western blot analysis of TIGAR protein expression in small intestine tissue of wild-type (WT) and $p53^{-/-}TAp73^{-/-}$ mice before (Con) and 72 hr after 10 Gy IR (+IR). n = 1 mouse per genotype per condition.

Altogether, these data suggest that maintenance of the basal expression of TIGAR is not dependent on p53 or TAp73 and induction of TIGAR following intestinal tissue damage does not depend on p53 or TAp73, but is through a different cellular mechanism.

4.5 Summary and Discussion

It has been shown in the previous chapter that TIGAR is induced following cisplatin- or IR-induced intestinal damage. In humans, TIGAR is a p53 target gene and found to play a role in conditions of mild stress to promote cell survival (Bensaad et al. 2006; Bensaad et al. 2009; Cheung et al. 2012). Here it was shown that TAp73 is able to transcriptionally activate the TIGAR promoter in human cells in an iRFP reporter assay. As IR can activate both p53 (Merritt et al. 1994) and TAp73 (Agami et al. 1999; Gong et al. 1999; Yuan et al. 1999), the hypothesis that the increase in TIGAR observed in the mouse intestine following IR is a response to p53 and/or TAp73 was tested.

Despite the potential for both p53 and TAp73 to activate TIGAR reporter constructs, it was found that while basal levels of TIGAR expression vary significantly between different mouse tissues, TIGAR protein expression was generally not affected by the loss of p53 or TAp73. Furthermore, the induction of TIGAR in mouse small intestine in response to IR was not dependent on p53 or TAp73. Mice deficient for both p53 and TAp73 also maintained a similar basal expression of TIGAR compared to WT animals and also retained the ability to upregulate the expression of TIGAR in the crypts of the small intestine following tissue ablation. Importantly, several previous studies have shown p53-responsive expression of TIGAR in mouse cells and tissues such as liver and heart, and p53 binding to the *Tigar* promoter was also previously shown detected in the liver (Kimata et al. 2010; Hoshino et al. 2012; Li et al. 2012a; Hamard et al. 2013). In contrast, only a minor reduction in TIGAR expression was found here in p53 or TAp73-deficient muscle. Taken together, these data suggest that while p53 can induce TIGAR in some mouse tissues, the p53-responsiveness of mouse TIGAR expression is lower than that observed in human cells. To some extent, this difference may reflect the binding of p53 to the different response elements in the mouse and human TIGAR encoding genes. However, it is also possible that tissue or stress-specific co-factors (that may show human/mouse differences in expression or availability) are required to allow p53 regulation of TIGAR expression. Given the function of TIGAR as a regulator of metabolism, it will be of particular interest to see whether p53 family proteins can associate with other co-

factors in order to participate in the induction of TIGAR in response to different forms of metabolic stress.

TIGAR has also been found to be elevated in several human tumour types (Wanka et al. 2012; Cheung et al. 2013; Sinha et al. 2013) and the expression of TIGAR under these conditions does not correlate with the maintenance of wild-type p53 (Won et al. 2012), suggesting that TIGAR overexpression in tumours can be uncoupled from the activity of p53. Moreover, other transcription factors such as SP1 (Zou et al. 2012) and CREB (Zou et al. 2013) have been shown to play a role in regulating the basal expression of TIGAR in liver cancer cell lines. It would be interesting to further investigate direct mechanisms or posttranslational modifications by which TIGAR activity could be regulated.

One of the major pathways in the small intestine that plays a key role in cell proliferation and promotes intestinal regeneration following tissue damage is the Wnt signalling pathway (Clevers and Nusse 2012). As the data presented in this chapter showed p53-independent mechanisms by which TIGAR is upregulated in the small intestine, the potential for the Wnt signalling pathway to influence TIGAR expression was further examined and will be presented in the following chapter. Future studies will be required to establish how TIGAR expression is regulated during stress and whether deregulation of these pathways explains the elevated expression of TIGAR seen in human tumours.

Chapter 5 TIGAR as a Wnt-Myc Signalling Target Gene

As TIGAR was found not to be dependent on p53 or p53 family members for its expression in the small intestine, we decided to investigate other transcriptional factors that might regulate TIGAR in the gut. The Wnt signalling pathway is particularly important in promoting cell proliferation in the small intestine and activation of this pathway can promote the transcriptional activation of its target genes through various mechanisms (Clevers and Nusse 2012). Activation of the Wnt signalling pathway results in the stabilization and nuclear translocation of β -catenin, which interacts with T-cell factor (TCF) and lymphoid enhancing factor (LEF) to directly regulate gene expression. A key downstream target of TCF/LEF is c-Myc, which has been shown to mediate the highly proliferative phenotype observed during activation of the Wnt signalling pathway (Sansom et al. 2007).

As TIGAR expression was increased in the small intestine following tissue ablation in a p53-independent manner, the induction of TIGAR expression in response to activation of the Wnt signalling pathway was examined. In addition, since Myc can induce several metabolic target genes including hexokinase 2 and pyruvate dehydrogenase kinase 1 (Dang 2009), it was also examined as a potential regulator of TIGAR downstream of the Wnt signalling pathway. To understand how the Wnt signalling pathway may contribute to the regulation of TIGAR, the expression of TIGAR was assessed after activation of the pathway using recombinant proteins *in vitro* as well as *in vivo* using known models of high Wnt pathway activation.

5.1 Activation of TIGAR expression by Wnt signalling

5.1.1 Induction of TIGAR Expression by Wnt Signalling *in vitro*

The expression of TIGAR was first assessed following treatment of cells with recombinant Wnt3a protein (rWnt3a), the activating ligand of the Wnt signalling pathway (Willert et al. 2003). MCF7 cells, which have low basal expression of TIGAR, were treated with increasing doses of rWnt3a (0 – 500 ng/ml) for 8 hours to determine the optimum dosage for future experimental use. A known Wnt target

gene, c-Myc (He et al. 1998), was used to assess activation of the signalling pathway after treatment. In this experiment, 200 ng/ml rWnt3a induced TIGAR expression in MCF7 cells, a dosage below that required to activate canonical Wnt pathway genes (Figure 5-1). Altogether, under these conditions, the Wnt response was not activated, despite an increase in TIGAR levels.

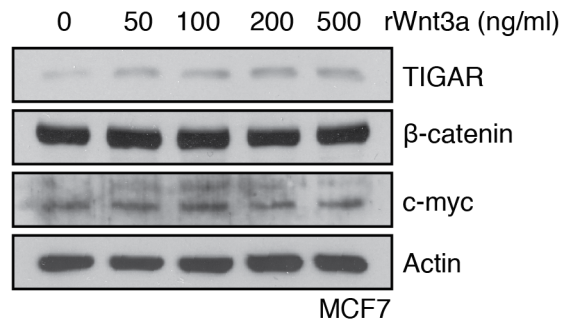


Figure 5-1 TIGAR expression in response to increasing doses of rWnt3a
Western blot analysis of MCF7 cells treated with increasing concentrations (0 – 500 ng/ml) of rWnt3a for 8 hr. n = 1 independent experiment.

To further investigate the induction of TIGAR through Wnt signalling, MCF7 cells were treated with 200 ng/ml rWnt3a for various time points (0 – 8 hours). A mouse cell line (L-cell), known to be responsive to rWnt3a (Willert et al. 2003), was also included to assess the activation of TIGAR in mouse cells. In MCF7 cells, treatment with rWnt3a was again able to induce the expression of TIGAR, however, no activation of the canonical Wnt signalling pathway was observed (Figure 5-2A). In the L-cells, an increase in TIGAR expression could also be seen following treatment with rWnt3a and the activation of the canonical Wnt signalling pathway was clearly observed in these cells through the increased levels of β -catenin and c-Myc (Figure 5-2B). However, in these 2D tissue culture systems, the changes in TIGAR protein expression were weak. Therefore, another method to investigate the potential role of Wnt signalling in regulating TIGAR was utilized.

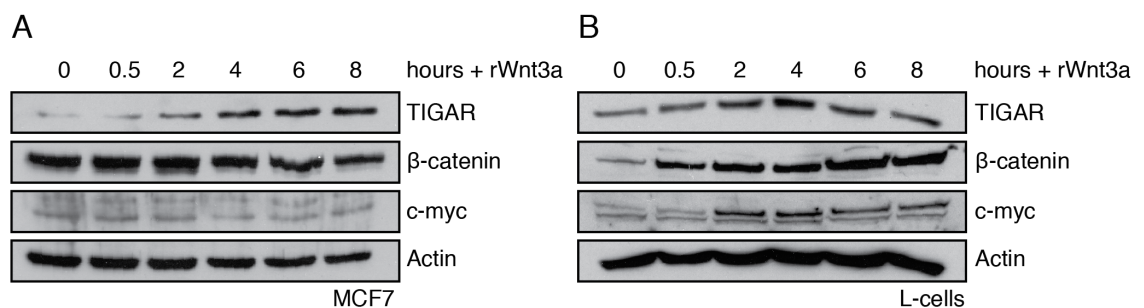


Figure 5-2 TIGAR expression in response to rWnt3a

Western blot analysis of MCF7 (A) and L-cells (B) treated with 200 ng/ml rWnt3a for the indicated time points (0 - 8 hr). n = 1 independent experiment.

As the Wnt signalling pathway plays an important role in regulating and supporting the proliferation of intestinal cells, the induction of TIGAR expression by Wnt signalling was tested in small intestinal crypt organoids harvested from WT animals (Sato et al. 2009). First, small intestinal crypt organoids were treated with increasing concentrations (0 – 500 ng/ml) of rWnt3a for 8 hours. No major morphological changes were seen in the crypts following treatment (Figure 5-3A). Protein expression was then assessed by Western blot. Both β -catenin and TIGAR expression were elevated following treatment with rWnt3a (Figure 5-3B). This

suggested that the Wnt signalling pathway may contribute to the induction of TIGAR in the mouse small intestine.

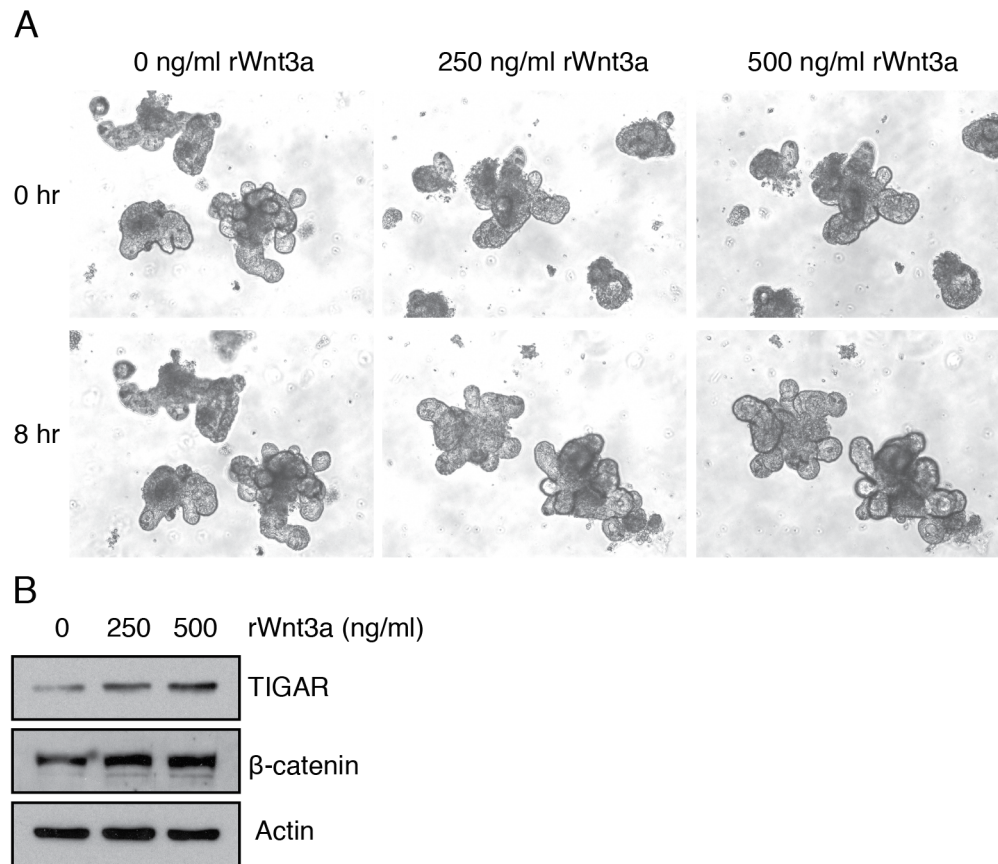


Figure 5-3 TIGAR in response to rWnt3a in intestinal crypt organoids

(A) Brightfield images of small intestinal crypt organoids treated at indicated concentrations (0 – 500 ng/ml) of rWnt3a for 8 hr. (B) Western blot analysis of small intestinal crypt organoids treated at indicated concentrations (0 – 500 ng/ml) of rWnt3a for 8 hr. $n = 3$ independent experiments.

To further examine how the Wnt pathway may promote TIGAR expression, small intestinal crypt organoids harvested from WT mice were compared to those harvested from *Apc*^{min/+} mice, which possess highly active Wnt signalling pathway due to a mutation in the adenomatous polyposis coli (*Apc*) gene (Moser et al. 1990). In this model, crypt organoids from *Apc*^{min/+} mice were cultured from the adenomas that form in these animals (Sato et al. 2011). While, WT crypts form buds during their culture as they differentiate, *Apc*^{min/+} crypts possess a spheroid shape due to their highly proliferative capacity and are devoid of differentiated cells (Figure 5-4A). A clear increase in TIGAR expression at both protein and mRNA was detected in organoid cultures from *Apc*^{min/+} mice (Figure 5-4B-C). Furthermore, an increase in the known Wnt target gene cyclin D1 (Tetsu and McCormick 1999) was detected in the *Apc*^{min/+} organoids. In order to confirm whether the elevation in TIGAR in the *Apc*^{min/+} organoids was due to Wnt signalling (and not p53), the expression of p53 and p21 were also assessed. Interestingly, there was no clear induction of either p53 or p21 protein or mRNA, suggesting that the increase in TIGAR observed was not dependent on p53 activity and is in agreement with the previously shown data (Figure 5-4B-C).

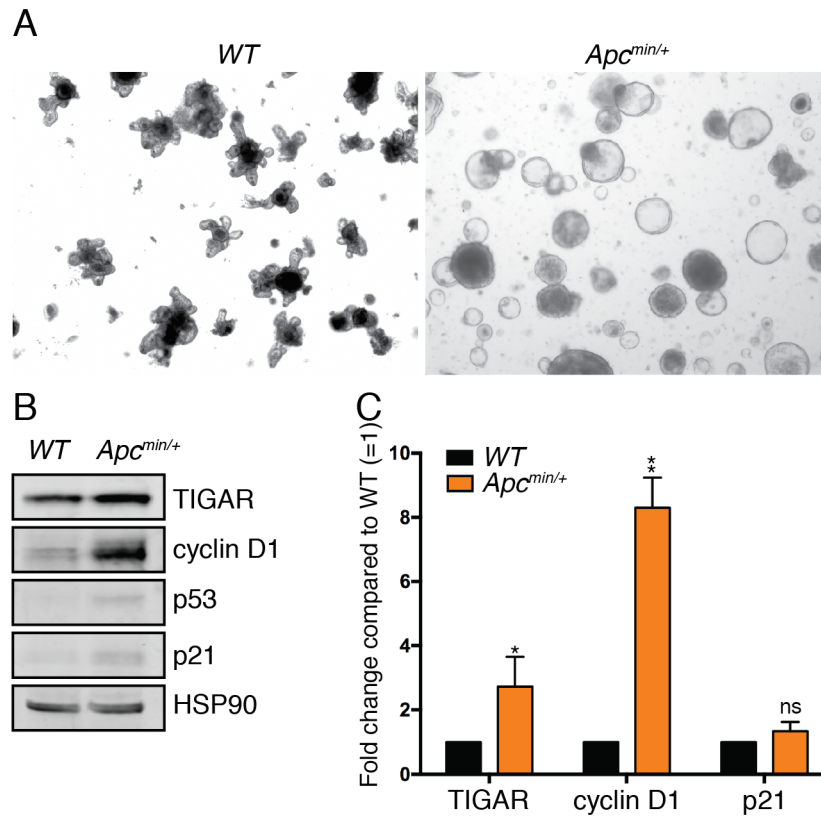


Figure 5-4 Increased TIGAR expression in *Apc^{min/+}* organoids

(A) Brightfield images of intestinal crypt organoids from wild-type (WT) and *Apc^{min/+}* mice. (B) Western blot analysis of intestinal crypt organoids from WT and *Apc^{min/+}* mice. n = 3 independent experiments. (C) mRNA expression of TIGAR, cyclin D1 and p21 in intestinal crypt organoids from WT and *Apc^{min/+}* mice. Values represent mean \pm SEM. n = 3 independent experiments with 3 technical replicates. *p < 0.05, **p < 0.005 compared to WT. NS, not significant.

The expression of TIGAR was also assessed following acute *Apc* deletion in intestinal crypt organoids. This was achieved by using intestinal crypts harvested from transgenic mice bearing a tamoxifen-dependent Cre recombinase expressed under the control of a regulatory region of the murine *villin* gene (*villin-Cre-ER^{T2}*). *Apc* was acutely deleted by treating intestinal crypts with a single dose of 4-hydroxytamoxifen in culture (el Marjou et al. 2004).

As seen in the *Apc^{min/+}* organoids, an increase in TIGAR expression at both protein and mRNA was observed along with an increase in cyclin D1 expression following 4-hydroxytamoxifen treatment. As with *Apc^{min/+}*, no clear induction of p53 or p21 was detected after 4-hydroxytamoxifen treatment (Figure 5-5). These results support previous observations that the expression of TIGAR is not strongly dependent on p53 and could be promoted by the Wnt signalling pathway in the mouse small intestine.

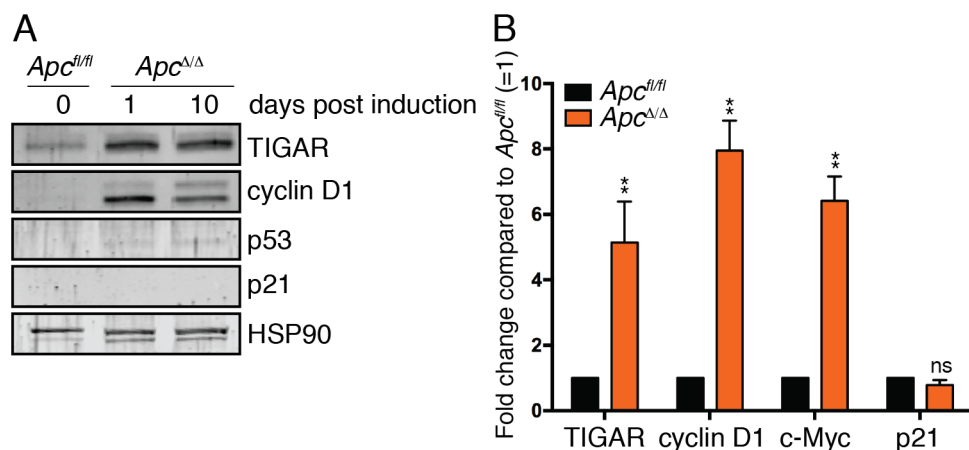


Figure 5-5 Increased TIGAR expression upon acute *Apc* loss

(A) Western blot analysis of intestinal crypt organoids from *villin-Cre-ER^{T2} Apc^{fl/fl}* animals before (*Apc^{fl/fl}*), and 1 or 10 days post tamoxifen induction (*Apc^{Δ/Δ}*). *n* = 1 independent experiment. (B) mRNA expression of TIGAR, cyclin D1, c-Myc and p21 in intestinal crypt organoids before (*Apc^{fl/fl}*) and 10 days post tamoxifen induction (*Apc^{Δ/Δ}*). Values represent mean \pm SEM. *n* = 1 independent experiment with 3 technical replicates. ***p* < 0.005 compared to *Apc^{fl/fl}*. NS, not significant.

5.1.2 Induction of TIGAR Expression by Wnt Signalling *in vivo*

To further understand the role of Wnt signalling in promoting TIGAR expression, another mouse model was utilized where high Wnt signalling was present. Conditional deletion of APC in the small intestine and liver was achieved by treating *AhCre⁺ Apc^{fl/fl}* mice with β -naphthoflavone (Sansom et al. 2004). Firstly, small intestines of *AhCre⁺ Apc^{fl/fl}* animals were harvested and using immunohistochemistry, the expression of TIGAR was assessed and found elevated in these animals when compared to WT mice (Figure 5-6A). This expression was similar to the high expression of β -catenin observed in the *AhCre⁺ Apc^{fl/fl}* animals, which indicated an increase in Wnt pathway activity following Cre induction (Figure 5-6A). Liver samples were also taken from WT and *AhCre⁺ Apc^{fl/fl}* animals and assessed for TIGAR expression. Much like in the small intestine, liver samples from *AhCre⁺ Apc^{fl/fl}* animals showed elevated levels of TIGAR protein as well as an increased expression of cyclin D1 (Figure 5-6B). In addition to protein levels, *AhCre⁺ Apc^{fl/fl}* liver samples also showed increased levels of TIGAR mRNA along with increased levels of known Wnt signalling target genes, Axin2, cyclin D1 and c-Myc when compared to liver samples from WT mice (Figure 5-6C).

Altogether, these results suggest that activation of the Wnt signalling pathway can promote the expression of TIGAR. Therefore, the potential mediator in this pathway driving TIGAR expression was further investigated.

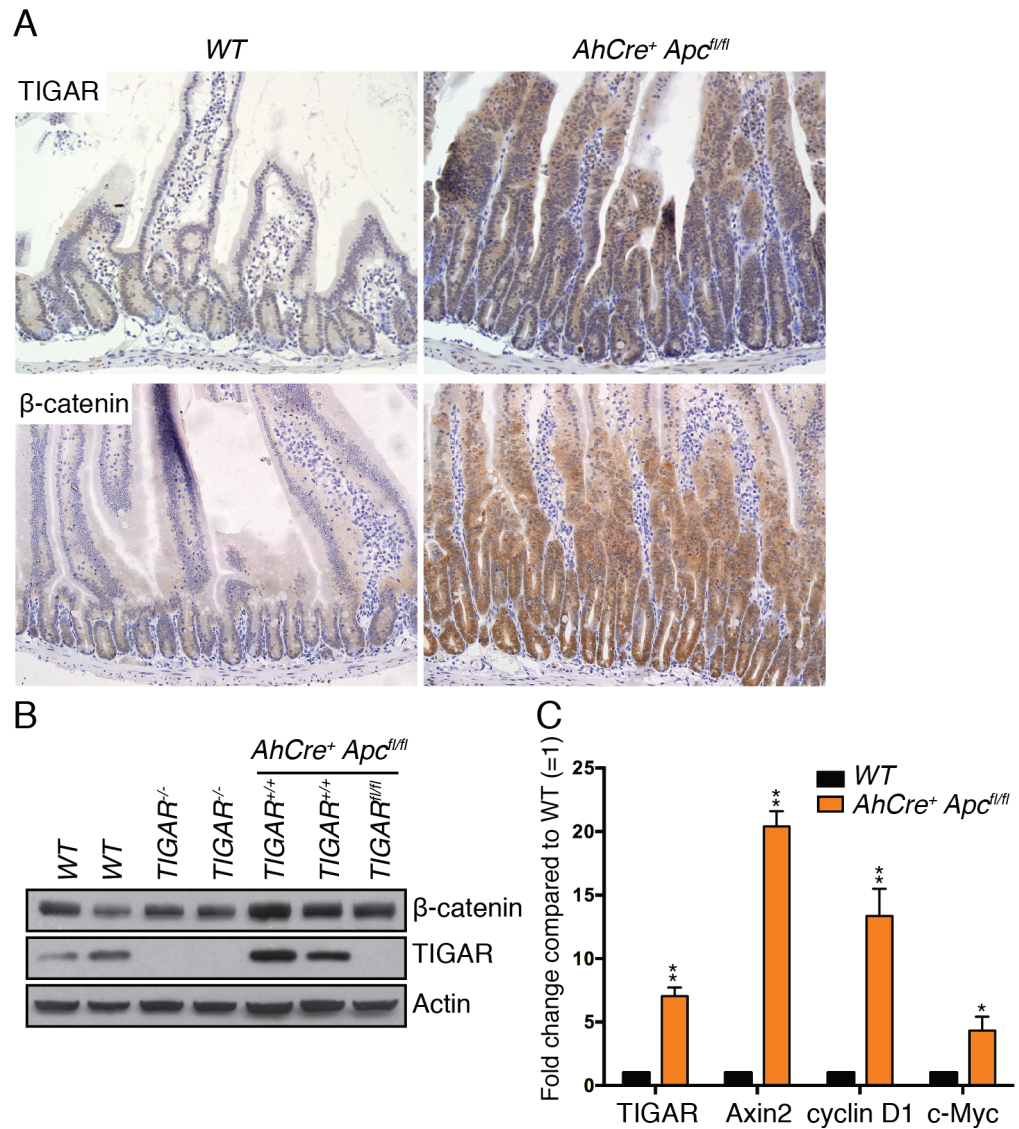


Figure 5-6 Increased TIGAR expression *in vivo* upon *Apc* loss

(A) Top: Immunohistochemistry for TIGAR on small intestines of wild-type (WT) and *AhCre⁺ Apc^{fl/fl}* mice. Bottom: Immunohistochemistry for β -catenin on small intestines of WT and *AhCre⁺ Apc^{fl/fl}* mice. $n = 3$ mice per genotype, each stained 3 times. (B) Western blot analysis of liver samples from WT ($n = 2$), *TIGAR^{-/-}* ($n = 2$), *AhCre⁺ Apc^{fl/fl}* ($n = 2$) and *AhCre⁺ Apc^{fl/fl} Tigar^{fl/fl}* ($n = 1$) mice. (C) mRNA expression of TIGAR, Axin2, cyclin D1, and c-Myc in liver samples of WT and *AhCre⁺ Apc^{fl/fl}* mice. Values represent mean \pm SEM. $n = 3$ mice per genotype with 3 technical replicates. * $p < 0.05$, ** $p < 0.005$ compared to WT.

5.2 Activation of TIGAR by c-Myc Downstream of the Wnt Pathway

As c-Myc is a known mediator of the proliferative effects of the Wnt signalling pathway (Sansom et al. 2007), the role of c-Myc in the induction of TIGAR expression downstream of Wnt pathway activation was considered.

5.2.1 Induction of TIGAR by c-Myc *in vitro*

Firstly, c-Myc was investigated *in vitro* using the MycER system in U2OS cells (U2OS-MycER). In this model, human c-Myc cDNA is fused with the oestrogen receptor ligand-binding domain (ER). The fusion protein, MycER, is activated upon 4-hydroxytamoxifen binding to the hormone binding domain, which initiates the translocation of the protein to the nucleus where it is transcriptionally active and drives the expression of c-Myc target genes.

Following 4-hydroxytamoxifen treatment, U2OS-MycER cells showed an induction of a known c-Myc target gene, hexokinase 2, on both protein as well as mRNA level. However, while TIGAR mRNA expression was elevated, no changes were observed in TIGAR protein levels (Figure 5-7).

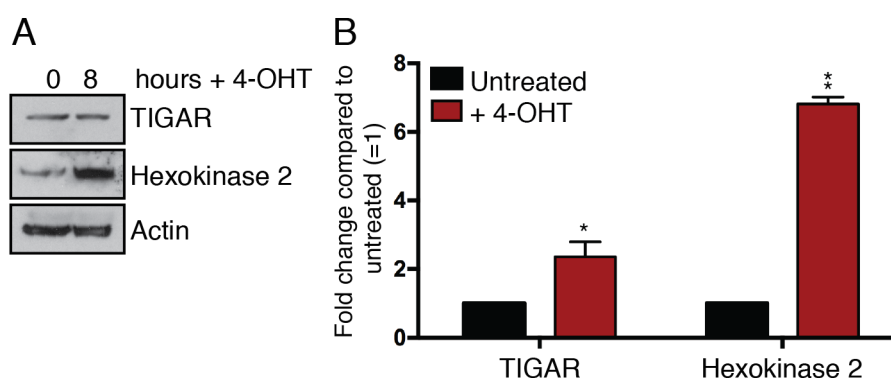


Figure 5-7 Induction of TIGAR by c-Myc *in vitro*

(A) Western blot analysis of U2OS-MycER cells treated with 500 nM 4-hydroxytamoxifen (4-OHT) for 8 hr. $n = 3$ independent experiments. (B) mRNA expression of TIGAR and hexokinase 2 in U2OS-MycER cells treated with 500 nM 4-hydroxytamoxifen (4-OHT) for 8 hr. Values represent mean \pm SEM. $n = 3$ independent experiments with 3 technical replicates. * $p < 0.05$, ** $p < 0.005$ compared to untreated.

5.2.2 Induction of TIGAR by c-Myc *in vivo*

To further understand whether Myc is important for the induction of TIGAR expression, the effects of simultaneous deletion of APC and Myc (*AhCre*⁺ *Apc*^{fl/fl} *Myc*^{fl/fl}) on TIGAR expression were examined in the small intestine. As previously shown by others (Sansom et al. 2007), loss of APC resulted in enhanced proliferation in the intestinal crypts as observed by Ki67 staining. However, when Myc was also lost, this significantly decreased the hyperproliferation seen in intestinal crypts in response to APC loss (Figure 5-8). As expected, the loss of Myc did not prevent the accumulation of β -catenin in these smaller crypts, as the expression of Myc is downstream of β -catenin during Wnt pathway activation (Figure 5-9). As observed previously (Figure 5-6), loss of APC resulted in increased TIGAR expression in the small intestine. Notably, deletion of Myc in addition to APC loss resulted in a failure to induce TIGAR expression in *AhCre*⁺ *Apc*^{fl/fl} *Myc*^{fl/fl} crypts (Figure 5-10). Furthermore, using the BioBase Match transcription factor programme (<http://www.gene-regulation.com/cgi-bin/pub/programs/match/bin/match.cgi>) and analyzing the sequence upstream and downstream of human *TIGAR* and mouse *Tigar* promoters, no potential TCF/LEF binding sites were found. Taken together, the results suggest that the induction of TIGAR may not be a direct response to β -catenin and its function as a co-activator for TCF/LEF transcriptional activity (Behrens et al. 1996), but rather a response to the activation of Myc downstream of the Wnt signalling pathway.

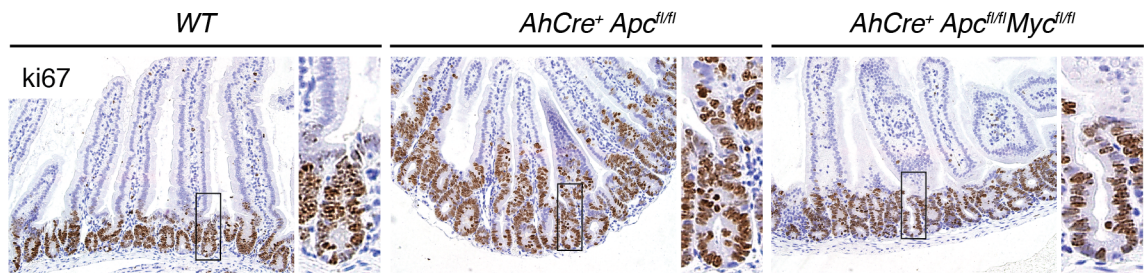


Figure 5-8 Loss of Myc attenuates Wnt-mediated proliferation

Immunohistochemistry for Ki67 on small intestines of wild-type (WT), *AhCre⁺ Apc^{fl/fl}* and *AhCre⁺ Apc^{fl/fl} Myc^{fl/fl}* mice. Panels show more detailed crypt structures indicated in the box. n = 3 mice per genotype.

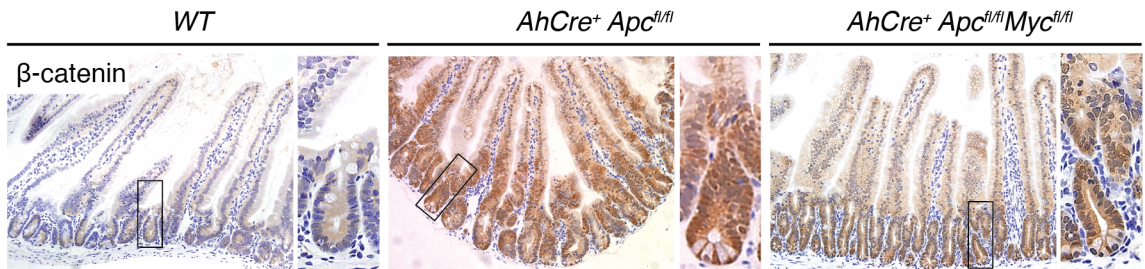


Figure 5-9 Loss of APC and Myc does not alter beta-catenin levels

Immunohistochemistry for beta-catenin on small intestines of wild-type (WT), *AhCre⁺ Apc^{fl/fl}* and *AhCre⁺ Apc^{fl/fl} Myc^{fl/fl}* mice. Panels show more detailed crypt structures indicated in the box. n = 3 mice per genotype.

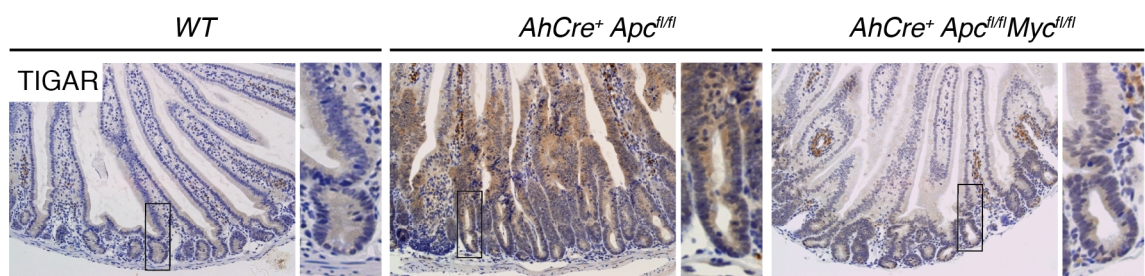


Figure 5-10 Loss of APC promotes TIGAR expression in a Myc-dependent manner

Immunohistochemistry for TIGAR on small intestines of wild-type (WT), *AhCre⁺ Apc^{fl/fl}* and *AhCre⁺ Apc^{fl/fl} Myc^{fl/fl}* mice. Panels show more detailed crypt structures indicated in the box. n = 3 mice per genotype, each stained 3 times.

Further support for Myc in regulating TIGAR expression was seen in transgenic mice expressing deregulated Myc. In the E μ -Myc mouse model, transgenic Myc is expressed from the IgH enhancer, leading to deregulated Myc expression in B-cells and the development of lymphomas within the first five months of age in E μ -Myc mice (Adams et al. 1985). Tissues of these mice were taken at two different stages, at approximately 35 days during which c-Myc is highly expressed in the spleen and bone marrow but does not result in the formation of lymphomas, and at approximately 75 days where tumours have formed in the thymus and lymph nodes.

The thymus was harvested from WT and E μ -Myc mice at 35 or 75 days. The thymus showed no increase in c-Myc expression at 35 days, as seen through the levels of cyclin D1, and this was also accompanied by no noticeable upregulation of TIGAR. However, a clear increase in TIGAR as well as cyclin D1 could be observed at 75 days (Figure 5-11). While these results suggest that Myc deregulation may contribute to TIGAR upregulation, there is also the possibility of indirect mechanisms driving TIGAR expression during the highly proliferative state of cells possessing high c-Myc levels.

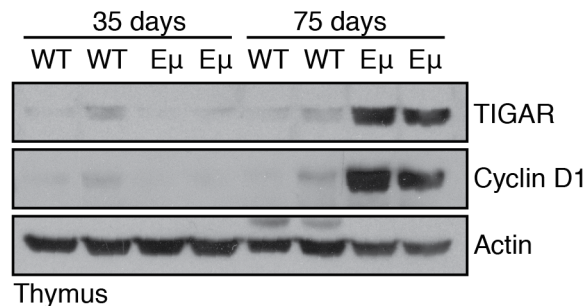


Figure 5-11 TIGAR expression in tissues of E μ -Myc mice

Western blot analysis of tissues harvested from thymus at 35 days (n = 2) or 75 days (n = 2) of wild-type (WT) and E μ -Myc (E μ) mice.

5.3 Activation of TIGAR Expression by ROS

5.3.1 Myc Promotes ROS upon APC Loss

Previous studies have shown that deletion of APC resulted in an increase of reactive oxygen species (ROS) in the mouse small intestine (Myant et al. 2013). To assess whether this elevation in ROS is Myc-dependent and also whether ROS itself can influence the expression of TIGAR, which normally functions to lower oxidative stress, small intestines of *AhCre⁺ Apc^{fl/fl}* and *AhCre⁺ Apc^{fl/fl} Myc^{fl/fl}* animals were stained for MDA, a marker for lipid peroxidation and thus oxidative stress. The induction of ROS following APC deletion could be observed in the crypts of the small intestine (Figure 5-12). Notably, this elevation in ROS was lost when Myc was also deleted, suggesting that the increase in ROS was dependent on the presence of Myc or rapid proliferation. Since TIGAR levels are also lower in *AhCre⁺ Apc^{fl/fl} Myc^{fl/fl}* crypts, the activation of TIGAR as a reflection of increased levels of ROS, in addition to Myc-dependent induction, was considered.

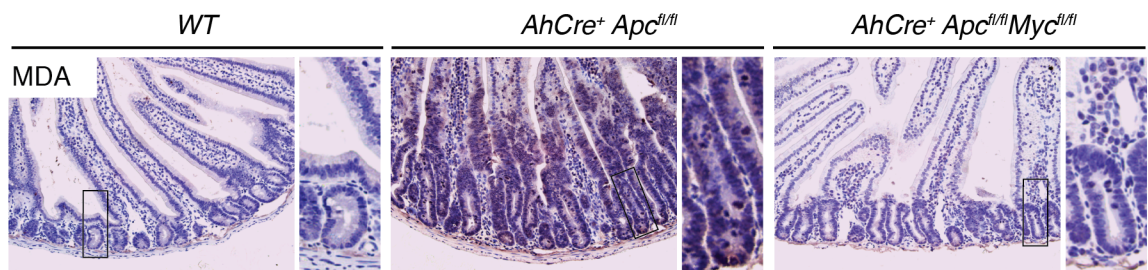


Figure 5-12 Loss of APC promotes oxidative stress in a Myc-dependent manner

Immunohistochemistry for malondialdehyde (MDA) on small intestines from wild-type (WT), *AhCre⁺ Apc^{fl/fl}* and *AhCre⁺ Apc^{fl/fl} Myc^{fl/fl}* mice. Panels show more detailed crypt structures indicated in the box. n = 3 mice per genotype, each stained 3 times.

5.3.2 The Response of TIGAR to Qualitative Differences in ROS

The potential effects of ROS in regulating TIGAR expression were assessed in small intestinal crypt organoids.

In order to induce oxidative stress, intestinal crypt organoids were treated for 24 hours with 250 μM hydrogen peroxide (H_2O_2) or 1 μM rotenone, an inhibitor of mitochondrial complex I, which acts to block the transfer of electrons in complex I to ubiquinone. By doing so, rotenone increases free electrons within the mitochondrial matrix and causes increased generation of superoxide ROS (Chance et al. 1963). Treatment of H_2O_2 or rotenone did not induce major cell death in these crypts. However, there was a slight decrease in growth in either condition when compared to the untreated organoids (Figure 5-13A). Following treatment with either condition, an increase in mRNA expression of the known ROS-responsive gene haem oxygenase-1 (HO-1) as well as of TIGAR was observed. However, there was no effect on the mRNA expression of cyclin D1, a c-Myc target gene (Figure 5-13B) or p21, a p53 target, suggesting neither c-Myc or p53 activity was activated by ROS in these crypts.

Next, changes in TIGAR expression were assessed in crypt organoids harvested from *Apc^{min/+}* animals, where a higher expression of TIGAR was previously observed (Figure 5-4). It would be predicted that these crypt organoids would possess greater levels of oxidative stress due to their proliferative phenotype and perhaps the high levels of TIGAR would assist in coping with this oxidative stress. To test this possibility, *Apc^{min/+}* crypt organoids were treated with 250 μM H_2O_2 or 1 μM rotenone for 24 hours. Following treatment, crypt organoids showed reduced growth compared to untreated organoids (Figure 5-14A). Treated crypts also exhibited increased TIGAR and HO-1 expression compared to controls as well as no change in cyclin D1 expression (Figure 5-14B). Interestingly, the magnitude of both TIGAR and HO-1 mRNA induction was much greater in treated *Apc^{min/+}* crypts compared to treated WT crypt organoids.

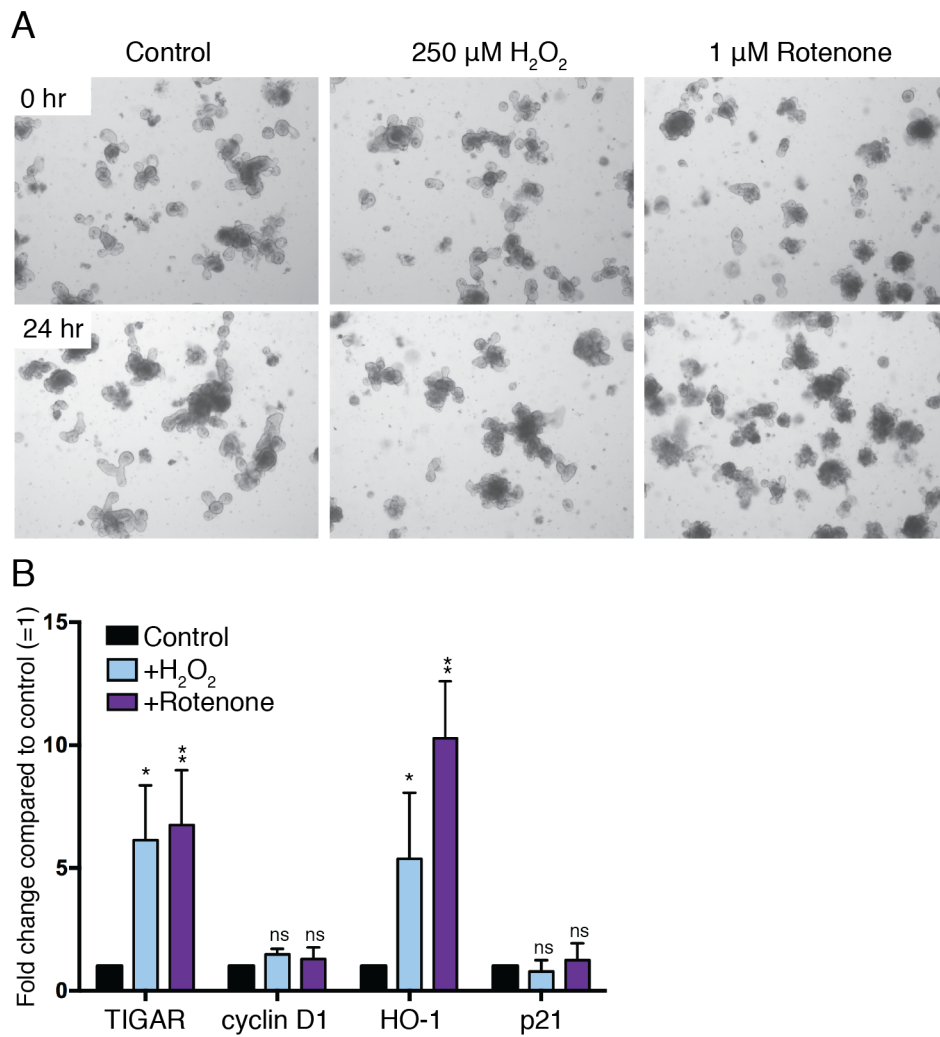


Figure 5-13 TIGAR expression in response to oxidants in WT intestinal organoids

(A) Brightfield images of small intestinal crypt organoids taken from wild-type (WT) mice treated with 250 μM hydrogen peroxide (H_2O_2) or 1 μM rotenone for 24 hr. (B) mRNA expression of TIGAR, cyclin D1, HO-1 and p21 in small intestinal crypt organoids taken from wild-type (WT) mice treated with 250 μM H_2O_2 or 1 μM rotenone for 24 hr. Values represent mean \pm SEM. $n = 3$ independent experiments with 3 technical replicates. * $p < 0.05$, ** $p < 0.005$ compared to control. NS, not significant.

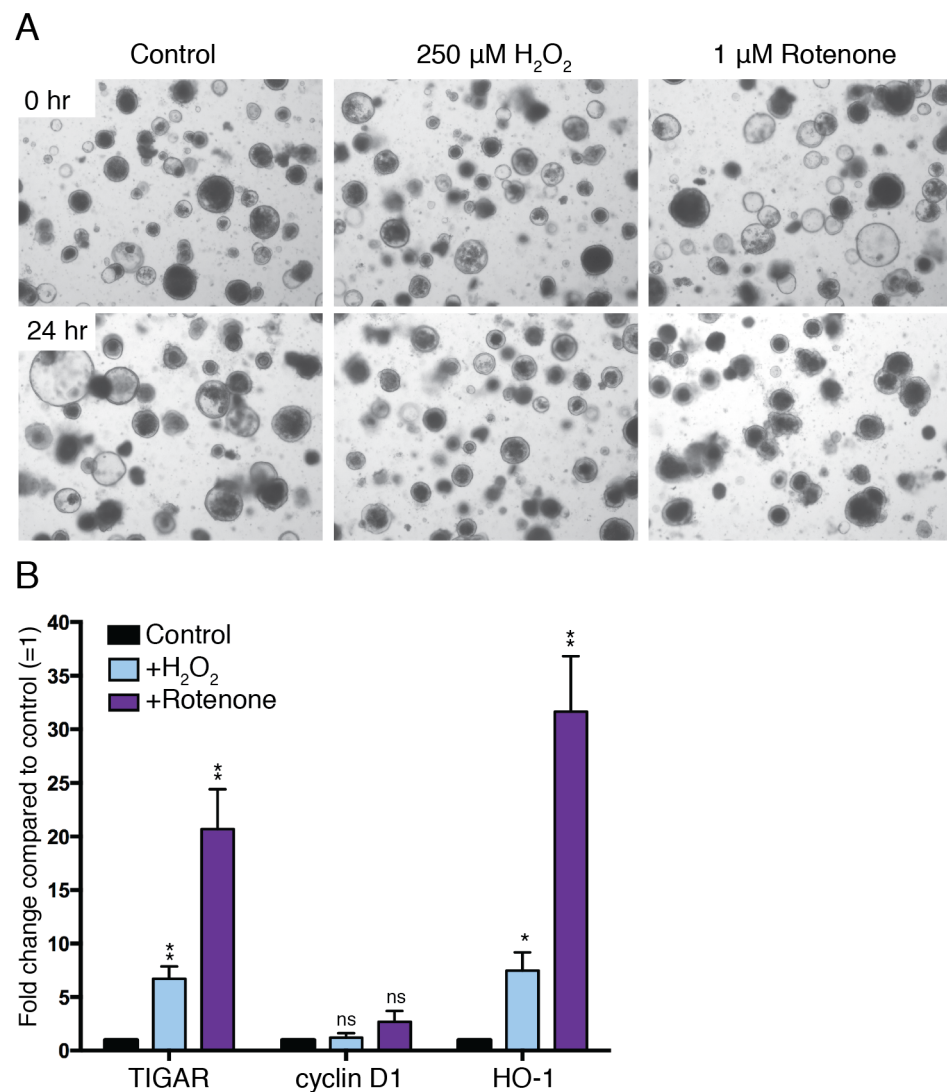


Figure 5-14 TIGAR expression in response to oxidants in *Apc*^{min/+} organoids
 (A) Brightfield images of organoids taken from *Apc*^{min/+} mice treated with 250 μ M hydrogen peroxide (H₂O₂) or 1 μ M rotenone for 24 hr. (B) mRNA expression of TIGAR, cyclin D1 and HO-1 in organoids taken from *Apc*^{min/+} mice treated with 250 μ M H₂O₂ or 1 μ M rotenone for 24 hr. Values represent mean \pm SEM. n = 3 independent experiments with 3 technical replicates. *p < 0.05, **p < 0.005 compared to control. NS, not significant.

As treatment with oxidants was able to increase the mRNA expression of TIGAR, it was hypothesised that ROS lowering treatments would result in decreased TIGAR expression. Previous work has suggested that signalling and damaging ROS may be generated through different mechanisms as well as in different cell compartments (Trachootham et al. 2009). ROS generated in mitochondria as a consequence of oxidative phosphorylation, by xanthine oxidase (XO) at the ER or nitric oxide (NO) generated by nitric oxide synthase (NOS) are generally

considered to produce ROS that is damaging to the cell by reacting with proteins, lipids and DNA (Porasuphatana et al. 2003; Abramov et al. 2007). If produced at excessive levels, this type of ROS can result in cell death.

Firstly, N-acetyl cysteine (NAC), a general antioxidant that is commonly used to lower ROS, was used. *Apc^{min/+}* organoids, which possess greater basal levels of TIGAR, were treated for 24 hours with 2 mM NAC and TIGAR mRNA was assessed as well as cyclin D1 and HO-1. Following treatment, while organoids showed an enhanced growth (Figure 5-15A), there were no changes in the mRNA expression of TIGAR or HO-1, suggesting perhaps that the high basal expression of TIGAR in *Apc^{min/+}* organoids was enough to cope with the changes in ROS balance. In addition, cyclin D1 expression was elevated, supporting the increased growth observed (Figure 5-15B).

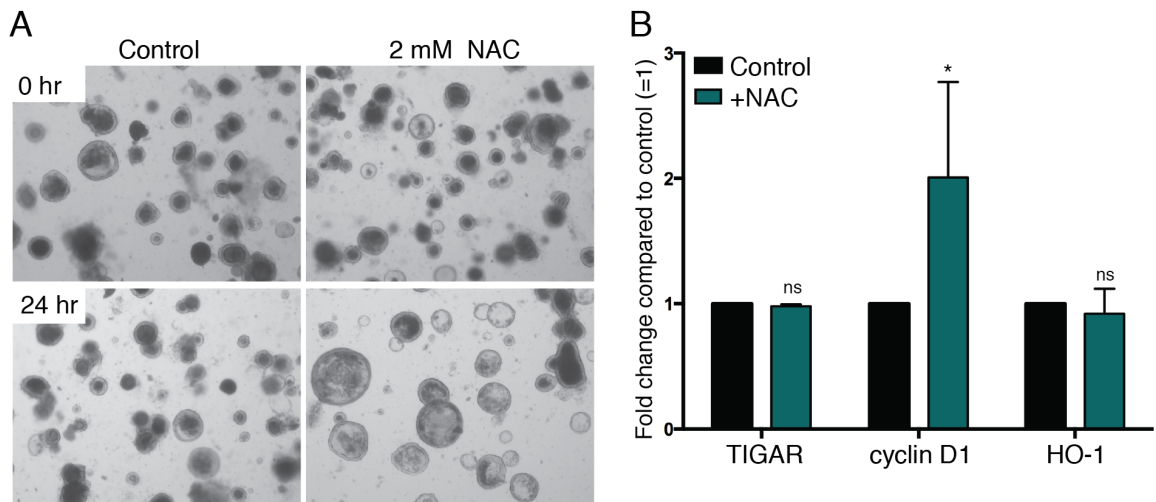


Figure 5-15 TIGAR expression upon NAC treatment in *Apc*^{min/+} organoids

(A) Brightfield images of organoids taken from *Apc*^{min/+} mice treated with 2 mM N-acetyl cysteine (NAC) for 24 hr. (B) mRNA expression of TIGAR, cyclin D1 and HO-1 in *Apc*^{min/+} organoids treated with 2 mM NAC for 24 hr. Values represent mean \pm SEM. $n = 2$ independent experiments with 3 technical replicates. * $p < 0.05$, ** $p < 0.005$ compared to control. NS, not significant.

Following on from this, in order to explore the effects of ROS from different sources on organoid growth, *Apc*^{min/+} organoids were treated with specific antioxidants including allopurinol (XO inhibitor), gallic acid (XO inhibitor) (Cheng and Sun 1994) and L-NG-nitroarginine methyl ester (L-NAME, NOS inhibitor) (Atlante et al. 1997). Organoids were treated with these antioxidants for 24 hours and their effects on TIGAR, cyclin D1 and HO-1 mRNA were assessed.

Following treatment with any of these antioxidants, the growth of the organoids was enhanced (Figure 5-16A). Notably, treatment with XO inhibitors resulted in a dramatic decrease in TIGAR mRNA expression (Figure 5-16B). This was accompanied by a decrease in HO-1 mRNA expression as well as an increase in cyclin D1, illustrating a drop in oxidative stress and a pro-growth phenotype. In contrast, inhibition of NOS resulted in no changes in mRNA expression of TIGAR, HO-1 or cyclin D1. As the nitric oxide generated by NOS can also be utilized as a signalling molecule, which has been well established in vasodilation (Schmidt and Walter 1994), it is possible that the enhanced growth of organoids observed following L-NAME treatment was through a different mechanism than what was

observed after treatment with XO inhibitors. Altogether, these data suggest that TIGAR expression is increased upon oxidative stress and decreased when ROS is lowered by antioxidants.

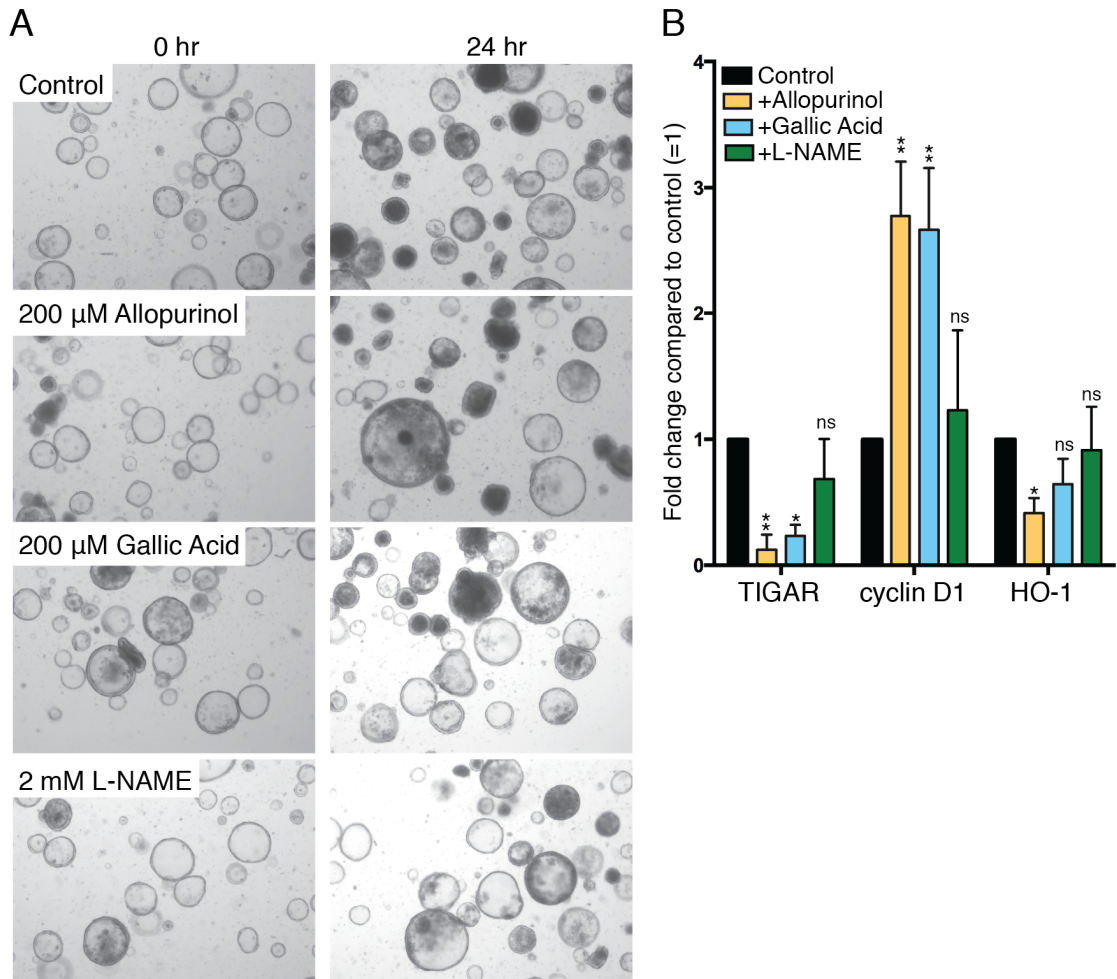


Figure 5-16 TIGAR expression in response to antioxidants in *Apc*^{min/+} organoids

(A) Brightfield images of organoids from *Apc*^{min/+} mice treated with 200 μ M allopurinol, 200 μ M gallic acid or 2 mM L-NAME for 24 hr. (B) mRNA expression of TIGAR, cyclin D1 and HO-1 in *Apc*^{min/+} organoids treated with 200 μ M allopurinol, 200 μ M gallic acid or 2 mM L-NAME for 24 hr. Values represent mean \pm SEM. n = 3 independent experiments with 3 technical replicates. *p < 0.05, **p < 0.005 compared to control. NS, not significant.

5.3.3 The Regulation of TIGAR by ROS in Human Cells

As ROS seems to be able to regulate the expression of TIGAR in mouse cells *in vitro*, the potential for ROS to also regulate TIGAR expression in human cells was investigated. To address this, experiments were performed in 2D tissue culture systems using human MCF7 cells, either possessing wild-type p53 or deficient for p53 (MCF7 p53^{-/-}). Induction of oxidative stress was first performed through treatment with hydrogen peroxide (H₂O₂) or tert-butyl hydroperoxide (tBHP), both of which result in a cytoplasmic increase in ROS. Cells were treated with 500 μM H₂O₂ or 100 μM tBHP for 24 hours and protein as well as mRNA expression were assessed.

Induction of oxidative stress following treatment with H₂O₂ led to an increase in the expression of known stress-responsive pathways such as p53 and its target gene p21 on protein and mRNA level (Figure 5-17B-C). MCF7 p53^{-/-} cells were less able to cope with oxidative stress, most likely due to the loss of the p53 stress response (Figure 5-17A). In addition to the p53 pathway, the response of ROS-induced genes to treatment was also assessed. Nuclear factor erythroid 2-related factor 2 (NRF2) is a transcription factor known to induce the transcription of antioxidant genes including HO-1 (Jian et al. 2011). While NRF2 protein and mRNA expression showed no change, which could be due to alterations in protein translocation rather than expression driving NRF2 activity (Sporn and Libby 2012), HO-1 was clearly induced on both protein and mRNA level following treatment with H₂O₂ (Figure 5-17B-C). The expression of TIGAR, however, was solely induced following induction of H₂O₂ in a p53-dependent manner (Figure 5-17B-C). The effects of cytosolic oxidative stress were further assessed using tBHP. Similar to what was observed upon treatment with H₂O₂, cells lacking p53 were less able to cope with oxidative stress (Figure 5-18A) and TIGAR expression was elevated in a p53-dependent manner regardless of NRF2 activity as shown by the elevation in HO-1 (Figure 5-18B).

As the ROS induced by H₂O₂ or tBHP was cytosolic, another manner to induce ROS was tested which would elevate mitochondrial ROS.

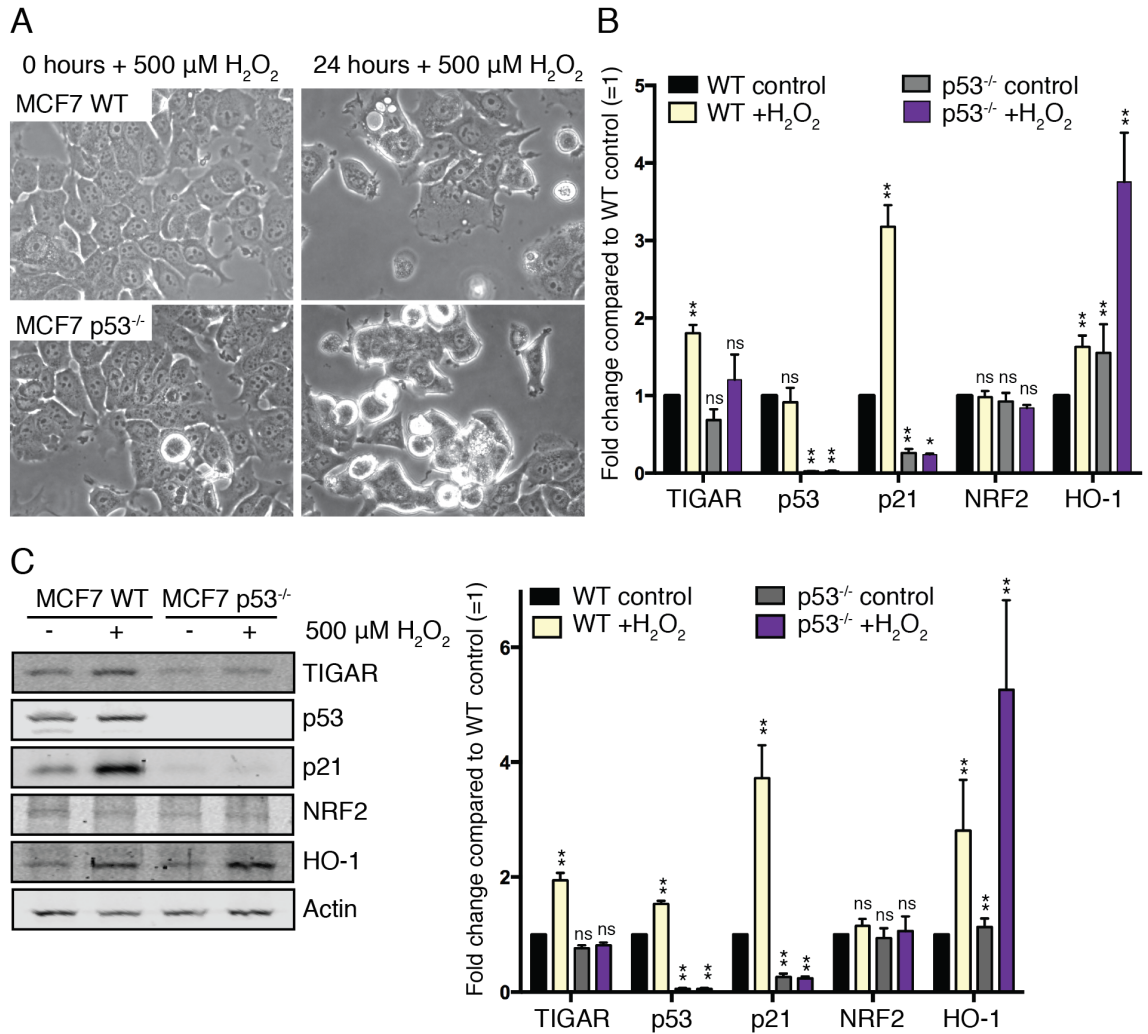
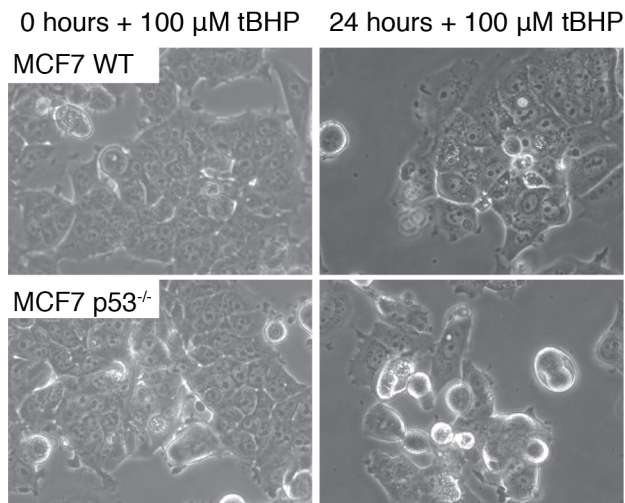


Figure 5-17 TIGAR expression in response to hydrogen peroxide

(A) Brightfield images of MCF7 wild-type (WT) and MCF7 p53-null (p53^{-/-}) treated with 500 μM hydrogen peroxide (H_2O_2) for 24 hr. (B) mRNA expression of TIGAR, p53, p21, NRF2 and HO-1 in MCF7 WT and MCF7 p53^{-/-} treated with 500 μM H_2O_2 for 24 hr. Values represent mean \pm SEM. $n = 3$ independent experiments with 3 technical replicates. (C) Left: Western blot analysis of MCF7 WT and MCF7 p53^{-/-} treated with 500 μM H_2O_2 for 24 hr. Right: Quantification of Western blots. Values represent mean \pm SEM. $n = 3$ independent experiments. * $p < 0.05$, ** $p < 0.005$ compared to WT control. NS, not significant.

A



B

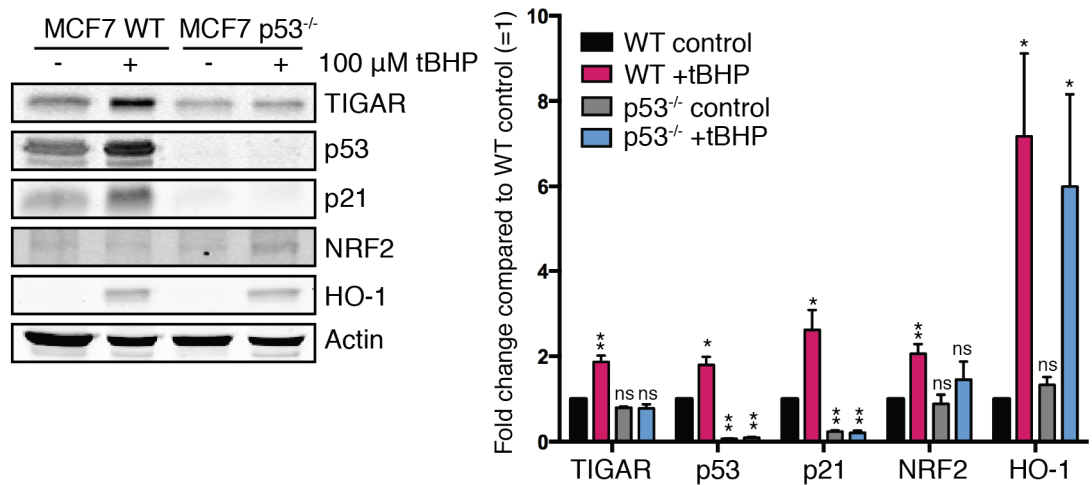


Figure 5-18 TIGAR expression in response to tert-butyl hydroperoxide

(A) Brightfield images of MCF7 wild-type (WT) and MCF7 p53-null (p53^{-/-}) treated with 100 μM tert-butyl hydroperoxide (tBHP) for 24 hr. (B) Left: Western blot analysis of MCF7 WT and MCF7 p53^{-/-} treated with 100 μM tBHP for 24 hr. Right: Quantification of Western blots. Values represent mean ± SEM. n = 3 independent experiments. *p < 0.05, **p < 0.005 compared to WT control. NS, not significant.

To test the effects of mitochondrial ROS on TIGAR, cells were treated with 1 μ M rotenone for 24 hours. Much like observed following treatment with H₂O₂ or tBHP, treatment with rotenone induced the expression of p53 and its target gene p21 as well as NRF2 and its target gene HO-1 (Figure 5-19B-C). Similarly, an elevation of TIGAR protein and mRNA were observed, however, this was again in a p53-dependent manner. In addition, these cells showed less cell death following rotenone treatment compared to H₂O₂ or tBHP treatment (Figure 5-19A). Altogether, these results suggest that ROS is also able to induce the expression of TIGAR in human cells, but in this scenario relies on p53.

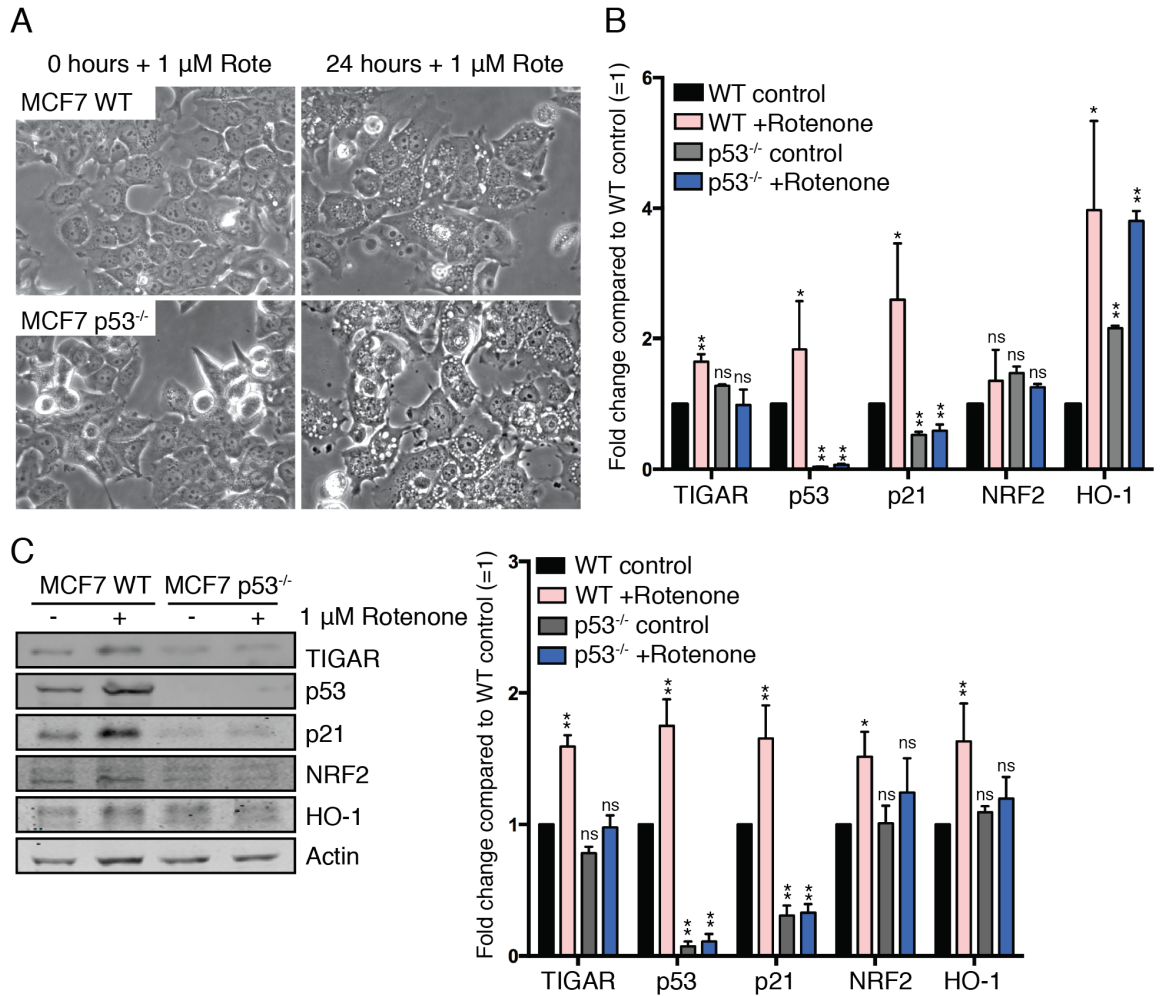


Figure 5-19 TIGAR expression in response to rotenone

(A) Brightfield images of MCF7 wild-type (WT) and MCF7 p53-null (p53^{-/-}) treated with 1 μ M rotenone (Rote) for 24 hr. (B) mRNA expression of TIGAR, p53, p21, NRF2 and HO-1 in MCF7 WT and MCF7 p53^{-/-} treated with 1 μ M rotenone for 24 hr. Values represent mean \pm SEM. n = 3 independent experiments with 3 technical replicates. (C) Left: Western blot analysis of MCF7 WT and MCF7 p53^{-/-} treated with 1 μ M rotenone for 24 hr. Right: Quantification of Western blots. Values represent mean \pm SEM. n = 3 independent experiments. *p < 0.05, **p < 0.005 compared to WT control. NS, not significant.

5.4 Summary & Discussion

It has previously been found that TIGAR can be induced in the small intestine following irradiation in a p53-independent manner, despite being a p53 target gene in humans (Chapter 4). As the Wnt signalling pathway plays a key role in promoting and mediating cell proliferation in the small intestine particularly during intestinal regeneration, the hypothesis that the Wnt signalling can induce TIGAR expression in the small intestine was tested.

As several metabolic genes have been found to be a target of the Wnt signalling pathway, through canonical as well as the non-canonical branches, it is possible that TIGAR may also be a target of this pathway. Recently, the Wnt pathway was found to increase aerobic glycolysis through the suppression of mitochondrial respiration by repressing the transcription of cytochrome c oxidase, a component of the ETC (Sherwood 2015). In colorectal cancer, canonical Wnt signalling can promote aerobic glycolysis by increasing the expression of pyruvate dehydrogenase kinase 1, thereby decreasing pyruvate oxidation and increasing the conversion of pyruvate to lactate. Similarly, the lactate transporter, monocarboxylate transporter 1 is also upregulated by Wnt in order to facilitate lactate secretion (Pate et al. 2014).

Our studies in cultured cells did not show a clear Wnt-dependent increase in TIGAR expression. However, upon treatment of rWnt3a ligand in small intestinal crypt organoids, a clear induction in the expression of TIGAR was observed. Comparison between WT small intestinal crypt organoids and those harvested from *Apc^{min/+}* mice showed higher levels of TIGAR expression in *Apc^{min/+}* organoids. Furthermore, an acute loss of APC in *villin-Cre-ER^{T2} Apc^{fl/fl}* organoids also promoted the expression of TIGAR. Upon further investigation *in vivo*, using models where loss of intestinal-specific APC resulted in high Wnt pathway signalling, a clear increase in TIGAR expression was also observed at both mRNA and protein level.

Downstream of the Wnt signalling pathway, the transcription factor c-Myc, acts to drive the majority of the hyperproliferative phenotype observed upon APC loss (Sansom et al. 2007), and can also influence the transcription of genes involved in

various metabolic pathways including glycolysis, nucleotide synthesis, lipid synthesis and glutaminolysis, all of which are important in promoting cell growth and proliferation (Dang 2012). β -catenin mediated c-Myc expression results in the upregulation of glucose transporter 1 (GLUT1), lactate dehydrogenase (LDH) and pyruvate kinase M2 (PKM2) to promote aerobic glycolysis in cancer cells (Pate et al. 2014). Assessment of TIGAR expression in the small intestine of *AhCre⁺ Apc^{fl/fl} Myc^{fl/fl}* mice showed that the APC-loss driven increase in TIGAR was c-Myc-dependent.

It is clear that ROS is able to support both cell proliferation and survival as well as result in damage and cell death (Sabharwal and Schumacker 2014). Malignant development is often associated with an increase in oxidative stress, which can be a result of a loss of normal cell environment as well as a consequence of increased metabolism to support enhanced cell proliferation. Several studies have shown that cancer cells are able to limit excessive levels of ROS to support their growth and survival (Budanov and Karin 2008; DeNicola et al. 2011). In addition, ROS generated in cancer cells can also directly affect the transcriptional activity of β -catenin. Studies in breast cancer have found that ROS is able to displace the interaction between β -catenin and TCF4 and facilitate the interaction between β -catenin and forkhead box O3 (FOXO3a). Through this, ROS can alter cell fate from a proliferative, cancer stem cell phenotype to a more differentiated state with reduced tumorigenesis (Dong et al. 2013). Oxidative stress can also alter Wnt signalling further upstream by influencing the activity of Dishevelled (Dsh). The interaction of Dsh with the thioredoxin family protein nucleoredoxin inhibits Dsh. This interaction can be abrogated through treatment with H_2O_2 , which promotes Wnt signalling independent of extracellular Wnt stimulation (Funato et al. 2006). As TIGAR plays an important role combatting oxidative stress in the small intestine and deletion of APC also promotes an increase in ROS (in a Myc-dependent manner), the role of ROS itself being able to regulate TIGAR was also investigated.

The intestinal crypt culture model was used to investigate p53-independent changes in TIGAR expression following treatment with oxidants as well as antioxidants. TIGAR expression was upregulated in the *Apc^{min/+}* crypt organoids

after treatment with hydrogen peroxide or rotenone. A decrease in TIGAR expression was also observed following treatment with antioxidants, showing how levels of ROS can influence the expression of TIGAR. This was further examined in human cells, where TIGAR expression was also increased upon treatment with oxidants, however, this was in a p53-dependent manner.

As ROS was able to influence the expression of TIGAR, the potential of NRF2 to drive TIGAR expression would be interesting to explore further. NRF2 is a well-established transcription factor that is activated in response to oxidative stress to drive the cellular antioxidant response. Therefore, the potential of TIGAR to be a NRF2 target gene could be considered in addition to being a p53 target gene. While initial studies have found that NRF2 is upregulated in small intestinal crypts of wild-type mice following irradiation much like the expression of TIGAR (data not shown), in 2D human cell cultures, activation of NRF2 using a chemical activator of NRF2, sulforaphane, did not influence TIGAR expression (data not shown). Notably, human p53-null cells treated with sulforaphane showed an increase in NRF2 and its target HO-1 but no increase in TIGAR (data not shown). It would be interesting to further investigate the potential for NRF2 to influence mouse TIGAR expression through the use of *in vitro* small intestinal organoids as well as using cancer models where NRF2 is upregulated to promote tumorigenesis as seen in the KRas pancreatic adenocarcinoma model (DeNicola et al. 2011). Other ROS-induced transcription factors could also be investigated for a role in promoting TIGAR such as FOXO3a, which can contribute to protection against oxidative stress by upregulating the transcription of manganese superoxide dismutase (MnSOD) and catalase (Kops et al. 2002a; Kops et al. 2002b; Nemoto and Finkel 2002). The activator protein (AP-1) family of transcription factors are also induced by ROS and can bind to antioxidant response elements (ARE) in genes involved in protecting cells against oxidative stress (Weitzman et al. 2000; Gerald et al. 2004; Tsuji 2005), which could include TIGAR.

Furthermore, it would be interesting to understand whether TIGAR is upregulated in other cancer types and how this may contribute to tumorigenesis, as basal expression of TIGAR is variable in different tissues.

Chapter 6 The Role of TIGAR *in vivo*

TIGAR functions as a fructose-2,6-bisphosphatase, decreasing the intracellular levels of fructose-2,6-bisphosphate and thereby lowering the activity of phosphofructokinase-1 (PFK-1) and flux through the glycolytic pathway (Bensaad et al. 2006; Wanka et al. 2012). As a consequence, glycolytic metabolites can be diverted into the pentose phosphate pathway (PPP) and TIGAR has been shown to increase the production of NADPH for antioxidant activity as well as ribose-5-phosphate (R5P) for nucleotide synthesis (Kimata et al. 2010; Pena-Rico et al. 2011). Several studies have shown the importance of TIGAR in regulating redox control in cells and elevated TIGAR expression has also been observed in various cancer types (Wanka et al. 2012; Won et al. 2012; Cheung et al. 2013; Sinha et al. 2013), suggesting that a deregulated expression of TIGAR may play a role in supporting rather than inhibiting cancer development and proliferation.

Activation of the Wnt signalling pathway increased TIGAR expression in the small intestine, therefore, the function of TIGAR in the small intestine was further investigated. In particular, the consequences of TIGAR loss *in vivo* were analysed as well as the functional role of TIGAR in a mouse model of intestinal regeneration.

6.1 Confirmation of Efficient TIGAR Deletion in Mice

Previous analyses of TIGAR function have been predominantly performed in human cancer cell lines (Jen and Cheung 2005; Bensaad et al. 2006; Bensaad et al. 2009; Hasegawa et al. 2009; Wanka et al. 2012). Therefore, a TIGAR-deficient mouse was generated to further study the role of TIGAR *in vivo* as well as the consequences of its loss (Cheung et al. 2013). To do so, a constitutive deletion was generated using a genetrapp construct from EUCOMM, where the targeting vector was inserted between exons 2 and 3 of the *Tigar* gene (Cheung et al. 2013). To validate this model, the deletion of TIGAR was confirmed by examining TIGAR expression in liver tissues from TIGAR-null ($TIGAR^{-/-}$) mice by Western blot and using liver samples from WT animals as a control (Figure 6-1). A loss of TIGAR did not affect developing embryos or unstressed adults (Cheung et al. 2013), suggesting that TIGAR expression is not essential for development and may play a role under conditions of stress in adult tissue.

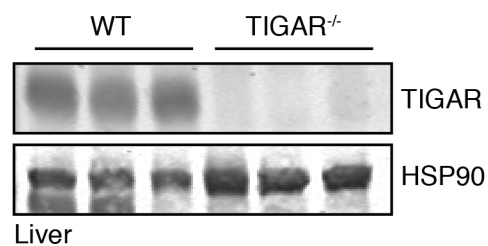


Figure 6-1 Confirmation of TIGAR-deficient mice

Loss of TIGAR protein expression was confirmed in $TIGAR^{-/-}$ animals by Western blot analysis of liver tissue samples. $n = 3$ mice per genotype.

6.2 TIGAR Expression is required for Small Intestine Proliferation after Acute Damage

The function of TIGAR in proliferation was further analysed using an intestinal regeneration model following tissue ablation caused by cisplatin or irradiation treatment, as previously described (Martin et al. 1998; Potten and Grant 1998; Metcalfe et al. 2014).

In agreement with published reports, TIGAR expression is relatively low in the untreated small intestines and is localised in the crypts of the small intestine where intestinal cell proliferation occurs. Moreover, TIGAR deficiency did not affect normal intestinal crypt architecture (Cheung et al. 2013). TIGAR expression in WT animals showed a sustained increase within the intestinal crypts following cisplatin treatment (Figure 6-2) as well as after irradiation (Figure 6-3). Loss of TIGAR was confirmed in the small intestine of *TIGAR*^{-/-} animals as no increase in TIGAR expression was observed following cisplatin (Figure 6-2) or irradiation treatment (Figure 6-3). This increase in TIGAR after irradiation was also observed in the small intestine by Western blot, where TIGAR-deficiency was again confirmed in *TIGAR*^{-/-} animals (Figure 6-4). Furthermore, the elevation in TIGAR RNA was also observed following irradiation by using RNAscope assays, a novel *in situ* hybridisation (ISH) method, which allows for the visualisation of single RNA molecules in samples mounted on slides. No increase in TIGAR RNA was seen in the *TIGAR*^{-/-} animals after irradiation (Figure 6-5). Altogether, these data show that both TIGAR protein and RNA are increased during intestinal regeneration and confirm complete ablation of TIGAR in *TIGAR*^{-/-} mice.

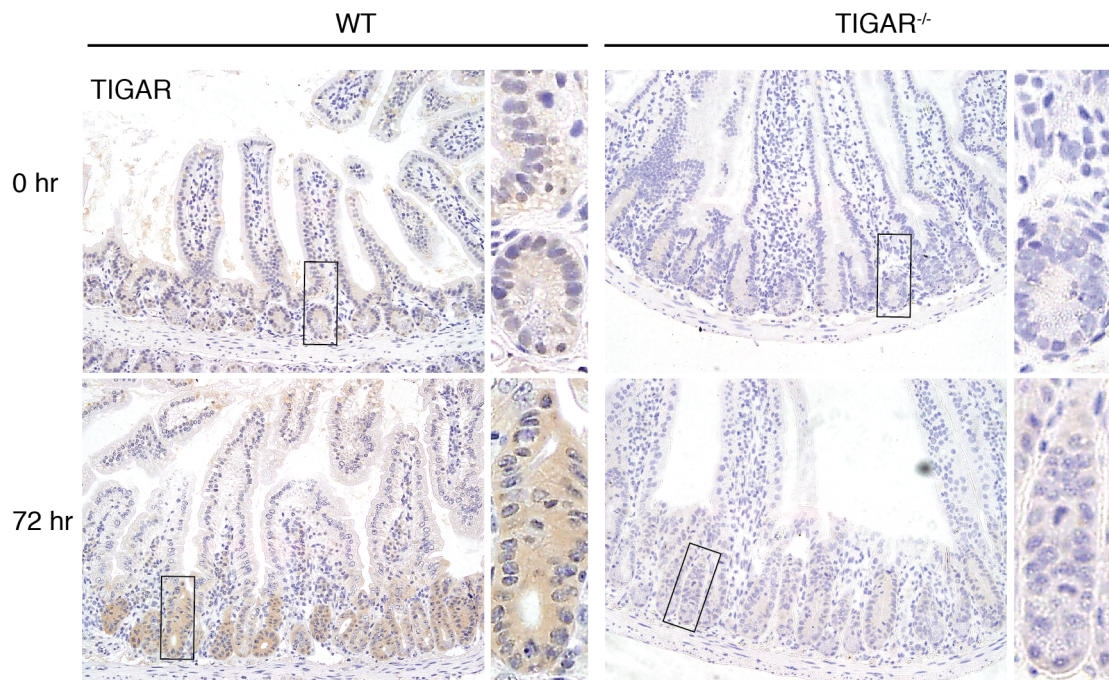


Figure 6-2 Increased TIGAR in the small intestine after cisplatin treatment
 Immunohistochemistry for TIGAR on wild-type (WT) and *TIGAR*^{-/-} animals before and 72 hr after cisplatin treatment. Panels show more detailed crypt structures indicated in the box. n = 3 mice per genotype per condition, each stained 3 times.

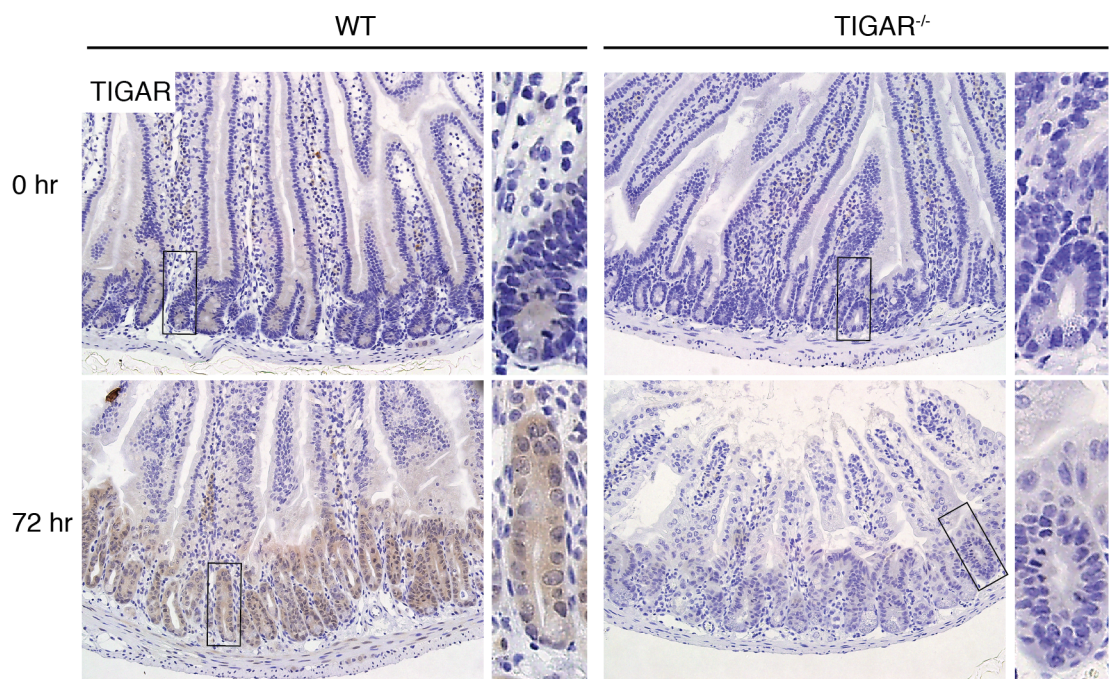


Figure 6-3 TIGAR expression increases in the small intestine after irradiation
 Immunohistochemistry for TIGAR on wild-type (WT) and *TIGAR*^{-/-} animals before and 72 hr after 14 Gy irradiation. Panels show more detailed crypt structures indicated in the box. n = 3 mice per genotype per condition, each stained 3 times.

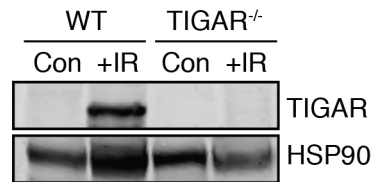


Figure 6-4 TIGAR expression increases in the small intestine after irradiation
Western blot showing an increase in TIGAR expression in the small intestine of wild-type (WT) and *TIGAR*^{-/-} animals before and after 10 Gy irradiation (IR). n = 1 mouse per genotype per condition.

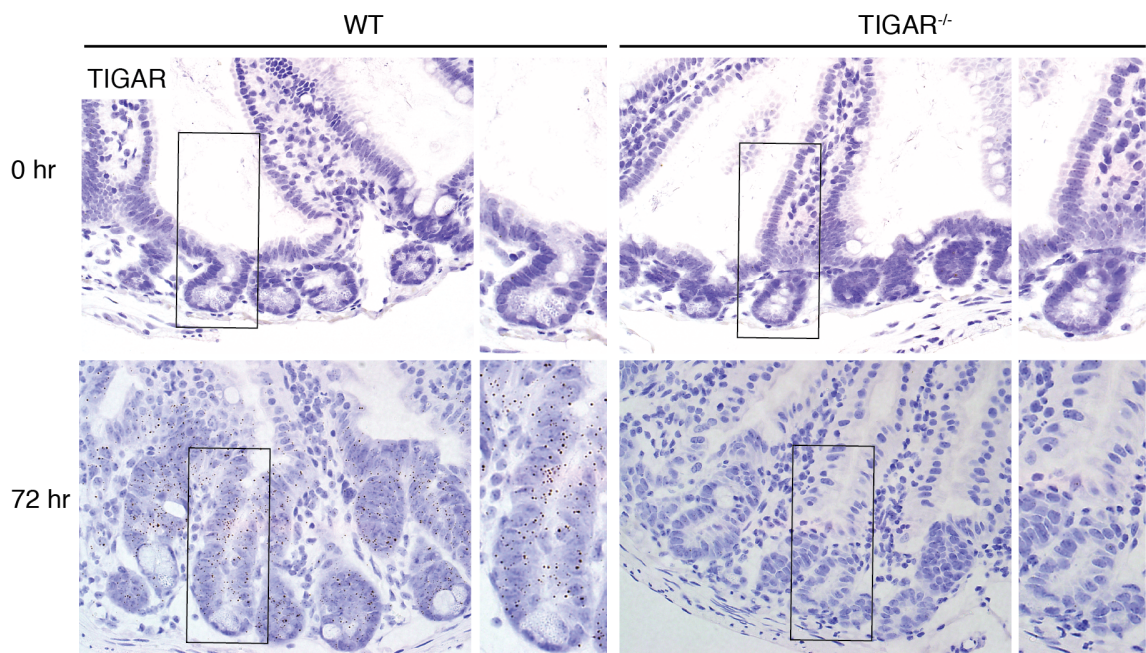


Figure 6-5 TIGAR RNA expression in the small intestine after irradiation
RNAscope assay for TIGAR on wild-type (WT) and *TIGAR*^{-/-} animals before and 72 hr after 14 Gy irradiation. Panels show more detailed crypt structures indicated in the box. n = 3 mice per genotype per condition, each stained 2 times

Next, the effects of TIGAR-deficiency on intestinal regeneration were assessed. Immunohistochemistry was performed for the proliferative marker Ki67, and while both WT and *TIGAR*^{-/-} animals showed an initial decrease in proliferation 24 hours post-IR, only WT animals were able to progress into a phase of rapid proliferation that was evident 48 and 72 hours post-IR, consistent with an outgrowth of new crypt structures (Figure 6-6A-B). *TIGAR*^{-/-} animals showed a clear defect in proliferation at these time points, suggesting a role for TIGAR in supporting intestinal regeneration after damage.

To further examine how TIGAR supports intestinal regeneration, oxidative stress in the small intestine was assessed following irradiation. Since TIGAR can contribute to the cellular antioxidant response by promoting the pentose phosphate pathway, it was hypothesized that TIGAR may support proliferation in the small intestine through this method.

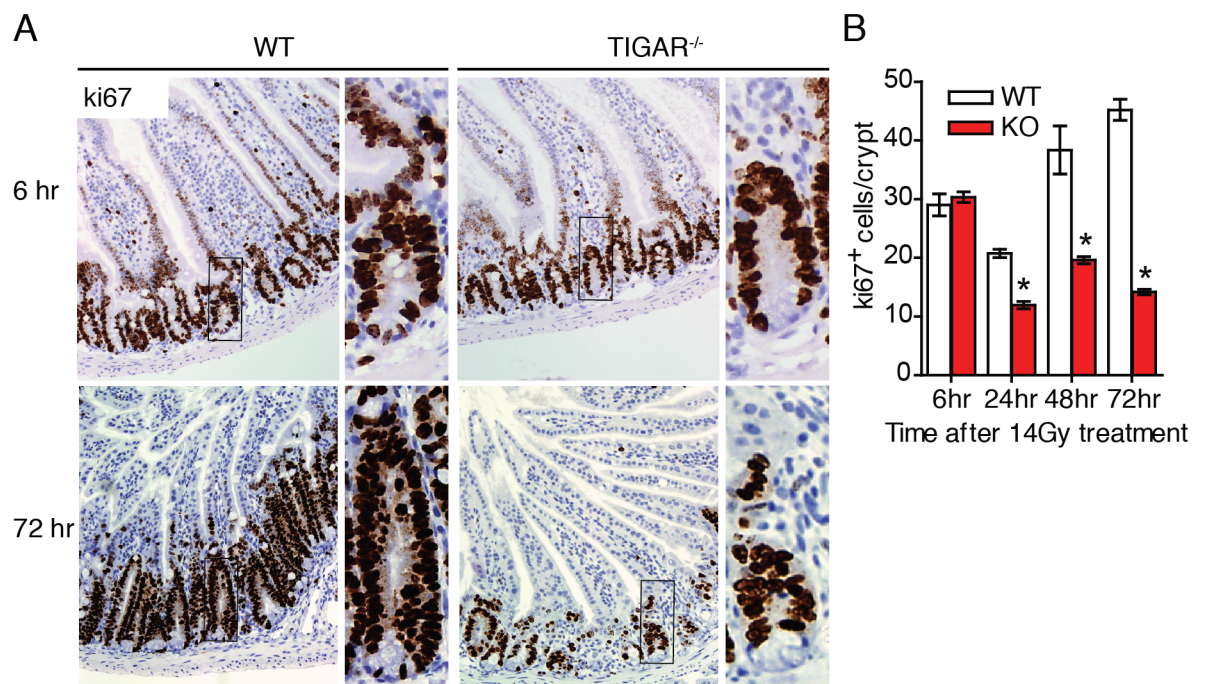


Figure 6-6 TIGAR-deficiency reduces regenerative capacity in intestinal crypts

(A) Immunohistochemistry for Ki67 on wild-type (WT) and *TIGAR*^{-/-} (KO) animals 6 and 72 hr after 14 Gy irradiation. Panels show more detailed crypt structures indicated in the box. n = at least 3 mice. (B) Quantification of Ki67 positive cells in WT and KO animals at the indicated times after 14 Gy IR. *p < 0.05 compared to WT. Data obtained from Eric Cheung.

6.3 Loss of TIGAR Leads to Increased Oxidative Stress After Irradiation

Previous work has demonstrated a role for TIGAR in lowering oxidative stress and TIGAR-deficient baby mouse kidney cells possess lower levels of GSH and are more sensitive to treatment with hydrogen peroxide (Bensaad et al. 2006; Bensaad et al. 2009; Cheung et al. 2013). To assess levels of oxidative stress in the *TIGAR*^{-/-} mice, the levels of malondialdehyde (MDA) were examined by immunohistochemistry. Following irradiation treatment, WT mice showed an increase in MDA in their intestinal crypts, indicating an increase in oxidative stress. Notably, animals deficient in TIGAR showed a greater increase in MDA levels compared to WT animals after irradiation (Figure 6-7). This indicates that TIGAR plays an important role in limiting ROS *in vivo* in order to support proliferation during intestinal regeneration.

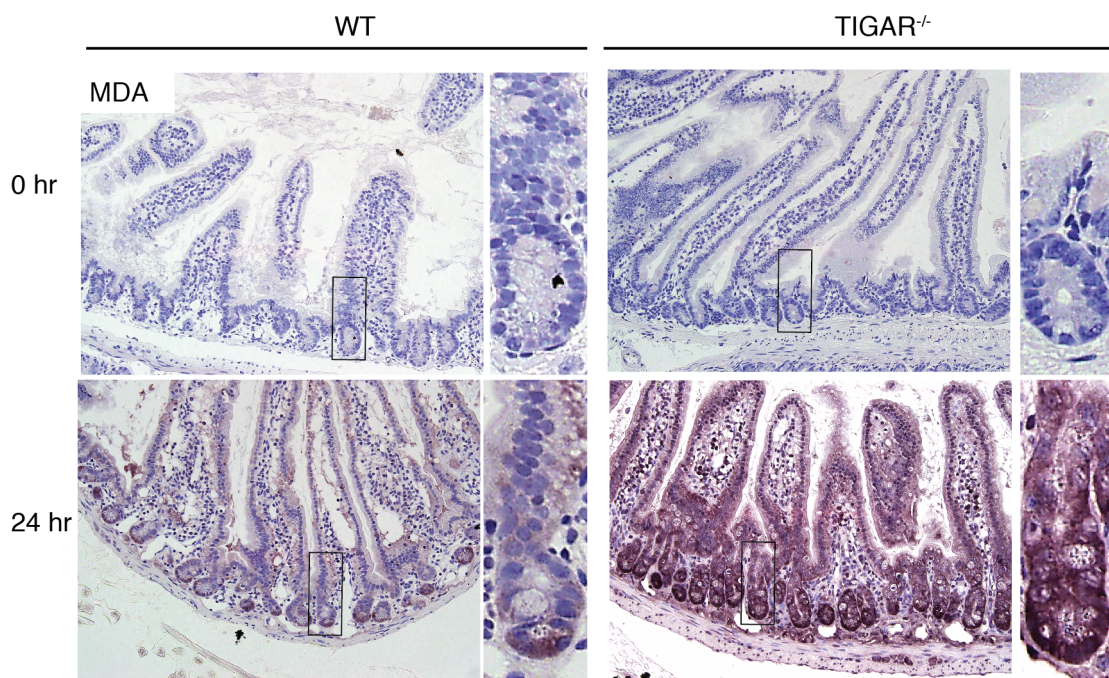


Figure 6-7 Loss of TIGAR leads to increased oxidative stress after irradiation

Immunohistochemistry for malondialdehyde (MDA) staining wild-type (WT) and *TIGAR*^{-/-} animals before and 24 hr after 14 Gy irradiation. Panels show more detailed crypt structures indicated in the box. n = 3 mice per genotype per condition, each stained 3 times.

6.4 TIGAR is Important in Tumour Development in an Intestinal Adenoma Model

The previous results show that TIGAR plays an important role in allowing for the growth and proliferation required for the repair of the damaged intestinal epithelium in adult mice. The modulation of metabolic pathways to allow anabolism and ROS limitation has also been proposed to play an important role in supporting tumourigenesis. Therefore, we decided to investigate whether TIGAR contributes to the abnormal proliferation of tumour cells in the small intestine. To address this, a model in which the tumour suppressor APC is deleted in LGR5⁺ intestinal stem cells resulting in the development of intestinal adenomas was used (*TIGAR*^{+/+} *Lgr5-EGFP-IRES-creER*^{T2/APC}^{fl/fl}) (Barker et al. 2009). Following multiple doses of tamoxifen in order to maximize the incidence of adenoma development, TIGAR was found highly expressed in the adenomas formed in *TIGAR*^{+/+} *Lgr5-EGFP-IRES-creER*^{T2/APC}^{fl/fl} mice compared to the surrounding tissue, consistent with a role for TIGAR in promoting proliferation in tumour tissues (Figure 6-8A). To test the role of TIGAR in these adenomas, these animals were then crossed with TIGAR-deficient mice to generate *TIGAR*^{-/-} *Lgr5-EGFP-IRES-creER*^{T2/APC}^{fl/fl}, where TIGAR was lost and APC could be deleted upon tamoxifen induction. Compared to *TIGAR*^{+/+} *Lgr5-EGFP-IRES-creER*^{T2/APC}^{fl/fl} mice, TIGAR-null animals showed less proliferation (less Ki67 staining) (Figure 6-8A) as well as a significant reduction in the number of tumours (Figure 6-8B), total tumour burden (Figure 6-8C) and average tumour size (Figure 6-8D). These results indicate that a loss of TIGAR limited tumour development. Importantly, this reduction in tumour burden correlated with an increased survival in mice lacking TIGAR (Figure 6-8E) (Cheung et al. 2013).

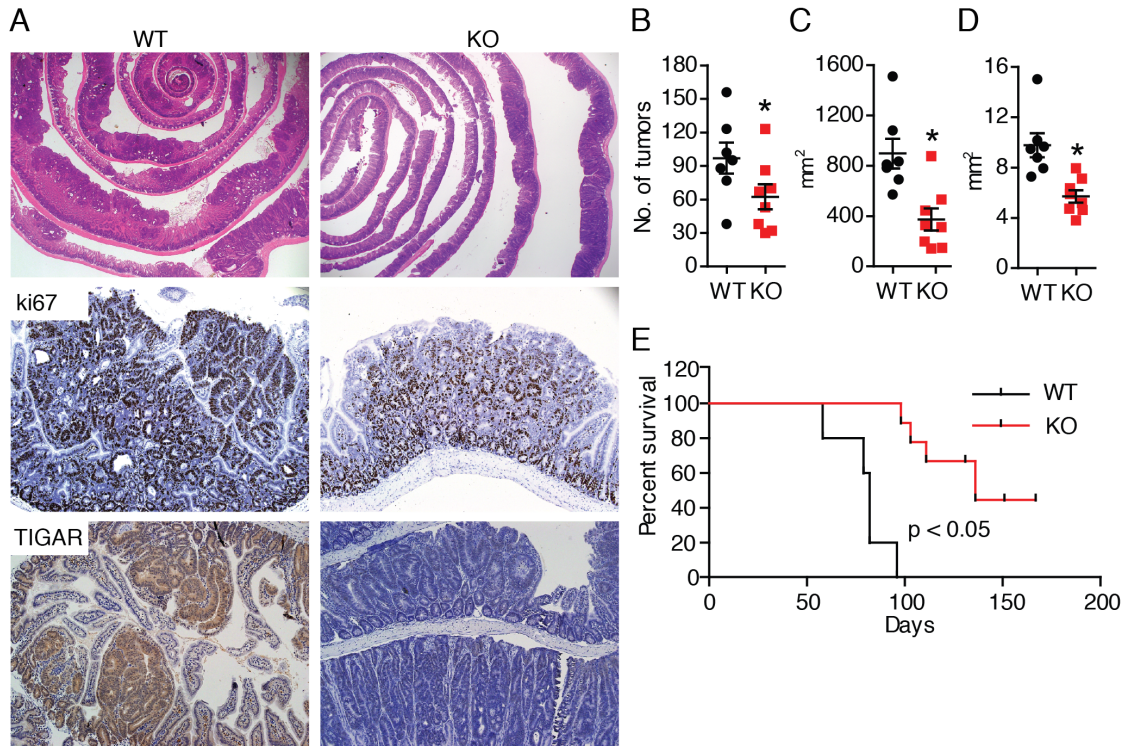


Figure 6-8 TIGAR loss reduces tumour burden in an intestinal adenoma model

(A) Top: H&E staining of small intestine of *TIGAR*^{+/+} *Lgr5-EGFP-IRES-creER*^{T2}/*Apc*^{fl/fl} (WT) and *TIGAR*^{-/-} *Lgr5-EGFP-IRES-creER*^{T2}/*Apc*^{fl/fl} (KO) mice after multiple rounds of tamoxifen induction and taken at clinical endpoint. Middle: Immunohistochemistry for Ki67 in the small intestine of WT and KO mice after multiple rounds of tamoxifen induction and taken at clinical endpoint. Bottom: Immunohistochemistry for TIGAR in small intestine of WT and KO mice after multiple rounds of tamoxifen induction and taken at clinical endpoint. (B) Number of tumours from WT and KO mice (C) Total tumour burden in the small intestine of WT and KO mice. (D) Average tumour size from WT and KO mice (E) Kaplan-Meier survival curves showing adenoma-free survival of WT (n = 5) and KO (n = 7) mice. Data represents and mean ± SEM. **p* < 0.05 compared to WT. Data obtained from Eric Cheung.

6.5 TIGAR Modulates Damaging ROS

Taken together, our data from the previous chapter suggest that TIGAR is induced in response to ROS. In addition, previous work has shown that TIGAR can function to promote the antioxidant defence in cells (Bensaad et al. 2006; Bensaad et al. 2009; Lui et al. 2010; Lui et al. 2011; Wanka et al. 2012; Yin et al. 2012). As previously discussed, signalling and damaging ROS may be generated through different mechanisms and in different cell compartments (Trachootham et al. 2009). ROS can be either pro-proliferative, as seen in ROS generated by NADPH oxidases (NOX) (Bedard and Krause 2007) or detrimental to cell growth or survival, as seen in ROS generated by the mitochondria, and the outcome can depend on the source, the levels and the forms of ROS. Therefore, whether the ROS signal induced by the loss of TIGAR is qualitatively different from the ROS induced by NOX was tested *in vivo*.

An APC model was used where TIGAR as well as another Wnt target gene, RAC1, which is also involved in redox homeostasis, were simultaneously deleted. The RAC1 GTPase has previously been shown to play an important role in promoting cell proliferation and is often overexpressed in human cancers (Sanz-Moreno et al. 2008; Krauthammer et al. 2012; Yang et al. 2012c). Alongside its cytoskeletal role, RAC1 functions as a mediator of NOX and a key contribution of RAC1 to support proliferation is through NOX-mediated ROS production, which has also been found important in supporting tumourigenesis. As with TIGAR, loss of APC in the mouse intestine results in the upregulation of RAC1, despite its opposing role to TIGAR in the regulation of ROS. Notably, loss of RAC1 in this model resulted in an inhibition of APC-driven hyperproliferation alongside a decrease in ROS levels (Myant et al. 2013).

Loss of APC resulted in hyperproliferation in the small intestine (Ki67 staining) due to high Wnt signalling as shown by an accumulation of β -catenin (Figure 6-9, Figure 6-10). In addition, APC loss resulted in increased levels of damaging ROS as shown by MDA staining (Figure 6-11), and increased expression of TIGAR (Figure 6-12). A co-deletion of APC and TIGAR resulted in a further increase in damaging ROS (Figure 6-11), but was accompanied with a decrease in proliferation (Ki67 staining and crypt size) (Figure 6-9). Interestingly, while co-

deletion of APC and RAC1 reduced the proliferation in the small intestine to a similar extent as when TIGAR was deleted alongside APC (Figure 6-9), there was no further increase in MDA staining (Figure 6-11). Furthermore, loss of RAC alongside APC deletion did not impair the increased expression of TIGAR in the small intestine or liver (Figure 6-13). This suggests that loss of RAC1 does not lower damaging ROS, which can induce TIGAR expression, but rather a distinct pool of ROS important in supporting proliferation. This notion was further supported when a simultaneous loss of both TIGAR (leading to an increase in damaging ROS) and RAC1 (leading to a decrease in growth signalling ROS) resulted in a greater inhibition of crypt proliferation in response to APC loss than deletion of either individually, despite a minor diminution in β -catenin levels (Figure 6-9, Figure 6-10). In addition, despite the inhibition of proliferation, *AhCre⁺ Apc^{fl/fl} TIGAR^{fl/fl} Rac1^{fl/fl}* cells retained high levels of damaging ROS (MDA staining), which was only found in the crypts (Figure 6-11).

Altogether, these data suggest that during the rapid proliferation induced upon APC loss, there is a selective modulation of two pools of ROS, which have different and opposing properties on cell growth, with RAC1 promoting signalling ROS and TIGAR limiting damaging ROS (Figure 6-14).

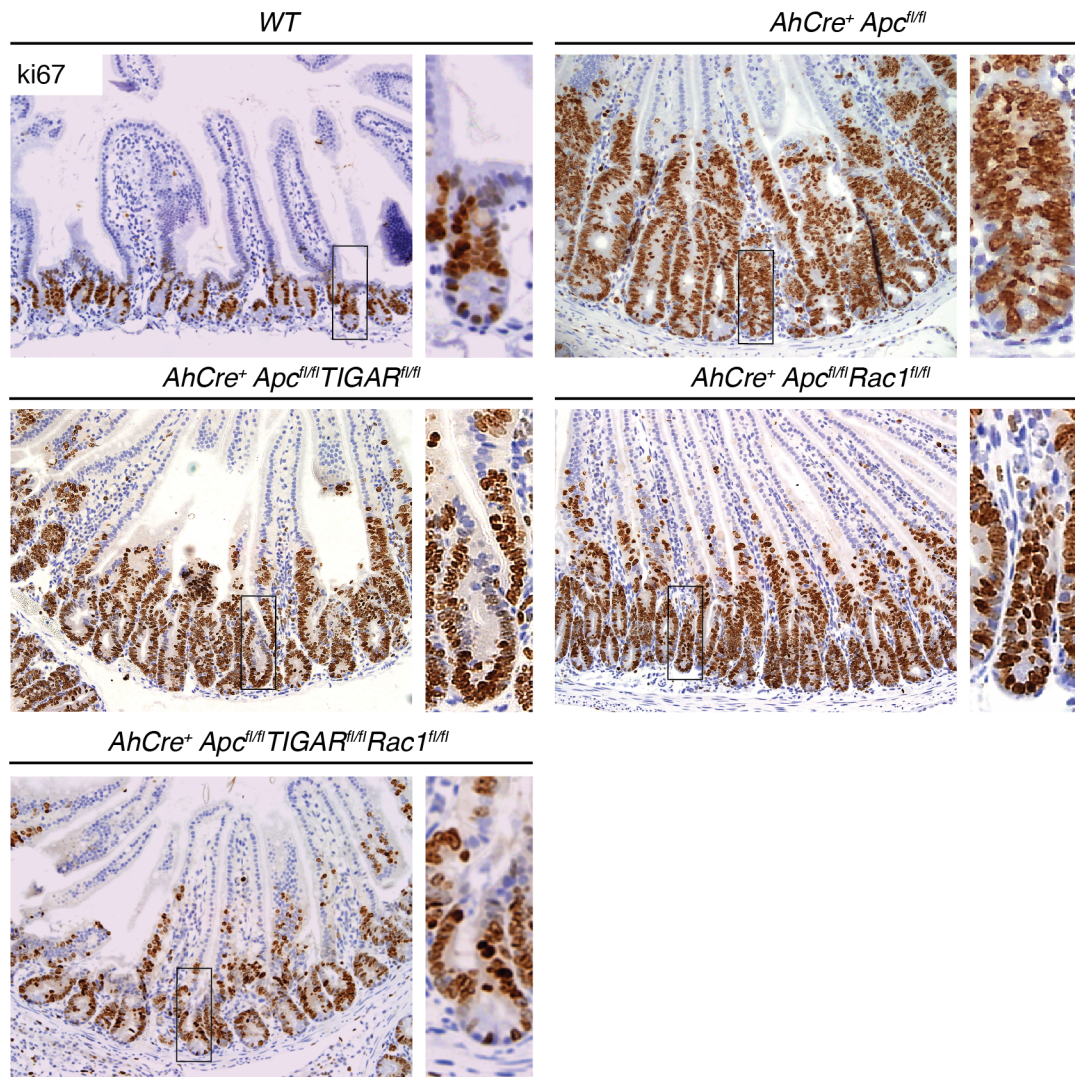


Figure 6-9 Loss of TIGAR and RAC1 reduces proliferation in an APC intestinal model

Immunohistochemistry for Ki67 on small intestines of wild-type (WT) and *AhCre⁺ Apc^{fl/fl}*, *AhCre⁺ Apc^{fl/fl} TIGAR^{fl/fl}*, *AhCre⁺ Apc^{fl/fl} Rac1^{fl/fl}* and *AhCre⁺ Apc^{fl/fl} TIGAR^{fl/fl} Rac1^{fl/fl}* mice. Panels show more detailed crypt structures indicated in the box. n = 3 mice per genotype.

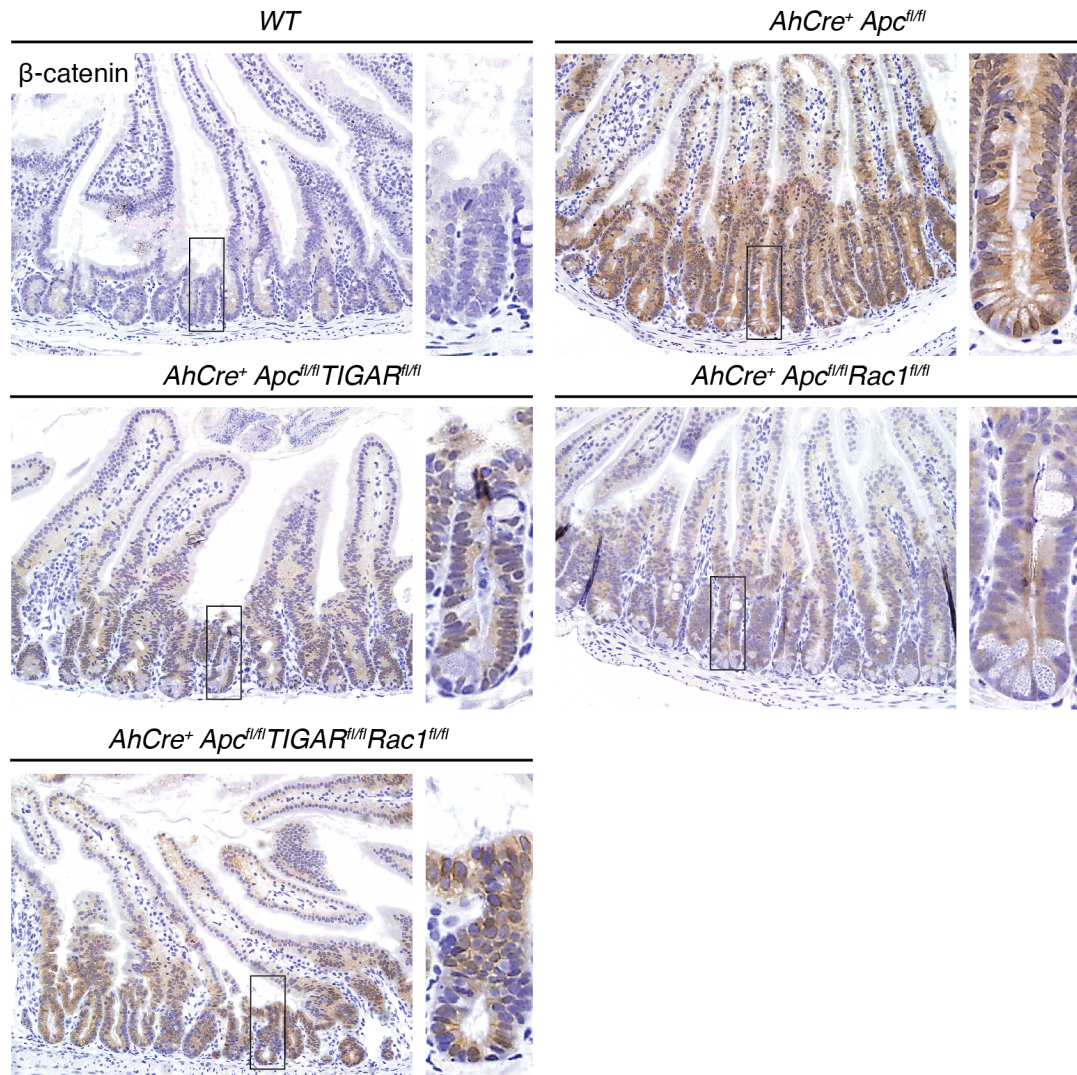


Figure 6-10 Loss of TIGAR and RAC1 lowers but does not completely abrogate Wnt signalling

Immunohistochemistry for β -catenin on small intestines of wild-type (WT) and $AhCre^+ Apc^{fl/fl}$, $AhCre^+ Apc^{fl/fl} TIGAR^{fl/fl}$, $AhCre^+ Apc^{fl/fl} Rac1^{fl/fl}$ and $AhCre^+ Apc^{fl/fl} TIGAR^{fl/fl} Rac1^{fl/fl}$ mice. Panels show more detailed crypt structures indicated in the box. $n = 3$ mice per genotype.

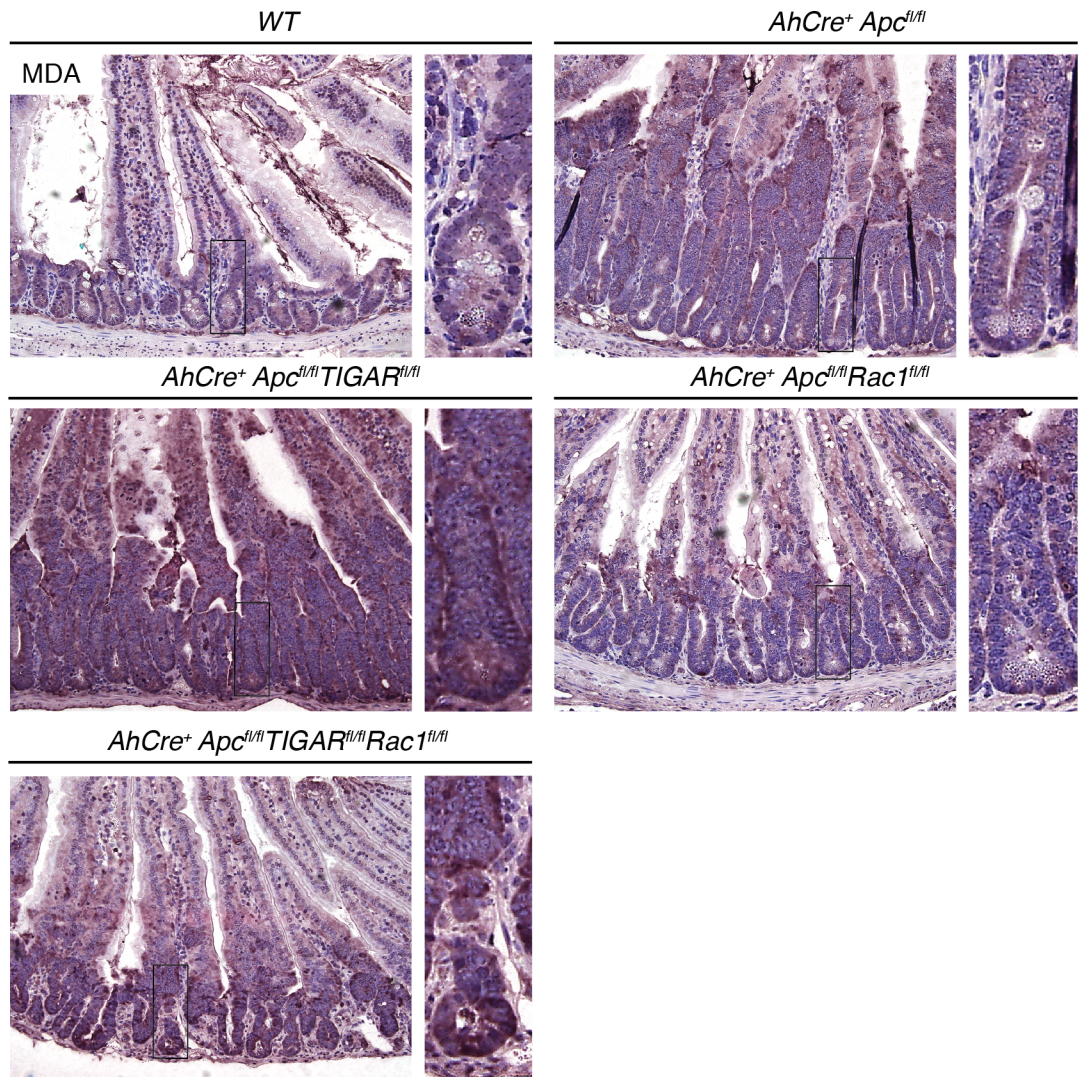


Figure 6-11 Loss of TIGAR, but not RAC1, results in increased damaging ROS in *Apc*-deficient intestinal crypts

Immunohistochemistry for MDA on small intestines of wild-type (WT) and $AhCre^+ Apc^{fl/fl}$, $AhCre^+ Apc^{fl/fl} TIGAR^{fl/fl}$, $AhCre^+ Apc^{fl/fl} Rac1^{fl/fl}$ and $AhCre^+ Apc^{fl/fl} TIGAR^{fl/fl} Rac1^{fl/fl}$ mice. Panels show more detailed crypt structures indicated in the box. n = 3 mice per genotype, each stained 3 times.

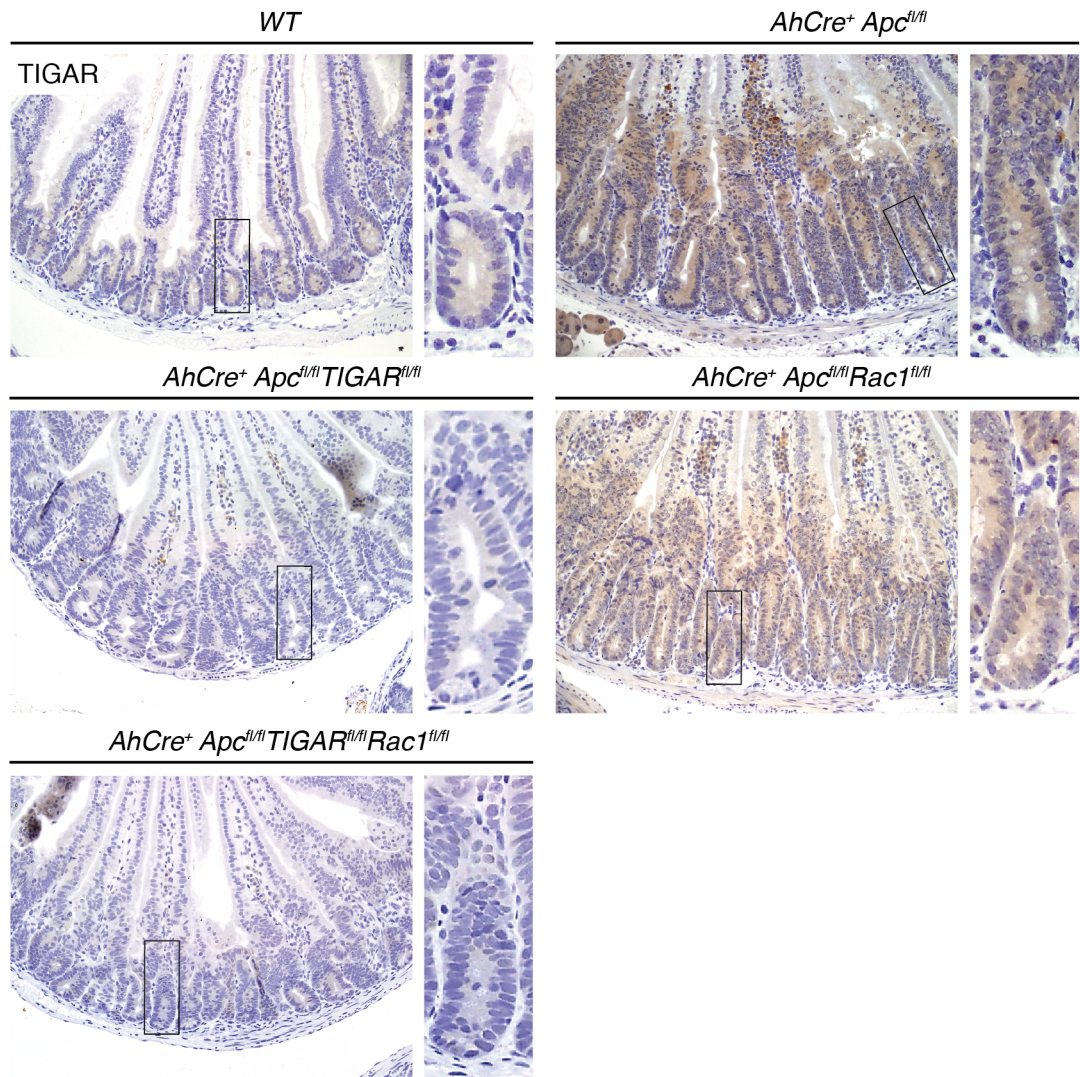


Figure 6-12 TIGAR expression upon APC and RAC1 loss

Immunohistochemistry for TIGAR on small intestines of wild-type (WT) and *AhCre⁺ Apc^{fl/fl}*, *AhCre⁺ Apc^{fl/fl} TIGAR^{fl/fl}*, *AhCre⁺ Apc^{fl/fl} Rac1^{fl/fl}* and *AhCre⁺ Apc^{fl/fl} TIGAR^{fl/fl} Rac1^{fl/fl}* mice. Panels show more detailed crypt structures indicated in the box. n = 3 mice per genotype.

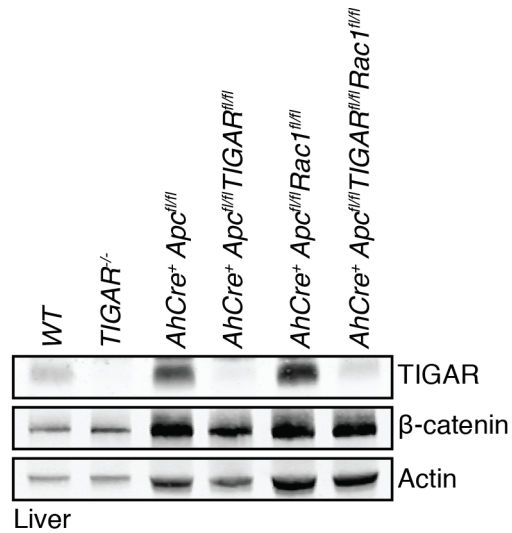


Figure 6-13 TIGAR expression upon APC and RAC1 loss in the liver

Western blot analysis of liver samples from wild-type (WT), *TIGAR*^{-/-}, *AhCre*⁺ *Apc*^{fl/fl}, *AhCre*⁺ *Apc*^{fl/fl} *TIGAR*^{fl/fl}, *AhCre*⁺ *Apc*^{fl/fl} *Rac1*^{fl/fl} and *AhCre*⁺ *Apc*^{fl/fl} *TIGAR*^{fl/fl} *Rac1*^{fl/fl} mice. n = 1 mouse per genotype.

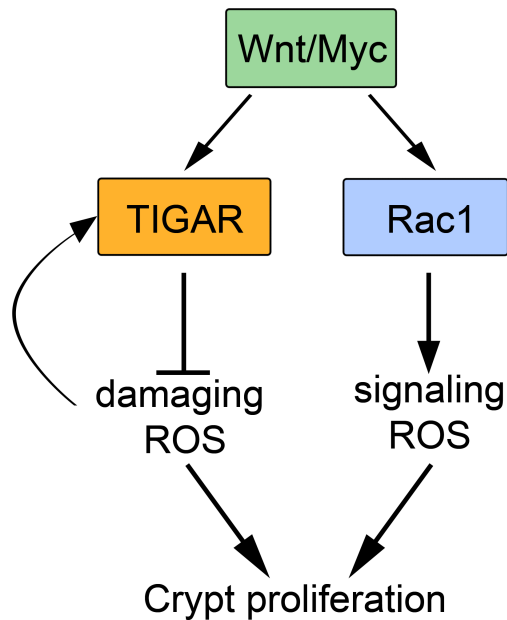


Figure 6-14 Proposed role of ROS after Wnt signalling activation

6.6 TIGAR Expression in Human Cancers

While the function of TIGAR in normal tissues is to allow for repair or adaptation following mild or transient stress as part of the p53 stress response, the results in mouse studies suggest that TIGAR expression may also be advantageous to tumour cells in order to lower damaging ROS. Therefore, the expression of TIGAR was examined in a panel of human cancer cell lines (MCF7, A2780, U2OS, HCT116 p53^{+/+}, HCT116 p53^{-/-}, H1299, HT29, A431 and SW480) to determine whether the expression of TIGAR was dependent on the presence of wild-type p53 in these cells.

It was found that the basal expression of TIGAR was not dependent on the maintenance of wild-type p53 as cell lines lacking p53 (HCT116 p53^{-/-} and H1299) or possessing mutant forms of p53 (HT29, A431 and SW480) were still able to express TIGAR protein (Figure 6-15). Notably, the A2780 cells possessing wild-type p53 showed the highest expression of TIGAR, while the A431 cells expressing mutant p53 showed the lowest (Figure 6-15). This suggests that the expression of TIGAR can become decoupled from p53 expression and there may be a selection for TIGAR expression during malignant progression.

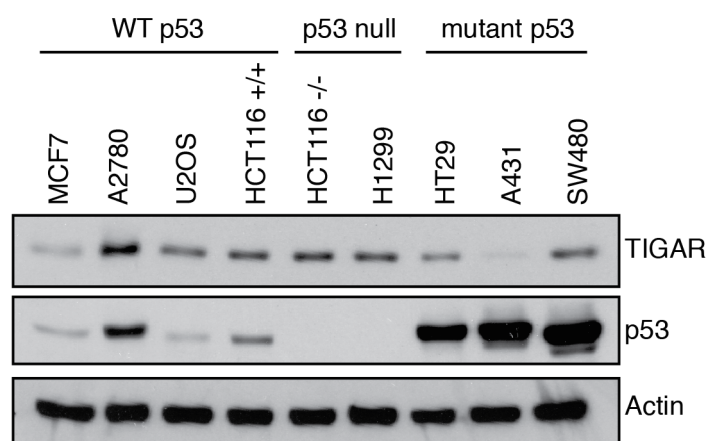


Figure 6-15 Basal TIGAR expression in human cancer cell lines

Western blot analysis of indicated human cancer cell lines with either wild-type (WT), p53-null or mutant p53 status. n = 1 independent experiment.

To establish whether TIGAR expression is also associated with the development of human cancers, a series of colon tissue microarrays were examined comparing normal, tumour and metastatic tissues from the same patient (Cheung et al. 2013). Staining for TIGAR expression by immunohistochemistry showed an increase in TIGAR protein in both the primary colon cancer and associated metastases compared to the normal tissue (Figure 6-16).

These observations were supported by expression data from the General Expression Across Normal and Tumor Tissue (GENT) database (<http://medical-genome.kribb.re.kr/GENT/>), which provides gene expression patterns across many human cancer and normal tissues. TIGAR was found overexpressed in many tumour types (red bars) compared to normal tissues (green bars) as profiled by the provided Affymetrix U133plus2 platform (Figure 6-17). These results are consistent with TIGAR expression supporting malignant development, potentially by promoting cell proliferation and an expansion of the abnormal lesion through the lowering of damaging ROS.

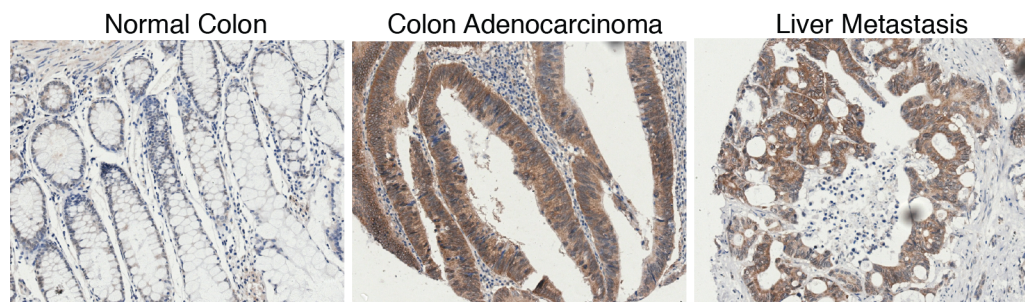


Figure 6-16 Increased TIGAR expression in primary human colon cancer and associated metastases

Example of TIGAR staining in matched samples of human normal colon, colon adenocarcinoma, and liver metastasis from the same patient. Data obtained from Eric Cheung.

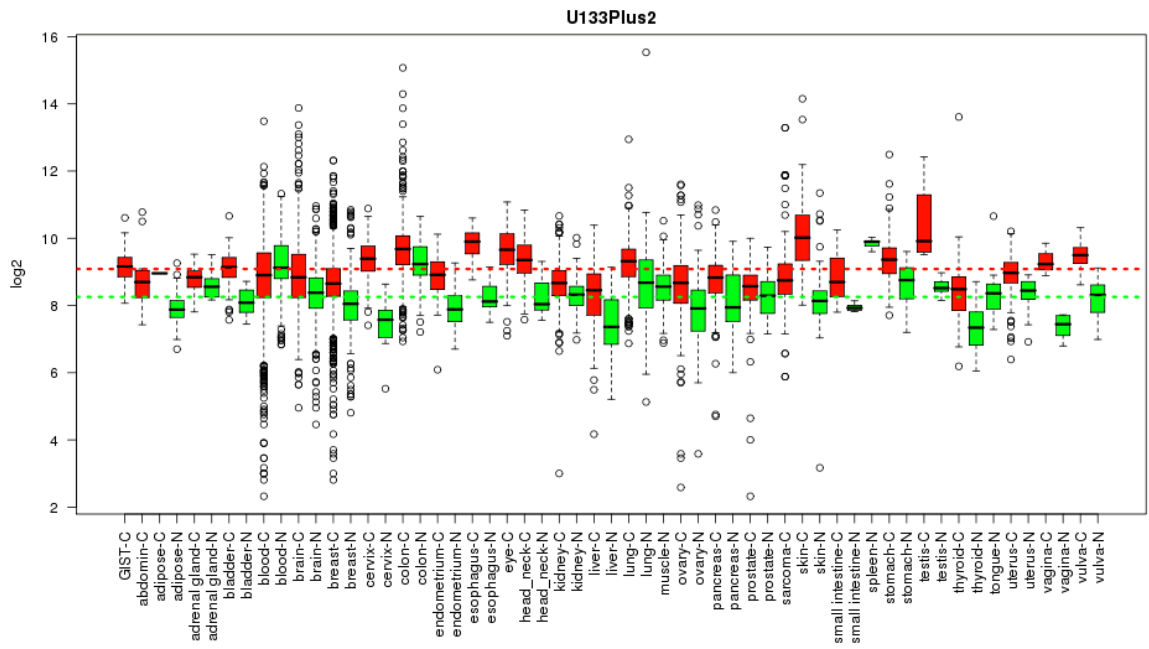


Figure 6-17 TIGAR is overexpressed in a number of human cancer types
 TIGAR expression in a variety of human tumour (red) and normal (green) tissues. Data obtained from General Expression Across Normal and Tumor Tissue (GENT) database using the Affymetrix U133plus2 platform.

6.7 Summary and Discussion

The generation of TIGAR-deficient mice was used to investigate the contribution of TIGAR to normal development and in rapidly proliferating cells after acute tissue damage. It has previously been shown that *TIGAR*^{-/-} animals do not show a clear developmental defect, suggesting that the role of TIGAR is not involved in embryogenesis or that a compensatory adaptation is present due to a constitutive lack of TIGAR during embryonic development (Cheung et al. 2013). However, it was found that TIGAR was necessary to support rapid proliferation in the adult tissue, as observed in the intestinal epithelium to allow for regeneration following tissue damage such as following irradiation or cisplatin treatment. The loss of TIGAR also resulted in increased oxidative damage in the TIGAR-deficient animals. This part of the study shows a role for TIGAR in tissue regeneration and that loss of TIGAR results in a failure to repair the damaged intestinal epithelium.

Further studies elucidated the role of TIGAR in contributing to the growth of malignancies in a mouse model of intestinal tumour induced by the deletion of APC in the intestinal stem cells (Barker et al. 2009; Cheung et al. 2013). TIGAR expression was found increased in these intestinal tumours. When these animals were also deficient for TIGAR, a reduction in tumour development as well as enhanced survival was observed. This suggests that while in healthy tissues, TIGAR can promote regeneration by lowering oxidative stress, in tumours, this same function may allow TIGAR to play a role in supporting cancer development. This is consistent with data showing increased TIGAR expression in human primary colon cancer and associated metastases. TIGAR overexpression has also been reported in other tumour types including invasive breast cancer (Won et al. 2012), glioblastoma (Wanka et al. 2012; Sinha et al. 2013), and nasopharyngeal carcinomas (Wong et al. 2015). This ability to support cancer growth has also been observed in other members of the PFK-2/FBPase-2 family. In particular, all *PFKFB* mRNAs were reported overexpressed in human lung cancers (Minchenko et al. 2005) and *PFKFB4* plays an essential role in the survival of glioma stem-like cells (Goidts et al. 2012).

Following studies understanding the role of TIGAR during intestinal regeneration, *in vivo* models were used to further understand the particular pool of ROS TIGAR

regulates. Wnt signalling results in the activation of both RAC1 (Myant et al. 2013), a component of NOX, as well as TIGAR. While loss of RAC1 results in decreased levels of ROS, due to decreased NOX activity, and decreased cell proliferation (Myant et al. 2013), loss of TIGAR results in increased levels of ROS, due to inefficient NADPH generation, but also decreased cell growth (Cheung et al. 2013). A single loss of either protein resulted in a decrease in the hyperproliferation usually observed upon APC loss. However, when both TIGAR and RAC1 proteins were simultaneously deleted, the hyperproliferation of crypts upon APC loss was attenuated even more, suggesting that TIGAR and RAC1 regulate independent pools of ROS with RAC1 generating signalling ROS to promote cell growth, while TIGAR provides antioxidant defence against damaging ROS.

Alongside multiple studies currently investigating altered metabolism in cancer progression, the metabolic alterations induced by the upregulation of TIGAR during tumourigenesis would be interesting to examine further. Furthermore, the dependence of cancer cells on antioxidants may make them more vulnerable to the inhibition of detoxifying systems compared to normal cells, which do not possess such a high burden of oxidative stress (DeNicola et al. 2011; Harris et al. 2015). This would make TIGAR an interesting target to inhibit for further studies in cancer models.

Chapter 7 Final Summary and Discussion

Taken together, the data presented here support the following conclusions:

- p53 is much less important in the regulation of TIGAR in mouse cells compared to human cells.
- Intestinal regeneration following irradiation or cisplatin treatment results in a strong induction of TIGAR expression in the mouse that is independent of p53 and TAp73.
- TIGAR expression is regulated by the Wnt/c-Myc signalling pathway through ROS.
- TIGAR functions to support intestinal regeneration by lowering oxidative stress.

While human TIGAR expression is activated in a p53-dependent manner, there was no clear p53-dependent increase in TIGAR in mouse cells. Upon further investigation of the promoter regions of human and mouse TIGAR, the p53-binding sites in the human TIGAR promoter were more responsive than those found in the mouse. Using ChIP, following cisplatin treatment in mouse cells, p53 was not recruited to the *Tigar* promoter, unlike the *p21* promoter. Further investigation found that TAp73 was also able to activate expression of mouse and human TIGAR p53-binding site reporters. However, p73 isoforms were unable to drive TIGAR protein expression in human cells.

To better understand whether mouse TIGAR was responsive to p53 or TAp73 *in vivo*, animals deficient in p53, TAp73 or both were assessed for their basal TIGAR expression and then for their ability to upregulate TIGAR following irradiation. TIGAR expression was generally not affected by the loss of p53 and/or TAp73 at a basal level or after irradiation. Altogether, these data show that the upregulation of TIGAR seen after irradiation is not dependent on p53 or its family member, TAp73.

In contrast to these observations, several previous studies have shown p53-responsive expression of TIGAR in mouse cells and tissues such as the liver and heart, and p53 binding to the *Tigar* promoter was also previously shown detected in the liver (Kimata et al. 2010; Hoshino et al. 2012; Hamard et al. 2013; Li et al. 2014b). However, while the published data suggest that p53 can induce TIGAR in some mouse tissues, the p53-responsiveness of mouse TIGAR expression is lower than observed in human cells. To some extent this difference reflects the binding of p53 to the different response elements in the mouse and human TIGAR encoding genes. However, it is also possible that tissue or stress-specific co-factors are required to allow p53 regulation of TIGAR expression, which may illustrate differences in human and mouse TIGAR expression and promoter availability. It will be of particular interest to see whether p53 family members can interact with other co-factors to participate in the induction of TIGAR in response to different forms of oxidative and metabolic stress.

The work presented here shows that mouse TIGAR expression is also regulated through p53-independent mechanisms since TIGAR is strongly activated in mouse small intestinal crypts following irradiation or cisplatin treatment. Studies by others have also shown p53-independent induction of TIGAR in primary neuron cells (Sun et al. 2015). While others have suggested a role for SP1 (Zou et al. 2012) and CREB (Zou et al. 2013) in supporting basal TIGAR expression in liver cancer cell lines, it would be interesting to further investigate other potential transcription factors which may drive TIGAR expression, particularly following cell stress or during tumourigenesis. Therefore, the role of the Wnt pathway was examined.

As several metabolic genes have been found to be a target of the Wnt signalling pathway, through canonical as well as the non-canonical branches, it is possible that TIGAR is a target of this pathway, particularly in the small intestine. Recently, the Wnt pathway was found to increase aerobic glycolysis through the suppression of mitochondrial respiration by repressing the transcription of cytochrome c oxidase, a component of the electron transport chain (Sherwood 2015). Furthermore, in colorectal cancer, canonical Wnt signalling can promote aerobic glycolysis by increasing the expression of pyruvate dehydrogenase kinase 1 (PDK1), thereby decreasing pyruvate oxidation and increasing the conversion of

pyruvate to lactate. The lactate transporter, monocarboxylate transporter 1 (MCT1) is also upregulated in order to facilitate lactate secretion (Pate et al. 2014). To address the potential role of the Wnt signalling pathway promoting TIGAR expression, the ability of extracellular Wnt stimulation to drive TIGAR expression was tested *in vitro*.

Firstly, treatment of cultured cells with recombinant Wnt3a (rWnt3a) ligand did not show a clear Wnt-dependent increase in TIGAR expression. However, upon treatment of rWnt3a in small intestinal crypt organoids (obtained from WT animals), a clear induction in the expression of TIGAR could be observed. Comparison between WT organoids and those harvested from the adenomas of *Apc^{min/+}* mice, which possess high Wnt signalling activity, showed higher levels of TIGAR in the *Apc^{min/+}* organoids. Furthermore, an acute loss of APC in *villin-Cre-ER^{T2} Apc^{fl/fl}* organoids through 4-hydroxytamoxifen treatment, resulting in high Wnt pathway activity, also promoted the expression of TIGAR. Upon further investigation *in vivo*, using models where loss of intestinal-specific APC results in high Wnt pathway signalling and intestinal hyperproliferation (*AhCre⁺ Apc^{fl/fl}*), a clear increase in TIGAR expression was observed at both mRNA and protein level.

Downstream of the Wnt signalling pathway, the transcription factor c-Myc, acts to drive the majority of the hyperproliferative phenotype observed upon APC loss in the small intestine (Sansom et al. 2007). Moreover, c-Myc itself can influence the transcription of various metabolic targets involved in glycolysis, nucleotide synthesis, lipid synthesis and glutaminolysis, all of which are important in promoting cell growth and proliferation (Dang 2009). In particular, β -catenin-mediated expression of c-Myc results in the upregulation of glucose transporter 1 (GLUT1), lactate dehydrogenase (LDH) and pyruvate kinase M2 (PKM2), all of which promote aerobic glycolysis in cancer cells (Yang et al. 2012a). Further assessment of TIGAR expression in the small intestine of *AhCre⁺ Apc^{fl/fl} Myc^{fl/fl}* mice, which have high Wnt signalling but lack the transcriptional output of c-Myc, showed that the increase in TIGAR observed upon APC deletion was c-Myc-dependent. This suggests that in the small intestine, TIGAR is a target of c-Myc. This was further observed in transgenic mouse models with deregulated Myc expression such as the E μ -Myc model of spontaneous lymphoma and leukaemia

of early B cells (Adams et al. 1985), where TIGAR expression was also upregulated in tissues possessing high Myc levels.

As TIGAR plays an important role in combatting oxidative stress and the deletion of APC promoted an increase in ROS in a c-Myc dependent manner, the role of ROS itself being able to regulate TIGAR was also investigated. Studies using the intestinal crypt culture model found that TIGAR expression was elevated following treatment with oxidants in a p53-independent manner. Furthermore, a decrease in TIGAR expression was observed following treatment using antioxidants. Others have also illustrated an upregulation in TIGAR protein expression by ROS in primary cortical neurons, which could also be attenuated through pre-treatment of cells with the antioxidant NADPH (Sun et al. 2015).

As ROS can regulate the expression of TIGAR in mouse cells, the ability of ROS to influence TIGAR expression was also considered in human cells. While ROS was also able to promote the expression of TIGAR in cultured human cells, it was induced in a p53-dependent manner. It would be interesting to further investigate whether TIGAR expression is also induced in cells with mutant p53, and whether this would also be p53-dependent. In addition, while TAp73 did not reveal any contribution to TIGAR expression in mouse tissues or in human Saos-2 cell lines with inducible TAp73, it is still possible that TAp73 can upregulate TIGAR expression in humans in response to cell stress, particularly as TAp73 has been shown by others to upregulate the expression of proteins involved in the pentose phosphate pathway such as glucose-6-phosphate dehydrogenase (Du et al. 2013; Agostini et al. 2014). Overall, this highlights the difference between the induction of TIGAR in mouse and human cells. While human TIGAR is induced by p53, another mechanism, perhaps through ROS itself or NRF2, promotes mouse TIGAR expression in response to stress. Preliminary studies found that NRF2 is upregulated in small intestinal crypts following irradiation (data not shown), however, in human cell cultures, activation of NRF2 did not influence TIGAR expression. It would be interesting to further investigate the potential for NRF2 to influence TIGAR expression through the use of *in vitro* small intestinal crypt organoids as well as using cancer models where NRF2 is upregulated to promote

tumorigenesis as seen in the KRas pancreatic adenocarcinoma model (DeNicola et al. 2011).

In addition, the regulation of TIGAR could also occur in other ways such as through transcriptional, translational, the control of protein stability or other posttranslational modifications on the protein. The half-life of TIGAR was investigated in human and mouse cell lines and the TIGAR protein was found to be relatively stable (data not shown). This could be due to the conditions cultured cells are grown in, which are much harsher than physiological conditions and thus may promote the maintenance of high TIGAR levels. TIGAR has also been found phosphorylated by ATM (personal communications), however the effects of this phosphorylation are not yet understood.

The activation of TIGAR by ROS places TIGAR into a group of ROS-induced genes that function to limit oxidative stress, which is particularly important in the cellular stress response as well as in promoting cell growth. TIGAR has previously been shown to lower oxidative stress by localising to the mitochondria in order to interact with hexokinase 2 and regulate mitochondrial membrane potential during hypoxia (Cheung et al. 2012). This has also been observed under ischaemia/reperfusion as well as oxygen glucose deprivation/reoxygenation conditions in primary neurons where TIGAR acts to protect mitochondrial functions and against ischaemia/reperfusion-induced injury (Li et al. 2014b).

It has also been speculated that an increased production of NADPH through the PPP (potentially by TIGAR) may also be used for ATP production in neurons (Herrero-Mendez et al. 2009; Stanton 2012). Furthermore, it is thought that an increased generation of ribose from the PPP may be used by cells for the rapid repair of DNA damage following oxidative stress during ischaemia/reperfusion. Preliminary studies by other groups have found that knockdown of TIGAR delayed the repair of drug-induced DNA breaks (Li et al. 2014b; Yu et al. 2015) and during the DNA damage response, TIGAR levels increased and relocated to the nucleus. PPP products such as NADPH and ribose could reverse the deleterious effects of TIGAR knockdown after DNA damage (Yu et al. 2015). Much like the ability of TIGAR to interact with hexokinase 2 at the mitochondria (Cheung et al. 2012), this ability of TIGAR was independent of its enzymatic activity as TIGAR was found to

contribute to the phosphorylation of ATM through CDK5 (Sinha et al. 2013; Yu et al. 2015).

In order to assess the *in vivo* functions of TIGAR, TIGAR-deficient mice were generated. While the loss of TIGAR did not influence embryonic development or unstressed adults (Cheung et al. 2013), the loss of TIGAR resulted in an inability to promote intestinal regeneration following tissue damage by irradiation or cisplatin treatment as well as an increase in oxidative stress in small intestine crypts. This data shows that TIGAR plays a role in regulating redox homeostasis in the small intestine and potentially other self-regenerating tissues by lowering oxidative stress following tissue damage in order to promote tissue regeneration. This phenotype was similar to other mouse models presenting increased sensitivity to oxidative stress such as the glutamate cysteine ligase modifier subunit (GCLM)-deficient mice, which have a compromised oxidative stress response due to decreased GSH synthesis (Yang et al. 2002). Ageing is associated with an impaired scavenging of ROS and TIGAR may also play a role here. TIGAR-null mice showed earlier age-related characteristics such as lower body weight compared to WT animals (personal communications). This phenotype shares similarities to the TAp73-null mice, which present more pronounced ageing with increased oxidative damage and senescence. This was found to be due to the loss of the TAp73 target mitochondrial complex IV subunit cytochrome C oxidase subunit 4 (Cox4i1), which normally regulates mitochondrial activity and thus prevents ROS accumulation (Rufini et al. 2012). While animals deficient in p63 also show accelerated ageing phenotypes in adults, this was attributed to enhanced cellular senescence upon p63 loss (Keyes et al. 2005).

Malignant development is often associated with an increase in oxidative stress, which can be a result of the loss of a normal cell environment as well as a consequence of increased metabolism to support enhanced cell growth and proliferation. Several studies have shown that cancer cells are able to limit excessive levels of ROS to support their growth and survival through the upregulation of antioxidant genes (Budanov and Karin 2008; DeNicola et al. 2011). In line with this, the activities of TIGAR in lowering ROS and promoting anabolic pathways suggest it has cancer-promoting capabilities. In an intestinal adenoma

mouse model, TIGAR was found highly expressed in the adenomas compared to the surrounding normal tissue, and mice deficient in TIGAR showed a reduction in total tumour burden in the small intestine compared to WT mice (Cheung et al. 2013). Notably, other ROS regulators are also overexpressed in a number of human cancers. NRF2, which was found overexpressed in lung, breast and ovarian carcinomas (Singh et al. 2006; Nioi and Nguyen 2007; Solis et al. 2010; Konstantinopoulos et al. 2011), can promote the transcription of genes involved in the pentose phosphate pathway such as glucose-6-phosphate dehydrogenase and phosphogluconate dehydrogenase to drive NADPH production to support cancer cell growth and proliferation. Furthermore, NRF2 can support GSH synthesis to maintain redox balance in cancer cells (Jaramillo and Zhang 2013). Mitochondrial manganese superoxide dismutase (MnSOD) expression has also been found upregulated in lung (Chung-man Ho et al. 2001), gastric and colon cancers (Hirose et al. 1993), and overexpression of glucose-6-phosphate dehydrogenase is associated with poor clinical outcome in gastric cancer (Wang et al. 2012).

ROS can exist in two separate pools, cytoplasmic, which is generated at the ER and by the NADPH oxidase (NOX) complex, and mitochondrial, which is generated by the mitochondrial electron transport chain. With distinct pools of ROS comes distinct cellular responses. Mitochondrial ROS generally inhibits cell growth and potentially damages cellular compartments while cytoplasmic ROS can both inhibit and promote cell growth depending on the source and levels. These differences in ROS levels, the forms of ROS as well as their source were further investigated *in vitro* and *in vivo* in relation to their ability to influence TIGAR expression as well as the contribution of TIGAR to these ROS pools.

While mitochondria are a primary source of ROS, the NOX family of membrane proteins also contribute significantly to ROS generation. While the activation of NOX is not completely understood, the Rho GTPase, RAC1, plays an important role in NOX activation and acts as an important signalling component in regulating various cell processes, including proliferation and invasion by influencing signalling pathway such as the NF- κ B pathway and ROS production (Bustelo et al. 2007). Upon GDP-GTP exchange by guanine nucleotide exchange factors (GEFs), active

GTP-bound RAC1 associates with NOX resulting in its activation and subsequent ROS production (Ueyama et al. 2006). RAC1 was previously identified to be upregulated after APC loss in a Myc-dependent manner and RAC1-associated GEFs are often overexpressed during tumourigenesis (Myant et al. 2013; Lindsay et al. 2015). Furthermore, the constitutive active form of RAC1, RAC1B, was found to promote lung tumourigenesis (Hodis et al. 2012; Krauthammer et al. 2012). While loss of RAC1 does not prevent the activation of the Wnt signalling pathway, it does result in an attenuation in the hyperproliferation usually observed following APC loss and subsequent tumourigenesis. This was found to be due to RAC1-mediated production of ROS as well as NF- κ B activation.

In vivo models were used to further understand the particular pool of ROS TIGAR regulates and whether this is qualitatively different from the ROS RAC1 regulates. Single loss of either RAC1 or TIGAR resulted in a decrease in the hyperproliferation usually seen in small intestine crypts when APC is lost (Cheung et al. 2013; Myant et al. 2013). However, when both proteins were simultaneously deleted, this hyperproliferation was further attenuated, suggesting that RAC1 and TIGAR regulate independent pools of ROS with RAC1 normally generating signalling ROS through NOX to promote cell growth, while TIGAR provides antioxidant defence against damaging ROS by NADPH generation.

As TIGAR was found overexpressed in a mouse model of intestinal adenoma, the expression of TIGAR in human cancers was further examined. Analysis of TIGAR expression in colon tissue microarrays revealed increased TIGAR levels in the primary colon cancer and associated metastases compared to normal tissue. Overexpression of TIGAR has also been described in many human tumour types. For example, glioblastoma have been found to show a high expression of TIGAR compared to normal brain tissue (Wanka et al. 2012; Sinha et al. 2013) and this was similarly observed in human breast cancer (Won et al. 2012). It would be interesting to understand whether TIGAR is upregulated in other cancer types and how this may contribute to tumourigenesis, as basal expression of TIGAR is variable in different tissues. As the expression of TIGAR was not found correlated with wild-type p53 expression, it may also be worth investigating the expression and role of TIGAR in human cancers associated with possessing mutant p53 such

as pancreatic and ovarian cancer. Cancer-associated p53 mutations can endow new activities to p53, which can contribute to tumour progression (Muller and Vousden 2013), therefore the potential ability of mutant p53 to upregulate TIGAR in tumours would be beneficial to cancer cell growth.

It has previously been found that TIGAR expression was responsive to hormones such as adrenaline, glucagon and hydrocortisone in the mouse brain, and insulin was found to decrease TIGAR expression (Sun et al. 2015). This would be interesting to examine in other tissues such as the liver where TIGAR is highly expressed and where these hormones play an important role in metabolic homeostasis. Furthermore, studies have found that TIGAR can play a role in promoting cell survival following nutrient starvation and metabolic stress (Bensaad et al. 2009). Alongside current studies investigating how the upregulation of TIGAR can alter the metabolism in tumours as well as the metabolic consequences of a systemic loss of TIGAR, it would be interesting to understand how further metabolic stresses and nutrient deprivation can influence tumourigenesis with alterations in TIGAR expression. For example, serine deprivation has been found to increase oxidative stress in cancer cells (Maddocks et al. 2013). Therefore, it would be interesting to see whether a combination of serine starvation and TIGAR loss would further attenuate cancer cell growth, particularly in the small intestinal crypt organoids where the greatest alterations in TIGAR have been observed.

The findings presented here suggest that TIGAR acts to lower damaging oxidative stress in the mouse small intestine in a p53-independent manner, and relies on Wnt/c-Myc signalling to drive its expression. The data presented here as well as results shown from other groups show that TIGAR is overexpressed in a number of human cancers, and loss of TIGAR is able to suppress tumourigenesis. As cancer cells have an increased burden in oxidative stress and TIGAR acts selectively on damaging ROS, inhibition of TIGAR could potentially be beneficial in inhibiting cancer cell growth as it would result in an increase in damaging ROS but have no effects on the pool of signalling ROS. Altogether, this illustrates a promising therapy strategy for treating cancer types, which show an overexpression of TIGAR or rely on antioxidant defence for their continued growth.

Bibliography

- Aberle H, Bauer A, Stappert J, Kispert A, Kemler R. 1997. beta-catenin is a target for the ubiquitin-proteasome pathway. *The EMBO journal* **16**: 3797-3804.
- Abramov AY, Scorziello A, Duchen MR. 2007. Three distinct mechanisms generate oxygen free radicals in neurons and contribute to cell death during anoxia and reoxygenation. *The Journal of neuroscience : the official journal of the Society for Neuroscience* **27**: 1129-1138.
- Adam J, Hatipoglu E, O'Flaherty L, Ternette N, Sahgal N, Lockstone H, Baban D, Nye E, Stamp GW, Wolhuter K et al. 2011. Renal cyst formation in Fh1-deficient mice is independent of the Hif/Phd pathway: roles for fumarate in KEAP1 succination and Nrf2 signaling. *Cancer Cell* **20**: 524-537.
- Adams JM, Cory S. 2007. Bcl-2-regulated apoptosis: mechanism and therapeutic potential. *Curr Opin Immunol* **19**: 488-496.
- Adams JM, Harris AW, Pinkert CA, Corcoran LM, Alexander WS, Cory S, Palmiter RD, Brinster RL. 1985. The c-myc oncogene driven by immunoglobulin enhancers induces lymphoid malignancy in transgenic mice. *Nature* **318**: 533-538.
- Agami R, Blandino G, Oren M, Shaul Y. 1999. Interaction of c-Abl and p73alpha and their collaboration to induce apoptosis. *Nature* **399**: 809-813.
- Agnoletto C, Melloni E, Casciano F, Rigolin GM, Rimondi E, Celeghini C, Brunelli L, Cuneo A, Secchiero P, Zauli G. 2014. Sodium dichloroacetate exhibits anti-leukemic activity in B-chronic lymphocytic leukemia (B-CLL) and synergizes with the p53 activator Nutlin-3. *Oncotarget* **5**: 4347-4360.
- Agostini M, Niklison-Chirou MV, Catani MV, Knight RA, Melino G, Rufini A. 2014. TAp73 promotes anti-senescence-anabolism not proliferation. *Aging* **6**: 921-930.
- Aguilar V, Fajas L. 2010. Cycling through metabolism. *EMBO Mol Med* **2**: 338-348.
- Alarcon R, Koumenis C, Geyer RK, Maki CG, Giaccia AJ. 1999. Hypoxia induces p53 accumulation through MDM2 down-regulation and inhibition of E6-mediated degradation. *Cancer research* **59**: 6046-6051.
- Almeida A, Bolanos JP, Moncada S. 2010. E3 ubiquitin ligase APC/C-Cdh1 accounts for the Warburg effect by linking glycolysis to cell proliferation. *Proceedings of the National Academy of Sciences of the United States of America* **107**: 738-741.
- Amaravadi RK, Yu DN, Lum JJ, Bui T, Christophorou MA, Evan GI, Thomas-Tikhonenko A, Thompson CB. 2007. Autophagy inhibition enhances therapy-induced apoptosis in a Myc-induced model of lymphoma. *J Clin Invest* **117**: 326-336.
- Ambs S, Ogunfusika MO, Merriam WG, Bennett WP, Billiar TR, Harris CC. 1998. Up-regulation of inducible nitric oxide synthase expression in cancer-prone p53 knockout mice. *Proceedings of the National Academy of Sciences of the United States of America* **95**: 8823-8828.
- Amelio I, Antonov AA, Catani MV, Massoud R, Bernassola F, Knight RA, Melino G, Rufini A. 2014. TAp73 promotes anabolism. *Oncotarget* **5**: 12820-12934.
- Anagnostou SH, Shepherd PR. 2008. Glucose induces an autocrine activation of the Wnt/beta-catenin pathway in macrophage cell lines. *The Biochemical journal* **416**: 211-218.
- Anastasiou D, Poulogiannis G, Asara JM, Boxer MB, Jiang JK, Shen M, Bellinger G, Sasaki AT, Locasale JW, Auld DS et al. 2011. Inhibition of pyruvate

- kinase M2 by reactive oxygen species contributes to cellular antioxidant responses. *Science* **334**: 1278-1283.
- Anastasiou D, Yu Y, Israelsen WJ, Jiang JK, Boxer MB, Hong BS, Tempel W, Dimov S, Shen M, Jha A et al. 2012. Pyruvate kinase M2 activators promote tetramer formation and suppress tumorigenesis. *Nature chemical biology* **8**: 839-847.
- Andl T, Reddy ST, Gaddapara T, Millar SE. 2002. WNT signals are required for the initiation of hair follicle development. *Developmental cell* **2**: 643-653.
- Apte U, Singh S, Zeng G, Cieply B, Virji MA, Wu T, Monga SP. 2009. Beta-catenin activation promotes liver regeneration after acetaminophen-induced injury. *Am J Pathol* **175**: 1056-1065.
- Armstrong JF, Kaufman MH, Harrison DJ, Clarke AR. 1995. High-frequency developmental abnormalities in p53-deficient mice. *Curr Biol* **5**: 931-936.
- Ashton GH, Morton JP, Myant K, Phesse TJ, Ridgway RA, Marsh V, Wilkins JA, Athineos D, Muncan V, Kemp R et al. 2010. Focal adhesion kinase is required for intestinal regeneration and tumorigenesis downstream of Wnt/c-Myc signaling. *Developmental cell* **19**: 259-269.
- Atlante A, Gagliardi S, Minervini GM, Ciotti MT, Marra E, Calissano P. 1997. Glutamate neurotoxicity in rat cerebellar granule cells: a major role for xanthine oxidase in oxygen radical formation. *Journal of neurochemistry* **68**: 2038-2045.
- Badciong JC, Haas AL. 2002. MdmX is a RING finger ubiquitin ligase capable of synergistically enhancing Mdm2 ubiquitination. *Journal of Biological Chemistry* **277**: 49668-49675.
- Bae YS, Kang SW, Seo MS, Baines IC, Tekle E, Chock PB, Rhee SG. 1997. Epidermal growth factor (EGF)-induced generation of hydrogen peroxide. Role in EGF receptor-mediated tyrosine phosphorylation. *The Journal of biological chemistry* **272**: 217-221.
- Bakkenist CJ, Kastan MB. 2003. DNA damage activates ATM through intermolecular autophosphorylation and dimer dissociation. *Nature* **421**: 499-506.
- Baltrusch S, Lenzen S, Okar DA, Lange AJ, Tiedge M. 2001. Characterization of glucokinase-binding protein epitopes by a phage-displayed peptide library. Identification of 6-phosphofructo-2-kinase/fructose-2,6-bisphosphatase as a novel interaction partner. *The Journal of biological chemistry* **276**: 43915-43923.
- Bando H, Atsumi T, Nishio T, Niwa H, Mishima S, Shimizu C, Yoshioka N, Bucala R, Koike T. 2005. Phosphorylation of the 6-phosphofructo-2-kinase/fructose 2,6-bisphosphatase/PFKFB3 family of glycolytic regulators in human cancer. *Clin Cancer Res* **11**: 5784-5792.
- Banziger C, Soldini D, Schutt C, Zipperlen P, Hausmann G, Basler K. 2006. Wntless, a conserved membrane protein dedicated to the secretion of Wnt proteins from signaling cells. *Cell* **125**: 509-522.
- Barbieri CE, Tang LJ, Brown KA, Pietenpol JA. 2006. Loss of p63 leads to increased cell migration and up-regulation of genes involved in invasion and metastasis. *Cancer research* **66**: 7589-7597.
- Barker N, Huch M, Kujala P, van de Wetering M, Snippert HJ, van Es JH, Sato T, Stange DE, Begthel H, van den Born M et al. 2010. Lgr5(+ve) stem cells drive self-renewal in the stomach and build long-lived gastric units in vitro. *Cell stem cell* **6**: 25-36.

- Barker N, Ridgway RA, van Es JH, van de Wetering M, Begthel H, van den Born M, Danenberg E, Clarke AR, Sansom OJ, Clevers H. 2009. Crypt stem cells as the cells-of-origin of intestinal cancer. *Nature* **457**: 608-611.
- Bartrons R, Hue L, Van Schaftingen E, Hers HG. 1983. Hormonal control of fructose 2,6-bisphosphate concentration in isolated rat hepatocytes. *The Biochemical journal* **214**: 829-837.
- Bedard K, Krause KH. 2007. The NOX family of ROS-generating NADPH oxidases: physiology and pathophysiology. *Physiological reviews* **87**: 245-313.
- Behrens J, von Kries JP, Kuhl M, Bruhn L, Wedlich D, Grosschedl R, Birchmeier W. 1996. Functional interaction of beta-catenin with the transcription factor LEF-1. *Nature* **382**: 638-642.
- Bell EL, Guarente L. 2011. The SirT3 divining rod points to oxidative stress. *Molecular cell* **42**: 561-568.
- Benard J, Douc-Rasy S, Ahomadegbe JC. 2003. TP53 family members and human cancers. *Hum Mutat* **21**: 182-191.
- Benassi B, Fanciulli M, Fiorentino F, Porrello A, Chiorino G, Loda M, Zupi G, Biroccio A. 2006. c-Myc phosphorylation is required for cellular response to oxidative stress. *Molecular cell* **21**: 509-519.
- Bensaad K, Cheung EC, Vousden KH. 2009. Modulation of intracellular ROS levels by TIGAR controls autophagy. *The EMBO journal* **28**: 3015-3026.
- Bensaad K, Tsuruta A, Selak MA, Vidal MN, Nakano K, Bartrons R, Gottlieb E, Vousden KH. 2006. TIGAR, a p53-inducible regulator of glycolysis and apoptosis. *Cell* **126**: 107-120.
- Bergamaschi D, Samuels Y, Sullivan A, Zvelebil M, Breysens H, Bisso A, Del Sal G, Syed N, Smith P, Gasco M et al. 2006. iASPP preferentially binds p53 proline-rich region and modulates apoptotic function of codon 72-polymorphic p53. *Nat Genet* **38**: 1133-1141.
- Bernard H, Garmy-Susini B, Ainaoui N, Van Den Berghe L, Peurichard A, Javerzat S, Bikfalvi A, Lane DP, Bourdon JC, Prats AC. 2013. The p53 isoform, Delta133p53alpha, stimulates angiogenesis and tumour progression. *Oncogene* **32**: 2150-2160.
- Bertout JA, Patel SA, Simon MC. 2008. The impact of O₂ availability on human cancer. *Nat Rev Cancer* **8**: 967-975.
- Bhanot P, Brink M, Samos CH, Hsieh JC, Wang Y, Macke JP, Andrew D, Nathans J, Nusse R. 1996. A new member of the frizzled family from Drosophila functions as a Wingless receptor. *Nature* **382**: 225-230.
- Bigl M, Jandrig B, Horn LC, Eschrich K. 2008. Aberrant methylation of human L- and M-fructose 1,6-bisphosphatase genes in cancer. *Biochemical and biophysical research communications* **377**: 720-724.
- Bobarykina AY, Minchenko DO, Opentanova IL, Moenner M, Caro J, Esumi H, Minchenko OH. 2006. Hypoxic regulation of PFKFB-3 and PFKFB-4 gene expression in gastric and pancreatic cancer cell lines and expression of PFKFB genes in gastric cancers. *Acta Biochim Pol* **53**: 789-799.
- Boidot R, Vegran F, Meulle A, Le Breton A, Dessy C, Sonveaux P, Lizard-Nacol S, Feron O. 2012. Regulation of Monocarboxylate Transporter MCT1 Expression by p53 Mediates Inward and Outward Lactate Fluxes in Tumors. *Cancer research* **72**: 939-948.
- Boroughs LK, DeBerardinis RJ. 2015. Metabolic pathways promoting cancer cell survival and growth. *Nature cell biology* **17**: 351-359.

- Bourdon A, Minai L, Serre V, Jais JP, Sarzi E, Aubert S, Chretien D, de Lonlay P, Paquis-Flucklinger V, Arakawa H et al. 2007. Mutation of RRM2B, encoding p53-controlled ribonucleotide reductase (p53R2), causes severe mitochondrial DNA depletion. *Nat Genet* **39**: 776-780.
- Bourdon JC, Fernandes K, Murray-Zmijewski F, Liu G, Diot A, Xirodimas DP, Saville MK, Lane DP. 2005. p53 isoforms can regulate p53 transcriptional activity. *Genes & development* **19**: 2122-2137.
- Bovolenta P, Esteve P, Ruiz JM, Cisneros E, Lopez-Rios J. 2008. Beyond Wnt inhibition: new functions of secreted Frizzled-related proteins in development and disease. *J Cell Sci* **121**: 737-746.
- Boyden LM, Mao J, Belsky J, Mitzner L, Farhi A, Mitnick MA, Wu D, Insogna K, Lifton RP. 2002. High bone density due to a mutation in LDL-receptor-related protein 5. *N Engl J Med* **346**: 1513-1521.
- Braeuning A. 2009. Regulation of cytochrome P450 expression by Ras- and beta-catenin-dependent signaling. *Curr Drug Metab* **10**: 138-158.
- Brown MD, Sacks DB. 2009. Protein scaffolds in MAP kinase signalling. *Cell Signal* **21**: 462-469.
- Brunelle JK, Bell EL, Quesada NM, Vercauteren K, Tiranti V, Zeviani M, Scarpulla RC, Chandel NS. 2005. Oxygen sensing requires mitochondrial ROS but not oxidative phosphorylation. *Cell metabolism* **1**: 409-414.
- Budanov AV, Karin M. 2008. p53 target genes sestrin1 and sestrin2 connect genotoxic stress and mTOR signaling. *Cell* **134**: 451-460.
- Budhidarmo R, Nakatani Y, Day CL. 2012. RINGs hold the key to ubiquitin transfer. *Trends Biochem Sci* **37**: 58-65.
- Burkhardt DL, Sage J. 2008. Cellular mechanisms of tumour suppression by the retinoblastoma gene. *Nat Rev Cancer* **8**: 671-682.
- Bustelo XR, Sauzeau V, Berenjano IM. 2007. GTP-binding proteins of the Rho/Rac family: regulation, effectors and functions in vivo. *Bioessays* **29**: 356-370.
- Cadore A, Ovejero C, Terris B, Souil E, Levy L, Lamers WH, Kitajewski J, Kahn A, Perret C. 2002. New targets of beta-catenin signaling in the liver are involved in the glutamine metabolism. *Oncogene* **21**: 8293-8301.
- Cairns P, Okami K, Halachmi S, Halachmi N, Esteller M, Herman JG, Jen J, Isaacs WB, Bova GS, Sidransky D. 1997. Frequent inactivation of PTEN/MMAC1 in primary prostate cancer. *Cancer research* **57**: 4997-5000.
- Cairns RA, Harris IS, Mak TW. 2011. Regulation of cancer cell metabolism. *Nat Rev Cancer* **11**: 85-95.
- Candi E, Rufini A, Terrinoni A, Dinsdale D, Ranalli M, Paradisi A, De Laurenzi V, Spagnoli LG, Catani MV, Ramadan S et al. 2006. Differential roles of p63 isoforms in epidermal development: selective genetic complementation in p63 null mice. *Cell death and differentiation* **13**: 1037-1047.
- Cano CE, Gommeaux J, Pietri S, Culcasi M, Garcia S, Seux M, Barelier S, Vasseur S, Spoto RP, Pebusque MJ et al. 2009. Tumor protein 53-induced nuclear protein 1 is a major mediator of p53 antioxidant function. *Cancer research* **69**: 219-226.
- Cantor JR, Sabatini DM. 2012. Cancer cell metabolism: one hallmark, many faces. *Cancer Discov* **2**: 881-898.
- Cao C, Leng Y, Huang W, Liu X, Kufe D. 2003. Glutathione peroxidase 1 is regulated by the c-Abl and Arg tyrosine kinases. *The Journal of biological chemistry* **278**: 39609-39614.
- Carmon KS, Gong X, Lin Q, Thomas A, Liu Q. 2011. R-spondins function as ligands of the orphan receptors LGR4 and LGR5 to regulate Wnt/beta-

- catenin signaling. *Proceedings of the National Academy of Sciences of the United States of America* **108**: 11452-11457.
- Casciano I, Mazzocco K, Boni L, Pagnan G, Banelli B, Allemanni G, Ponzoni M, Tonini GP, Romani M. 2002. Expression of DeltaNp73 is a molecular marker for adverse outcome in neuroblastoma patients. *Cell death and differentiation* **9**: 246-251.
- Cavallo RA, Cox RT, Moline MM, Roose J, Polevoy GA, Clevers H, Peifer M, Bejsovec A. 1998. Drosophila Tcf and Groucho interact to repress Wingless signalling activity. *Nature* **395**: 604-608.
- Celli J, Duijf P, Hamel BC, Bamshad M, Kramer B, Smits AP, Newbury-Ecob R, Hennekam RC, Van Buggenhout G, van Haeringen A et al. 1999. Heterozygous germline mutations in the p53 homolog p63 are the cause of EEC syndrome. *Cell* **99**: 143-153.
- Chafey P, Finzi L, Boisgard R, Cauzac M, Clary G, Broussard C, Pegorier JP, Guillonneau F, Mayeux P, Camoin L et al. 2009. Proteomic analysis of beta-catenin activation in mouse liver by DIGE analysis identifies glucose metabolism as a new target of the Wnt pathway. *Proteomics* **9**: 3889-3900.
- Chan WM, Mak MC, Fung TK, Lau A, Siu WY, Poon RYC. 2006. Ubiquitination of p53 at multiple sites in the DNA-binding domain. *Molecular Cancer Research* **4**: 15-25.
- Chance B, Williams GR, Hollunger G. 1963. Inhibition of electron and energy transfer in mitochondria. I. Effects of Amytal, thiopental, rotenone, progesterone, and methylene glycol. *The Journal of biological chemistry* **238**: 418-431.
- Chandel NS, Maltepe E, Goldwasser E, Mathieu CE, Simon MC, Schumacker PT. 1998. Mitochondrial reactive oxygen species trigger hypoxia-induced transcription. *Proceedings of the National Academy of Sciences of the United States of America* **95**: 11715-11720.
- Chandel NS, McClintock DS, Feliciano CE, Wood TM, Melendez JA, Rodriguez AM, Schumacker PT. 2000. Reactive oxygen species generated at mitochondrial complex III stabilize hypoxia-inducible factor-1alpha during hypoxia: a mechanism of O2 sensing. *The Journal of biological chemistry* **275**: 25130-25138.
- Chaneton B, Hillmann P, Zheng L, Martin AC, Maddocks OD, Chokkathukalam A, Coyle JE, Jankevics A, Holding FP, Vousden KH et al. 2012. Serine is a natural ligand and allosteric activator of pyruvate kinase M2. *Nature* **491**: 458-462.
- Chehab NH, Malikzay A, Appel M, Halazonetis TD. 2000. Chk2/hCds1 functions as a DNA damage checkpoint in G(1) by stabilizing p53. *Genes & development* **14**: 278-288.
- Chen CL, Ip SM, Cheng D, Wong LC, Ngan HY. 2000. P73 gene expression in ovarian cancer tissues and cell lines. *Clin Cancer Res* **6**: 3910-3915.
- Chen J, Marechal V, Levine AJ. 1993. Mapping of the p53 and mdm-2 interaction domains. *Molecular and cellular biology* **13**: 4107-4114.
- Chen M, Zhang J, Li N, Qian Z, Zhu M, Li Q, Zheng J, Wang X, Shi G. 2011. Promoter hypermethylation mediated downregulation of FBP1 in human hepatocellular carcinoma and colon cancer. *Plos One* **6**: e25564.
- Chen RE, Thorner J. 2007. Function and regulation in MAPK signaling pathways: lessons learned from the yeast *Saccharomyces cerevisiae*. *Biochimica et biophysica acta* **1773**: 1311-1340.

- Chen S, Li P, Li J, Wang Y, Du Y, Chen X, Zang W, Wang H, Chu H, Zhao G et al. 2015. MiR-144 inhibits proliferation and induces apoptosis and autophagy in lung cancer cells by targeting TIGAR. *Cell Physiol Biochem* **35**: 997-1007.
- Chen W, Jiang T, Wang H, Tao S, Lau A, Fang D, Zhang DD. 2012. Does Nrf2 contribute to p53-mediated control of cell survival and death? *Antioxidants & redox signaling* **17**: 1670-1675.
- Chen W, ten Berge D, Brown J, Ahn S, Hu LA, Miller WE, Caron MG, Barak LS, Nusse R, Lefkowitz RJ. 2003. Dishevelled 2 recruits beta-arrestin 2 to mediate Wnt5A-stimulated endocytosis of Frizzled 4. *Science* **301**: 1391-1394.
- Chen WM, Sun Z, Wang XJ, Jiang T, Huang ZP, Fang DY, Zhang DD. 2009. Direct Interaction between Nrf2 and p21(Cip1/WAF1) Upregulates the Nrf2-Mediated Antioxidant Response. *Molecular cell* **34**: 663-673.
- Cheng JC, Chang HM, Leung PCK. 2011. Wild-Type p53 Attenuates Cancer Cell Motility by Inducing Growth Differentiation Factor-15 Expression. *Endocrinology* **152**: 2987-2995.
- Cheng N, Chytil A, Shyr Y, Joly A, Moses HL. 2008. Transforming growth factor-beta signaling-deficient fibroblasts enhance hepatocyte growth factor signaling in mammary carcinoma cells to promote scattering and invasion. *Molecular cancer research : MCR* **6**: 1521-1533.
- Cheng Q, Chen LH, Li ZY, Lane WS, Chen JD. 2009. ATM activates p53 by regulating MDM2 oligomerization and E3 processivity. *Embo Journal* **28**: 3857-3867.
- Cheng Y, Sun AY. 1994. Oxidative mechanisms involved in kainate-induced cytotoxicity in cortical neurons. *Neurochemical research* **19**: 1557-1564.
- Chesney J, Mitchell R, Benigni F, Bacher M, Spiegel L, Al-Abed Y, Han JH, Metz C, Bucala R. 1999. An inducible gene product for 6-phosphofructo-2-kinase with an AU-rich instability element: role in tumor cell glycolysis and the Warburg effect. *Proceedings of the National Academy of Sciences of the United States of America* **96**: 3047-3052.
- Cheung EC, Athineos D, Lee P, Ridgway RA, Lambie W, Nixon C, Strathdee D, Blyth K, Sansom OJ, Vousden KH. 2013. TIGAR is required for efficient intestinal regeneration and tumorigenesis. *Developmental cell* **25**: 463-477.
- Cheung EC, Ludwig RL, Vousden KH. 2012. Mitochondrial localization of TIGAR under hypoxia stimulates HK2 and lowers ROS and cell death. *Proceedings of the National Academy of Sciences of the United States of America* **109**: 20491-20496.
- Chikri M, Rousseau GG. 1995. Rat gene coding for heart 6-phosphofructo-2-kinase/fructose-2,6-bisphosphatase: characterization of an unusual promoter region and identification of four mRNAs. *Biochemistry* **34**: 8876-8884.
- Cho Y, Gorina S, Jeffrey PD, Pavletich NP. 1994. Crystal structure of a p53 tumor suppressor-DNA complex: understanding tumorigenic mutations. *Science* **265**: 346-355.
- Chocarro-Calvo A, Garcia-Martinez JM, Ardila-Gonzalez S, De la Vieja A, Garcia-Jimenez C. 2013. Glucose-induced beta-catenin acetylation enhances Wnt signaling in cancer. *Molecular cell* **49**: 474-486.
- Choi J, Liu RM, Forman HJ. 1997. Adaptation to oxidative stress: quinone-mediated protection of signaling in rat lung epithelial L2 cells. *Biochem Pharmacol* **53**: 987-993.

- Chow VT, Quek HH, Tock EP. 1993. Alternative splicing of the p53 tumor suppressor gene in the Molt-4 T-lymphoblastic leukemia cell line. *Cancer Lett* **73**: 141-148.
- Christodoulides C, Scarda A, Granzotto M, Milan G, Dalla Nora E, Keogh J, De Pergola G, Stirling H, Pannacciulli N, Sethi JK et al. 2006. WNT10B mutations in human obesity. *Diabetologia* **49**: 678-684.
- Christofk HR, Vander Heiden MG, Harris MH, Ramanathan A, Gerszten RE, Wei R, Fleming MD, Schreiber SL, Cantley LC. 2008a. The M2 splice isoform of pyruvate kinase is important for cancer metabolism and tumour growth. *Nature* **452**: 230-233.
- Christofk HR, Vander Heiden MG, Wu N, Asara JM, Cantley LC. 2008b. Pyruvate kinase M2 is a phosphotyrosine-binding protein. *Nature* **452**: 181-186.
- Chuikov S, Kurash JK, Wilson JR, Xiao B, Justin N, Ivanov GS, McKinney K, Tempst P, Prives C, Gamblin SJ et al. 2004. Regulation of p53 activity through lysine methylation. *Nature* **432**: 353-360.
- Chung-man Ho J, Zheng S, Comhair SA, Farver C, Erzurum SC. 2001. Differential expression of manganese superoxide dismutase and catalase in lung cancer. *Cancer research* **61**: 8578-8585.
- Ciccio A, Elledge SJ. 2010. The DNA damage response: making it safe to play with knives. *Molecular cell* **40**: 179-204.
- Clem B, Telang S, Clem A, Yalcin A, Meier J, Simmons A, Rasku MA, Arumugam S, Dean WL, Eaton J et al. 2008. Small-molecule inhibition of 6-phosphofructo-2-kinase activity suppresses glycolytic flux and tumor growth. *Mol Cancer Ther* **7**: 110-120.
- Clements CM, McNally RS, Conti BJ, Mak TW, Ting JP. 2006. DJ-1, a cancer- and Parkinson's disease-associated protein, stabilizes the antioxidant transcriptional master regulator Nrf2. *Proceedings of the National Academy of Sciences of the United States of America* **103**: 15091-15096.
- Clevers H. 2006. Wnt/beta-catenin signaling in development and disease. *Cell* **127**: 469-480.
- Clevers H, Nusse R. 2012. Wnt/beta-catenin signaling and disease. *Cell* **149**: 1192-1205.
- Clore GM, Ernst J, Clubb R, Omichinski JG, Kennedy WM, Sakaguchi K, Appella E, Gronenborn AM. 1995. Refined solution structure of the oligomerization domain of the tumour suppressor p53. *Nat Struct Biol* **2**: 321-333.
- Clower CV, Chatterjee D, Wang Z, Cantley LC, Vander Heiden MG, Krainer AR. 2010. The alternative splicing repressors hnRNP A1/A2 and PTB influence pyruvate kinase isoform expression and cell metabolism. *Proceedings of the National Academy of Sciences of the United States of America* **107**: 1894-1899.
- Connor KM, Subbaram S, Regan KJ, Nelson KK, Mazurkiewicz JE, Bartholomew PJ, Aplin AE, Tai YT, Aguirre-Ghiso J, Flores SC et al. 2005. Mitochondrial H2O2 regulates the angiogenic phenotype via PTEN oxidation. *The Journal of biological chemistry* **280**: 16916-16924.
- Contente A, Dittmer A, Koch MC, Roth J, Dobbelsstein M. 2002. A polymorphic microsatellite that mediates induction of PIG3 by p53. *Nat Genet* **30**: 315-320.
- Contractor T, Harris CR. 2012. p53 Negatively Regulates Transcription of the Pyruvate Dehydrogenase Kinase Pdk2. *Cancer research* **72**: 560-567.
- Corn PG, Kuerbitz SJ, van Noesel MM, Esteller M, Compitello N, Baylin SB, Herman JG. 1999. Transcriptional silencing of the p73 gene in acute

- lymphoblastic leukemia and Burkitt's lymphoma is associated with 5' CpG island methylation. *Cancer research* **59**: 3352-3356.
- Coudreuse DY, Roel G, Betist MC, Destree O, Korswagen HC. 2006. Wnt gradient formation requires retromer function in Wnt-producing cells. *Science* **312**: 921-924.
- Crack PJ, Taylor JM. 2005. Reactive oxygen species and the modulation of stroke. *Free Radic Biol Med* **38**: 1433-1444.
- Crichton D, O'Prey J, Bell HS, Ryan KM. 2007. p73 regulates DRAM-independent autophagy that does not contribute to programmed cell death. *Cell death and differentiation* **14**: 1071-1079.
- Crichton D, Wilkinson S, O'Prey J, Syed N, Smith P, Harrison PR, Gasco M, Garrone O, Crook T, Ryan KM. 2006. DRAM, a p53-induced modulator of autophagy, is critical for apoptosis. *Cell* **126**: 121-134.
- D'Alessandro A, Amelio I, Berkers CR, Antonov A, Vousden KH, Melino G, Zolla L. 2014. Metabolic effect of TAp63alpha: enhanced glycolysis and pentose phosphate pathway, resulting in increased antioxidant defense. *Oncotarget* **5**: 7722-7733.
- Dahia PL. 2014. Pheochromocytoma and paraganglioma pathogenesis: learning from genetic heterogeneity. *Nat Rev Cancer* **14**: 108-119.
- Dai HM, Smith A, Meng XW, Schneider PA, Pang YP, Kaufmann SH. 2011. Transient binding of an activator BH3 domain to the Bak BH3-binding groove initiates Bak oligomerization. *Journal of Cell Biology* **194**: 38-47.
- Dai MS, Zeng SX, Jin YT, Sun XX, David L, Lu H. 2004. Ribosomal protein L23 activates p53 by inhibiting MDM2 function in response to ribosomal perturbation but not to translation inhibition. *Molecular and cellular biology* **24**: 7654-7668.
- Dai Q, Yin Y, Liu W, Wei L, Zhou Y, Li Z, You Q, Lu N, Guo Q. 2013. Two p53-related metabolic regulators, TIGAR and SCO2, contribute to oroxylin A-mediated glucose metabolism in human hepatoma HepG2 cells. *Int J Biochem Cell Biol* **45**: 1468-1478.
- Dameron KM, Volpert OV, Tainsky MA, Bouck N. 1994. Control of Angiogenesis in Fibroblasts by P53 Regulation of Thrombospondin-1. *Science* **265**: 1582-1584.
- Dang CV. 2009. MYC, microRNAs and glutamine addiction in cancers. *Cell cycle* **8**: 3243-3245.
- . 2012. Links between metabolism and cancer. *Genes & development* **26**: 877-890.
- Dang CV, Kim JW, Gao P, Yustein J. 2008. The interplay between MYC and HIF in cancer. *Nat Rev Cancer* **8**: 51-56.
- Dann CE, Hsieh JC, Rattner A, Sharma D, Nathans J, Leahy DJ. 2001. Insights into Wnt binding and signalling from the structures of two Frizzled cysteine-rich domains. *Nature* **412**: 86-90.
- Darville MI, Antoine IV, Rousseau GG. 1992. Characterization of an enhancer upstream from the muscle-type promoter of a gene encoding 6-phosphofructo-2-kinase/fructose-2,6-bisphosphatase. *Nucleic Acids Res* **20**: 3575-3583.
- DasGupta R, Fuchs E. 1999. Multiple roles for activated LEF/TCF transcription complexes during hair follicle development and differentiation. *Development* **126**: 4557-4568.

- David CJ, Chen M, Assanah M, Canoll P, Manley JL. 2010. HnRNP proteins controlled by c-Myc deregulate pyruvate kinase mRNA splicing in cancer. *Nature* **463**: 364-368.
- Davidson B, Hadar R, Schlossberg A, Sternlicht T, Slipicevic A, Skrede M, Risberg B, Florenes VA, Kopolovic J, Reich R. 2008. Expression and clinical role of DJ-1, a negative regulator of PTEN, in ovarian carcinoma. *Human pathology* **39**: 87-95.
- Davidson G, Wu W, Shen J, Bilic J, Fenger U, Stannek P, Glinka A, Niehrs C. 2005. Casein kinase 1 gamma couples Wnt receptor activation to cytoplasmic signal transduction. *Nature* **438**: 867-872.
- de Graaf P, Little NA, Ramos YFM, Meulmeester E, Letteboer SJF, Jochemsen AG. 2003. Hdmx protein stability is regulated by the ubiquitin ligase activity of Mdm2. *Journal of Biological Chemistry* **278**: 38315-38324.
- de Lau W, Barker N, Low TY, Koo BK, Li VS, Teunissen H, Kujala P, Haegebarth A, Peters PJ, van de Wetering M et al. 2011. Lgr5 homologues associate with Wnt receptors and mediate R-spondin signalling. *Nature* **476**: 293-297.
- De Laurenzi V, Costanzo A, Barcaroli D, Terrinoni A, Falco M, Annicchiarico-Petruzzelli M, Levrero M, Melino G. 1998. Two new p73 splice variants, gamma and delta, with different transcriptional activity. *The Journal of experimental medicine* **188**: 1763-1768.
- De Laurenzi V, Rossi A, Terrinoni A, Barcaroli D, Levrero M, Costanzo A, Knight RA, Guerrieri P, Melino G. 2000. p63 and p73 transactivate differentiation gene promoters in human keratinocytes. *Biochemical and biophysical research communications* **273**: 342-346.
- DeBerardinis RJ, Cheng T. 2010. Q's next: the diverse functions of glutamine in metabolism, cell biology and cancer. *Oncogene* **29**: 313-324.
- DeBerardinis RJ, Lum JJ, Hatzivassiliou G, Thompson CB. 2008. The biology of cancer: metabolic reprogramming fuels cell growth and proliferation. *Cell metabolism* **7**: 11-20.
- DeNicola GM, Karreth FA, Humpton TJ, Gopinathan A, Wei C, Frese K, Mangal D, Yu KH, Yeo CJ, Calhoun ES et al. 2011. Oncogene-induced Nrf2 transcription promotes ROS detoxification and tumorigenesis. *Nature* **475**: 106-109.
- Deprez J, Vertommen D, Alessi DR, Hue L, Rider MH. 1997. Phosphorylation and activation of heart 6-phosphofructo-2-kinase by protein kinase B and other protein kinases of the insulin signaling cascades. *The Journal of biological chemistry* **272**: 17269-17275.
- Dhillon AS, Hagan S, Rath O, Kolch W. 2007. MAP kinase signalling pathways in cancer. *Oncogene* **26**: 3279-3290.
- Dohn M, Zhang S, Chen X. 2001. p63alpha and DeltaNp63alpha can induce cell cycle arrest and apoptosis and differentially regulate p53 target genes. *Oncogene* **20**: 3193-3205.
- Donehower LA, Harvey M, Slagle BL, McArthur MJ, Montgomery CA, Jr., Butel JS, Bradley A. 1992. Mice deficient for p53 are developmentally normal but susceptible to spontaneous tumours. *Nature* **356**: 215-221.
- Dong C, Yuan T, Wu Y, Wang Y, Fan TW, Miriyala S, Lin Y, Yao J, Shi J, Kang T et al. 2013. Loss of FBP1 by Snail-mediated repression provides metabolic advantages in basal-like breast cancer. *Cancer Cell* **23**: 316-331.
- Du W, Jiang P, Mancuso A, Stonestrom A, Brewer MD, Minn AJ, Mak TW, Wu M, Yang X. 2013. TAp73 enhances the pentose phosphate pathway and supports cell proliferation. *Nature cell biology* **15**: 991-1000.

- Duncan CG, Barwick BG, Jin G, Rago C, Kapoor-Vazirani P, Powell DR, Chi JT, Bigner DD, Vertino PM, Yan H. 2012. A heterozygous IDH1R132H/WT mutation induces genome-wide alterations in DNA methylation. *Genome Res* **22**: 2339-2355.
- Dupriez VJ, Darville MI, Antoine IV, Gegonne A, Ghysdael J, Rousseau GG. 1993. Characterization of a hepatoma mRNA transcribed from a third promoter of a 6-phosphofructo-2-kinase/fructose-2,6-bisphosphatase-encoding gene and controlled by ets oncogene-related products. *Proceedings of the National Academy of Sciences of the United States of America* **90**: 8224-8228.
- Edinger AL, Thompson CB. 2002. Akt maintains cell size and survival by increasing mTOR-dependent nutrient uptake. *Mol Biol Cell* **13**: 2276-2288.
- Egler RA, Fernandes E, Rothermund K, Sereika S, de Souza-Pinto N, Jaruga P, Dizdaroglu M, Prochownik EV. 2005. Regulation of reactive oxygen species, DNA damage, and c-Myc function by peroxiredoxin 1. *Oncogene* **24**: 8038-8050.
- el Marjou F, Janssen KP, Chang BH, Li M, Hindie V, Chan L, Louvard D, Chambon P, Metzger D, Robine S. 2004. Tissue-specific and inducible Cre-mediated recombination in the gut epithelium. *Genesis* **39**: 186-193.
- el-Deiry WS, Kern SE, Pietenpol JA, Kinzler KW, Vogelstein B. 1992. Definition of a consensus binding site for p53. *Nat Genet* **1**: 45-49.
- el-Deiry WS, Tokino T, Velculescu VE, Levy DB, Parsons R, Trent JM, Lin D, Mercer WE, Kinzler KW, Vogelstein B. 1993. WAF1, a potential mediator of p53 tumor suppression. *Cell* **75**: 817-825.
- Elchuri S, Oberley TD, Qi W, Eisenstein RS, Jackson Roberts L, Van Remmen H, Epstein CJ, Huang TT. 2005. CuZnSOD deficiency leads to persistent and widespread oxidative damage and hepatocarcinogenesis later in life. *Oncogene* **24**: 367-380.
- Elstrom RL, Bauer DE, Buzzai M, Karnauskas R, Harris MH, Plas DR, Zhuang H, Cinalli RM, Alavi A, Rudin CM et al. 2004. Akt stimulates aerobic glycolysis in cancer cells. *Cancer research* **64**: 3892-3899.
- Fan Y, Dickman KG, Zong WX. 2010. Akt and c-Myc differentially activate cellular metabolic programs and prime cells to bioenergetic inhibition. *The Journal of biological chemistry* **285**: 7324-7333.
- Fang M, Shen Z, Huang S, Zhao L, Chen S, Mak TW, Wang X. 2010. The ER UDPase ENTPD5 promotes protein N-glycosylation, the Warburg effect, and proliferation in the PTEN pathway. *Cell* **143**: 711-724.
- Fang SY, Jensen JP, Ludwig RL, Vousden KH, Weissman AM. 2000. Mdm2 is a RING finger-dependent ubiquitin protein ligase for itself and p53. *Journal of Biological Chemistry* **275**: 8945-8951.
- Faraonio R, Vergara P, Di Marzo D, Pierantoni MG, Napolitano M, Russo T, Cimino F. 2006. p53 suppresses the Nrf2-dependent transcription of antioxidant response genes. *Journal of Biological Chemistry* **281**: 39776-39784.
- Feng LJ, Lin TX, Uranishi H, Gu W, Xu Y. 2005. Functional analysis of the roles of posttranslational modifications at the p53 C terminus in regulating p53 stability and activity. *Molecular and cellular biology* **25**: 5389-5395.
- Feng ZH, Hu WW, de Stanchina E, Teresky AK, Jin SK, Lowe S, Levine AJ. 2007. The regulation of AMPK beta 1, TSC2, and PTEN expression by p53: Stress, cell and tissue specificity, and the role of these gene products in

- modulating the IGF-1-AKT-mTOR pathways. *Cancer research* **67**: 3043-3053.
- Finkel T. 2003. Oxidant signals and oxidative stress. *Curr Opin Cell Biol* **15**: 247-254.
- . 2012. From sulfenylation to sulfhydration: what a thiolate needs to tolerate. *Sci Signal* **5**: pe10.
- Finley LW, Carracedo A, Lee J, Souza A, Egia A, Zhang J, Teruya-Feldstein J, Moreira PI, Cardoso SM, Clish CB et al. 2011. SIRT3 opposes reprogramming of cancer cell metabolism through HIF1alpha destabilization. *Cancer Cell* **19**: 416-428.
- Flaman JM, Waridel F, Estreicher A, Vannier A, Limacher JM, Gilbert D, Iggo R, Frebourg T. 1996. The human tumour suppressor gene p53 is alternatively spliced in normal cells. *Oncogene* **12**: 813-818.
- Flinn LJ, Keatinge M, Breaud S, Mortiboys H, Matsui H, De Felice E, Woodroof HI, Brown L, McTighe A, Soellner R et al. 2013. TigarB causes mitochondrial dysfunction and neuronal loss in PINK1 deficiency. *Ann Neurol* **74**: 837-847.
- Flores ER, Sengupta S, Miller JB, Newman JJ, Bronson R, Crowley D, Yang A, McKeon F, Jacks T. 2005. Tumor predisposition in mice mutant for p63 and p73: evidence for broader tumor suppressor functions for the p53 family. *Cancer Cell* **7**: 363-373.
- Frenzel J, Schellenberger W, Eschrich K, Hofmann E. 1988. Control of the fructose 6-phosphate/fructose 2,6-bisphosphate cycle by sn-glycerol 3-phosphate. *Biomed Biochim Acta* **47**: 461-470.
- Freytag SO, Geddes TJ. 1992. Reciprocal regulation of adipogenesis by Myc and C/EBP alpha. *Science* **256**: 379-382.
- Fu M, Rao M, Bouras T, Wang C, Wu K, Zhang X, Li Z, Yao TP, Pestell RG. 2005. Cyclin D1 inhibits peroxisome proliferator-activated receptor gamma-mediated adipogenesis through histone deacetylase recruitment. *The Journal of biological chemistry* **280**: 16934-16941.
- Funato Y, Michiue T, Asashima M, Miki H. 2006. The thioredoxin-related redox-regulating protein nucleoredoxin inhibits Wnt-beta-catenin signalling through dishevelled. *Nature cell biology* **8**: 501-508.
- Gallenne T, Gautier F, Oliver L, Hervouet E, Noel B, Hickman JA, Geneste O, Cartron PF, Vallette FM, Manon S et al. 2009. Bax activation by the BH3-only protein Puma promotes cell dependence on antiapoptotic Bcl-2 family members. *Journal of Cell Biology* **185**: 279-290.
- Galli LM, Barnes TL, Secret SS, Kadowaki T, Burrus LW. 2007. Porcupine-mediated lipid-modification regulates the activity and distribution of Wnt proteins in the chick neural tube. *Development* **134**: 3339-3348.
- Gao P, Tchernyshyov I, Chang TC, Lee YS, Kita K, Ochi T, Zeller KI, De Marzo AM, Van Eyk JE, Mendell JT et al. 2009. c-Myc suppression of miR-23a/b enhances mitochondrial glutaminase expression and glutamine metabolism. *Nature* **458**: 762-765.
- Gao X, Wang H, Yang JJ, Liu X, Liu ZR. 2012. Pyruvate kinase M2 regulates gene transcription by acting as a protein kinase. *Molecular cell* **45**: 598-609.
- Gat U, DasGupta R, Degenstein L, Fuchs E. 1998. De Novo hair follicle morphogenesis and hair tumors in mice expressing a truncated beta-catenin in skin. *Cell* **95**: 605-614.

- Gerald D, Berra E, Frapart YM, Chan DA, Giaccia AJ, Mansuy D, Pouyssegur J, Yaniv M, Mechta-Grigoriou F. 2004. JunD reduces tumor angiogenesis by protecting cells from oxidative stress. *Cell* **118**: 781-794.
- Gerin I, Noel G, Bolsee J, Haumont O, Van Schaffingen E, Bommer GT. 2014. Identification of TP53-induced glycolysis and apoptosis regulator (TIGAR) as the phosphoglycolate-independent 2,3-bisphosphoglycerate phosphatase. *The Biochemical journal* **458**: 439-448.
- Ghosh A, Stewart D, Matlashewski G. 2004. Regulation of human p53 activity and cell localization by alternative splicing. *Molecular and cellular biology* **24**: 7987-7997.
- Ghosh S, Mendoza T, Ortiz LA, Hoyle GW, Fermin CD, Brody AR, Friedman M, Morris GF. 2002. Bleomycin sensitivity of mice expressing dominant-negative p53 in the lung epithelium. *Am J Respir Crit Care Med* **166**: 890-897.
- Giacobbe A, Bongiorno-Borbone L, Bernassola F, Terrinoni A, Markert EK, Levine AJ, Feng Z, Agostini M, Zolla L, Agro AF et al. 2013. p63 regulates glutaminase 2 expression. *Cell cycle* **12**: 1395-1405.
- Glinka A, Dolde C, Kirsch N, Huang YL, Kazanskaya O, Ingelfinger D, Boutros M, Cruciat CM, Niehrs C. 2011. LGR4 and LGR5 are R-spondin receptors mediating Wnt/beta-catenin and Wnt/PCP signalling. *EMBO Rep* **12**: 1055-1061.
- Goidts V, Bageritz J, Puccio L, Nakata S, Zapatka M, Barbus S, Toedt G, Campos B, Korshunov A, Momma S et al. 2012. RNAi screening in glioma stem-like cells identifies PFKFB4 as a key molecule important for cancer cell survival. *Oncogene* **31**: 3235-3243.
- Gong JG, Costanzo A, Yang HQ, Melino G, Kaelin WG, Jr., Levrero M, Wang JY. 1999. The tyrosine kinase c-Abl regulates p73 in apoptotic response to cisplatin-induced DNA damage. *Nature* **399**: 806-809.
- Gong Y, Slee RB, Fukai N, Rawadi G, Roman-Roman S, Reginato AM, Wang H, Cundy T, Glorieux FH, Lev D et al. 2001. LDL receptor-related protein 5 (LRP5) affects bone accrual and eye development. *Cell* **107**: 513-523.
- Grant SF, Thorleifsson G, Reynisdottir I, Benediktsson R, Manolescu A, Sainz J, Helgason A, Stefansson H, Emilsson V, Helgadóttir A et al. 2006. Variant of transcription factor 7-like 2 (TCF7L2) gene confers risk of type 2 diabetes. *Nat Genet* **38**: 320-323.
- Grier JD, Xiong S, Elizondo-Fraire AC, Parant JM, Lozano G. 2006. Tissue-specific differences of p53 inhibition by Mdm2 and Mdm4. *Molecular and cellular biology* **26**: 192-198.
- Gross S, Cairns RA, Minden MD, Driggers EM, Bittinger MA, Jang HG, Sasaki M, Jin S, Schenkein DP, Su SM et al. 2010. Cancer-associated metabolite 2-hydroxyglutarate accumulates in acute myelogenous leukemia with isocitrate dehydrogenase 1 and 2 mutations. *The Journal of experimental medicine* **207**: 339-344.
- Gu W, Roeder RG. 1997. Activation of p53 sequence-specific DNA binding by acetylation of the p53 C-terminal domain. *Cell* **90**: 595-606.
- Guertin DA, Sabatini DM. 2007. Defining the role of mTOR in cancer. *Cancer Cell* **12**: 9-22.
- Guzy RD, Hoyos B, Robin E, Chen H, Liu L, Mansfield KD, Simon MC, Hammerling U, Schumacker PT. 2005. Mitochondrial complex III is required for hypoxia-induced ROS production and cellular oxygen sensing. *Cell metabolism* **1**: 401-408.

- Hagiwara K, McMenamin MG, Miura K, Harris CC. 1999. Mutational analysis of the p63/p73L/p51/p40/CUSP/KET gene in human cancer cell lines using intronic primers. *Cancer research* **59**: 4165-4169.
- Hamard PJ, Barthelery N, Hogstad B, Mungamuri SK, Tonnessen CA, Carvajal LA, Senturk E, Gillespie V, Aaronson SA, Merad M et al. 2013. The C terminus of p53 regulates gene expression by multiple mechanisms in a target- and tissue-specific manner in vivo. *Genes & development* **27**: 1868-1885.
- Hammond EM, Denko NC, Dorie MJ, Abraham RT, Giaccia AJ. 2002. Hypoxia links ATR and p53 through replication arrest. *Molecular and cellular biology* **22**: 1834-1843.
- Hanahan D, Weinberg RA. 2000. The hallmarks of cancer. *Cell* **100**: 57-70.
- . 2011. Hallmarks of cancer: the next generation. *Cell* **144**: 646-674.
- Harper JW, Adami GR, Wei N, Keyomarsi K, Elledge SJ. 1993. The P21 Cdk-Interacting Protein Cip1 Is a Potent Inhibitor of G1 Cyclin-Dependent Kinases. *Cell* **75**: 805-816.
- Harper JW, Elledge SJ, Keyomarsi K, Dynlacht B, Tsai LH, Zhang PM, Dobrowolski S, Bai C, Connellcrowley L, Swindell E et al. 1995. Inhibition of Cyclin-Dependent Kinases by P21. *Mol Biol Cell* **6**: 387-400.
- Harris AW, Pinkert CA, Crawford M, Langdon WY, Brinster RL, Adams JM. 1988. The E mu-myc transgenic mouse. A model for high-incidence spontaneous lymphoma and leukemia of early B cells. *The Journal of experimental medicine* **167**: 353-371.
- Harris IS, Treloar AE, Inoue S, Sasaki M, Gorrini C, Lee KC, Yung KY, Brenner D, Knobbe-Thomsen CB, Cox MA et al. 2015. Glutathione and thioredoxin antioxidant pathways synergize to drive cancer initiation and progression. *Cancer Cell* **27**: 211-222.
- Hasegawa H, Yamada Y, Iha H, Tsukasaki K, Nagai K, Atogami S, Sugahara K, Tsuruda K, Ishizaki A, Kamihira S. 2009. Activation of p53 by Nutlin-3a, an antagonist of MDM2, induces apoptosis and cellular senescence in adult T-cell leukemia cells. *Leukemia* **23**: 2090-2101.
- Haupt Y, Maya R, Kazaz A, Oren M. 1997. Mdm2 promotes the rapid degradation of p53. *Nature* **387**: 296-299.
- Hausmann G, Banziger C, Basler K. 2007. Helping Wingless take flight: how WNT proteins are secreted. *Nature reviews Molecular cell biology* **8**: 331-336.
- Hayes JD, McMahon M, Chowdhry S, Dinkova-Kostova AT. 2010. Cancer chemoprevention mechanisms mediated through the Keap1-Nrf2 pathway. *Antioxidants & redox signaling* **13**: 1713-1748.
- He TC, Sparks AB, Rago C, Hermeking H, Zawel L, da Costa LT, Morin PJ, Vogelstein B, Kinzler KW. 1998. Identification of c-MYC as a target of the APC pathway. *Science* **281**: 1509-1512.
- He X, Semenov M, Tamai K, Zeng X. 2004. LDL receptor-related proteins 5 and 6 in Wnt/beta-catenin signaling: arrows point the way. *Development* **131**: 1663-1677.
- He Z, Liu H, Agostini M, Yousefi S, Perren A, Tschan MP, Mak TW, Melino G, Simon HU. 2013. p73 regulates autophagy and hepatocellular lipid metabolism through a transcriptional activation of the ATG5 gene. *Cell death and differentiation* **20**: 1415-1424.
- Heine-Suner D, Diaz-Guillen MA, Lange AJ, Rodriguez de Cordoba S. 1998. Sequence and structure of the human 6-phosphofructo-2-kinase/fructose-

- 2,6-bisphosphatase heart isoform gene (PFKFB2). *Eur J Biochem* **254**: 103-110.
- Herrero-Mendez A, Almeida A, Fernandez E, Maestre C, Moncada S, Bolanos JP. 2009. The bioenergetic and antioxidant status of neurons is controlled by continuous degradation of a key glycolytic enzyme by APC/C-Cdh1. *Nature cell biology* **11**: 747-752.
- Hibi K, Trink B, Patturajan M, Westra WH, Caballero OL, Hill DE, Ratovitski EA, Jen J, Sidransky D. 2000. AIS is an oncogene amplified in squamous cell carcinoma. *Proceedings of the National Academy of Sciences of the United States of America* **97**: 5462-5467.
- Hirao A, Kong YY, Matsuoka S, Wakeham A, Ruland J, Yoshida H, Liu D, Elledge SJ, Mak TW. 2000. DNA damage-induced activation of p53 by the checkpoint kinase Chk2. *Science* **287**: 1824-1827.
- Hirata T, Watanabe M, Miura S, Ijichi K, Fukasawa M, Sakakibara R. 2000. Inhibition of tumor cell growth by a specific 6-phosphofructo-2-kinase inhibitor, N-bromoacetyethanolamine phosphate, and its analogues. *Biosci Biotechnol Biochem* **64**: 2047-2052.
- Hirose K, Longo DL, Oppenheim JJ, Matsushima K. 1993. Overexpression of mitochondrial manganese superoxide dismutase promotes the survival of tumor cells exposed to interleukin-1, tumor necrosis factor, selected anticancer drugs, and ionizing radiation. *FASEB J* **7**: 361-368.
- Hitosugi T, Kang S, Vander Heiden MG, Chung TW, Elf S, Lythgoe K, Dong S, Lonial S, Wang X, Chen GZ et al. 2009. Tyrosine phosphorylation inhibits PKM2 to promote the Warburg effect and tumor growth. *Sci Signal* **2**: ra73.
- Hoang B, Moos M, Jr., Vukicevic S, Luyten FP. 1996. Primary structure and tissue distribution of FRZB, a novel protein related to Drosophila frizzled, suggest a role in skeletal morphogenesis. *The Journal of biological chemistry* **271**: 26131-26137.
- Hock AK, Lee P, Maddocks OD, Mason SM, Blyth K, Vousden KH. 2014. iRFP is a sensitive marker for cell number and tumor growth in high-throughput systems. *Cell cycle* **13**: 220-226.
- Hodis E, Watson IR, Kryukov GV, Arold ST, Imielinski M, Theurillat JP, Nickerson E, Auclair D, Li L, Place C et al. 2012. A landscape of driver mutations in melanoma. *Cell* **150**: 251-263.
- Hofmann K. 2000. A superfamily of membrane-bound O-acyltransferases with implications for wnt signaling. *Trends Biochem Sci* **25**: 111-112.
- Holmgren A. 1989. Thioredoxin and glutaredoxin systems. *The Journal of biological chemistry* **264**: 13963-13966.
- Honda R, Tanaka H, Yasuda H. 1997. Oncoprotein MDM2 is a ubiquitin ligase E3 for tumor suppressor p53. *Febs Lett* **420**: 25-27.
- Honda R, Yasuda H. 2000. Activity of MDM2, a ubiquitin Ligase, toward p53 or itself is dependent on the RING finger domain of the ligase. *Oncogene* **19**: 1473-1476.
- Hoshino A, Matoba S, Iwai-Kanai E, Nakamura H, Kimata M, Nakaoka M, Katamura M, Okawa Y, Ariyoshi M, Mita Y et al. 2012. p53-TIGAR axis attenuates mitophagy to exacerbate cardiac damage after ischemia. *Journal of molecular and cellular cardiology* **52**: 175-184.
- Hsieh JC, Kodjabachian L, Rebbert ML, Rattner A, Smallwood PM, Samos CH, Nusse R, Dawid IB, Nathans J. 1999. A new secreted protein that binds to Wnt proteins and inhibits their activities. *Nature* **398**: 431-436.

- Hu W, Zhang C, Wu R, Sun Y, Levine A, Feng Z. 2010. Glutaminase 2, a novel p53 target gene regulating energy metabolism and antioxidant function. *Proceedings of the National Academy of Sciences of the United States of America* **107**: 7455-7460.
- Huang Y, Guerrero-Preston R, Ratovitski EA. 2012. Phospho-DeltaNp63alpha-dependent regulation of autophagic signaling through transcription and micro-RNA modulation. *Cell cycle* **11**: 1247-1259.
- Ide T, Brown-Endres L, Chu K, Ongusaha PP, Ohtsuka T, El-Deiry WS, Aaronson SA, Lee SW. 2009. GAMT, a p53-Inducible Modulator of Apoptosis, Is Critical for the Adaptive Response to Nutrient Stress (Retracted article. See vol. 51, pg. 552, 2013). *Molecular cell* **36**: 379-392.
- Iggo R, Gatter K, Bartek J, Lane D, Harris AL. 1990. Increased Expression of Mutant Forms of the P53 Oncogene in Primary Lung-Cancer. *Brit J Cancer* **62**: 505-505.
- Imamura K, Ogura T, Kishimoto A, Kaminishi M, Esumi H. 2001. Cell cycle regulation via p53 phosphorylation by a 5'-AMP activated protein kinase activator, 5-aminoimidazole-4-carboxamide-1-beta-D-ribofuranoside, in a human hepatocellular carcinoma cell line. *Biochemical and biophysical research communications* **287**: 562-567.
- Imamura K, Tanaka T. 1972. Multimolecular forms of pyruvate kinase from rat and other mammalian tissues. I. Electrophoretic studies. *J Biochem* **71**: 1043-1051.
- Inoki K, Corradetti MN, Guan KL. 2005. Dysregulation of the TSC-mTOR pathway in human disease. *Nat Genet* **37**: 19-24.
- Inoki K, Ouyang H, Zhu T, Lindvall C, Wang Y, Zhang X, Yang Q, Bennett C, Harada Y, Stankunas K et al. 2006. TSC2 integrates Wnt and energy signals via a coordinated phosphorylation by AMPK and GSK3 to regulate cell growth. *Cell* **126**: 955-968.
- Inoki K, Zhu T, Guan KL. 2003. TSC2 mediates cellular energy response to control cell growth and survival. *Cell* **115**: 577-590.
- Inoue S, Tomasini R, Rufini A, Elia AJ, Agostini M, Amelio I, Cescon D, Dinsdale D, Zhou L, Harris IS et al. 2014. TAp73 is required for spermatogenesis and the maintenance of male fertility. *Proceedings of the National Academy of Sciences of the United States of America* **111**: 1843-1848.
- Ireland H, Kemp R, Houghton C, Howard L, Clarke AR, Sansom OJ, Winton DJ. 2004. Inducible Cre-mediated control of gene expression in the murine gastrointestinal tract: effect of loss of beta-catenin. *Gastroenterology* **126**: 1236-1246.
- Ishikawa K, Takenaga K, Akimoto M, Koshikawa N, Yamaguchi A, Imanishi H, Nakada K, Honma Y, Hayashi J. 2008. ROS-generating mitochondrial DNA mutations can regulate tumor cell metastasis. *Science* **320**: 661-664.
- Ishimoto O, Kawahara C, Enjo K, Obinata M, Nukiwa T, Ikawa S. 2002. Possible oncogenic potential of DeltaNp73: a newly identified isoform of human p73. *Cancer research* **62**: 636-641.
- Israelsen WJ, Dayton TL, Davidson SM, Fiske BP, Hosios AM, Bellinger G, Li J, Yu Y, Sasaki M, Horner JW et al. 2013. PKM2 isoform-specific deletion reveals a differential requirement for pyruvate kinase in tumor cells. *Cell* **155**: 397-409.
- Itahana K, Mao H, Jin AW, Itahana Y, Clegg HV, Lindstrom MS, Bhat KP, Godfrey VL, Evan GI, Zhang YP. 2007. Targeted inactivation of mdm2 RING finger

- e3 ubiquitin ligase activity in the mouse reveals mechanistic insights into p53 regulation. *Cancer Cell* **12**: 355-366.
- Ito A, Lai CH, Zhao X, Saito S, Hamilton MH, Appella E, Yao TP. 2001. p300/CBP-mediated p53 acetylation is commonly induced by p53-activating agents and inhibited by MDM2. *Embo Journal* **20**: 1331-1340.
- Jaks V, Barker N, Kasper M, van Es JH, Snippert HJ, Clevers H, Toftgard R. 2008. Lgr5 marks cycling, yet long-lived, hair follicle stem cells. *Nat Genet* **40**: 1291-1299.
- Janda CY, Waghray D, Levin AM, Thomas C, Garcia KC. 2012. Structural basis of Wnt recognition by Frizzled. *Science* **337**: 59-64.
- Jansson M, Durant ST, Cho EC, Sheahan S, Edelmann M, Kessler B, La Thangue NB. 2008. Arginine methylation regulates the p53 response. *Nature cell biology* **10**: 1431-U1122.
- Jaramillo MC, Zhang DD. 2013. The emerging role of the Nrf2-Keap1 signaling pathway in cancer. *Genes & development* **27**: 2179-2191.
- Jen KY, Cheung VG. 2005. Identification of novel p53 target genes in ionizing radiation response. *Cancer research* **65**: 7666-7673.
- Jenne DE, Reimann H, Nezu J, Friedel W, Loff S, Jeschke R, Muller O, Back W, Zimmer M. 1998. Peutz-Jeghers syndrome is caused by mutations in a novel serine threonine kinase. *Nat Genet* **18**: 38-43.
- Jeong AY, Lee MY, Lee SH, Park JH, Han HJ. 2009. PPARdelta agonist-mediated ROS stimulates mouse embryonic stem cell proliferation through cooperation of p38 MAPK and Wnt/beta-catenin. *Cell cycle* **8**: 611-619.
- Ji H, Ramsey MR, Hayes DN, Fan C, McNamara K, Kozlowski P, Torrice C, Wu MC, Shimamura T, Perera SA et al. 2007. LKB1 modulates lung cancer differentiation and metastasis. *Nature* **448**: 807-810.
- Jia S, Liu Z, Zhang S, Liu P, Zhang L, Lee SH, Zhang J, Signoretti S, Loda M, Roberts TM et al. 2008. Essential roles of PI(3)K-p110beta in cell growth, metabolism and tumorigenesis. *Nature* **454**: 776-779.
- Jian Z, Li K, Liu L, Zhang Y, Zhou Z, Li C, Gao T. 2011. Heme oxygenase-1 protects human melanocytes from H2O2-induced oxidative stress via the Nrf2-ARE pathway. *The Journal of investigative dermatology* **131**: 1420-1427.
- Jiang L, Kon N, Li TY, Wang SJ, Su T, Hibshoosh H, Baer R, Gu W. 2015. Ferroptosis as a p53-mediated activity during tumour suppression. *Nature* **520**: 57-+.
- Jiang P, Du W, Mancuso A, Wellen KE, Yang X. 2013. Reciprocal regulation of p53 and malic enzymes modulates metabolism and senescence. *Nature* **493**: 689-693.
- Jiang P, Du W, Wang X, Mancuso A, Gao X, Wu M, Yang X. 2011. p53 regulates biosynthesis through direct inactivation of glucose-6-phosphate dehydrogenase. *Nature cell biology* **13**: 310-316.
- Jiang Y, Zou L, Zhang C, He S, Cheng C, Xu J, Lu W, Zhang Y, Zhang H, Wang D et al. 2009. PPARgamma and Wnt/beta-Catenin pathway in human breast cancer: expression pattern, molecular interaction and clinical/prognostic correlations. *J Cancer Res Clin Oncol* **135**: 1551-1559.
- Jin A, Itahana K, O'Keefe K, Zhang Y. 2004. Inhibition of HDM2 and activation of p53 by ribosomal protein L23. *Molecular and cellular biology* **24**: 7669-7680.

- Jones RG, Plas DR, Kubek S, Buzzai M, Mu J, Xu Y, Birnbaum MJ, Thompson CB. 2005. AMP-activated protein kinase induces a p53-dependent metabolic checkpoint. *Molecular cell* **18**: 283-293.
- Jones SN, Roe AE, Donehower LA, Bradley A. 1995. Rescue of embryonic lethality in Mdm2-deficient mice by absence of p53. *Nature* **378**: 206-208.
- Jost CA, Marin MC, Kaelin WG, Jr. 1997. p73 is a simian [correction of human] p53-related protein that can induce apoptosis. *Nature* **389**: 191-194.
- Kaelin WG, Jr., Ratcliffe PJ. 2008. Oxygen sensing by metazoans: the central role of the HIF hydroxylase pathway. *Molecular cell* **30**: 393-402.
- Kaghad M, Bonnet H, Yang A, Creancier L, Biscan JC, Valent A, Minty A, Chalon P, Lelias JM, Dumont X et al. 1997. Monoallelically expressed gene related to p53 at 1p36, a region frequently deleted in neuroblastoma and other human cancers. *Cell* **90**: 809-819.
- Kahle PJ, Waak J, Gasser T. 2009. DJ-1 and prevention of oxidative stress in Parkinson's disease and other age-related disorders. *Free Radic Biol Med* **47**: 1354-1361.
- Kamiguti AS, Serrander L, Lin K, Harris RJ, Cawley JC, Allsup DJ, Slupsky JR, Krause KH, Zuzel M. 2005. Expression and activity of NOX5 in the circulating malignant B cells of hairy cell leukemia. *J Immunol* **175**: 8424-8430.
- Kanazawa A, Tsukada S, Sekine A, Tsunoda T, Takahashi A, Kashiwagi A, Tanaka Y, Babazono T, Matsuda M, Kaku K et al. 2004. Association of the gene encoding wingless-type mammary tumor virus integration-site family member 5B (WNT5B) with type 2 diabetes. *Am J Hum Genet* **75**: 832-843.
- Kawai H, Lopez-Pajares V, Kim MM, Wiederschain D, Yuan ZM. 2007. RING domain-mediated interaction is a requirement for MDM2's E3 ligase activity. *Cancer research* **67**: 6026-6030.
- Kawai H, Wiederschain D, Yuan ZM. 2003. Critical contribution of the MDM2 acidic domain to p53 ubiquitination. *Molecular and cellular biology* **23**: 4939-4947.
- Kawano S, Miller CW, Gombart AF, Bartram CR, Matsuo Y, Asou H, Sakashita A, Said J, Tatsumi E, Koeffler HP. 1999. Loss of p73 gene expression in leukemias/lymphomas due to hypermethylation. *Blood* **94**: 1113-1120.
- Kazanskaya O, Glinka A, del Barco Barrantes I, Stanek P, Niehrs C, Wu W. 2004. R-Spondin2 is a secreted activator of Wnt/beta-catenin signaling and is required for *Xenopus* myogenesis. *Developmental cell* **7**: 525-534.
- Keyes WM, Wu Y, Vogel H, Guo X, Lowe SW, Mills AA. 2005. p63 deficiency activates a program of cellular senescence and leads to accelerated aging. *Genes & development* **19**: 1986-1999.
- Khatri S, Yepiskoposyan H, Gallo CA, Tandon P, Plas DR. 2010. FOXO3a regulates glycolysis via transcriptional control of tumor suppressor TSC1. *The Journal of biological chemistry* **285**: 15960-15965.
- Khosravi R, Maya R, Gottlieb T, Oren M, Shiloh Y, Shkedy D. 1999. Rapid ATM-dependent phosphorylation of MDM2 precedes p53 accumulation in response to DNA damage. *Proceedings of the National Academy of Sciences of the United States of America* **96**: 14973-14977.
- Kim J, Devalaraja-Narashimha K, Padanilam BJ. 2015. TIGAR regulates glycolysis in ischemic kidney proximal tubules. *Am J Physiol Renal Physiol* **308**: F298-308.
- Kim JW, Tchernyshyov I, Semenza GL, Dang CV. 2006. HIF-1-mediated expression of pyruvate dehydrogenase kinase: a metabolic switch required for cellular adaptation to hypoxia. *Cell metabolism* **3**: 177-185.

- Kim MS, Chang X, LeBron C, Nagpal JK, Lee J, Huang Y, Yamashita K, Trink B, Ratovitski EA, Sidransky D. 2010a. Neurofilament heavy polypeptide regulates the Akt-beta-catenin pathway in human esophageal squamous cell carcinoma. *Plos One* **5**: e9003.
- Kim RH, Peters M, Jang Y, Shi W, Pintilie M, Fletcher GC, DeLuca C, Liepa J, Zhou L, Snow B et al. 2005. DJ-1, a novel regulator of the tumor suppressor PTEN. *Cancer Cell* **7**: 263-273.
- Kim YR, Oh JE, Kim MS, Kang MR, Park SW, Han JY, Eom HS, Yoo NJ, Lee SH. 2010b. Oncogenic NRF2 mutations in squamous cell carcinomas of oesophagus and skin. *J Pathol* **220**: 446-451.
- Kimata M, Matoba S, Iwai-Kanai E, Nakamura H, Hoshino A, Nakaoka M, Katamura M, Okawa Y, Mita Y, Okigaki M et al. 2010. p53 and TIGAR regulate cardiac myocyte energy homeostasis under hypoxic stress. *American journal of physiology Heart and circulatory physiology* **299**: H1908-1916.
- King A, Selak MA, Gottlieb E. 2006. Succinate dehydrogenase and fumarate hydratase: linking mitochondrial dysfunction and cancer. *Oncogene* **25**: 4675-4682.
- Kinzler KW, Vogelstein B. 1996. Lessons from hereditary colorectal cancer. *Cell* **87**: 159-170.
- Kitamura N, Nakamura Y, Miyamoto Y, Miyamoto T, Kabu K, Yoshida M, Futamura M, Ichinose S, Arakawa H. 2011. Mieap, a p53-Inducible Protein, Controls Mitochondrial Quality by Repairing or Eliminating Unhealthy Mitochondria. *Plos One* **6**.
- Komekado H, Yamamoto H, Chiba T, Kikuchi A. 2007. Glycosylation and palmitoylation of Wnt-3a are coupled to produce an active form of Wnt-3a. *Genes Cells* **12**: 521-534.
- Kondoh H, Leonart ME, Gil J, Wang J, Degan P, Peters G, Martinez D, Carnero A, Beach D. 2005. Glycolytic enzymes can modulate cellular life span. *Cancer research* **65**: 177-185.
- Konstantinopoulos PA, Spentzos D, Fountzilas E, Francoeur N, Sanisetty S, Grammatikos AP, Hecht JL, Cannistra SA. 2011. Keap1 mutations and Nrf2 pathway activation in epithelial ovarian cancer. *Cancer research* **71**: 5081-5089.
- Kops GJPL, Dansen TB, Polderman PE, Saarloos I, Wirtz KWA, Coffey PJ, Huang TT, Bos JL, Medema RH, Burgering BMT. 2002a. Forkhead transcription factor FOXO3a protects quiescent cells from oxidative stress. *Nature* **419**: 316-321.
- Kops GJPL, Medema RH, Glassford J, Essers MAG, Dijkers PF, Coffey PJ, Lam EWF, Burgering BMT. 2002b. Control of cell cycle exit and entry by protein kinase B-regulated Forkhead transcription factors. *Molecular and cellular biology* **22**: 2025-2036.
- Korinek V, Barker N, Moerer P, van Donselaar E, Huls G, Peters PJ, Clevers H. 1998. Depletion of epithelial stem-cell compartments in the small intestine of mice lacking Tcf-4. *Nat Genet* **19**: 379-383.
- Korsmeyer SJ. 1992. Bcl-2 initiates a new category of oncogenes: regulators of cell death. *Blood* **80**: 879-886.
- Korswagen HC, Herman MA, Clevers HC. 2000. Distinct beta-catenins mediate adhesion and signalling functions in *C. elegans*. *Nature* **406**: 527-532.

- Koster MI, Marinari B, Payne AS, Kantaputra PN, Costanzo A, Roop DR. 2009. DeltaNp63 knockdown mice: A mouse model for AEC syndrome. *Am J Med Genet A* **149A**: 1942-1947.
- Krauthammer M, Kong Y, Ha BH, Evans P, Bacchicocchi A, McCusker JP, Cheng E, Davis MJ, Goh G, Choi M et al. 2012. Exome sequencing identifies recurrent somatic RAC1 mutations in melanoma. *Nat Genet* **44**: 1006-1014.
- Krummel KA, Lee CJ, Toledo F, Wahl GM. 2005. The C-terminal lysines fine-tune P53 stress responses in a mouse model but are not required for stability control or transactivation. *Proceedings of the National Academy of Sciences of the United States of America* **102**: 10188-10193.
- Kubbutat MH, Ludwig RL, Levine AJ, Vousden KH. 1999. Analysis of the degradation function of Mdm2. *Cell Growth Differ* **10**: 87-92.
- Kuhajda FP. 2008. AMP-activated protein kinase and human cancer: cancer metabolism revisited. *Int J Obes (Lond)* **32 Suppl 4**: S36-41.
- Kulawiec M, Ayyasamy V, Singh KK. 2009. p53 regulates mtDNA copy number and mitochekpoint pathway. *J Carcinog* **8**: 8.
- Kulikov R, Winter M, Blattner C. 2006. Binding of p53 to the central domain of Mdm2 is regulated by phosphorylation. *Journal of Biological Chemistry* **281**: 28575-28583.
- Kumar B, Koul S, Khandrika L, Meacham RB, Koul HK. 2008. Oxidative stress is inherent in prostate cancer cells and is required for aggressive phenotype. *Cancer research* **68**: 1777-1785.
- Labuschagne CF, van den Broek NJ, Mackay GM, Vousden KH, Maddocks OD. 2014. Serine, but not glycine, supports one-carbon metabolism and proliferation of cancer cells. *Cell Rep* **7**: 1248-1258.
- Lagathu C, Christodoulides C, Virtue S, Cawthorn WP, Franzin C, Kimber WA, Nora ED, Campbell M, Medina-Gomez G, Cheyette BN et al. 2009. Dact1, a nutritionally regulated preadipocyte gene, controls adipogenesis by coordinating the Wnt/beta-catenin signaling network. *Diabetes* **58**: 609-619.
- Lammi L, Arte S, Somer M, Jarvinen H, Lahermo P, Thesleff I, Pirinen S, Nieminen P. 2004. Mutations in AXIN2 cause familial tooth agenesis and predispose to colorectal cancer. *Am J Hum Genet* **74**: 1043-1050.
- Lang GA, Iwakuma T, Suh YA, Liu G, Rao VA, Parant JM, Valentin-Vega YA, Terzian T, Caldwell LC, Strong LC et al. 2004. Gain of function of a p53 hot spot mutation in a mouse model of Li-Fraumeni syndrome. *Cell* **119**: 861-872.
- Larman TC, DePalma SR, Hadjipanayis AG, Cancer Genome Atlas Research N, Protopopov A, Zhang J, Gabriel SB, Chin L, Seidman CE, Kucherlapati R et al. 2012. Spectrum of somatic mitochondrial mutations in five cancers. *Proceedings of the National Academy of Sciences of the United States of America* **109**: 14087-14091.
- Latina A, Viticchie G, Lena AM, Piro MC, Annicchiarico-Petruzzelli M, Melino G, Candi E. 2015. DeltaNp63 targets cytoglobin to inhibit oxidative stress-induced apoptosis in keratinocytes and lung cancer. *Oncogene*.
- Le A, Lane AN, Hamaker M, Bose S, Gouw A, Barbi J, Tsukamoto T, Rojas CJ, Slusher BS, Zhang H et al. 2012. Glucose-independent glutamine metabolism via TCA cycling for proliferation and survival in B cells. *Cell metabolism* **15**: 110-121.
- Lee CW, La Thangue NB. 1999. Promoter specificity and stability control of the p53-related protein p73. *Oncogene* **18**: 4171-4181.

- Lee P, Vousden KH, Cheung EC. 2014. TIGAR, TIGAR, burning bright. *Cancer & metabolism* **2**: 1.
- Lee SR, Yang KS, Kwon J, Lee C, Jeong W, Rhee SG. 2002. Reversible inactivation of the tumor suppressor PTEN by H₂O₂. *The Journal of biological chemistry* **277**: 20336-20342.
- Lee SY, Jeon HM, Ju MK, Kim CH, Yoon G, Han SI, Park HG, Kang HS. 2012. Wnt/Snail signaling regulates cytochrome C oxidase and glucose metabolism. *Cancer research* **72**: 3607-3617.
- Leone G, DeGregori J, Yan Z, Jakoi L, Ishida S, Williams RS, Nevins JR. 1998. E2F3 activity is regulated during the cell cycle and is required for the induction of S phase. *Genes & development* **12**: 2120-2130.
- Leslie NR, Bennett D, Lindsay YE, Stewart H, Gray A, Downes CP. 2003. Redox regulation of PI 3-kinase signalling via inactivation of PTEN. *The EMBO journal* **22**: 5501-5510.
- Li B, Qiu B, Lee DS, Walton ZE, Ochocki JD, Mathew LK, Mancuso A, Gade TP, Keith B, Nissim I et al. 2014a. Fructose-1,6-bisphosphatase opposes renal carcinoma progression. *Nature* **513**: 251-255.
- Li H, Jogi G. 2009. Structural and biochemical studies of TIGAR (TP53-induced glycolysis and apoptosis regulator). *The Journal of biological chemistry* **284**: 1748-1754.
- Li M, Sun M, Cao L, Gu JH, Ge J, Chen J, Han R, Qin YY, Zhou ZP, Ding Y et al. 2014b. A TIGAR-regulated metabolic pathway is critical for protection of brain ischemia. *The Journal of neuroscience : the official journal of the Society for Neuroscience* **34**: 7458-7471.
- Li MY, Luo JY, Brooks CL, Gu W. 2002. Acetylation of p53 inhibits its ubiquitination by Mdm2. *Journal of Biological Chemistry* **277**: 50607-50611.
- Li N, He Y, Wang L, Mo C, Zhang J, Zhang W, Li J, Liao Z, Tang X, Xiao H. 2011. D-galactose induces necroptotic cell death in neuroblastoma cell lines. *J Cell Biochem* **112**: 3834-3844.
- Li T, Kon N, Jiang L, Tan M, Ludwig T, Zhao Y, Baer R, Gu W. 2012a. Tumor suppression in the absence of p53-mediated cell-cycle arrest, apoptosis, and senescence. *Cell* **149**: 1269-1283.
- Li VS, Ng SS, Boersema PJ, Low TY, Karthaus WR, Gerlach JP, Mohammed S, Heck AJ, Maurice MM, Mahmoudi T et al. 2012b. Wnt signaling through inhibition of beta-catenin degradation in an intact Axin1 complex. *Cell* **149**: 1245-1256.
- Linares LK, Hengstermann A, Ciechanover A, Muller S, Scheffner M. 2003. HdmX stimulates Hdm2-mediated ubiquitination and degradation of p53. *Proceedings of the National Academy of Sciences of the United States of America* **100**: 12009-12014.
- Lindsay CR, Li A, Faller W, Ozanne B, Welch H, Machesky LM, Sansom OJ. 2015. A Rac1-independent role for P-Rex1 in melanoblasts. *The Journal of investigative dermatology* **135**: 314-318.
- Linke K, Mace PD, Smith CA, Vaux DL, Silke J, Day CL. 2008. Structure of the MDM2/MDMX RING domain heterodimer reveals dimerization is required for their ubiquitylation in trans. *Cell death and differentiation* **15**: 841-848.
- Little RD, Carulli JP, Del Mastro RG, Dupuis J, Osborne M, Folz C, Manning SP, Swain PM, Zhao SC, Eustace B et al. 2002. A mutation in the LDL receptor-related protein 5 gene results in the autosomal dominant high-bone-mass trait. *Am J Hum Genet* **70**: 11-19.

- Liu G, Chen X. 2005. The C-terminal sterile alpha motif and the extreme C terminus regulate the transcriptional activity of the alpha isoform of p73. *The Journal of biological chemistry* **280**: 20111-20119.
- Liu G, Chen XB. 2002. The ferredoxin reductase gene is regulated by the p53 family and sensitizes cells to oxidative stress-induced apoptosis. *Oncogene* **21**: 7195-7204.
- Liu G, Nozell S, Xiao H, Chen X. 2004. DeltaNp73beta is active in transactivation and growth suppression. *Molecular and cellular biology* **24**: 487-501.
- Liu J, Wang H, Zuo Y, Farmer SR. 2006. Functional interaction between peroxisome proliferator-activated receptor gamma and beta-catenin. *Molecular and cellular biology* **26**: 5827-5837.
- Liu W, Dong X, Mai M, Seelan RS, Taniguchi K, Krishnadath KK, Halling KC, Cunningham JM, Boardman LA, Qian C et al. 2000. Mutations in AXIN2 cause colorectal cancer with defective mismatch repair by activating beta-catenin/TCF signalling. *Nat Genet* **26**: 146-147.
- Liu Z, Habener JF. 2009. Stromal cell-derived factor-1 promotes survival of pancreatic beta cells by the stabilisation of beta-catenin and activation of transcription factor 7-like 2 (TCF7L2). *Diabetologia* **52**: 1589-1598.
- Livera G, Petre-Lazar B, Guerquin MJ, Trautmann E, Coffigny H, Habert R. 2008. p63 null mutation protects mouse oocytes from radio-induced apoptosis. *Reproduction* **135**: 3-12.
- Locasale JW, Grassian AR, Melman T, Lyssiotis CA, Mattaini KR, Bass AJ, Heffron G, Metallo CM, Muranen T, Sharfi H et al. 2011. Phosphoglycerate dehydrogenase diverts glycolytic flux and contributes to oncogenesis. *Nat Genet* **43**: 869-874.
- Logan CY, Nusse R. 2004. The Wnt signaling pathway in development and disease. *Annu Rev Cell Dev Biol* **20**: 781-810.
- Lohrum MAE, Ludwig RL, Kubbutat MHG, Hanlon M, Vousden KH. 2003. Regulation of HDM2 activity by the ribosomal protein L11. *Cancer Cell* **3**: 577-587.
- Longo KA, Wright WS, Kang S, Gerin I, Chiang SH, Lucas PC, Opp MR, MacDougald OA. 2004. Wnt10b inhibits development of white and brown adipose tissues. *The Journal of biological chemistry* **279**: 35503-35509.
- Lou YW, Chen YY, Hsu SF, Chen RK, Lee CL, Khoo KH, Tonks NK, Meng TC. 2008. Redox regulation of the protein tyrosine phosphatase PTP1B in cancer cells. *FEBS J* **275**: 69-88.
- Lowe SW, Lin AW. 2000. Apoptosis in cancer. *Carcinogenesis* **21**: 485-495.
- Lu C, Ward PS, Kapoor GS, Rohle D, Turcan S, Abdel-Wahab O, Edwards CR, Khanin R, Figueroa ME, Melnick A et al. 2012. IDH mutation impairs histone demethylation and results in a block to cell differentiation. *Nature* **483**: 474-478.
- Lu CW, Lin SC, Chen KF, Lai YY, Tsai SJ. 2008. Induction of pyruvate dehydrogenase kinase-3 by hypoxia-inducible factor-1 promotes metabolic switch and drug resistance. *The Journal of biological chemistry* **283**: 28106-28114.
- Lu YP, Lou YR, Yen P, Newmark HL, Mirochnitchenko OI, Inouye M, Huang MT. 1997. Enhanced skin carcinogenesis in transgenic mice with high expression of glutathione peroxidase or both glutathione peroxidase and superoxide dismutase. *Cancer research* **57**: 1468-1474.

- Luftner D, Mesterharm J, Akrivakis C, Geppert R, Petrides PE, Wernecke KD, Possinger K. 2000. Tumor type M2 pyruvate kinase expression in advanced breast cancer. *Anticancer Res* **20**: 5077-5082.
- Lui VW, Lau CP, Cheung CS, Ho K, Ng MH, Cheng SH, Hong B, Tsao SW, Tsang CM, Lei KI et al. 2010. An RNA-directed nucleoside anti-metabolite, 1-(3-C-ethynyl-beta-d-ribo-pentofuranosyl)cytosine (ECyd), elicits antitumor effect via TP53-induced Glycolysis and Apoptosis Regulator (TIGAR) downregulation. *Biochem Pharmacol* **79**: 1772-1780.
- Lui VW, Wong EY, Ho K, Ng PK, Lau CP, Tsui SK, Tsang CM, Tsao SW, Cheng SH, Ng MH et al. 2011. Inhibition of c-Met downregulates TIGAR expression and reduces NADPH production leading to cell death. *Oncogene* **30**: 1127-1134.
- Luo W, Hu H, Chang R, Zhong J, Knabel M, O'Meally R, Cole RN, Pandey A, Semenza GL. 2011. Pyruvate kinase M2 is a PHD3-stimulated coactivator for hypoxia-inducible factor 1. *Cell* **145**: 732-744.
- Lustig B, Jerchow B, Sachs M, Weiler S, Pietsch T, Karsten U, van de Wetering M, Clevers H, Schlag PM, Birchmeier W et al. 2002. Negative feedback loop of Wnt signaling through upregulation of conductin/axin2 in colorectal and liver tumors. *Molecular and cellular biology* **22**: 1184-1193.
- Lv L, Li D, Zhao D, Lin R, Chu Y, Zhang H, Zha Z, Liu Y, Li Z, Xu Y et al. 2011. Acetylation targets the M2 isoform of pyruvate kinase for degradation through chaperone-mediated autophagy and promotes tumor growth. *Molecular cell* **42**: 719-730.
- Ma J, Meng Y, Kwiatkowski DJ, Chen X, Peng H, Sun Q, Zha X, Wang F, Wang Y, Jing Y et al. 2010. Mammalian target of rapamycin regulates murine and human cell differentiation through STAT3/p63/Jagged/Notch cascade. *J Clin Invest* **120**: 103-114.
- MacDonald BT, Tamai K, He X. 2009. Wnt/beta-catenin signaling: components, mechanisms, and diseases. *Developmental cell* **17**: 9-26.
- Maclean KH, Dorsey FC, Cleveland JL, Kastan MB. 2008. Targeting lysosomal degradation induces p53-dependent cell death and prevents cancer in mouse models of lymphomagenesis (vol 118, pg 79, 2008). *J Clin Invest* **118**: 1584-1584.
- Maddocks OD, Berkers CR, Mason SM, Zheng L, Blyth K, Gottlieb E, Vousden KH. 2013. Serine starvation induces stress and p53-dependent metabolic remodelling in cancer cells. *Nature* **493**: 542-546.
- Maiuri MC, Galluzzi L, Morselli E, Kepp O, Malik SA, Kroemer G. 2010. Autophagy regulation by p53. *Current Opinion in Cell Biology* **22**: 181-185.
- Major MB, Camp ND, Berndt JD, Yi X, Goldenberg SJ, Hubbert C, Biechele TL, Gingras AC, Zheng N, Maccoss MJ et al. 2007. Wilms tumor suppressor WTX negatively regulates WNT/beta-catenin signaling. *Science* **316**: 1043-1046.
- Malhotra JD, Kaufman RJ. 2007. Endoplasmic reticulum stress and oxidative stress: a vicious cycle or a double-edged sword? *Antioxidants & redox signaling* **9**: 2277-2293.
- Malkin D, Li FP, Strong LC, Fraumeni JF, Nelson CE, Kim DH, Kassel J, Gryka MA, Bischoff FZ, Tainsky MA et al. 1990. Germ Line P53 Mutations in a Familial Syndrome of Breast-Cancer, Sarcomas, and Other Neoplasms. *Science* **250**: 1233-1238.
- Mamane Y, Petroulakis E, Rong L, Yoshida K, Ler LW, Sonenberg N. 2004. eIF4E--from translation to transformation. *Oncogene* **23**: 3172-3179.

- Mantovani F, Tocco F, Girardini J, Smith P, Gasco M, Lu X, Crook T, Del Sal G. 2007. The prolyl isomerase Pin1 orchestrates p53 acetylation and dissociation from the apoptosis inhibitor iASPP. *Nat Struct Mol Biol* **14**: 912-920.
- Mao B, Wu W, Davidson G, Marhold J, Li M, Mechler BM, Delius H, Hoppe D, Stanek P, Walter C et al. 2002. Kremen proteins are Dickkopf receptors that regulate Wnt/beta-catenin signalling. *Nature* **417**: 664-667.
- Mao J, Wang J, Liu B, Pan W, Farr GH, 3rd, Flynn C, Yuan H, Takada S, Kimelman D, Li L et al. 2001. Low-density lipoprotein receptor-related protein-5 binds to Axin and regulates the canonical Wnt signaling pathway. *Molecular cell* **7**: 801-809.
- Marcel V, Perrier S, Aoubala M, Ageorges S, Groves MJ, Diot A, Fernandes K, Tauro S, Bourdon JC. 2010. Delta160p53 is a novel N-terminal p53 isoform encoded by Delta133p53 transcript. *Febs Lett* **584**: 4463-4468.
- Marsin AS, Bertrand L, Rider MH, Deprez J, Beauloye C, Vincent MF, Van den Berghe G, Carling D, Hue L. 2000. Phosphorylation and activation of heart PFK-2 by AMPK has a role in the stimulation of glycolysis during ischaemia. *Curr Biol* **10**: 1247-1255.
- Martin K, Potten CS, Roberts SA, Kirkwood TB. 1998. Altered stem cell regeneration in irradiated intestinal crypts of senescent mice. *J Cell Sci* **111** (Pt 16): 2297-2303.
- Mashimo T, Watabe M, Hirota S, Hosobe S, Miura K, Tegtmeyer PJ, Rinker-Shaeffer CW, Watabe K. 1998. The expression of the KAI1 gene, a tumor metastasis suppressor, is directly activated by p53. *Proceedings of the National Academy of Sciences of the United States of America* **95**: 11307-11311.
- Massa L, Baltrusch S, Okar DA, Lange AJ, Lenzen S, Tiedge M. 2004. Interaction of 6-phosphofructo-2-kinase/fructose-2,6-bisphosphatase (PFK-2/FBPase-2) with glucokinase activates glucose phosphorylation and glucose metabolism in insulin-producing cells. *Diabetes* **53**: 1020-1029.
- Massion PP, Taflan PM, Jamshedur Rahman SM, Yildiz P, Shyr Y, Edgerton ME, Westfall MD, Roberts JR, Pietenpol JA, Carbone DP et al. 2003. Significance of p63 amplification and overexpression in lung cancer development and prognosis. *Cancer research* **63**: 7113-7121.
- Matoba S, Kang JG, Patino WD, Wragg A, Boehm M, Gavrilova O, Hurley PJ, Bunz F, Hwang PM. 2006. p53 regulates mitochondrial respiration. *Science* **312**: 1650-1653.
- Matsuoka S, Rotman G, Ogawa A, Shiloh Y, Tamai K, Elledge SJ. 2000. Ataxia telangiectasia-mutated phosphorylates Chk2 in vivo and in vitro. *Proceedings of the National Academy of Sciences of the United States of America* **97**: 10389-10394.
- Matthew EM, Hart LS, Astrinidis A, Navaraj A, Dolloff NG, Dicker DT, Henske EP, El-Deiry WS. 2009. The p53 target Plk2 interacts with TSC proteins impacting mTOR signaling, tumor growth and chemosensitivity under hypoxic conditions. *Cell cycle* **8**: 4168-4175.
- Maya R, Balass M, Kim ST, Shkedy D, Leal JFM, Shifman O, Moas M, Buschmann T, Ronai Z, Shiloh Y et al. 2001. ATM-dependent phosphorylation of Mdm2 on serine 395: role in p53 activation by DNA damage. *Genes & development* **15**: 1067-1077.
- Mazurek S. 2011. Pyruvate kinase type M2: a key regulator of the metabolic budget system in tumor cells. *Int J Biochem Cell Biol* **43**: 969-980.

- Melino G, De Laurenzi V, Vousden KH. 2002. p73: Friend or foe in tumorigenesis. *Nat Rev Cancer* **2**: 605-615.
- Melino G, Lu X, Gasco M, Crook T, Knight RA. 2003. Functional regulation of p73 and p63: development and cancer. *Trends Biochem Sci* **28**: 663-670.
- Menendez JA, Lupu R. 2007. Fatty acid synthase and the lipogenic phenotype in cancer pathogenesis. *Nat Rev Cancer* **7**: 763-777.
- Menon S, Yecies JL, Zhang HH, Howell JJ, Nicholatos J, Harputlugil E, Bronson RT, Kwiatkowski DJ, Manning BD. 2012. Chronic activation of mTOR complex 1 is sufficient to cause hepatocellular carcinoma in mice. *Sci Signal* **5**: ra24.
- Merritt AJ, Potten CS, Kemp CJ, Hickman JA, Balmain A, Lane DP, Hall PA. 1994. The role of p53 in spontaneous and radiation-induced apoptosis in the gastrointestinal tract of normal and p53-deficient mice. *Cancer research* **54**: 614-617.
- Metcalfe C, Klijavin NM, Ybarra R, de Sauvage FJ. 2014. Lgr5+ stem cells are indispensable for radiation-induced intestinal regeneration. *Cell stem cell* **14**: 149-159.
- Meulmeester E, Frenk R, Stad R, de Graaf P, Marine JC, Vousden KH, Jochemsen AG. 2003. Critical role for a central part of Mdm2 in the ubiquitylation of p53. *Molecular and cellular biology* **23**: 4929-4938.
- Miceli AP, Saporita AJ, Weber JD. 2012. Hypergrowth mTORC1 Signals Translationally Activate the ARF Tumor Suppressor Checkpoint. *Molecular and cellular biology* **32**: 348-364.
- Migliorini D, Denchi EL, Danovi D, Jochemsen A, Capillo M, Gobbi A, Helin K, Pelicci PG, Marine JC. 2002. Mdm4 (Mdmx) regulates p53-induced growth arrest and neuronal cell death during early embryonic mouse development. *Molecular and cellular biology* **22**: 5527-5538.
- Mills AA, Zheng B, Wang XJ, Vogel H, Roop DR, Bradley A. 1999. p63 is a p53 homologue required for limb and epidermal morphogenesis. *Nature* **398**: 708-713.
- Minchenko DO, Mykhalchenko VG, Tsuchihara K, Kanehara S, Yavorovsky OP, Zavgorodny IV, Paustovsky YO, Komisarenko SV, Esumi H, Minchenko OH. 2008. Alternative splice variants of rat 6-phosphofructo-2-kinase/fructose-2,6-bisphosphatase-4 mRNA. *Ukr Biokhim Zh (1999)* **80**: 66-73.
- Minchenko O, Opentanova I, Caro J. 2003. Hypoxic regulation of the 6-phosphofructo-2-kinase/fructose-2,6-bisphosphatase gene family (PFKFB-1-4) expression in vivo. *Febs Lett* **554**: 264-270.
- Minchenko O, Opentanova I, Minchenko D, Ogura T, Esumi H. 2004. Hypoxia induces transcription of 6-phosphofructo-2-kinase/fructose-2,6-bisphosphatase-4 gene via hypoxia-inducible factor-1 alpha activation. *Febs Lett* **576**: 14-20.
- Minchenko OH, Ogura T, Opentanova IL, Minchenko DO, Ochiai A, Caro J, Komisarenko SV, Esumi H. 2005. 6-Phosphofructo-2-kinase/fructose-2,6-bisphosphatase gene family overexpression in human lung tumor. *Ukr Biokhim Zh* **77**: 46-50.
- Miralpeix M, Katz NR, Bartrons R. 1990. Effects of vanadate on 6-phosphofructo 2-kinase activity and fructose 2,6-bisphosphate levels in cultured rat hepatocytes. *Cell Biochem Funct* **8**: 237-241.
- Miyashita T, Reed JC. 1995. Tumor-Suppressor P53 Is a Direct Transcriptional Activator of the Human Bax Gene. *Cell* **80**: 293-299.

- Mojena M, Bosca L, Hue L. 1985. Effect of glutamine on fructose 2,6-bisphosphate and on glucose metabolism in HeLa cells and in chick-embryo fibroblasts. *The Biochemical journal* **232**: 521-527.
- Molchadsky A, Shats I, Goldfinger N, Pevsner-Fischer M, Olson M, Rinon A, Tzahor E, Lozano G, Zipori D, Sarig R et al. 2008. p53 Plays a Role in Mesenchymal Differentiation Programs, in a Cell Fate Dependent Manner. *Plos One* **3**.
- Molenaar M, Roose J, Peterson J, Venanzi S, Clevers H, Destree O. 1998. Differential expression of the HMG box transcription factors XTcf-3 and XLef-1 during early xenopus development. *Mech Dev* **75**: 151-154.
- Moll UM, Slade N. 2004. p63 and p73: roles in development and tumor formation. *Molecular cancer research : MCR* **2**: 371-386.
- Momand J, Zambetti GP, Olson DC, George D, Levine AJ. 1992. The Mdm-2 Oncogene Product Forms a Complex with the P53 Protein and Inhibits P53-Mediated Transactivation. *Cell* **69**: 1237-1245.
- Montes de Oca Luna R, Wagner DS, Lozano G. 1995. Rescue of early embryonic lethality in mdm2-deficient mice by deletion of p53. *Nature* **378**: 203-206.
- Moon JS, Jin WJ, Kwak JH, Kim HJ, Yun MJ, Kim JW, Park SW, Kim KS. 2011. Androgen stimulates glycolysis for de novo lipid synthesis by increasing the activities of hexokinase 2 and 6-phosphofructo-2-kinase/fructose-2,6-bisphosphatase 2 in prostate cancer cells. *The Biochemical journal* **433**: 225-233.
- Mordier S, Deval C, Bechet D, Tassa A, Ferrara M. 2000. Leucine limitation induces autophagy and activation of lysosome-dependent proteolysis in C2C12 myotubes through a mammalian target of rapamycin-independent signaling pathway. *Journal of Biological Chemistry* **275**: 29900-29906.
- Morin PJ, Sparks AB, Korinek V, Barker N, Clevers H, Vogelstein B, Kinzler KW. 1997. Activation of beta-catenin-Tcf signaling in colon cancer by mutations in beta-catenin or APC. *Science* **275**: 1787-1790.
- Morselli E, Galluzzi L, Kepp O, Vicencio JM, Criollo A, Maiuri MC, Kroemer G. 2009. Anti- and pro-tumor functions of autophagy. *Bba-Mol Cell Res* **1793**: 1524-1532.
- Moser AR, Pitot HC, Dove WF. 1990. A dominant mutation that predisposes to multiple intestinal neoplasia in the mouse. *Science* **247**: 322-324.
- Muller FL, Liu Y, Van Remmen H. 2004. Complex III releases superoxide to both sides of the inner mitochondrial membrane. *The Journal of biological chemistry* **279**: 49064-49073.
- Muller PA, Vousden KH. 2013. p53 mutations in cancer. *Nature cell biology* **15**: 2-8.
- Mungamuri SK, Yang YH, Thor AD, Somasundaram K. 2006. Survival signaling by Notch1: Mammalian target of rapamycin (mTOR)-dependent inhibition of p53. *Cancer research* **66**: 4715-4724.
- Murphy MP. 2009. How mitochondria produce reactive oxygen species. *The Biochemical journal* **417**: 1-13.
- Murray-Zmijewski F, Lane DP, Bourdon JC. 2006. p53/p63/p73 isoforms: an orchestra of isoforms to harmonise cell differentiation and response to stress. *Cell death and differentiation* **13**: 962-972.
- Myant KB, Cammareri P, McGhee EJ, Ridgway RA, Huels DJ, Cordero JB, Schwitalla S, Kalna G, Ogg EL, Athineos D et al. 2013. ROS production and NF-kappaB activation triggered by RAC1 facilitate WNT-driven intestinal

- stem cell proliferation and colorectal cancer initiation. *Cell stem cell* **12**: 761-773.
- Nakano K, Vousden KH. 2001. PUMA, a novel proapoptotic gene, is induced by p53. *Molecular cell* **7**: 683-694.
- Narendra DP, Jin SM, Tanaka A, Suen DF, Gautier CA, Shen J, Cookson MR, Youle RJ. 2010. PINK1 is selectively stabilized on impaired mitochondria to activate Parkin. *PLoS Biol* **8**: e1000298.
- Navarro-Sabate A, Manzano A, Riera L, Rosa JL, Ventura F, Bartrons R. 2001. The human ubiquitous 6-phosphofructo-2-kinase/fructose-2,6-bisphosphatase gene (PFKFB3): promoter characterization and genomic structure. *Gene* **264**: 131-138.
- Negrini S, Gorgoulis VG, Halazonetis TD. 2010. Genomic instability--an evolving hallmark of cancer. *Nature reviews Molecular cell biology* **11**: 220-228.
- Nemoto S, Finkel T. 2002. Redox regulation of forkhead proteins through a p66shc-dependent signaling pathway. *Science* **295**: 2450-2452.
- Nevins JR. 2001. The Rb/E2F pathway and cancer. *Hum Mol Genet* **10**: 699-703.
- Ng SW, Yiu GK, Liu Y, Huang LW, Palnati M, Jun SH, Berkowitz RS, Mok SC. 2000. Analysis of p73 in human borderline and invasive ovarian tumor. *Oncogene* **19**: 1885-1890.
- Nioi P, Nguyen T. 2007. A mutation of Keap1 found in breast cancer impairs its ability to repress Nrf2 activity. *Biochemical and biophysical research communications* **362**: 816-821.
- Nissler K, Petermann H, Wenz I, Brox D. 1995. Fructose 2,6-bisphosphate metabolism in Ehrlich ascites tumour cells. *J Cancer Res Clin Oncol* **121**: 739-745.
- Noguchi T, Inoue H, Tanaka T. 1986. The M1- and M2-type isozymes of rat pyruvate kinase are produced from the same gene by alternative RNA splicing. *The Journal of biological chemistry* **261**: 13807-13812.
- Nowicki S, Gottlieb E. 2015. Oncometabolites: tailoring our genes. *FEBS J* **282**: 2796-2805.
- Nozell S, Wu Y, McNaughton K, Liu G, Willis A, Paik JC, Chen X. 2003. Characterization of p73 functional domains necessary for transactivation and growth suppression. *Oncogene* **22**: 4333-4347.
- Nusse R, Varmus HE. 1982. Many tumors induced by the mouse mammary tumor virus contain a provirus integrated in the same region of the host genome. *Cell* **31**: 99-109.
- Nusslein-Volhard C, Wieschaus E. 1980. Mutations affecting segment number and polarity in *Drosophila*. *Nature* **287**: 795-801.
- Obach M, Navarro-Sabate A, Caro J, Kong XG, Duran J, Gomez M, Perales JC, Ventura F, Rosa JL, Bartrons R. 2004. 6-phosphofructo-2-kinase (pfkfb3) gene promoter contains hypoxia-inducible factor-1 binding sites necessary for transactivation in response to hypoxia. *Journal of Biological Chemistry* **279**: 53562-53570.
- Oda E, Ohki R, Murasawa H, Nemoto J, Shibue T, Yamashita T, Tokino T, Taniguchi T, Tanaka N. 2000. Nora, a BH3-only member of the Bcl-2 family and candidate mediator of p53-induced apoptosis. *Science* **288**: 1053-1058.
- Offer H, Erez N, Zurer I, Tang X, Milyavsky M, Goldfinger N, Rotter V. 2002. The onset of p53-dependent DNA repair or apoptosis is determined by the level of accumulated damaged DNA. *Carcinogenesis* **23**: 1025-1032.

- Ogasawara MA, Zhang H. 2009. Redox regulation and its emerging roles in stem cells and stem-like cancer cells. *Antioxidants & redox signaling* **11**: 1107-1122.
- Ohta T, Iijima K, Miyamoto M, Nakahara I, Tanaka H, Ohtsuji M, Suzuki T, Kobayashi A, Yokota J, Sakiyama T et al. 2008. Loss of Keap1 function activates Nrf2 and provides advantages for lung cancer cell growth. *Cancer research* **68**: 1303-1309.
- Okar DA, Manzano A, Navarro-Sabate A, Riera L, Bartrons R, Lange AJ. 2001. PFK-2/FBPase-2: maker and breaker of the essential biofactor fructose-2,6-bisphosphate. *Trends Biochem Sci* **26**: 30-35.
- Okorokov AL, Milner J. 1999. An ATP/ADP-dependent molecular switch regulates the stability of p53-DNA complexes. *Molecular and cellular biology* **19**: 7501-7510.
- Oliner JD, Pietenpol JA, Thiagalingam S, Gvuris J, Kinzler KW, Vogelstein B. 1993. Oncoprotein Mdm2 Conceals the Activation Domain of Tumor Suppressor-P53. *Nature* **362**: 857-860.
- Ooi A, Wong JC, Petillo D, Roossien D, Perrier-Trudova V, Whitten D, Min BW, Tan MH, Zhang Z, Yang XJ et al. 2011. An antioxidant response phenotype shared between hereditary and sporadic type 2 papillary renal cell carcinoma. *Cancer Cell* **20**: 511-523.
- Osada M, Nagakawa Y, Park HL, Yamashita K, Wu G, Kim MS, Fomenkov A, Trink B, Sidransky D. 2005a. p63-specific activation of the BPAG-1e promoter. *The Journal of investigative dermatology* **125**: 52-60.
- Osada M, Ohba M, Kawahara C, Ishioka C, Kanamaru R, Katoh I, Ikawa Y, Nimura Y, Nakagawara A, Obinata M et al. 1998. Cloning and functional analysis of human p51, which structurally and functionally resembles p53. *Nat Med* **4**: 839-843.
- Osada M, Park HL, Nagakawa Y, Yamashita K, Fomenkov A, Kim MS, Wu G, Nomoto S, Trink B, Sidransky D. 2005b. Differential recognition of response elements determines target gene specificity for p53 and p63. *Molecular and cellular biology* **25**: 6077-6089.
- Ostman A, Frijhoff J, Sandin A, Bohmer FD. 2011. Regulation of protein tyrosine phosphatases by reversible oxidation. *J Biochem* **150**: 345-356.
- Palmero I, Pantoja C, Serrano M. 1998. p19(ARF) links the tumour suppressor p53 to Ras. *Nature* **395**: 125-126.
- Pan Y, Chen JD. 2003. MDM2 promotes ubiquitination and degradation of MDMX. *Molecular and cellular biology* **23**: 5113-5121.
- Papandreou I, Cairns RA, Fontana L, Lim AL, Denko NC. 2006. HIF-1 mediates adaptation to hypoxia by actively downregulating mitochondrial oxygen consumption. *Cell metabolism* **3**: 187-197.
- Parant J, Chavez-Reyes A, Little NA, Yan W, Reinke V, Jochemsen AG, Lozano G. 2001. Rescue of embryonic lethality in Mdm4-null mice by loss of Trp53 suggests a nonoverlapping pathway with MDM2 to regulate p53. *Nat Genet* **29**: 92-95.
- Parma P, Radi O, Vidal V, Chaboissier MC, Dellambra E, Valentini S, Guerra L, Schedl A, Camerino G. 2006. R-spondin1 is essential in sex determination, skin differentiation and malignancy. *Nat Genet* **38**: 1304-1309.
- Parsa R, Yang A, McKeon F, Green H. 1999. Association of p63 with proliferative potential in normal and neoplastic human keratinocytes. *The Journal of investigative dermatology* **113**: 1099-1105.

- Pate KT, Stringari C, Sprowl-Tanio S, Wang K, TeSlaa T, Hoverter NP, McQuade MM, Garner C, Digman MA, Teitell MA et al. 2014. Wnt signaling directs a metabolic program of glycolysis and angiogenesis in colon cancer. *The EMBO journal* **33**: 1454-1473.
- Patel BP, Rawal UM, Dave TK, Rawal RM, Shukla SN, Shah PM, Patel PS. 2007. Lipid peroxidation, total antioxidant status, and total thiol levels predict overall survival in patients with oral squamous cell carcinoma. *Integr Cancer Ther* **6**: 365-372.
- Patra KC, Hay N. 2014. The pentose phosphate pathway and cancer. *Trends Biochem Sci* **39**: 347-354.
- Payne DM, Rossomando AJ, Martino P, Erickson AK, Her JH, Shabanowitz J, Hunt DF, Weber MJ, Sturgill TW. 1991. Identification of the regulatory phosphorylation sites in pp42/mitogen-activated protein kinase (MAP kinase). *The EMBO journal* **10**: 885-892.
- Peifer M, McCrea PD, Green KJ, Wieschaus E, Gumbiner BM. 1992. The vertebrate adhesive junction proteins beta-catenin and plakoglobin and the Drosophila segment polarity gene armadillo form a multigene family with similar properties. *J Cell Biol* **118**: 681-691.
- Pelicano H, Xu RH, Du M, Feng L, Sasaki R, Carew JS, Hu Y, Ramdas L, Hu L, Keating MJ et al. 2006. Mitochondrial respiration defects in cancer cells cause activation of Akt survival pathway through a redox-mediated mechanism. *J Cell Biol* **175**: 913-923.
- Pena-Rico MA, Calvo-Vidal MN, Villalonga-Planells R, Martinez-Soler F, Gimenez-Bonafe P, Navarro-Sabate A, Tortosa A, Bartrons R, Manzano A. 2011. TP53 induced glycolysis and apoptosis regulator (TIGAR) knockdown results in radiosensitization of glioma cells. *Radiotherapy and oncology : journal of the European Society for Therapeutic Radiology and Oncology* **101**: 132-139.
- Petitjean A, Mathe E, Kato S, Ishioka C, Tavtigian SV, Hainaut P, Olivier M. 2007. Impact of mutant p53 functional properties on TP53 mutation patterns and tumor phenotype: Lessons from recent developments in the IARC TP53 database. *Hum Mutat* **28**: 622-629.
- Pilkis SJ, Claus TH, Kurland IJ, Lange AJ. 1995. 6-Phosphofructo-2-kinase/fructose-2,6-bisphosphatase: a metabolic signaling enzyme. *Annu Rev Biochem* **64**: 799-835.
- Pinson KI, Brennan J, Monkley S, Avery BJ, Skarnes WC. 2000. An LDL-receptor-related protein mediates Wnt signalling in mice. *Nature* **407**: 535-538.
- Piruat JI, Pintado CO, Ortega-Saenz P, Roche M, Lopez-Barneo J. 2004. The mitochondrial SDHD gene is required for early embryogenesis, and its partial deficiency results in persistent carotid body glomus cell activation with full responsiveness to hypoxia. *Molecular and cellular biology* **24**: 10933-10940.
- Pomerantz J, Schreiber-Agus N, Liegeois NJ, Silverman A, Alland L, Chin L, Potes J, Chen K, Orlow I, Lee HW et al. 1998. The Ink4a tumor suppressor gene product, p19(Arf), interacts with MDM2 and neutralizes MDM2's inhibition of p53. *Cell* **92**: 713-723.
- Porasuphatana S, Tsai P, Rosen GM. 2003. The generation of free radicals by nitric oxide synthase. *Comparative biochemistry and physiology Toxicology & pharmacology : CBP* **134**: 281-289.

- Port F, Kuster M, Herr P, Furger E, Banziger C, Hausmann G, Basler K. 2008. Wingless secretion promotes and requires retromer-dependent cycling of Wntless. *Nature cell biology* **10**: 178-185.
- Potten CS, Grant HK. 1998. The relationship between ionizing radiation-induced apoptosis and stem cells in the small and large intestine. *Br J Cancer* **78**: 993-1003.
- Poyurovsky MV, Priest C, Kentsis A, Borden KLB, Pan ZQ, Pavletich N, Prives C. 2007. The Mdm2 RING domain C-terminus is required for supramolecular assembly and ubiquitin ligase activity. *Embo Journal* **26**: 90-101.
- Pozniak CD, Radinovic S, Yang A, McKeon F, Kaplan DR, Miller FD. 2000. An anti-apoptotic role for the p53 family member, p73, during developmental neuron death. *Science* **289**: 304-306.
- Preston-Martin S, Pike MC, Ross RK, Jones PA, Henderson BE. 1990. Increased cell division as a cause of human cancer. *Cancer research* **50**: 7415-7421.
- Prestwich TC, Macdougald OA. 2007. Wnt/beta-catenin signaling in adipogenesis and metabolism. *Curr Opin Cell Biol* **19**: 612-617.
- Puente XS, Velasco G, Gutierrez-Fernandez A, Bertranpetit J, King MC, Lopez-Otin C. 2006. Comparative analysis of cancer genes in the human and chimpanzee genomes. *BMC Genomics* **7**: 15.
- Ramos JW. 2008. The regulation of extracellular signal-regulated kinase (ERK) in mammalian cells. *Int J Biochem Cell Biol* **40**: 2707-2719.
- Rao RK, Clayton LW. 2002. Regulation of protein phosphatase 2A by hydrogen peroxide and glutathionylation. *Biochemical and biophysical research communications* **293**: 610-616.
- Reid MA, Wang WI, Rosales KR, Welliver MX, Pan M, Kong M. 2013. The B55alpha subunit of PP2A drives a p53-dependent metabolic adaptation to glutamine deprivation. *Molecular cell* **50**: 200-211.
- Reya T, Clevers H. 2005. Wnt signalling in stem cells and cancer. *Nature* **434**: 843-850.
- Rider MH, Bertrand L, Vertommen D, Michels PA, Rousseau GG, Hue L. 2004. 6-phosphofructo-2-kinase/fructose-2,6-bisphosphatase: head-to-head with a bifunctional enzyme that controls glycolysis. *The Biochemical journal* **381**: 561-579.
- Rijsewijk F, Schuermann M, Wagenaar E, Parren P, Weigel D, Nusse R. 1987. The *Drosophila* homolog of the mouse mammary oncogene *int-1* is identical to the segment polarity gene *wingless*. *Cell* **50**: 649-657.
- Rivera A, Maxwell SA. 2005. The p53-induced gene-6 (proline oxidase) mediates apoptosis through a calcineurin-dependent pathway. *Journal of Biological Chemistry* **280**: 29346-29354.
- Robey RB, Hay N. 2009. Is Akt the "Warburg kinase"?-Akt-energy metabolism interactions and oncogenesis. *Semin Cancer Biol* **19**: 25-31.
- Rodriguez MS, Desterro JMP, Lain S, Lane DP, Hay RT. 2000. Multiple C-terminal lysine residues target p53 for ubiquitin-proteasome-mediated degradation. *Molecular and cellular biology* **20**: 8458-8467.
- Romano RA, Ortt K, Birkaya B, Smalley K, Sinha S. 2009. An active role of the DeltaN isoform of p63 in regulating basal keratin genes K5 and K14 and directing epidermal cell fate. *Plos One* **4**: e5623.
- Roose J, Molenaar M, Peterson J, Hurenkamp J, Brantjes H, Moerer P, van de Wetering M, Destree O, Clevers H. 1998. The *Xenopus* Wnt effector XTcf-3 interacts with Groucho-related transcriptional repressors. *Nature* **395**: 608-612.

- Ros S, Santos CR, Moco S, Baenke F, Kelly G, Howell M, Zamboni N, Schulze A. 2012. Functional metabolic screen identifies 6-phosphofructo-2-kinase/fructose-2,6-bisphosphatase 4 as an important regulator of prostate cancer cell survival. *Cancer Discov* **2**: 328-343.
- Ros S, Schulze A. 2013. Balancing glycolytic flux: the role of 6-phosphofructo-2-kinase/fructose 2,6-bisphosphatases in cancer metabolism. *Cancer & metabolism* **1**: 8.
- Rosenbluth JM, Mays DJ, Jiang A, Shyr Y, Pietenpol JA. 2011. Differential regulation of the p73 cistrome by mammalian target of rapamycin reveals transcriptional programs of mesenchymal differentiation and tumorigenesis. *Proceedings of the National Academy of Sciences of the United States of America* **108**: 2076-2081.
- Rosenbluth JM, Mays DJ, Pino MF, Tang LJ, Pietenpol JA. 2008. A gene signature-based approach identifies mTOR as a regulator of p73. *Molecular and cellular biology* **28**: 5951-5964.
- Rosenbluth JM, Pietenpol JA. 2009. mTOR regulates autophagy-associated genes downstream of p73. *Autophagy* **5**: 114-116.
- Roth M, Chen WY. 2014. Sorting out functions of sirtuins in cancer. *Oncogene* **33**: 1609-1620.
- Rubinfeld B, Albert I, Porfiri E, Munemitsu S, Polakis P. 1997. Loss of beta-catenin regulation by the APC tumor suppressor protein correlates with loss of structure due to common somatic mutations of the gene. *Cancer research* **57**: 4624-4630.
- Rubinsztein DC, Codogno P, Levine B. 2012. Autophagy modulation as a potential therapeutic target for diverse diseases. *Nature Reviews Drug Discovery* **11**: 709-U784.
- Rufini A, Niklison-Chirou MV, Inoue S, Tomasini R, Harris IS, Marino A, Federici M, Dinsdale D, Knight RA, Melino G et al. 2012. TAp73 depletion accelerates aging through metabolic dysregulation. *Genes & development* **26**: 2009-2014.
- Ruiz-Lozano P, Hixon ML, Wagner MW, Flores AI, Ikawa S, Baldwin AS, Chien KR, Gualberto A. 1999. p53 is a transcriptional activator of the muscle-specific phosphoglycerate mutase gene and contributes in vivo to the control of its cardiac expression. *Cell Growth & Differentiation* **10**: 295-306.
- Rulifson IC, Karnik SK, Heiser PW, ten Berge D, Chen H, Gu X, Taketo MM, Nusse R, Hebrok M, Kim SK. 2007. Wnt signaling regulates pancreatic beta cell proliferation. *Proceedings of the National Academy of Sciences of the United States of America* **104**: 6247-6252.
- Sabbisetti V, Di Napoli A, Seeley A, Amato AM, O'Regan E, Ghebremichael M, Loda M, Signoretti S. 2009. p63 promotes cell survival through fatty acid synthase. *Plos One* **4**: e5877.
- Sabharwal SS, Schumacker PT. 2014. Mitochondrial ROS in cancer: initiators, amplifiers or an Achilles' heel? *Nat Rev Cancer* **14**: 709-721.
- Saifudeen Z, Diavolitsis V, Stefkova J, Dipp S, Fan H, El-Dahr SS. 2005. Spatiotemporal switch from DeltaNp73 to TAp73 isoforms during nephrogenesis: impact on differentiation gene expression. *The Journal of biological chemistry* **280**: 23094-23102.
- Sakata J, Abe Y, Uyeda K. 1991. Molecular cloning of the DNA and expression and characterization of rat testes fructose-6-phosphate,2-kinase:fructose-2,6-bisphosphatase. *The Journal of biological chemistry* **266**: 15764-15770.

- Salmeen A, Andersen JN, Myers MP, Meng TC, Hinks JA, Tonks NK, Barford D. 2003. Redox regulation of protein tyrosine phosphatase 1B involves a sulphenyl-amide intermediate. *Nature* **423**: 769-773.
- Samuels Y, Diaz LA, Jr., Schmidt-Kittler O, Cummins JM, Delong L, Cheong I, Rago C, Huso DL, Lengauer C, Kinzler KW et al. 2005. Mutant PIK3CA promotes cell growth and invasion of human cancer cells. *Cancer Cell* **7**: 561-573.
- Samuels Y, Wang Z, Bardelli A, Silliman N, Ptak J, Szabo S, Yan H, Gazdar A, Powell SM, Riggins GJ et al. 2004. High frequency of mutations of the PIK3CA gene in human cancers. *Science* **304**: 554.
- Sansom OJ, Meniel VS, Muncan V, Pheese TJ, Wilkins JA, Reed KR, Vass JK, Athineos D, Clevers H, Clarke AR. 2007. Myc deletion rescues Apc deficiency in the small intestine. *Nature* **446**: 676-679.
- Sansom OJ, Reed KR, Hayes AJ, Ireland H, Brinkmann H, Newton IP, Batlle E, Simon-Assmann P, Clevers H, Nathke IS et al. 2004. Loss of Apc in vivo immediately perturbs Wnt signaling, differentiation, and migration. *Genes & development* **18**: 1385-1390.
- Santos CR, Schulze A. 2012. Lipid metabolism in cancer. *FEBS J* **279**: 2610-2623.
- Sanz-Moreno V, Gadea G, Ahn J, Paterson H, Marra P, Pinner S, Sahai E, Marshall CJ. 2008. Rac activation and inactivation control plasticity of tumor cell movement. *Cell* **135**: 510-523.
- Sasaki Y, Naishiro Y, Oshima Y, Imai K, Nakamura Y, Tokino T. 2005. Identification of pigment epithelium-derived factor as a direct target of the p53 family member genes. *Oncogene* **24**: 5131-5136.
- Sato T, van Es JH, Snippert HJ, Stange DE, Vries RG, van den Born M, Barker N, Shroyer NF, van de Wetering M, Clevers H. 2011. Paneth cells constitute the niche for Lgr5 stem cells in intestinal crypts. *Nature* **469**: 415-418.
- Sato T, Vries RG, Snippert HJ, van de Wetering M, Barker N, Stange DE, van Es JH, Abo A, Kujala P, Peters PJ et al. 2009. Single Lgr5 stem cells build crypt-villus structures in vitro without a mesenchymal niche. *Nature* **459**: 262-265.
- Savic D, Ye H, Aneas I, Park SY, Bell GI, Nobrega MA. 2011. Alterations in TCF7L2 expression define its role as a key regulator of glucose metabolism. *Genome Res* **21**: 1417-1425.
- Sayan BS, Sayan AE, Yang AL, Aqeilan RI, Candi E, Cohen GM, Knight RA, Croce CM, Melino G. 2007. Cleavage of the transactivation-inhibitory domain of p63 by caspases enhances apoptosis. *Proceedings of the National Academy of Sciences of the United States of America* **104**: 10871-10876.
- Schinner S, Ulgen F, Papewalis C, Schott M, Woelk A, Vidal-Puig A, Scherbaum WA. 2008. Regulation of insulin secretion, glucokinase gene transcription and beta cell proliferation by adipocyte-derived Wnt signalling molecules. *Diabetologia* **51**: 147-154.
- Schmale H, Bamberger C. 1997. A novel protein with strong homology to the tumor suppressor p53. *Oncogene* **15**: 1363-1367.
- Schmidt HH, Walter U. 1994. NO at work. *Cell* **78**: 919-925.
- Schneider J, Neu K, Grimm H, Velcovsky HG, Weisse G, Eigenbrodt E. 2002. Tumor M2-pyruvate kinase in lung cancer patients: immunohistochemical detection and disease monitoring. *Anticancer Res* **22**: 311-318.

- Schwartzenberg-Bar-Yoseph F, Armoni M, Karnieli E. 2004. The tumor suppressor p53 down-regulates glucose transporters GLUT1 and GLUT4 gene expression. *Cancer research* **64**: 2627-2633.
- Sdek P, Ying HQ, Zheng HW, Margulis A, Tang XR, Tian K, Xiao ZXJ. 2004. The central acidic domain of MDM2 is critical in inhibition of retinoblastoma-mediated suppression of E2F and cell growth. *Journal of Biological Chemistry* **279**: 53317-53322.
- Seifert JR, Mlodzik M. 2007. Frizzled/PCP signalling: a conserved mechanism regulating cell polarity and directed motility. *Nat Rev Genet* **8**: 126-138.
- Semenov M, Tamai K, He X. 2005. SOST is a ligand for LRP5/LRP6 and a Wnt signaling inhibitor. *The Journal of biological chemistry* **280**: 26770-26775.
- Semenov MV, Tamai K, Brott BK, Kuhl M, Sokol S, He X. 2001. Head inducer Dickkopf-1 is a ligand for Wnt coreceptor LRP6. *Curr Biol* **11**: 951-961.
- Semenza GL. 2002. HIF-1 and tumor progression: pathophysiology and therapeutics. *Trends Mol Med* **8**: S62-67.
- . 2010. HIF-1: upstream and downstream of cancer metabolism. *Curr Opin Genet Dev* **20**: 51-56.
- Sena LA, Chandel NS. 2012. Physiological roles of mitochondrial reactive oxygen species. *Molecular cell* **48**: 158-167.
- Senoo M, Pinto F, Crum CP, McKeon F. 2007. p63 is essential for the proliferative potential of stem cells in stratified epithelia. *Cell* **129**: 523-536.
- Seo M, Kim JD, Neau D, Sehgal I, Lee YH. 2011. Structure-based development of small molecule PFKFB3 inhibitors: a framework for potential cancer therapeutic agents targeting the Warburg effect. *Plos One* **6**: e24179.
- Serber Z, Lai HC, Yang A, Ou HD, Sigal MS, Kelly AE, Darimont BD, Duijf PH, Van Bokhoven H, McKeon F et al. 2002. A C-terminal inhibitory domain controls the activity of p63 by an intramolecular mechanism. *Molecular and cellular biology* **22**: 8601-8611.
- Serrano M, Lin AW, McCurrach ME, Beach D, Lowe SW. 1997. Oncogenic ras provokes premature cell senescence associated with accumulation of p53 and p16(INK4a). *Cell* **88**: 593-602.
- Sethi JK, Vidal-Puig A. 2010. Wnt signalling and the control of cellular metabolism. *The Biochemical journal* **427**: 1-17.
- Shackelford DB, Shaw RJ. 2009. The LKB1-AMPK pathway: metabolism and growth control in tumour suppression. *Nat Rev Cancer* **9**: 563-575.
- Shaul YD, Seger R. 2007. The MEK/ERK cascade: from signaling specificity to diverse functions. *Biochimica et biophysica acta* **1773**: 1213-1226.
- Shaulsky G, Goldfinger N, Ben-Ze'ev A, Rotter V. 1990. Nuclear accumulation of p53 protein is mediated by several nuclear localization signals and plays a role in tumorigenesis. *Molecular and cellular biology* **10**: 6565-6577.
- Shaw RJ, Cantley LC. 2006. Ras, PI(3)K and mTOR signalling controls tumour cell growth. *Nature* **441**: 424-430.
- Sherwood V. 2015. WNT signaling: an emerging mediator of cancer cell metabolism? *Molecular and cellular biology* **35**: 2-10.
- Shibata T, Kokubu A, Gotoh M, Ojima H, Ohta T, Yamamoto M, Hirohashi S. 2008a. Genetic alteration of Keap1 confers constitutive Nrf2 activation and resistance to chemotherapy in gallbladder cancer. *Gastroenterology* **135**: 1358-1368, 1368 e1351-1354.
- Shibata T, Ohta T, Tong KI, Kokubu A, Odogawa R, Tsuta K, Asamura H, Yamamoto M, Hirohashi S. 2008b. Cancer related mutations in NRF2 impair its recognition by Keap1-Cul3 E3 ligase and promote malignancy.

Proceedings of the National Academy of Sciences of the United States of America **105**: 13568-13573.

- Shieh SY, Ahn J, Tamai K, Taya Y, Prives C. 2000. The human homologs of checkpoint kinases Chk1 and Cds1 (Chk2) phosphorylate p53 at multiple DNA damage-inducible sites. *Genes & development* **14**: 289-300.
- Shinozaki T, Nota A, Taya Y, Okamoto K. 2003. Functional role of Mdm2 phosphorylation by ATR in attenuation of p53 nuclear export. *Oncogene* **22**: 8870-8880.
- Shloush J, Vlassov JE, Engson I, Duan SL, Saridakis V, Dhe-Paganon S, Raught B, Sheng Y, Arrowsmith CH. 2011. Structural and Functional Comparison of the RING Domains of Two p53 E3 Ligases, Mdm2 and Pirh2. *Journal of Biological Chemistry* **286**: 4796-4808.
- Shu L, Sauter NS, Schulthess FT, Matveyenko AV, Oberholzer J, Maedler K. 2008. Transcription factor 7-like 2 regulates beta-cell survival and function in human pancreatic islets. *Diabetes* **57**: 645-653.
- Siliciano JD, Canman CE, Taya Y, Sakaguchi K, Appella E, Kastan MB. 1997. DNA damage induces phosphorylation of the amino terminus of p53. *Genes & development* **11**: 3471-3481.
- Singh A, Misra V, Thimmulappa RK, Lee H, Ames S, Hoque MO, Herman JG, Baylin SB, Sidransky D, Gabrielson E et al. 2006. Dysfunctional KEAP1-NRF2 interaction in non-small-cell lung cancer. *PLoS Med* **3**: e420.
- Sinha S, Ghildiyal R, Mehta VS, Sen E. 2013. ATM-NFkappaB axis-driven TIGAR regulates sensitivity of glioma cells to radiomimetics in the presence of TNFalpha. *Cell death & disease* **4**: e615.
- Solis LM, Behrens C, Dong W, Suraokar M, Ozburn NC, Moran CA, Corvalan AH, Biswal S, Swisher SG, Bekele BN et al. 2010. Nrf2 and Keap1 abnormalities in non-small cell lung carcinoma and association with clinicopathologic features. *Clin Cancer Res* **16**: 3743-3753.
- Soussi T, Lozano G. 2005. p53 mutation heterogeneity in cancer. *Biochemical and biophysical research communications* **331**: 834-842.
- Sporn MB, Liby KT. 2012. NRF2 and cancer: the good, the bad and the importance of context. *Nat Rev Cancer* **12**: 564-571.
- Stadeli R, Hoffmans R, Basler K. 2006. Transcription under the control of nuclear Arm/beta-catenin. *Curr Biol* **16**: R378-385.
- Stanton RC. 2012. Glucose-6-phosphate dehydrogenase, NADPH, and cell survival. *IUBMB Life* **64**: 362-369.
- Straub WE, Weber TA, Schafer B, Candi E, Durst F, Ou HD, Rajalingam K, Melino G, Dotsch V. 2010. The C-terminus of p63 contains multiple regulatory elements with different functions. *Cell death & disease* **1**: e5.
- Su X, Gi YJ, Chakravarti D, Chan IL, Zhang A, Xia X, Tsai KY, Flores ER. 2012. TAp63 is a master transcriptional regulator of lipid and glucose metabolism. *Cell metabolism* **16**: 511-525.
- Su X, Paris M, Gi YJ, Tsai KY, Cho MS, Lin YL, Biernaskie JA, Sinha S, Prives C, Pevny LH et al. 2009. TAp63 prevents premature aging by promoting adult stem cell maintenance. *Cell stem cell* **5**: 64-75.
- Subbaramaiah K, Altorki N, Chung WJ, Mestre JR, Sampat A, Dannenberg AJ. 1999. Inhibition of cyclooxygenase-2 gene expression by p53. *Journal of Biological Chemistry* **274**: 10911-10915.
- Sudarshan S, Sourbier C, Kong HS, Block K, Valera Romero VA, Yang Y, Galindo C, Mollapour M, Scroggins B, Goode N et al. 2009. Fumarate hydratase deficiency in renal cancer induces glycolytic addiction and hypoxia-inducible

- transcription factor 1alpha stabilization by glucose-dependent generation of reactive oxygen species. *Molecular and cellular biology* **29**: 4080-4090.
- Suh EK, Yang A, Kettenbach A, Bamberger C, Michaelis AH, Zhu Z, Elvin JA, Bronson RT, Crum CP, McKeon F. 2006. p63 protects the female germ line during meiotic arrest. *Nature* **444**: 624-628.
- Sullivan LB, Chandel NS. 2014. Mitochondrial metabolism in TCA cycle mutant cancer cells. *Cell cycle* **13**: 347-348.
- Sullivan LB, Martinez-Garcia E, Nguyen H, Mullen AR, Dufour E, Sudarshan S, Licht JD, Deberardinis RJ, Chandel NS. 2013. The proto-oncometabolite fumarate binds glutathione to amplify ROS-dependent signaling. *Molecular cell* **51**: 236-248.
- Sun M, Li M, Huang Q, Han F, Gu JH, Xie J, Han R, Qin ZH, Zhou Z. 2015. Ischemia/reperfusion-induced upregulation of TIGAR in brain is mediated by SP1 and modulated by ROS and hormones involved in glucose metabolism. *Neurochem Int* **80**: 99-109.
- Sundaresan M, Yu ZX, Ferrans VJ, Irani K, Finkel T. 1995. Requirement for generation of H₂O₂ for platelet-derived growth factor signal transduction. *Science* **270**: 296-299.
- Suzuki S, Tanaka T, Poyurovsky MV, Nagano H, Mayama T, Ohkubo S, Lokshin M, Hosokawa H, Nakayama T, Suzuki Y et al. 2010. Phosphate-activated glutaminase (GLS2), a p53-inducible regulator of glutamine metabolism and reactive oxygen species. *Proceedings of the National Academy of Sciences of the United States of America* **107**: 7461-7466.
- Tahir SA, Yang G, Goltsov A, Song KD, Ren C, Wang J, Chang W, Thompson TC. 2013. Caveolin-1-LRP6 signaling module stimulates aerobic glycolysis in prostate cancer. *Cancer research* **73**: 1900-1911.
- Takada R, Satomi Y, Kurata T, Ueno N, Norioka S, Kondoh H, Takao T, Takada S. 2006. Monounsaturated fatty acid modification of Wnt protein: its role in Wnt secretion. *Developmental cell* **11**: 791-801.
- Tamai K, Zeng X, Liu C, Zhang X, Harada Y, Chang Z, He X. 2004. A mechanism for Wnt coreceptor activation. *Molecular cell* **13**: 149-156.
- Tan X, Apte U, Micsenyi A, Kotsagrelis E, Luo JH, Ranganathan S, Monga DK, Bell A, Michalopoulos GK, Monga SP. 2005. Epidermal growth factor receptor: a novel target of the Wnt/beta-catenin pathway in liver. *Gastroenterology* **129**: 285-302.
- Tanaka K, Kitagawa Y, Kadowaki T. 2002. Drosophila segment polarity gene product porcupine stimulates the posttranslational N-glycosylation of wingless in the endoplasmic reticulum. *The Journal of biological chemistry* **277**: 12816-12823.
- Tang Y, Zhao WH, Chen Y, Zhao YM, Gu W. 2008. Acetylation is indispensable for p53 activation. *Cell* **133**: 612-626.
- Tanimura S, Ohtsuka S, Mitsui K, Shirouzu K, Yoshimura A, Ohtsubo M. 1999. MDM2 interacts with MDMX through their RING finger domains. *Febs Lett* **447**: 5-9.
- Tello D, Balsa E, Acosta-Iborra B, Fuertes-Yebra E, Elorza A, Ordonez A, Corral-Escariz M, Soro I, Lopez-Bernardo E, Perales-Clemente E et al. 2011. Induction of the mitochondrial NDUFA4L2 protein by HIF-1alpha decreases oxygen consumption by inhibiting Complex I activity. *Cell metabolism* **14**: 768-779.

- Teodoro JG, Parker AE, Zhu XC, Green MR. 2006. p53-mediated inhibition of angiogenesis through up-regulation of a collagen prolyl hydroxylase. *Science* **313**: 968-971.
- Tetsu O, McCormick F. 1999. Beta-catenin regulates expression of cyclin D1 in colon carcinoma cells. *Nature* **398**: 422-426.
- Thompson CB. 2014. Wnt meets Warburg: another piece in the puzzle? *The EMBO journal* **33**: 1420-1422.
- Tibbetts RS, Brumbaugh KM, Williams JM, Sarkaria JN, Cliby WA, Shieh SY, Taya Y, Prives C, Abraham RT. 1999. A role for ATR in the DNA damage-induced phosphorylation of p53. *Genes & development* **13**: 152-157.
- Tomasini R, Tsuchihara K, Wilhelm M, Fujitani M, Rufini A, Cheung CC, Khan F, Itie-Youten A, Wakeham A, Tsao MS et al. 2008. TAp73 knockout shows genomic instability with infertility and tumor suppressor functions. *Genes & development* **22**: 2677-2691.
- Tominaga K, Kawahara T, Sano T, Toida K, Kuwano Y, Sasaki H, Kawai T, Teshima-Kondo S, Rokutan K. 2007. Evidence for cancer-associated expression of NADPH oxidase 1 (Nox1)-based oxidase system in the human stomach. *Free Radic Biol Med* **43**: 1627-1638.
- Toomes C, Bottomley HM, Jackson RM, Towns KV, Scott S, Mackey DA, Craig JE, Jiang L, Yang Z, Trembath R et al. 2004. Mutations in LRP5 or FZD4 underlie the common familial exudative vitreoretinopathy locus on chromosome 11q. *Am J Hum Genet* **74**: 721-730.
- Trachootham D, Alexandre J, Huang P. 2009. Targeting cancer cells by ROS-mediated mechanisms: a radical therapeutic approach? *Nat Rev Drug Discov* **8**: 579-591.
- Trachootham D, Zhou Y, Zhang H, Demizu Y, Chen Z, Pelicano H, Chiao PJ, Achanta G, Arlinghaus RB, Liu J et al. 2006. Selective killing of oncogenically transformed cells through a ROS-mediated mechanism by beta-phenylethyl isothiocyanate. *Cancer Cell* **10**: 241-252.
- Tsao SM, Yin MC, Liu WH. 2007. Oxidant stress and B vitamins status in patients with non-small cell lung cancer. *Nutr Cancer* **59**: 8-13.
- Tseng YH, Butte AJ, Kokkotou E, Yechoor VK, Taniguchi CM, Kriauciunas KM, Cypess AM, Niinobe M, Yoshikawa K, Patti ME et al. 2005. Prediction of preadipocyte differentiation by gene expression reveals role of insulin receptor substrates and necdin. *Nature cell biology* **7**: 601-611.
- Tsuji Y. 2005. JunD activates transcription of the human ferritin H gene through an antioxidant response element during oxidative stress. *Oncogene* **24**: 7567-7578.
- Tsukamoto H, She H, Hazra S, Cheng J, Wang J. 2008. Fat paradox of steatohepatitis. *J Gastroenterol Hepatol* **23 Suppl 1**: S104-107.
- Turcan S, Rohle D, Goenka A, Walsh LA, Fang F, Yilmaz E, Campos C, Fabius AW, Lu C, Ward PS et al. 2012. IDH1 mutation is sufficient to establish the glioma hypermethylator phenotype. *Nature* **483**: 479-483.
- Ueyama T, Geiszt M, Leto TL. 2006. Involvement of Rac1 in activation of multicomponent Nox1- and Nox3-based NADPH oxidases. *Molecular and cellular biology* **26**: 2160-2174.
- Uldrijan S, Pannekoek WJ, Vousden KH. 2007. An essential function of the extreme C-terminus of MDM2 can be provided by MDMX. *Embo Journal* **26**: 102-112.
- van Amerongen R, Mikels A, Nusse R. 2008. Alternative wnt signaling is initiated by distinct receptors. *Sci Signal* **1**: re9.

- van Schaftingen E, Davies DR, Hers HG. 1982. Fructose-2,6-bisphosphatase from rat liver. *Eur J Biochem* **124**: 143-149.
- Vander Heiden MG, Cantley LC, Thompson CB. 2009. Understanding the Warburg effect: the metabolic requirements of cell proliferation. *Science* **324**: 1029-1033.
- Varghese B, Swaminathan G, Plotnikov A, Tzimas C, Yang N, Rui H, Fuchs SY. 2010. Prolactin inhibits activity of pyruvate kinase M2 to stimulate cell proliferation. *Mol Endocrinol* **24**: 2356-2365.
- Vaseva AV, Marchenko ND, Ji K, Tsirka SE, Holzmann S, Moll UM. 2012. p53 opens the mitochondrial permeability transition pore to trigger necrosis. *Cell* **149**: 1536-1548.
- Velletri T, Romeo F, Tucci P, Peschiaroli A, Annicchiarico-Petruzzelli M, Niklison-Chirou M, Amelio I, Knight R, Mak T, Melino G et al. 2015. GLS2 is transcriptionally regulated by p73 and contributes to neuronal differentiation. *Cell cycle* **14**: 1611-1612.
- Venot C, Maratrat M, Dureuil C, Conseiller E, Bracco L, Debussche L. 1998. The requirement for the p53 proline-rich functional domain for mediation of apoptosis is correlated with specific PIG3 gene transactivation and with transcriptional repression. *The EMBO journal* **17**: 4668-4679.
- Venot C, Maratrat M, Sierra V, Conseiller E, Debussche L. 1999. Definition of a p53 transactivation function-deficient mutant and characterization of two independent p53 transactivation subdomains. *Oncogene* **18**: 2405-2410.
- Viticchie G, Agostini M, Lena AM, Mancini M, Zhou H, Zolla L, Dinsdale D, Saintigny G, Melino G, Candi E. 2015. p63 supports aerobic respiration through hexokinase II. *Proceedings of the National Academy of Sciences of the United States of America*.
- Wallace M, Worrall E, Pettersson S, Hupp TR, Ball KL. 2006. Dual-site regulation of MDM2 E3-ubiquitin ligase activity. *Molecular cell* **23**: 251-263.
- Wang J, Yuan W, Chen Z, Wu S, Chen J, Ge J, Hou F, Chen Z. 2012. Overexpression of G6PD is associated with poor clinical outcome in gastric cancer. *Tumour Biol* **33**: 95-101.
- Wang TY, Chen BF, Yang YC, Chen H, Wang Y, Cviko A, Quade BJ, Sun D, Yang A, McKeon FD et al. 2001. Histologic and immunophenotypic classification of cervical carcinomas by expression of the p53 homologue p63: a study of 250 cases. *Human pathology* **32**: 479-486.
- Wang X, Reid Sutton V, Omar Peraza-Llanes J, Yu Z, Rosetta R, Kou YC, Eble TN, Patel A, Thaller C, Fang P et al. 2007a. Mutations in X-linked PORCN, a putative regulator of Wnt signaling, cause focal dermal hypoplasia. *Nat Genet* **39**: 836-838.
- Wang XW, Zhao XC, Gao X, Mei YD, Wu MA. 2013. A new role of p53 in regulating lipid metabolism. *J Mol Cell Biol* **5**: 147-150.
- Wang YV, Wade M, Wong E, Li YC, Rodewald LW, Wahl GM. 2007b. Quantitative analyses reveal the importance of regulated Hdmx degradation for P53 activation. *Proceedings of the National Academy of Sciences of the United States of America* **104**: 12365-12370.
- Wanka C, Steinbach JP, Rieger J. 2012. Tp53-induced glycolysis and apoptosis regulator (TIGAR) protects glioma cells from starvation-induced cell death by up-regulating respiration and improving cellular redox homeostasis. *The Journal of biological chemistry* **287**: 33436-33446.
- Warburg O, Wind F, Negelein E. 1927. The Metabolism of Tumors in the Body. *J Gen Physiol* **8**: 519-530.

- Ward PS, Thompson CB. 2012. Metabolic reprogramming: a cancer hallmark even warburg did not anticipate. *Cancer Cell* **21**: 297-308.
- Waypa GB, Marks JD, Guzy R, Mungai PT, Schriewer J, Dokic D, Schumacker PT. 2010. Hypoxia triggers subcellular compartmental redox signaling in vascular smooth muscle cells. *Circ Res* **106**: 526-535.
- Wei Q, Yokota C, Semenov MV, Doble B, Woodgett J, He X. 2007. R-spondin1 is a high affinity ligand for LRP6 and induces LRP6 phosphorylation and beta-catenin signaling. *The Journal of biological chemistry* **282**: 15903-15911.
- Weinberg F, Hamanaka R, Wheaton WW, Weinberg S, Joseph J, Lopez M, Kalyanaraman B, Mutlu GM, Budinger GR, Chandel NS. 2010. Mitochondrial metabolism and ROS generation are essential for Kras-mediated tumorigenicity. *Proceedings of the National Academy of Sciences of the United States of America* **107**: 8788-8793.
- Weitzman JB, Fiette L, Matsuo K, Yaniv M. 2000. JunD protects cells from p53-dependent senescence and apoptosis. *Molecular cell* **6**: 1109-1119.
- Whibley C, Pharoah PD, Hollstein M. 2009. p53 polymorphisms: cancer implications. *Nat Rev Cancer* **9**: 95-107.
- Wilhelm MT, Rufini A, Wetzel MK, Tsuchihara K, Inoue S, Tomasini R, Itie-Youten A, Wakeham A, Arsenian-Henriksson M, Melino G et al. 2010. Isoform-specific p73 knockout mice reveal a novel role for delta Np73 in the DNA damage response pathway. *Genes & development* **24**: 549-560.
- Willert K, Brown JD, Danenberg E, Duncan AW, Weissman IL, Reya T, Yates JR, 3rd, Nusse R. 2003. Wnt proteins are lipid-modified and can act as stem cell growth factors. *Nature* **423**: 448-452.
- Wingo SN, Gallardo TD, Akbay EA, Liang MC, Contreras CM, Boren T, Shimamura T, Miller DS, Sharpless NE, Bardeesy N et al. 2009. Somatic LKB1 mutations promote cervical cancer progression. *Plos One* **4**: e5137.
- Won KY, Lim SJ, Kim GY, Kim YW, Han SA, Song JY, Lee DK. 2012. Regulatory role of p53 in cancer metabolism via SCO2 and TIGAR in human breast cancer. *Human pathology* **43**: 221-228.
- Wong EY, Wong SC, Chan CM, Lam EK, Ho LY, Lau CP, Au TC, Chan AK, Tsang CM, Tsao SW et al. 2015. -induced glycolysis and apoptosis regulator promotes proliferation and invasiveness of nasopharyngeal carcinoma cells. *Oncol Lett* **9**: 569-574.
- Woo DK, Green PD, Santos JH, D'Souza AD, Walther Z, Martin WD, Christian BE, Chandel NS, Shadel GS. 2012. Mitochondrial genome instability and ROS enhance intestinal tumorigenesis in APC(Min/+) mice. *Am J Pathol* **180**: 24-31.
- Wood LD, Parsons DW, Jones S, Lin J, Sjoblom T, Leary RJ, Shen D, Boca SM, Barber T, Ptak J et al. 2007. The genomic landscapes of human breast and colorectal cancers. *Science* **318**: 1108-1113.
- Wu G, Nomoto S, Hoque MO, Dracheva T, Osada M, Lee CC, Dong SM, Guo Z, Benoit N, Cohen Y et al. 2003. DeltaNp63alpha and TAp63alpha regulate transcription of genes with distinct biological functions in cancer and development. *Cancer research* **63**: 2351-2357.
- Wu H, Li Z, Yang P, Zhang L, Fan Y, Li Z. 2014. PKM2 depletion induces the compensation of glutaminolysis through beta-catenin/c-Myc pathway in tumor cells. *Cell Signal* **26**: 2397-2405.
- Xiao M, Yang H, Xu W, Ma S, Lin H, Zhu H, Liu L, Liu Y, Yang C, Xu Y et al. 2012. Inhibition of alpha-KG-dependent histone and DNA demethylases by

- fumarate and succinate that are accumulated in mutations of FH and SDH tumor suppressors. *Genes & development* **26**: 1326-1338.
- Xie JM, Li B, Yu HP, Gao QG, Li W, Wu HR, Qin ZH. 2014. TIGAR has a dual role in cancer cell survival through regulating apoptosis and autophagy. *Cancer research* **74**: 5127-5138.
- Xu Q, Wang Y, Dabdoub A, Smallwood PM, Williams J, Woods C, Kelley MW, Jiang L, Tasman W, Zhang K et al. 2004. Vascular development in the retina and inner ear: control by Norrin and Frizzled-4, a high-affinity ligand-receptor pair. *Cell* **116**: 883-895.
- Xu W, Yang H, Liu Y, Yang Y, Wang P, Kim SH, Ito S, Yang C, Wang P, Xiao MT et al. 2011. Oncometabolite 2-hydroxyglutarate is a competitive inhibitor of alpha-ketoglutarate-dependent dioxygenases. *Cancer Cell* **19**: 17-30.
- Yahagi N, Shimano H, Matsuzaka T, Najima Y, Sekiya M, Nakagawa Y, Ide T, Tomita S, Okazaki H, Tamura Y et al. 2003. P53 activation in adipocytes of obese mice. *Journal of Biological Chemistry* **278**: 25395-25400.
- Yahagi N, Shimano H, Matsuzaka T, Sekiya M, Najima Y, Okazaki S, Okazaki H, Tamura Y, Iizuka Y, Inoue N et al. 2004. P53 involvement in the pathogenesis of fatty liver disease. *Journal of Biological Chemistry* **279**: 20571-20575.
- Yalcin A, Telang S, Clem B, Chesney J. 2009. Regulation of glucose metabolism by 6-phosphofructo-2-kinase/fructose-2,6-bisphosphatases in cancer. *Exp Mol Pathol* **86**: 174-179.
- Yamamoto A, Nagano T, Takehara S, Hibi M, Aizawa S. 2005. Shisa promotes head formation through the inhibition of receptor protein maturation for the caudalizing factors, Wnt and FGF. *Cell* **120**: 223-235.
- Yan H, Parsons DW, Jin G, McLendon R, Rasheed BA, Yuan W, Kos I, Batinic-Haberle I, Jones S, Riggins GJ et al. 2009. IDH1 and IDH2 mutations in gliomas. *N Engl J Med* **360**: 765-773.
- Yang A, Kaghad M, Wang Y, Gillett E, Fleming MD, Dotsch V, Andrews NC, Caput D, McKeon F. 1998. p63, a p53 homolog at 3q27-29, encodes multiple products with transactivating, death-inducing, and dominant-negative activities. *Molecular cell* **2**: 305-316.
- Yang A, Walker N, Bronson R, Kaghad M, Oosterwegel M, Bonnin J, Vagner C, Bonnet H, Dikkes P, Sharpe A et al. 2000. p73-deficient mice have neurological, pheromonal and inflammatory defects but lack spontaneous tumours. *Nature* **404**: 99-103.
- Yang H, Brosel S, Acin-Perez R, Slavkovich V, Nishino I, Khan R, Goldberg IJ, Graziano J, Manfredi G, Schon EA. 2010. Analysis of mouse models of cytochrome c oxidase deficiency owing to mutations in Sco2. *Hum Mol Genet* **19**: 170-180.
- Yang PT, Lorenowicz MJ, Silhankova M, Coudreuse DY, Betist MC, Korswagen HC. 2008. Wnt signaling requires retromer-dependent recycling of MIG-14/Wntless in Wnt-producing cells. *Developmental cell* **14**: 140-147.
- Yang W, Xia Y, Hawke D, Li X, Liang J, Xing D, Aldape K, Hunter T, Alfred Yung WK, Lu Z. 2012a. PKM2 phosphorylates histone H3 and promotes gene transcription and tumorigenesis. *Cell* **150**: 685-696.
- Yang W, Xia Y, Ji H, Zheng Y, Liang J, Huang W, Gao X, Aldape K, Lu Z. 2011. Nuclear PKM2 regulates beta-catenin transactivation upon EGFR activation. *Nature* **480**: 118-122.
- Yang W, Zheng Y, Xia Y, Ji H, Chen X, Guo F, Lyssiotis CA, Aldape K, Cantley LC, Lu Z. 2012b. ERK1/2-dependent phosphorylation and nuclear

- translocation of PKM2 promotes the Warburg effect. *Nature cell biology* **14**: 1295-1304.
- Yang WH, Lan HY, Huang CH, Tai SK, Tzeng CH, Kao SY, Wu KJ, Hung MC, Yang MH. 2012c. RAC1 activation mediates Twist1-induced cancer cell migration. *Nature cell biology* **14**: 366-374.
- Yang Y, Dieter MZ, Chen Y, Shertzer HG, Nebert DW, Dalton TP. 2002. Initial characterization of the glutamate-cysteine ligase modifier subunit Gclm(-/-) knockout mouse. Novel model system for a severely compromised oxidative stress response. *The Journal of biological chemistry* **277**: 49446-49452.
- Ye L, Zhao X, Lu J, Qian G, Zheng JC, Ge S. 2013. Knockdown of TIGAR by RNA interference induces apoptosis and autophagy in HepG2 hepatocellular carcinoma cells. *Biochemical and biophysical research communications* **437**: 300-306.
- Yee KS, Wilkinson S, James J, Ryan KM, Vousden KH. 2009. PUMA- and Bax-induced autophagy contributes to apoptosis. *Cell death and differentiation* **16**: 1135-1145.
- Yi W, Clark PM, Mason DE, Keenan MC, Hill C, Goddard WA, 3rd, Peters EC, Driggers EM, Hsieh-Wilson LC. 2012. Phosphofructokinase 1 glycosylation regulates cell growth and metabolism. *Science* **337**: 975-980.
- Yin L, Kosugi M, Kufe D. 2012. Inhibition of the MUC1-C oncoprotein induces multiple myeloma cell death by down-regulating TIGAR expression and depleting NADPH. *Blood* **119**: 810-816.
- Yin Y, Stephen CW, Luciani MG, Fahraeus R. 2002. p53 Stability and activity is regulated by Mdm2-mediated induction of alternative p53 translation products. *Nature cell biology* **4**: 462-467.
- Yoo NJ, Kim HR, Kim YR, An CH, Lee SH. 2012. Somatic mutations of the KEAP1 gene in common solid cancers. *Histopathology* **60**: 943-952.
- Yoon KA, Nakamura Y, Arakawa H. 2004. Identification of ALDH4 as a p53-inducible gene and its protective role in cellular stresses. *J Hum Genet* **49**: 134-140.
- Young TW, Mei FC, Yang G, Thompson-Lanza JA, Liu J, Cheng X. 2004. Activation of antioxidant pathways in ras-mediated oncogenic transformation of human surface ovarian epithelial cells revealed by functional proteomics and mass spectrometry. *Cancer research* **64**: 4577-4584.
- Yu HP, Xie JM, Li B, Sun YH, Gao QG, Ding ZH, Wu HR, Qin ZH. 2015. TIGAR regulates DNA damage and repair through pentosephosphate pathway and Cdk5-ATM pathway. *Sci Rep* **5**: 9853.
- Yu Z, Zhao X, Huang L, Zhang T, Yang F, Xie L, Song S, Miao P, Zhao L, Sun X et al. 2013. Proviral insertion in murine lymphomas 2 (PIM2) oncogene phosphorylates pyruvate kinase M2 (PKM2) and promotes glycolysis in cancer cells. *The Journal of biological chemistry* **288**: 35406-35416.
- Yuan ZM, Shioya H, Ishiko T, Sun X, Gu J, Huang YY, Lu H, Kharbanda S, Weichselbaum R, Kufe D. 1999. p73 is regulated by tyrosine kinase c-Abl in the apoptotic response to DNA damage. *Nature* **399**: 814-817.
- Yuen HF, Chan YP, Law S, Srivastava G, El-Tanani M, Mak TW, Chan KW. 2008. DJ-1 could predict worse prognosis in esophageal squamous cell carcinoma. *Cancer Epidemiol Biomarkers Prev* **17**: 3593-3602.
- Yun J, Rago C, Cheong I, Pagliarini R, Angenendt P, Rajagopalan H, Schmidt K, Willson JK, Markowitz S, Zhou S et al. 2009. Glucose deprivation

- contributes to the development of KRAS pathway mutations in tumor cells. *Science* **325**: 1555-1559.
- Zaika A, Irwin M, Sansome C, Moll UM. 2001. Oncogenes induce and activate endogenous p73 protein. *The Journal of biological chemistry* **276**: 11310-11316.
- Zamble DB, Jacks T, Lippard SJ. 1998. p53-Dependent and -independent responses to cisplatin in mouse testicular teratocarcinoma cells. *Proceedings of the National Academy of Sciences of the United States of America* **95**: 6163-6168.
- Zaugg K, Yao Y, Reilly PT, Kannan K, Kiarash R, Mason J, Huang P, Sawyer SK, Fuerth B, Faubert B et al. 2011. Carnitine palmitoyltransferase 1C promotes cell survival and tumor growth under conditions of metabolic stress. *Genes & development* **25**: 1041-1051.
- Zeng X, Tamai K, Doble B, Li S, Huang H, Habas R, Okamura H, Woodgett J, He X. 2005. A dual-kinase mechanism for Wnt co-receptor phosphorylation and activation. *Nature* **438**: 873-877.
- Zhang H, Gu C, Yu J, Wang Z, Yuan X, Yang L, Wang J, Jia Y, Liu J, Liu F. 2014. Radiosensitization of glioma cells by TP53-induced glycolysis and apoptosis regulator knockdown is dependent on thioredoxin-1 nuclear translocation. *Free Radic Biol Med* **69**: 239-248.
- Zhang YP, Wolf GW, Bhat K, Jin A, Allio T, Burkhart WA, Xiong Y. 2003. Ribosomal protein L11 negatively regulates oncoprotein MDM2 and mediates a p53-dependent ribosomal-stress checkpoint pathway. *Molecular and cellular biology* **23**: 8902-8912.
- Zhao YF, Chaiswing L, Velez JM, Batinic-Haberle I, Colburn NH, Oberley TD, St Clair DK. 2005. p53 translocation to mitochondria precedes its nuclear translocation and targets mitochondrial oxidative defense protein-manganese superoxide dismutase. *Cancer research* **65**: 3745-3750.
- Zhao YG, Zhao HY, Miao L, Wang L, Sun F, Zhang H. 2012. The p53-induced Gene Ei24 Is an Essential Component of the Basal Autophagy Pathway. *Journal of Biological Chemistry* **287**: 42053-42063.
- Zheng CF, Guan KL. 1994. Activation of MEK family kinases requires phosphorylation of two conserved Ser/Thr residues. *The EMBO journal* **13**: 1123-1131.
- Zhou Y, Hileman EO, Plunkett W, Keating MJ, Huang P. 2003. Free radical stress in chronic lymphocytic leukemia cells and its role in cellular sensitivity to ROS-generating anticancer agents. *Blood* **101**: 4098-4104.
- Zhu J, Jiang J, Zhou W, Chen X. 1998. The potential tumor suppressor p73 differentially regulates cellular p53 target genes. *Cancer research* **58**: 5061-5065.
- Zindy F, Eischen CM, Randle DH, Kamijo T, Cleveland JL, Sherr CJ, Roussel MF. 1998. Myc signaling via the ARF tumor suppressor regulates p53-dependent apoptosis and immortalization. *Genes & development* **12**: 2424-2433.
- Zoncu R, Efeyan A, Sabatini DM. 2011. mTOR: from growth signal integration to cancer, diabetes and ageing. *Nature reviews Molecular cell biology* **12**: 21-35.
- Zou S, Gu Z, Ni P, Liu X, Wang J, Fan Q. 2012. SP1 plays a pivotal role for basal activity of TIGAR promoter in liver cancer cell lines. *Molecular and cellular biochemistry* **359**: 17-23.

- Zou S, Wang X, Deng L, Wang Y, Huang B, Zhang N, Fan Q, Luo J. 2013. CREB, another culprit for TIGAR promoter activity and expression. *Biochemical and biophysical research communications* **439**: 481-486.
- Zuckerman V, Wolyniec K, Sionov RV, Haupt S, Haupt Y. 2009. Tumour suppression by p53: the importance of apoptosis and cellular senescence. *J Pathol* **219**: 3-15.

p53- and p73-independent activation of TIGAR expression *in vivo*

P Lee¹, AK Hock¹, KH Vousden*¹ and EC Cheung*¹

TIGAR (*TP53*-induced glycolysis and apoptosis regulator) functions as a fructose-2,6-bisphosphatase and its expression results in a dampening of the glycolytic pathway, while increasing antioxidant capacity by increasing NADPH and GSH levels. In addition to being a p53 target, p53-independent expression of TIGAR is also seen in many human cancer cell lines that lack wild-type p53. Although human TIGAR expression can be induced by p53, TAp63 and TAp73, mouse TIGAR is less responsive to the p53 family members and basal levels of TIGAR expression does not depend on p53 or TAp73 expression in most mouse tissues *in vivo*. Although mouse TIGAR expression is clearly induced in the intestines of mice following DNA-damaging stress such as ionising radiation, this is also not dependent on p53 or TAp73.

Cell Death and Disease (2015) 6, e1842; doi:10.1038/cddis.2015.205; published online 6 August 2015

TIGAR (*TP53*-induced glycolysis and apoptosis regulator) is a metabolic enzyme sharing structural similarities to the FBPase-2 domain of phosphofructokinase-2/fructose-2,6-bisphosphatase. TIGAR can act to lower the levels of fructose-2,6-bisphosphate (F-2,6-P₂), an allosteric activator of phosphofructokinase-1 (PFK-1) in the glycolytic pathway. Lowering F-2,6-P₂ levels results in decreased PFK-1 activity, thereby decreasing flux through glycolysis and potentially allowing for the diversion of glycolytic metabolites to other pathways such as the pentose phosphate pathway or the hexosamine pathway.^{1,2} Although the detailed effects of TIGAR expression on metabolism remain to be determined, it is clear that TIGAR functions in many cell systems to mediate antioxidant defence through an increase in NADPH and GSH.^{3–8} TIGAR has also been found to act as a 2,3-bisphosphoglycerate phosphatase, which catalyses the conversion of 2,3-bisphosphoglycerate into 3-phosphoglycerate,⁹ although the physiological significance of this activity remains unclear.

TIGAR was identified in human cells as a transcriptional target of the tumour-suppressor protein p53. The human *TIGAR* possesses two p53-binding sites, human p53-binding site (hBS) 1 and hBS2, where hBS2 is the functional p53-binding site.² In the mouse genome, *Tigar* shows a similar organisation with two potential p53-binding sites, mBS1 and mBS2, in a similar arrangement as human *TIGAR*.¹⁰ As a p53 target, TIGAR would be predicted to play a role in tumour suppression and the antioxidant functions of TIGAR would be consistent with a role in protecting from the acquisition of damage. However, TIGAR expression has been found to be elevated in a number of cancer models and tumour types^{4,11,12} through a mechanism that is not dependent on the maintenance of wild-type (WT) p53. Moreover, the expression of TIGAR in human breast cancer was found inversely correlated

to the levels of p53.¹³ Taken together, these data suggest that TIGAR can function in a tumour suppressor pathway as part of a p53 response, but may also contribute to cancer development when TIGAR expression is deregulated and uncoupled from p53. In mouse models, loss of TIGAR has been shown to result in a decreased ability to regenerate damaged intestinal epithelium and a restraint on tumour development, both situations where ROS limitation is important.¹¹ These results are consistent with the model that the expression of TIGAR may support tumour progression.

Little is known about p53-independent expression of TIGAR, although other transcription factors such as SP1 and CREB^{14,15} have been implicated. Other members of the p53 family (p63 and p73) are able to activate promoters of p53 targets such as p21^{16,17} and these p53 family proteins can also contribute to the regulation of metabolic gene expression. It is therefore possible that p63 and p73 can also regulate TIGAR expression.

To further understand the regulation of TIGAR, we investigate the differences in TIGAR regulation by p53 and its family members. Although both p53 and TAp73 showed activity in promoting the expression of both human and mouse TIGAR reporters in cells, we found that the activation of expression of mouse TIGAR in response to genotoxic stress is not dependent on p53 or TAp73.

Results

TIGAR expression is varied across tissues. Although we have previously shown TIGAR to be expressed in several mouse tissues, to assess the relative levels of TIGAR expression, protein levels were evaluated across various tissues from WT mice (Figure 1a). TIGAR protein was

¹Cancer Research-UK Beatson Institute, Switchback Road, Glasgow G61 1BD, UK

*Corresponding author: KH Vousden or EC Cheung, CRUK Beatson Institute, Switchback Road, Glasgow G61 1BD, UK. Tel: +44 141 330 2424; Fax: +44 141 942 0372; E-mail: k.vousden@beatson.gla.ac.uk or e.cheung@beatson.gla.ac.uk

Abbreviations: BPAG1, bullous pemphigoid antigen 1; CDDP, cisplatin; DMEM, Dulbecco's modified Eagle's medium; F-2,6-P₂, fructose-2,6-bisphosphate; hBS, human p53-binding site; IR, irradiation; iRFP, infrared fluorescent protein; PFK-1, phosphofructokinase-1; PFK-2/FBPase-2, phosphofructokinase-2/fructose-2,6-bisphosphatase; TIFs, tert-immortalised fibroblasts; TIGAR, *TP53*-induced glycolysis and apoptosis regulator; WT, wild type

Received 25.3.15; revised 17.6.15; accepted 26.6.15; Edited by G Melino

detected in all tissues examined, with highest levels in the muscle and brain. Antibody specificity was confirmed using small intestine tissue from WT and TIGAR-deficient animals after treatment with irradiation (IR), which we have previously shown to increase TIGAR expression.¹¹ As expected, TIGAR protein expression increased following IR in the WT animals and was not detected in TIGAR^{-/-} animals (Supplementary Figure 1a). Interestingly, TIGAR protein expression in tissues was not completely mirrored by mRNA expression (Figure 1b). For example, the protein expression of TIGAR in the liver and pancreas are similar, however, the levels of TIGAR mRNA in the pancreas are much lower than in the

liver. This suggests additional mechanisms to regulate TIGAR protein levels may exist in some tissues.

Mouse TIGAR is not responsive to p53 during genotoxic stress *in vitro*. Published studies have shown that mouse TIGAR can also be responsive to p53's transcriptional activity^{10,18,19} and p53-deficient mice lose the ability to induce TIGAR expression following myocardial injury.^{19,20} However, TIGAR was also shown to be induced in mouse primary neurons following oxygen and glucose deprivation/reoxygenation in a p53-independent manner.⁸ To compare the p53-induced expression of TIGAR in mouse and human

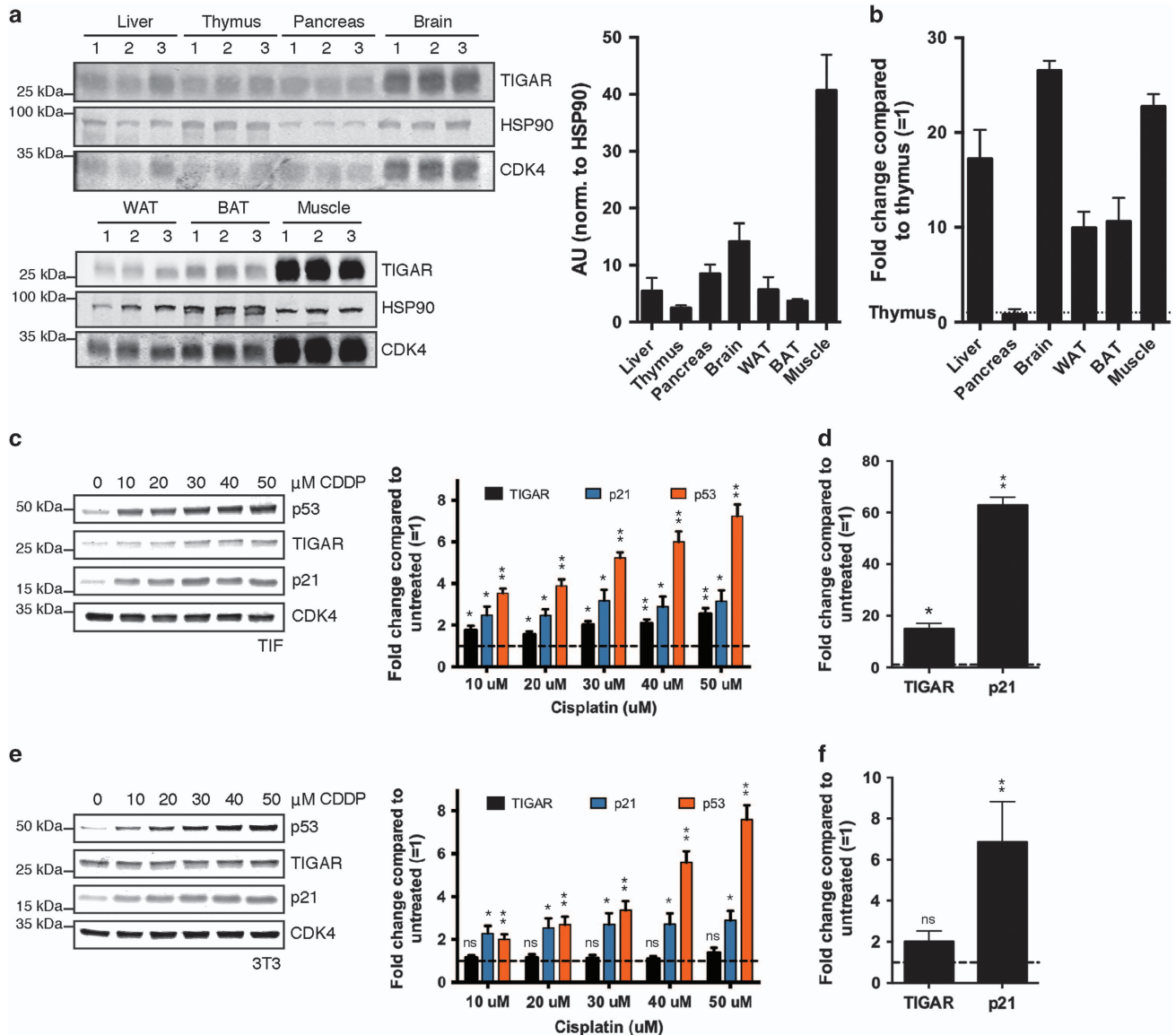


Figure 1 Basal TIGAR expression and its response to p53 activation. (a) Left: Western blot analysis of indicated tissues from three different wild-type (WT) animals. Right: Graph represents quantification of western blots. (b) mRNA expression of TIGAR in indicated tissues of WT animals. (c) Left: Western blot analysis of Tert-Immortalised Fibroblasts (TIFs) treated with indicated concentrations of cisplatin (CDDP) for 24 h. Right: Graph represents quantification of western blots with fold change compared with untreated. (d) mRNA expression of TIGAR and p21 following 24 h of CDDP treatment (50 μ M) in TIFs. (e) Left: Western blot analysis of 3T3s treated with indicated concentrations of CDDP for 24 h. Right: Graph represents quantification of western blots with fold change compared with untreated. (f) mRNA expression of TIGAR and p21 following 24 h of CDDP treatment (50 μ M) in 3T3s. Right: Graph represents quantification of western blots with fold change compared with untreated. Values represent mean \pm S.E.M. of three independent experiments unless otherwise indicated. * $P < 0.05$, ** $P < 0.005$ compared with untreated unless otherwise indicated. NS, not significant

cells, we treated human tert-immortalised fibroblasts (TIFs) and mouse 3T3s with increasing concentrations of cisplatin (CDDP) to activate p53, but not induce cell death. After treatment, TIFs showed an increase in p53 protein level, along with an increased expression of TIGAR and a known p53 target, p21 (Figure 1c). However, although mouse 3T3s showed an elevation in p53 and p21, the expression of TIGAR was not detectably affected after treatment (Figure 1e). Similarly, using qRT-PCR to examine mRNA expression, human TIFs showed a significant increase in TIGAR mRNA expression after CDDP treatment that was not seen in the mouse cells (Figures 1d and f). These results suggest that p53 activation in mouse cells in culture does not consistently induce TIGAR expression.

Loss of p53 does not affect expression of TIGAR *in vivo* following IR. Previous work has shown that TIGAR expression levels are increased in the crypts of WT mice during intestinal regeneration following tissue ablation.¹¹ As p53 is also upregulated in the small intestine following IR,²¹ we examined whether TIGAR expression is controlled by p53 in mice *in vivo*. The basal TIGAR protein levels were examined in various organs of WT and p53^{-/-} mice. No significant reduction in TIGAR expression was seen in response to loss of p53 at either the protein level (Figure 2a) or the mRNA level (Figure 2b) – with a possible exception of a slight reduction in TIGAR mRNA in p53-null muscle. By contrast, p21 showed a very clear decrease in mRNA expression in all the p53^{-/-} organs examined.

To extend these studies, we tested whether a p53-dependent increase in TIGAR expression would occur *in vivo* after damage, focusing on the intestinal system in which we have previously shown increased TIGAR in response to IR. Antibody specificity for TIGAR immunohistochemistry was confirmed using small intestine tissue from WT and TIGAR-deficient animals after treatment with IR to induce TIGAR expression. As shown previously,¹¹ TIGAR expression increased in the crypts of WT mice following IR, whereas no staining was observed in TIGAR^{-/-} animals (Supplementary Figure 1b). Comparison of WT and p53^{-/-} mice showed normal crypt architecture and similar levels of proliferation, as indicated by Ki67 staining, under unstressed conditions (Figure 2c). The basal expression of p53, p21 and TIGAR was also low in the crypts of WT and p53^{-/-} animals (Figure 2c). Tissue ablation of the intestinal epithelium by IR was followed by a period of recovery during which rapid tissue regeneration and proliferation occurred in WT and p53^{-/-} mice.²² Moreover, TIGAR expression increased in the crypts of both WT and p53^{-/-} animals, whereas p21 induction was clearly lower in the p53^{-/-} animals (Figure 2c). These data show that p53 is not necessary to maintain basal expression of TIGAR in many tissues or induce TIGAR expression following tissue damage in the small intestine.

Comparison of human and mouse TIGAR p53-binding site activity. The *in vitro* and *in vivo* data suggest that murine TIGAR is only weakly responsive to p53, possibly due to the differences in p53-binding sites between human and mouse TIGAR (Figure 3a). To investigate the differences between the human (hBS1 and hBS2) and mouse

(mBS1 and mBS2) p53-binding sites of TIGAR directly, sequences corresponding to each p53-binding sites were cloned into infrared fluorescent protein (iRFP) reporter constructs.²³ These constructs were co-transfected into HCT116 p53^{-/-} cells with increasing amounts of human or mouse p53 (Figures 3b and c). Each of these p53-binding site reporters were activated by both human and mouse p53. TIGAR-hBS2, the more efficient of the two human p53-binding sites, is efficiently activated by either human or mouse p53 (Figure 3d). By contrast, TIGAR-mBS1 is more responsive to p53 than TIGAR-mBS2, and slightly more responsive than TIGAR-hBS1, although less active than TIGAR-hBS2. Interestingly, mouse p53 was slightly more effective in the induction of all the binding site reporters, with the exception of TIGAR-mBS2. Taken together, the results suggest that the weaker p53-binding site (BS1) is structurally and functionally conserved between mouse and human but the stronger BS2 in humans is only very weakly active in the mouse.

To determine whether p53 can bind to either of the two putative binding sites in the mouse *Tigar* promoter, chromatin-immunoprecipitation was carried out in mouse 3T3 cells treated with CDDP to activate p53 (Figure 3e). Although p53 was clearly recruited to the p21 promoter following treatment, no increased binding of p53 to either mBS1 or mBS2 could be detected in these cells. The failure to recruit p53 to the *Tigar* promoter can explain the observed inefficiency of p53-dependent activation of mouse TIGAR expression seen in several cell types *in vitro* and *in vivo*.

Tap73 α can activate the human TIGAR p53-binding site reporter. We further investigated the potential role of other p53 family members in the regulation of TIGAR expression. We first focused on the functional human p53-binding site (hBS2), co-transfecting the TIGAR-hBS2 iRFP reporter construct with p53, Tap63 α or Tap73 α to assess transcriptional activity. As positive controls we used iRFP expression constructs containing p53 response element encoding repeats of a known p53-binding sequence (p53RE), the p53-binding site of p21 (WAF1²⁴) and a p63 response element from the skin-specific promoter of bullous pemphigoid antigen 1 (BPAG1²⁵). Both Tap63 α and Tap73 α induced a response from the human TIGAR-hBS2 iRFP reporter construct, although the activity of Tap63 α was extremely weak. The pattern of expression from TIGAR-hBS2 was similar to that seen with the p53RE or WAF1, where p53 was the most efficient, followed by Tap73 α , then Tap63 α . Strong activity for Tap63 α was only measured using the BPAG1 promoter, although even here Tap73 α was more active (Figures 4a–c). In light of these results, we focused on Tap73 isoforms as potential activators of TIGAR expression.

The Tap73 α isoform has been shown to contain an inhibitory domain that limits its activity, making it less efficient than other isoforms.²⁶ We therefore examined the activity of p73 isoforms, Tap73 α , Tap73 β , Tap73 γ or Δ Np73 α , in these assays. Although full-length Tap73 isoforms can induce p53 target genes,²⁷ Δ Np73 isoforms, which lack the N-terminal activation domain,²⁸ have been shown to inhibit Tap73 transcriptional activity as well as regulating an additional set of target genes.²⁹ As expected,^{30,31} Tap73 β was consistently more effective in driving expression from p53RE, WAF1 or

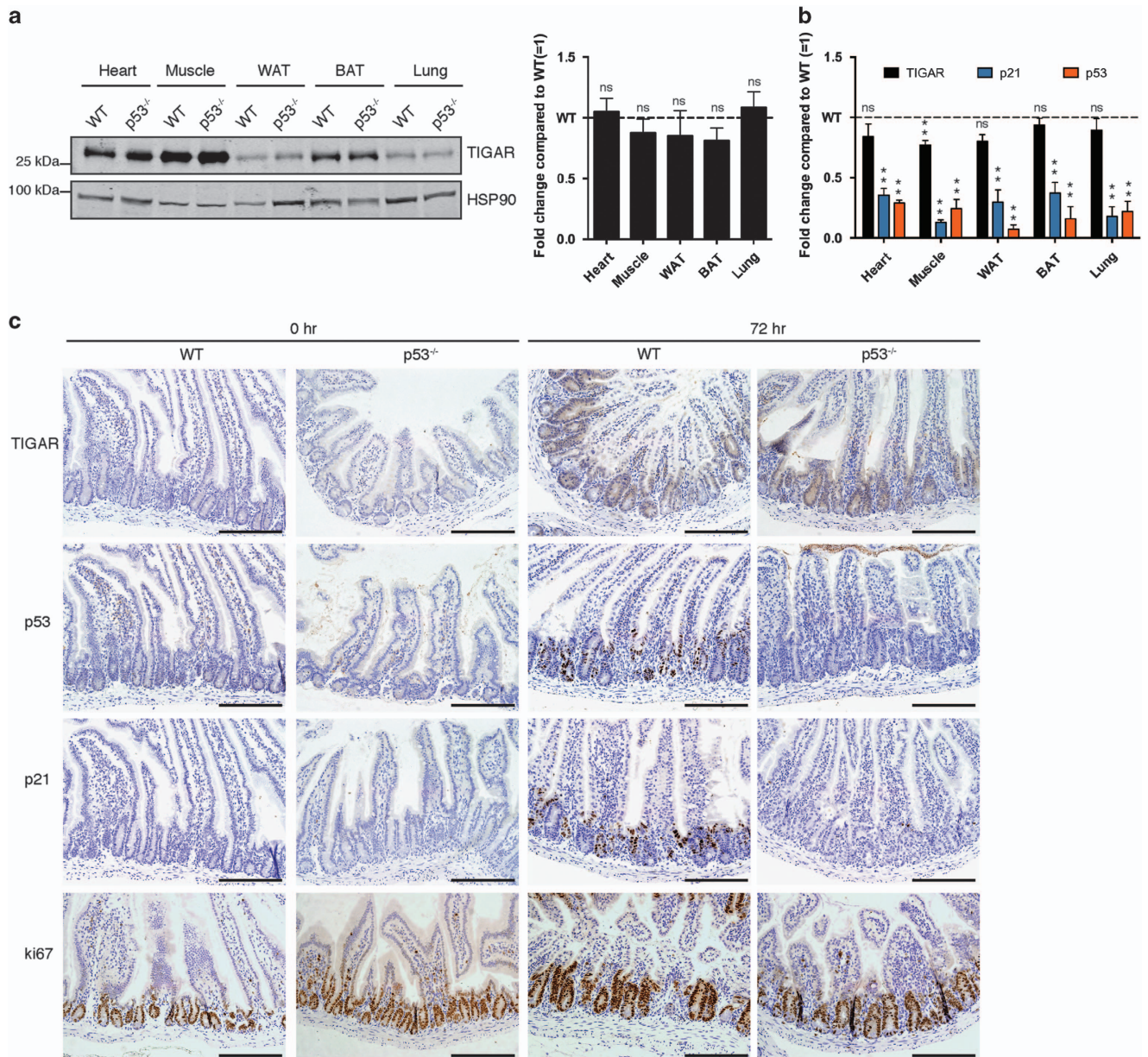


Figure 2 TIGAR expression in p53-null animals. (a) Left: Western blot analysis of TIGAR protein expression in organs of wild-type (WT) and p53^{-/-} mice. Right: Graph represents quantification of western blots with fold change compared with WT. (b) mRNA expression of TIGAR, p21 and p53 in organs of WT and p53^{-/-} mice. (c) Immunohistochemistry on small intestines from WT and p53^{-/-} animals 72 h after 10 Gy IR. Scale bar, 20 μ m. Values represent mean \pm S.E.M. of three independent experiments. * $P < 0.05$, ** $P < 0.005$ compared with WT. NS, not significant. WAT, white adipose tissue. BAT, brown adipose tissue

BPAG1 promoters. In these assays, Tap73 γ and Δ Np73 α did not show strong transcriptional activity. Turning to the reporter constructs containing TIGAR p53-binding sites (hBS2, mBS1 and mBS2), we found that Tap73 α more effectively induced expression from hBS2, whereas both Tap73 α and Tap73 β modestly induced expression from mBS1 and mBS2 (Figures 4d–f). Taken together, the data suggest that like p53, Tap73 has the potential to drive the expression of both mouse and human TIGAR.

Loss of Tap73 does not affect expression of TIGAR *in vivo* following IR. p73 can be activated by DNA damage,^{32–34} potentially mediating the induction of TIGAR

expression in response to IR independently of p53. To investigate this, we examined TIGAR expression in Tap73-deficient (Tap73^{-/-}) mice. First, the basal expression of TIGAR was assessed in various organs of untreated WT and Tap73^{-/-} mice (Figure 5a). As seen in p53^{-/-} mice, no clear significant decrease in TIGAR expression was seen in Tap73^{-/-} tissues, with a possible small reduction in protein and mRNA levels in the muscle (Figure 5b). Following IR, intestines of Tap73^{-/-} mice underwent rapid proliferation, as shown by the proliferative marker Ki67 (Figure 5c). Although induction of Tap73 was limited to the WT mice, TIGAR expression was increased in the crypts of both WT and Tap73^{-/-} animals, showing that this induction of expression

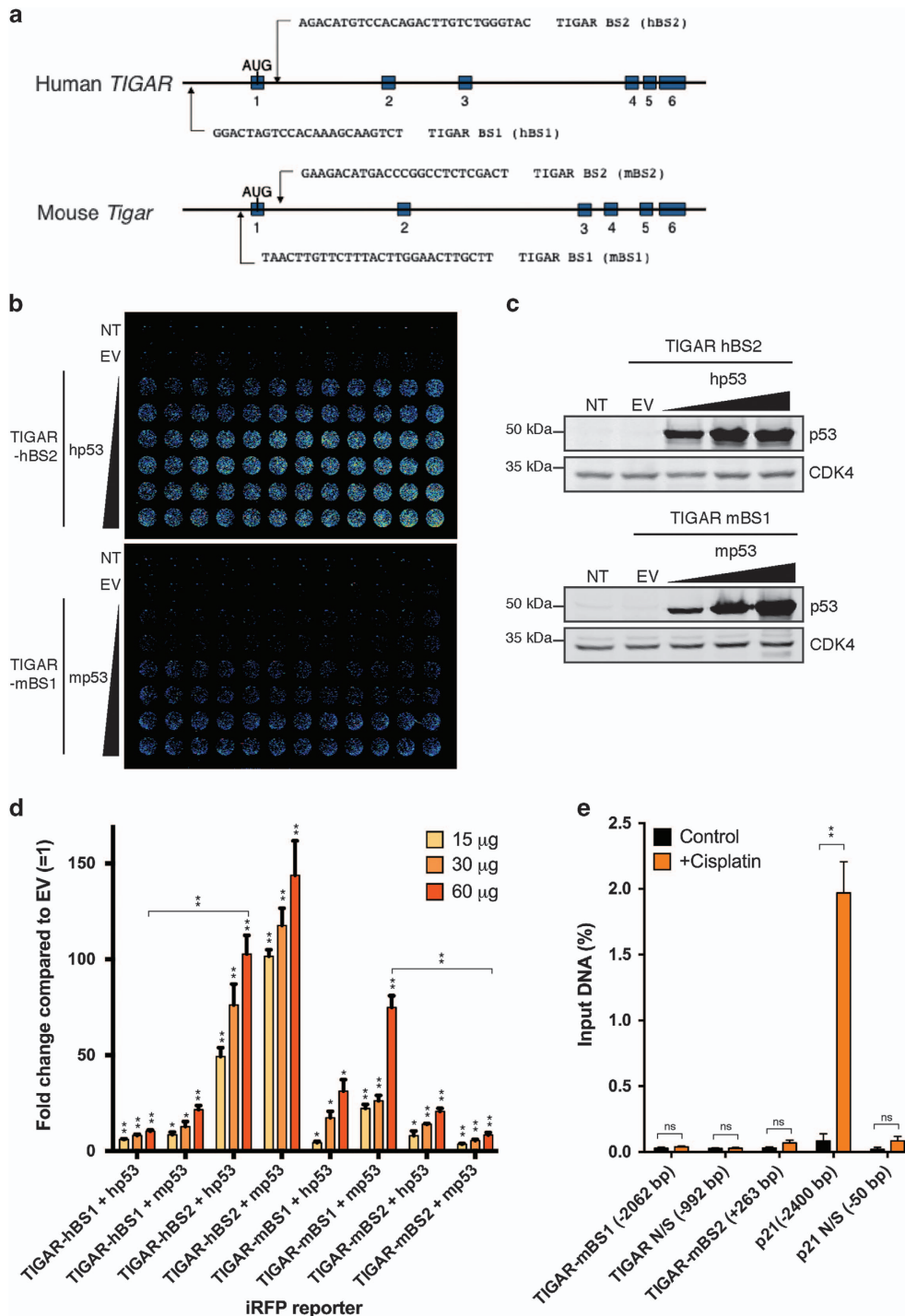


Figure 3 Comparison of human and mouse p53-binding sites on the *TIGAR* promoter. (a) Possible p53-binding sites along human and mouse *TIGAR*. (b) Representative iRFP reporter assay scan of HCT116 p53^{-/-} cells 24 h after co-transfection with TIGAR-hBS2 or TIGAR-mBS1 iRFP reporter and increasing amounts of human p53 or mouse p53. (c) Western blot analysis of HCT116 p53^{-/-} cells transfected with increasing amounts of human p53 or mouse p53. (d) Quantification of iRFP reporter scans on human (hBS1 and hBS2) and mouse (mBS1 and mBS2) TIGAR promoter-binding sites with increasing levels of human or mouse p53. (e) Chromatin-immunoprecipitation (ChIP) was performed for p53 with quantitative PCR for mBS1 (-2062 bp), mBS2 (+263 bp), a p53 response element on the *p21* promoter (-2400 bp) and non-specific (N/S) binding regions on the *Tigar* (-992 bp) and *p21* promoter (-50 bp), using 3T3s treated with 50 μ M cisplatin for 24 h. Values represent mean \pm S.E.M. of three independent experiments. **P* < 0.05, ***P* < 0.005 compared with empty vector (EV) or control. NT, non-transfected; NS, not significant

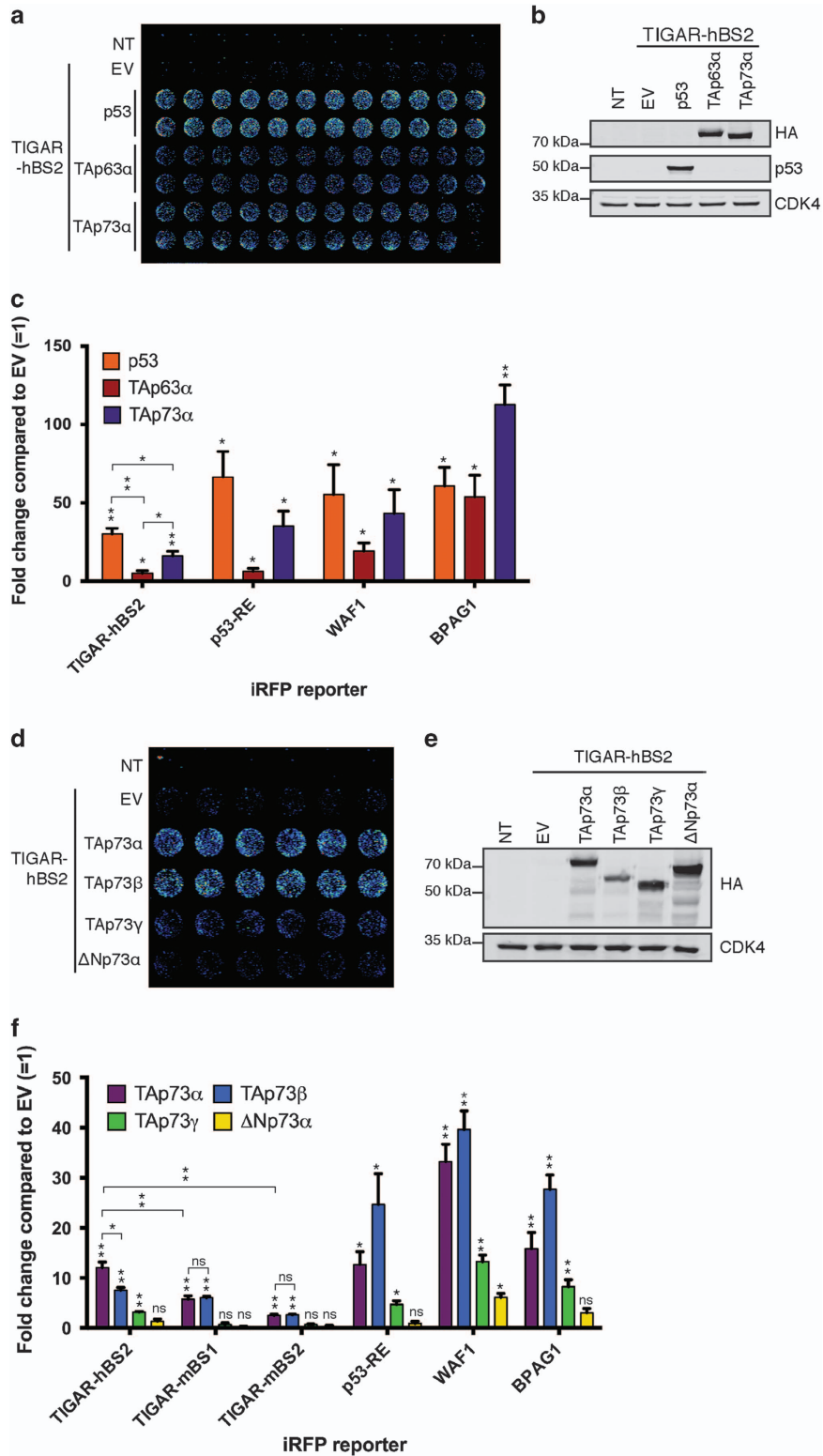


Figure 4 TAp63 α and TAp73 α can activate the TIGAR-hBS2 reporter. (a) Representative iRFP reporter assay scan of HCT116 p53 $^{-/-}$ cells 24 h after co-transfection with TIGAR-hBS2 iRFP reporter along with human p53, HA-tagged TAp63 α or HA-tagged TAp73 α . (b) Western blot analysis of HCT116 p53 $^{-/-}$ cells with transfected p53, HA-tagged TAp63 α or HA-tagged TAp73 α . (c) Quantification of iRFP reporter scans. (d) Representative iRFP reporter assay scan of HCT116 p53 $^{-/-}$ cells 24 h after co-transfection with TIGAR-hBS2 iRFP reporter along with TAp73 α , TAp73 β , TAp73 γ or Δ Np73 α . (e) Western blot analysis of HCT116 p53 $^{-/-}$ cells with transfected HA-tagged TAp73 α , HA-tagged TAp73 β , HA-tagged TAp73 γ or HA-tagged Δ Np73 α . (f) Quantification of iRFP reporter scans on human (hBS2) and mouse (mBS1 and mBS2) TIGAR promoter-binding sites. Values represent mean \pm S.E.M. of three independent experiments. * $P < 0.05$, ** $P < 0.005$ compared with empty vector (EV). NT, non-transfected; NS, not significant

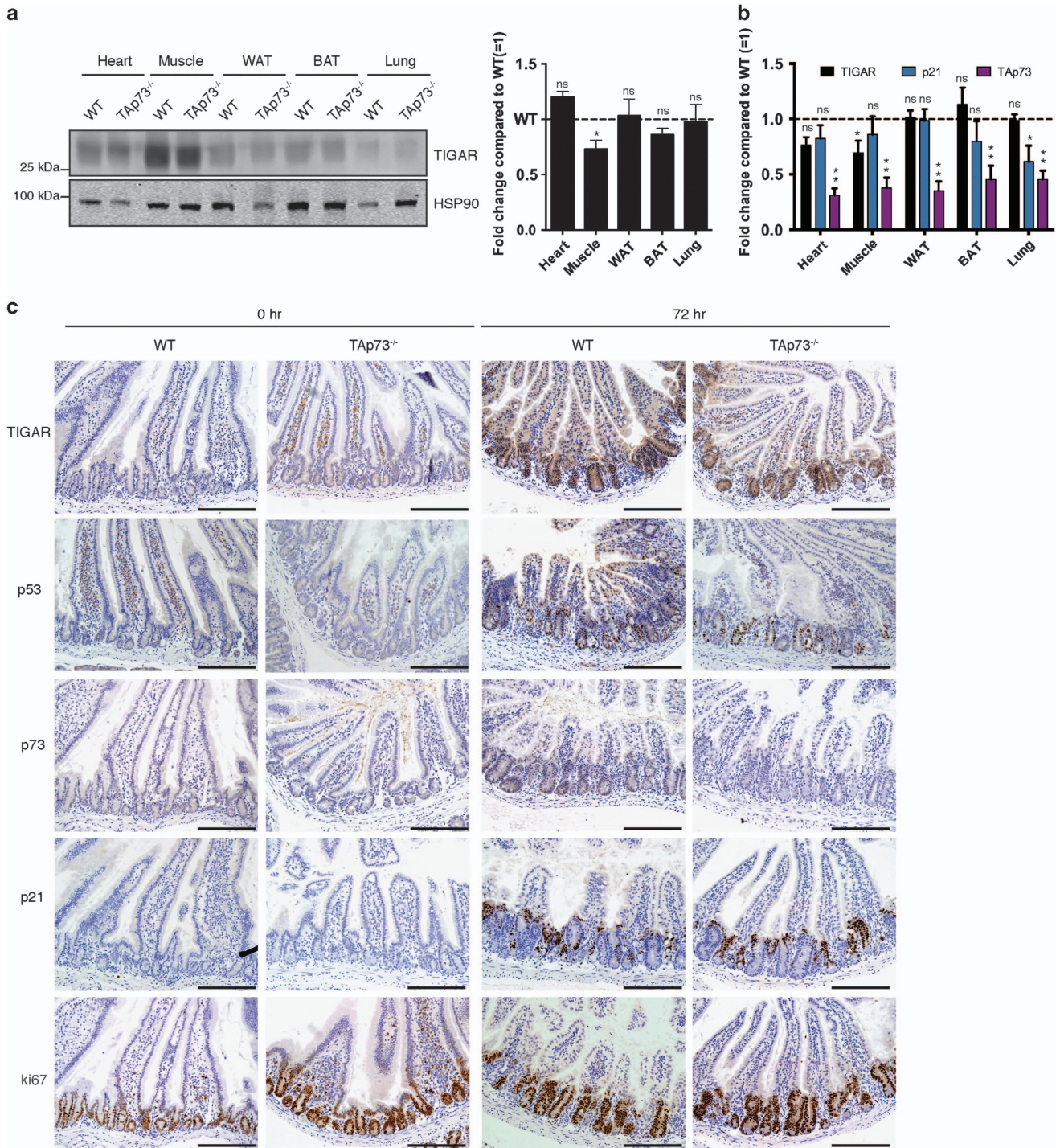


Figure 5 TIGAR expression in TAp73-null animals. (a) Left: Western blot analysis of TIGAR protein expression in organs of wild-type (WT) and TAp73^{-/-} mice. Right: Graph represents quantification of western blots with fold change compared with WT. (b) mRNA expression of TIGAR, p21 and TAp73 in organs of WT and TAp73^{-/-} mice. (c) Immunohistochemistry on small intestines from WT and TAp73^{-/-} animals 72 h after 10 Gy IR. Scale bar, 20 μ m. Values represent mean \pm S.E.M. of three independent experiments. * P < 0.05, ** P < 0.005 compared with WT. NS, not significant; WAT, white adipose tissue; BAT, brown adipose tissue

was not dependent on TAp73. p21 levels were also induced, reflecting the accumulation of p53 in response to IR in the TAp73^{-/-} animals (Figure 5c).

Finally, we examined possible redundancy between p53 and TAp73 in the induction of TIGAR expression after IR, by examining the effect of simultaneous deletion of

both transcription factors. Compared with WT animals, there was no significant decrease in TIGAR expression in the organs of p53^{-/-}TAp73^{-/-} mice (Figure 6a). Intestinal tissue from both WT and p53^{-/-}TAp73^{-/-} animals showed a similar increase in TIGAR protein expression following IR that was detected by western blot of tissue samples

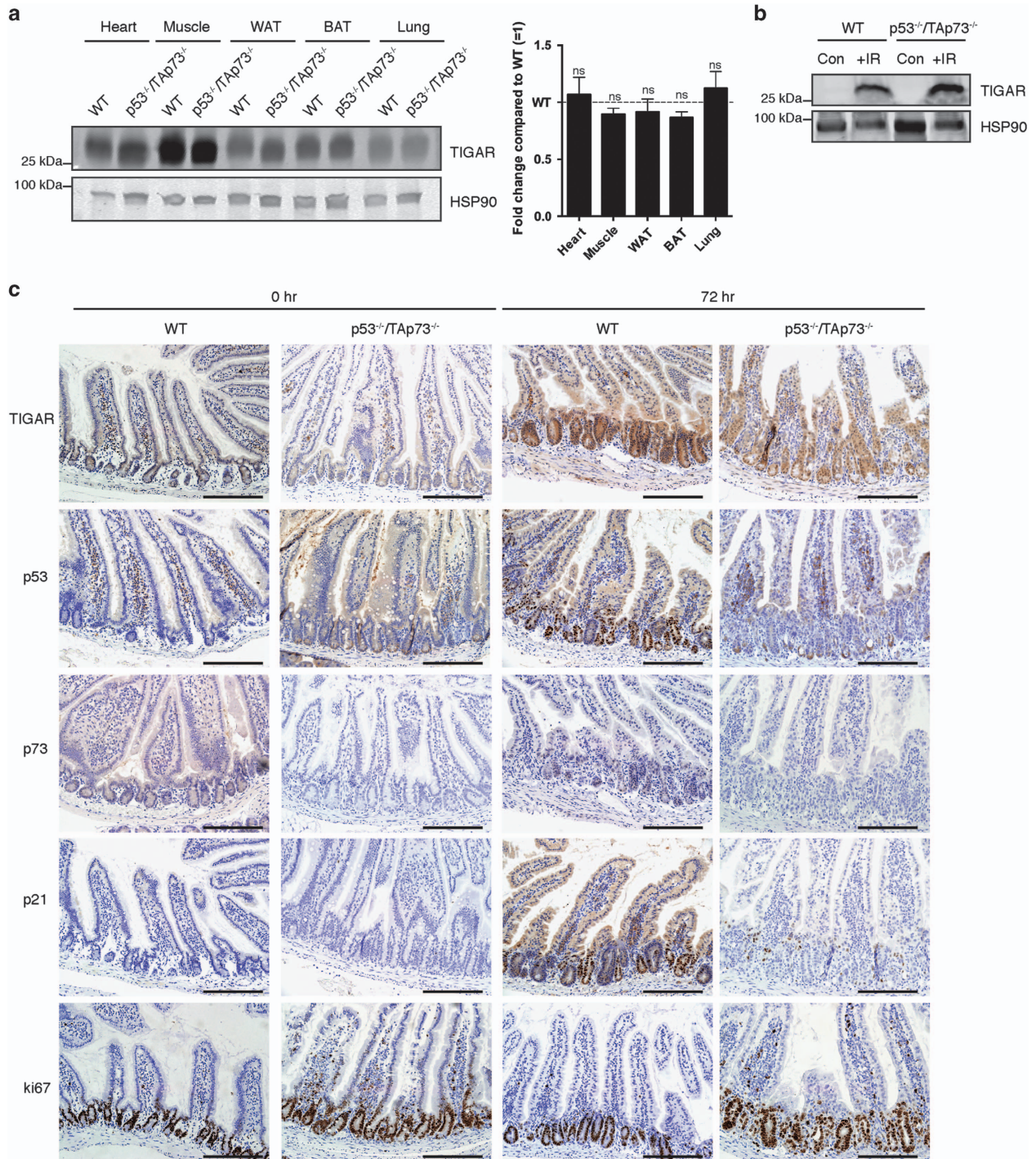


Figure 6 TIGAR expression in p53- and TAp73-null animals. (a) Left: Western blot analysis of TIGAR protein expression in organs of wild-type (WT) and p53^{-/-}/TAp73^{-/-} mice. Right: Graph represents quantification of western blots with fold change compared with WT. (b) Western blot analysis of TIGAR protein expression in small intestine tissue of WT and p53^{-/-}/TAp73^{-/-} mice 72 h after 10 Gy IR. Tissues were harvested from one experiment. (c) Immunohistochemistry on small intestines from WT and p53^{-/-}/TAp73^{-/-} animals 72 h after 10 Gy IR. Scale bar, 20 μ m. Values represent mean \pm S.E.M. of two independent experiments unless otherwise indicated. NS, not significant; WAT, white adipose tissue; BAT, brown adipose tissue

or IHC of crypts (Figures 6b and c). Taken together, these data show that the increase in TIGAR expression seen following IR and gut regeneration is not dependent on p53 or TAp73 in mouse.

Discussion

We have previously shown that TIGAR is induced following IR-induced intestinal damage and supports regeneration in the mouse. In humans, TIGAR is a p53 target gene and found to

have a role in conditions of mild stress to promote cell survival.^{2,5} We showed here that TAp73 can also activate expression from the TIGAR promoter in human cells. As IR can activate both p53²¹ and TAp73,^{32–34} we sought to test the hypothesis that the increase in TIGAR seen in mouse intestine following IR is a response to p53 and/or TAp73.

Our studies in cultured cells did not show a clear p53-dependent increase in TIGAR expression in mouse cells. A closer examination of the transcriptional control regions of human and mouse TIGAR showed that the principal p53-responsive element in human TIGAR is not well conserved in mouse TIGAR and is much less responsive to p53. The second, weaker binding site in humans seems to be conserved and somewhat more responsive to p53 in mouse. However, overall, the p53-binding sites in the human TIGAR promoter appear to be more responsive than those found in the mouse. TAp73 was also able to activate expression of mouse and human TIGAR-binding site reporters.

Despite the potential for both p53 and TAp73 to activate TIGAR expression, we found that although basal levels of TIGAR expression vary significantly between different mouse tissues, they are generally not affected by the loss of p53 or TAp73. Furthermore, the induction of TIGAR in mouse small intestine in response to IR does not depend on p53 or TAp73. Mice deficient for both p53 and TAp73 maintain a similar basal expression of TIGAR to WT animals and retain the ability to upregulate the expression of TIGAR in the crypts of the small intestine following tissue ablation. Importantly, several previous studies have shown p53-responsive expression of TIGAR in mouse cells and tissues such as the liver and heart, and p53 binding to the *Tigar* promoter was also detected in the liver.^{10,18–20} We also found a significant, but minor, reduction in TIGAR expression in p53 or TAp73-deficient muscle (Figures 2 and 5). Taken together, the data suggest that although p53 can induce TIGAR in some mouse tissues, the p53-responsiveness of mouse TIGAR expression is lower than observed in human cells. To some extent this difference reflects the binding of p53 to the different response elements in the mouse and human TIGAR-encoding genes. However, it is also possible that tissue or stress-specific co-factors (that may show human/mouse differences in expression or availability) are required to allow p53 regulation of TIGAR expression. Given the function of TIGAR as a regulator of metabolism, it will be of particular interest to see whether p53 family proteins with other co-factors can participate in the induction of TIGAR in response to different forms of metabolic stress.

TIGAR has been found to be elevated in several human tumour types.^{4,11,12} The expression of TIGAR under these conditions does not correlate with the maintenance of WT p53,¹³ suggesting that TIGAR overexpression in tumours can be uncoupled from the activity of p53. Our data show that mouse TIGAR expression is also regulated through p53-independent mechanisms, and is strongly activated in intestinal crypts following IR and APC deletion.¹¹ These observations suggest that activation of the Wnt signalling pathway may contribute to the regulation of TIGAR, particularly in the small intestine where this pathway has a key role in cell proliferation. Moreover, other transcription factors such as SP1 and CREB^{14,15} have been shown to have a role in regulating the basal expression of TIGAR in liver cancer cell

lines. Future studies will be required to establish how TIGAR expression is regulated during stress and whether deregulation of these pathways explains the elevated expression of TIGAR seen in human tumours.

Materials and Methods

Cell culture. All cell lines were cultured in Dulbecco's modified Eagle's medium (DMEM) supplemented with 10% of fetal bovine serum, 1% of glutamine, 1% of penicillin/streptomycin (Life Technologies, Paisley, UK), grown in a 37 °C incubator at 5% CO₂. CDDP (Sigma-Aldrich, St. Louis, MO, USA) was used at the indicated concentrations and times.

Small intestinal crypt culture. Small intestinal crypt culture was performed as previously described.³⁵ Small intestine was washed in cold PBS and villi were scraped off using a glass coverslip. The small intestine was then cut into small pieces and further washed in cold PBS. This was then transferred into PBS containing 2 mM EDTA and incubated for 30 min. Crypts were then obtained via mechanical pipetting and the supernatant containing the crypts was collected. The crypts were centrifuged at a low speed (700 r.p.m., 3 min) to remove single cells and the final pellet was resuspended in growth factor reduced Matrigel (BD, Franklin Lakes, NJ, USA). Crypts were cultured in Advanced DMEM/F-12 (Life Technologies) supplemented with 1% of glutamine, 1% of penicillin/streptomycin, 0.1% of AlbuMAX I (Life Technologies), 10 mM HEPES (Life Technologies), 0.05 µg/ml EGF (Peprotech, Rockyhill, NJ, USA), 0.1 µg/ml Noggin (Peprotech) and 0.5 µg/ml mR-spondin (R&D Systems, Minneapolis, MN, USA).

Animals. All animal work was carried out in-line with the Animals (Scientific Procedures) Act 1986 and the EU Directive 2010 and sanctioned by Local Ethical Review Process (University of Glasgow). The p53^{-/-36} and TAp73^{-/-37} animals have been previously described.

Western blot. Cell lysates were prepared in RIPA buffer with complete protease inhibitors (Roche, Penzberg, Germany), resolved via PAGE and transferred to nitrocellulose membranes. The following primary antibodies were used: Actin 1-I9-R (Santa Cruz Biotechnology, Dallas, TX, USA), cyclin D1 (Cell Signalling Technology, Danvers, MA, USA), CDK4 C-22 (Santa Cruz Biotechnology), HA.11 16B12 (Covance, Princeton, NJ, USA), HSP90 (Cell Signalling Technology), p21 C-19 (Santa Cruz Biotechnology), p53 1C12 (Cell Signalling Technology), p53 DO-1 (Santa Cruz Biotechnology), TIGAR G-2 (Santa Cruz Biotechnology) and TIGAR M-209 (Santa Cruz Biotechnology). Secondary antibodies were IRDye800CW-conjugated (LiCor Biosciences, Lincoln, NE, USA) and detection was performed using an Odyssey infrared scanner (LiCor Biosciences).

Gene expression analyses. RNA was isolated from cells or mouse tissue using the RNeasy RNA Isolation kit according to the manufacturer's instructions (Qiagen, Valencia, CA, USA). Mouse TIGAR primer was purchased from Qiagen and mouse GAPDH was used as murine housekeeping gene (Primer Design, Southampton, UK).

mRNA primer sequences (5' → 3'):

Human TIGAR for	CGGCATGGAGAAAGAAGATT
Human TIGAR rev	TCCTTTCCCGAAGTCTTGAG
Human p21 for	CTGGAGACTCTCAGGGTCGAAA
Human p21 rev	GATTAGGGCTTCTCTTGAGAGAA
Human p53 for	CCCTTCCAGAAAACCTACC
Human p53 rev	CTCCGTCATGTGCTGTGACT
Human RPLP0 for	GCAATGTTGCCAGTGTCTG
Human RPLP0 rev	GCCTTGACCTTTTCAGCAA
Mouse p21 for	GGCCCCGAACATCTCAGG
Mouse p21 rev	AAATCTGTCAAGGCTGGTCTGC
Mouse p53 for	CACGTACTCTCCTCCCCTCAAT
Mouse p53 rev	AACTGCACAGGGCACGTCTT
Mouse TAp73 for	GCACCTACTTTGACCTCCCC
Mouse TAp73 rev	GCACTACTTGACAAATTGAAAC

IR treatment. Gamma IR-induced intestinal damage was performed as previously described.³⁸

Immunohistochemistry. Immunohistochemistry was performed as previously described.³⁹ Primary antibodies used were: TIGAR (Merck Millipore, Darmstadt, Germany), p53 CM-5 (Vector Laboratories, Peterborough, UK), p21 M-19 (Santa Cruz Biotechnology), p73 S-20 (Santa Cruz Biotechnology) and Ki67 (Thermo Scientific, Waltham, MA, USA).

Plasmids. pcDNA3.1+ (Invitrogen, Grand Island, NY, USA) was used as empty vector control. iRFP reporter constructs were generated as previously described.²³ Reporter elements were ligated into vectors using the InFusion HD Eco Dry system (Clontech, Saint-Germain-en-Laye, France) according to the manufacturer's instructions.

Insert primer sequences (5' → 3'):

TIGAR hBS1 for	GGACTAGTCCACAAAGCAAGTCT
TIGAR hBS1 rev	AGACTTGTCTTTGTGGACTAGTCC
TIGAR-hBS2 for	AGACATGTCCACGACTTGTCTGGGTAC
TIGAR-hBS2 rev	GTACCCAGACAAGTCTGTGGACATGTCT
TIGAR-mBS1 for	TAACCTGTTCTTTACTTGGAACTTGCTT
TIGAR-mBS1 rev	AAGCAAGTTCCAAGTAAAGAACAAGTTA
TIGAR-mBS2 for	GAAGACATGTCCCGGCCTCTCGACT
TIGAR-mBS2 rev	AGTCGAGAGGCCGGGTCATGTCTTC
p53RE for	GGACATGCCCGGGCATGTCCCCAGAGACAT
	GTCCAGACATGTCCCGAGGAACATGTCCCAA
	CATGTTGTCCAGGAGACATGTCCAGACATGTC
	CCCAGGAACATGTCCCAACATGTTGT
p53RE rev	ACAACATGTTGGGACATGTTCTGGGACATG
	TCTGGACATGTCTCTGGACAACATGTTGGGA
	CATGTTCTGGGACATGTCTGGACATGTCTC
	TGGGGACATGCCCGGGCATGTCC
WAF1 for	GAACATGTCCCAACATGTTG
WAF1 rev	CAACATGTTGGGACATGTTT
BPAG1 for	CGCCATGCATGAATCCGCGTTCTGCCTGCT
	TTGTTCACTAGTTAGGCACTAGTTAGGCGTGTA
BPAG1 rev	TACACGCCTAAGTGCCTACAAGTATGAACA
	AAGCAGGCAGAACGCGGAATTCATGCATGGCC

Transient transfections and irfp reporter assays. Cells were seeded on 6-well plates for protein expression analysis or 96-well CellBIND clear bottom black microplates (Corning, Corning, NY, USA) for iRFP reporter assays and grown overnight prior to being transfected using GeneJuice (Merck Millipore) according to the manufacturer's manual. Twenty-four hours after co-transfection, cells were harvested as described above for protein expression analysis or scanned using an Odyssey infrared scanner (LiCor Biosciences). For quantification, plates were scanned at 169 μm resolution, 3.5 mm offset and a low-intensity setting.²³

Chromatin-immunoprecipitation. Assays were performed as previously described.⁴⁰ Cells were seeded in a 10-cm plate in DMEM and allowed to grow for 24 h before treatment with CDDP for 24 h.

Quantification and statistical analysis. Image Studio software (LiCor, V2.1.10) was used to quantify western blots as well as iRFP reporter assays on 96-well plates. The data represent mean values ± S.E.M. from at least three independent experiments ($n=3$) unless otherwise noted. All P values were obtained using a t -test.

Conflict of Interest

The authors declare no conflict of interest.

Acknowledgements. We are extremely thankful to Dimitris Athineos and Karen Blyth for providing p53 and Tap73 null mice, Cancer Research UK Glasgow Centre (C596/A18076), Cancer Research UK Beatson Institute Biological Services (C596/A17196) and Histology Service for technical assistance. We also acknowledge generous funding from Cancer Research UK grant C596/A10419, ERC Grant 322842-METABOp53 and an MRC studentship.

1. Lee P, Vousden KH, TIGAR Cheung EC. TIGAR, burning bright. *Cancer Metab* 2014; **2**: 1.
2. Bensaad K, Tsuruta A, Selak MA, Vidal MN, Nakano K, Bartrons R et al. TIGAR, a p53-inducible regulator of glycolysis and apoptosis. *Cell* 2006; **126**: 107–120.

3. Cheung EC, Ludwig RL, Vousden KH. Mitochondrial localization of TIGAR under hypoxia stimulates HK2 and lowers ROS and cell death. *Proc Natl Acad Sci USA* 2012; **109**: 20491–20496.
4. Wanka C, Steinbach JP, Rieger J. Tp53-induced glycolysis and apoptosis regulator (TIGAR) protects glioma cells from starvation-induced cell death by up-regulating respiration and improving cellular redox homeostasis. *J Biol Chem* 2012; **287**: 33436–33446.
5. Bensaad K, Cheung EC, Vousden KH. Modulation of intracellular ROS levels by TIGAR controls autophagy. *The EMBO J* 2009; **28**: 3015–3026.
6. Yin L, Kosugi M, Kufe D. Inhibition of the MUC1-C oncoprotein induces multiple myeloma cell death by down-regulating TIGAR expression and depleting NADPH. *Blood* 2012; **119**: 810–816.
7. Lui VW, Wong EY, Ho K, Ng PK, Lau CP, Tsui SK et al. Inhibition of c-Met downregulates TIGAR expression and reduces NADPH production leading to cell death. *Oncogene* 2011; **30**: 1127–1134.
8. Li M, Sun M, Cao L, Gu JH, Ge J, Chen J et al. A TIGAR-regulated metabolic pathway is critical for protection of brain ischemia. *J Neurosci* 2014; **34**: 7458–7471.
9. Gerin I, Noel G, Bolsee J, Haumont O, Van Schaefingen E, Bommer GT. Identification of TP53-induced glycolysis and apoptosis regulator (TIGAR) as the phosphoglycolate-independent 2,3-bisphosphoglycerate phosphatase. *Biochem J* 2014; **458**: 439–448.
10. Hamard PJ, Barthelemy N, Hogstad B, Mungamuri SK, Tonnessen CA, Carvajal LA et al. The C terminus of p53 regulates gene expression by multiple mechanisms in a target- and tissue-specific manner in vivo. *Genes Dev* 2013; **27**: 1868–1885.
11. Cheung EC, Athineos D, Lee P, Ridgway RA, Lambie W, Nixon C et al. TIGAR is required for efficient intestinal regeneration and tumorigenesis. *Dev Cell* 2013; **25**: 463–477.
12. Sinha S, Ghildiyal R, Mehta VS, Sen E. ATM-NFκB axis-driven TIGAR regulates sensitivity of glioma cells to radiomimetics in the presence of TNFα. *Cell Death Dis* 2013; **4**: e615.
13. Won KY, Lim SJ, Kim GY, Kim YW, Han SA, Song JY et al. Regulatory role of p53 in cancer metabolism via SCO2 and TIGAR in human breast cancer. *Hum Pathol* 2012; **43**: 221–228.
14. Zou S, Gu Z, Ni P, Liu X, Wang J, Fan Q. SP1 plays a pivotal role for basal activity of TIGAR promoter in liver cancer cell lines. *Mol Cell Biochem* 2012; **359**: 17–23.
15. Zou S, Wang X, Deng L, Wang Y, Huang B, Zhang N et al. CREB, another culprit for TIGAR promoter activity and expression. *Biochem Biophys Res Commun* 2013; **439**: 481–486.
16. Lee CW, La Thangue NB. Promoter specificity and stability control of the p53-related protein p73. *Oncogene* 1999; **18**: 4171–4181.
17. Yang A, Kaghad M, Wang Y, Gillett E, Fleming MD, Dotsch V et al. p63, a p53 homolog at 3q27-29, encodes multiple products with transactivating, death-inducing, and dominant-negative activities. *Mol Cell* 1998; **2**: 305–316.
18. Li T, Kon N, Jiang L, Tan M, Ludwig T, Zhao Y et al. Tumor suppression in the absence of p53-mediated cell-cycle arrest, apoptosis, and senescence. *Cell* 2012; **149**: 1269–1283.
19. Kimata M, Matoba S, Iwai-Kanai E, Nakamura H, Hoshino A, Nakaoka M et al. p53 and TIGAR regulate cardiac myocyte energy homeostasis under hypoxic stress. *Am J Physiol Heart Circ Physiol* 2010; **299**: H1908–H1916.
20. Hoshino A, Matoba S, Iwai-Kanai E, Nakamura H, Kimata M, Nakaoka M et al. p53-TIGAR axis attenuates mitophagy to exacerbate cardiac damage after ischemia. *J Mol Cell Cardiol* 2012; **52**: 175–184.
21. Merritt AJ, Potten CS, Kemp CJ, Hickman JA, Balmain A, Lane DP et al. The role of p53 in spontaneous and radiation-induced apoptosis in the gastrointestinal tract of normal and p53-deficient mice. *Cancer Res* 1994; **54**: 614–617.
22. Komarova EA, Kondratov RV, Wang K, Christov K, Golovkina TV, Goldblum JR et al. Dual effect of p53 on radiation sensitivity in vivo: p53 promotes hematopoietic injury, but protects from gastro-intestinal syndrome in mice. *Oncogene* 2004; **23**: 3265–3271.
23. Hock AK, Lee P, Maddocks OD, Mason SM, Blyth K, Vousden KH. iRFP is a sensitive marker for cell number and tumor growth in high-throughput systems. *Cell Cycle* 2014; **13**: 220–226.
24. el-Deiry WS, Tokino T, Velculescu VE, Levy DB, Parsons R, Trent JM et al. WAF1, a potential mediator of p53 tumor suppression. *Cell* 1993; **75**: 817–825.
25. Osada M, Nagakawa Y, Park HL, Yamashita K, Wu G, Kim MS et al. p63-specific activation of the BPAG-1 promoter. *J Invest Dermatol* 2005; **125**: 52–60.
26. Liu G, Chen X. The C-terminal sterile alpha motif and the extreme C terminus regulate the transcriptional activity of the alpha isoform of p73. *J Biol Chem* 2005; **280**: 20111–20119.
27. Zhu J, Jiang J, Zhou W, Chen X. The potential tumor suppressor p73 differentially regulates cellular p53 target genes. *Cancer Res* 1998; **58**: 5061–5065.
28. Ishimoto O, Kawahara C, Enjo K, Obinata M, Nukiwa T, Ikawa S. Possible oncogenic potential of DeltaNp73: a newly identified isoform of human p73. *Cancer Res* 2002; **62**: 636–641.
29. Liu G, Nozell S, Xiao H, Chen X. DeltaNp73beta is active in transactivation and growth suppression. *Mol Cell Biol* 2004; **24**: 487–501.
30. Moll UM, Slade N. p63 and p73: roles in development and tumor formation. *Mol Cancer Res* 2004; **2**: 371–386.
31. Nozell S, Wu Y, McNaughton K, Liu G, Willis A, Paik JC et al. Characterization of p73 functional domains necessary for transactivation and growth suppression. *Oncogene* 2003; **22**: 4333–4347.
32. Agami R, Blandino G, Oren M, Shaul Y. Interaction of c-Abl and p73alpha and their collaboration to induce apoptosis. *Nature* 1999; **399**: 809–813.

33. Gong JG, Costanzo A, Yang HQ, Melino G, Kaelin WG Jr., Levrero M *et al*. The tyrosine kinase c-Abl regulates p73 in apoptotic response to cisplatin-induced DNA damage. *Nature* 1999; **399**: 806–809.
34. Yuan ZM, Shioya H, Ishiko T, Sun X, Gu J, Huang YY *et al*. p73 is regulated by tyrosine kinase c-Abl in the apoptotic response to DNA damage. *Nature* 1999; **399**: 814–817.
35. Sato T, Vries RG, Snippert HJ, van de Wetering M, Barker N, Stange DE *et al*. Single Lgr5 stem cells build crypt-villus structures in vitro without a mesenchymal niche. *Nature* 2009; **459**: 262–265.
36. Donehower LA, Harvey M, Slagle BL, McArthur MJ, Montgomery CA Jr., Butel JS *et al*. Mice deficient for p53 are developmentally normal but susceptible to spontaneous tumours. *Nature* 1992; **356**: 215–221.
37. Tomasini R, Tsuchihara K, Wilhelm M, Fujitani M, Rufini A, Cheung CC *et al*. TAp73 knockout shows genomic instability with infertility and tumor suppressor functions. *Genes Dev* 2008; **22**: 2677–2691.
38. Ashton GH, Morton JP, Myant K, Pheasant TJ, Ridgway RA, Marsh V *et al*. Focal adhesion kinase is required for intestinal regeneration and tumorigenesis downstream of Wnt/c-Myc signaling. *Dev Cell* 2010; **19**: 259–269.
39. Sansom OJ, Reed KR, Hayes AJ, Ireland H, Brinkmann H, Newton IP *et al*. Loss of Apc in vivo immediately perturbs Wnt signaling, differentiation, and migration. *Genes Dev* 2004; **18**: 1385–1390.
40. Vigneron AM, Ludwig RL, Vousden KH. Cytoplasmic ASPP1 inhibits apoptosis through the control of YAP. *Genes Dev* 2010; **24**: 2430–2439.



Cell Death and Disease is an open-access journal published by **Nature Publishing Group**. This work is licensed under a **Creative Commons Attribution 4.0 International License**. The images or other third party material in this article are included in the article's Creative Commons license, unless indicated otherwise in the credit line; if the material is not included under the Creative Commons license, users will need to obtain permission from the license holder to reproduce the material. To view a copy of this license, visit <http://creativecommons.org/licenses/by/4.0/>

Supplementary Information accompanies this paper on Cell Death and Disease website (<http://www.nature.com/cddis>)

TIGAR Is Required for Efficient Intestinal Regeneration and Tumorigenesis

Eric C. Cheung,¹ Dimitris Athineos,¹ Pearl Lee,¹ Rachel A. Ridgway,¹ Wendy Lambie,¹ Colin Nixon,¹ Douglas Strathdee,¹ Karen Blyth,¹ Owen J. Sansom,¹ and Karen H. Vousden^{1,*}

¹CR-UK Beatson Institute, Switchback Road, Glasgow G61 1BD, UK

*Correspondence: k.vousden@beatson.gla.ac.uk

<http://dx.doi.org/10.1016/j.devcel.2013.05.001>

Open access under [CC BY-NC-ND license](https://creativecommons.org/licenses/by-nc-nd/4.0/).

SUMMARY

Regulation of metabolic pathways plays an important role in controlling cell growth, proliferation, and survival. TIGAR acts as a fructose-2,6-bisphosphatase, potentially promoting the pentose phosphate pathway to produce NADPH for antioxidant function and ribose-5-phosphate for nucleotide synthesis. The functions of TIGAR were dispensable for normal growth and development in mice but played a key role in allowing intestinal regeneration *in vivo* and in *ex vivo* cultures, where growth defects due to lack of TIGAR were rescued by ROS scavengers and nucleosides. In a mouse intestinal adenoma model, TIGAR deficiency decreased tumor burden and increased survival, while elevated expression of TIGAR in human colon tumors suggested that deregulated TIGAR supports cancer progression. Our study demonstrates the importance of TIGAR in regulating metabolism for regeneration and cancer development and identifies TIGAR as a potential therapeutic target in diseases such as ulcerative colitis and intestinal cancer.

INTRODUCTION

The ability to regulate metabolic pathways is key to maintaining normal health and homeostasis, and defects in these responses contribute to major diseases such as diabetes and cancer. Modulation of metabolic pathways plays an important role in tumorigenesis, where metabolic transformation underpins the abnormal growth, proliferation, and survival of cancer cells. The expression of the M2 isoform of pyruvate kinase, for example, allows the diversion of glycolytic intermediates into various anabolic pathways (including the pentose phosphate pathway [PPP]) to support cancer cell growth (Anastasiou et al., 2011; Ye et al., 2012). The use of glutamine for anaplerosis (Wise and Thompson, 2010) and the expression of mutant forms of isocitrate dehydrogenase (Borodovsky et al., 2012) are further examples where altered metabolism plays a role in promoting oncogenic transformation. Components of many metabolic pathways are modified by both tumor suppressors and oncogenes, and drugs that target metabolic enzymes are being developed as cancer therapies (Cairns et al., 2011; Dang, 2012). How-

ever, the contribution of these enzymes to tumor development and the balance between their roles in allowing normal cell growth and supporting cancer progression are not well explored *in vivo*, possibly due to the fact that modulation of many of these enzymes is deleterious to embryonic development (Piruat et al., 2004; Pollard et al., 2007; Yang et al., 2010b).

TIGAR functions as a fructose-2,6-bisphosphatase (Fru-2,6-BPase), decreasing the intracellular levels of fructose-2,6-bisphosphate (Fru-2,6-BP) and thereby lowering the activity of PFK1 and flux through the main glycolytic pathway. As a consequence, glucose metabolism may be diverted into the PPP, and TIGAR has been shown to support increased production of NADPH and antioxidant activity through the generation of reduced glutathione (Bensaad et al., 2006; Bensaad and Vousden, 2007; Li and Jogi, 2009; Wanka et al., 2012). Several studies have shown the importance of TIGAR in controlling reactive oxygen species (ROS) in tissue culture systems (Bensaad et al., 2006, 2009; Yin et al., 2012) and elevated expression of TIGAR has been reported in some cancer models (Wanka et al., 2012; Won et al., 2012).

The potential importance of TIGAR in tumor development is illustrated by a study showing that the depletion of PFKFB4 (an enzyme with fructose-2,6-bisphosphatase activity like TIGAR) and the subsequent decrease in ROS scavengers can inhibit tumor growth in a xenograph model (Ros et al., 2012). An RNA interference screen in glioma stem-like cells also identified *PFKFB4* as an essential gene for tumor survival (Gojts et al., 2012). Furthermore, additional consequences of promotion of the PPP, including the support of other anabolic reactions that require NADPH, such as fatty acid synthesis, and the generation of ribose phosphate for DNA synthesis and repair (Deberardinis et al., 2008; Kroemer and Pouyssegur, 2008; Tong et al., 2009; Vander Heiden et al., 2009) may play a role in tumor development. Taken together, it is possible that expression of TIGAR and subsequent changes in metabolic pathway utilization could help to promote tumor development. However, the overall contribution of TIGAR to normal growth and development has not been determined.

TIGAR was initially identified as a transcriptional target of p53 (Bensaad et al., 2006). p53 is a critical tumor suppressor protein that functions to prevent the growth or survival of cells that are undergoing malignant progression by inducing apoptosis or senescence in response to oncogenic stress. However, more recent studies have shown that p53 can also function to control metabolism (Vousden and Ryan, 2009), and TIGAR contributes to this activity of p53. The activation of TIGAR and other genes by p53 promotes an antioxidant response (Bensaad et al.,

2006; Budanov et al., 2004; Cosentino et al., 2011), which helps cells to survive transient or low levels of stress, and has recently also been suggested to play a key role in preventing malignant progression (Li et al., 2012). However, TIGAR overexpression has also been described in a few tumor types (Wanka et al., 2012; Won et al., 2012), raising the possibility that deregulated expression of TIGAR may play a role in supporting, rather than inhibiting, cancer development.

In order to determine the role of TIGAR in normal development and its contribution to proliferation under conditions of tissue repair or malignant growth, we generated TIGAR-deficient mice. While TIGAR does not appear to be essential for normal development, animals lacking TIGAR show a clear defect in their ability to mount a proliferative response in adult tissue, either in response to tissue damage or tumor development. TIGAR levels are elevated in mouse and human tumors and tumor cell lines, regardless of the presence or absence of wild-type (WT) p53, and a reduction of TIGAR increased survival in a mouse model of intestinal adenoma. Taken together, our data show that TIGAR contributes to both tissue regeneration and tumor development.

RESULTS

Generation of TIGAR-Deficient Mice

Two independent approaches were taken to generate TIGAR-deficient mice. A constitutive deletion was generated using a genetrapp construct from EUCOMM, in which the targeting vector was inserted between exons 2 and 3 of the *TIGAR* gene (Figure S1A available online). Lack of TIGAR protein expression was confirmed by western blotting lysates from various tissues derived from these mice (Figure 1A). Deletion of *TIGAR* did not lead to obvious developmental problems, and *TIGAR*^{-/-} mice were born at the expected Mendelian ratio (Figure 1B). In parallel, we also generated a conditional *TIGAR*^{fl/fl} mouse by targeting exon 3, the deletion of which resulted in a frame shift and complete loss of expression of TIGAR protein in the presence of the germline deleter cre (Figures S1B and S1C).

Much of the analysis of TIGAR function to date has been carried out in human cells (Bensaad et al., 2006; Li and Jogi, 2009), and to confirm a similar function of mouse TIGAR, we tested baby mouse kidney (BMK) cells derived from *TIGAR*^{-/-} mice for Fru-2,6-BP levels and reduced glutathione (GSH)/oxidized glutathione (GSSG) ratios (Figures 1C–1E). Cells lacking TIGAR showed increased Fru-2,6-BP levels and lower GSH/GSSG ratios. These results are therefore consistent with the described role of human TIGAR as a Fru-2,6-BPase that increases NADPH and subsequently lowers the GSH/GSSG ratio (Bensaad et al., 2006; Li and Jogi, 2009). As expected, TIGAR-deficient cells were more sensitive to oxidative stress following treatment with H₂O₂ (Figure 1F). Reintroduction of human TIGAR into these cells to levels comparable with those seen in WT cells (Figure 1C) rescued these phenotypes (Figures 1D and 1F), confirming that the effects seen were due to the lack of TIGAR in these cells and that mouse TIGAR functions similarly to human TIGAR.

TIGAR Is Required for Small Intestine Proliferation after Acute Damage

While lack of TIGAR in developing embryos or unstressed adults did not result in a clear change in phenotype, we considered that

TIGAR expression may play a more important role under conditions of stress in adult tissue. To address this question, we focused on the intestine as an organ in which cell proliferation plays an important role during regeneration following tissue ablation. Analysis of small intestine (Figure 1G) or colon (Figure 1H) from untreated mice showed normal intestinal crypt architecture and proliferation in TIGAR-deficient mice compared to WT animals. TIGAR protein expression in WT animals was localized mainly in the intestinal crypt (Figures 1G and 1H), where most of the proliferation occurs. Importantly, no staining was seen in the intestines or colon of TIGAR-null mice.

To examine the role of TIGAR in proliferation and regeneration of adult intestinal epithelium, we turned to well-defined models in which ablation of intestinal epithelium by irradiation (IR) or treatment with a genotoxic drug is followed by a period of recovery and rapid tissue regeneration. In WT mice, small intestinal regeneration is characterized by a rapid regrowth of intestinal crypts, which can be seen 72 hr following treatment with 14 Gy IR (Figures 2A and 2B). By comparison, TIGAR-deficient mice showed a significant reduction in both the size and number of regenerating crypts (Figures 2A and 2B). To determine the underlying cause of this defect, we examined both proliferation and cell death in the small intestine of mice after IR. Using the proliferation marker Ki67, it was clear that while both WT and *TIGAR*^{-/-} mice showed an initial decrease in proliferation 24 hr post-IR, only the WT animals moved to a phase of rapid proliferation that was evident 48 and 72 hr post-IR and was consistent with the outgrowth of new crypt structures (Figures 2C and 2D). The *TIGAR*^{-/-} mice showed a clear defect in proliferation at these time points (Figures 2C and 2D). Measurements of cell death in the intestine indicated an increase in the number of dying cells in the *TIGAR*^{-/-} compared to WT intestines 6 hr post-IR (Figures 2E and 2F), although by 24 or 48 hr minimal cell death was detected in mice of either genotype. Analysis of progenitor cells using immunohistochemistry of markers such as LGR5 or Olfm4 (van der Flier et al., 2009) revealed a similar staining pattern between *TIGAR*^{-/-} and WT animals (Figure S2A). The staining intensity was somewhat reduced in TIGAR-deficient animals after acute injury (Figure S2A), although the interpretation of this effect is limited by the difficulty in finding intact crypts to stain after damage. Taken together with the data showing only a transient increase in apoptosis in TIGAR-null intestines 6 hr after damage (Figures 2E and 2F), these results suggest that the defects in proliferation in the absence of TIGAR are not simply the result of massive apoptosis during the period of maximal regeneration (24–48 hr) or complete depletion of the stem cell population at an earlier time point, but also reflect a failure to proliferate.

Consistent with the role of TIGAR in supporting intestinal proliferation after damage, TIGAR immunostaining in WT tissues revealed a marked and sustained increase in TIGAR expression in intestinal crypts 24 and 72 hr after IR (Figure 2G). Previous studies have demonstrated a role of TIGAR in lowering ROS (Bensaad et al., 2006; Li and Jogi, 2009; Wanka et al., 2012), and we have shown that TIGAR-deficient BMK cells have less GSH and are more sensitive to H₂O₂ (Figures 1E and 1F). Analysis of intestinal tissue for markers of ROS accumulation also showed an increase in MDA (malondialdehyde, an indicator for lipid peroxidation) staining after IR in *TIGAR*^{-/-} mice compared to WT animals (Figure 2H), indicating that TIGAR is also important to limit

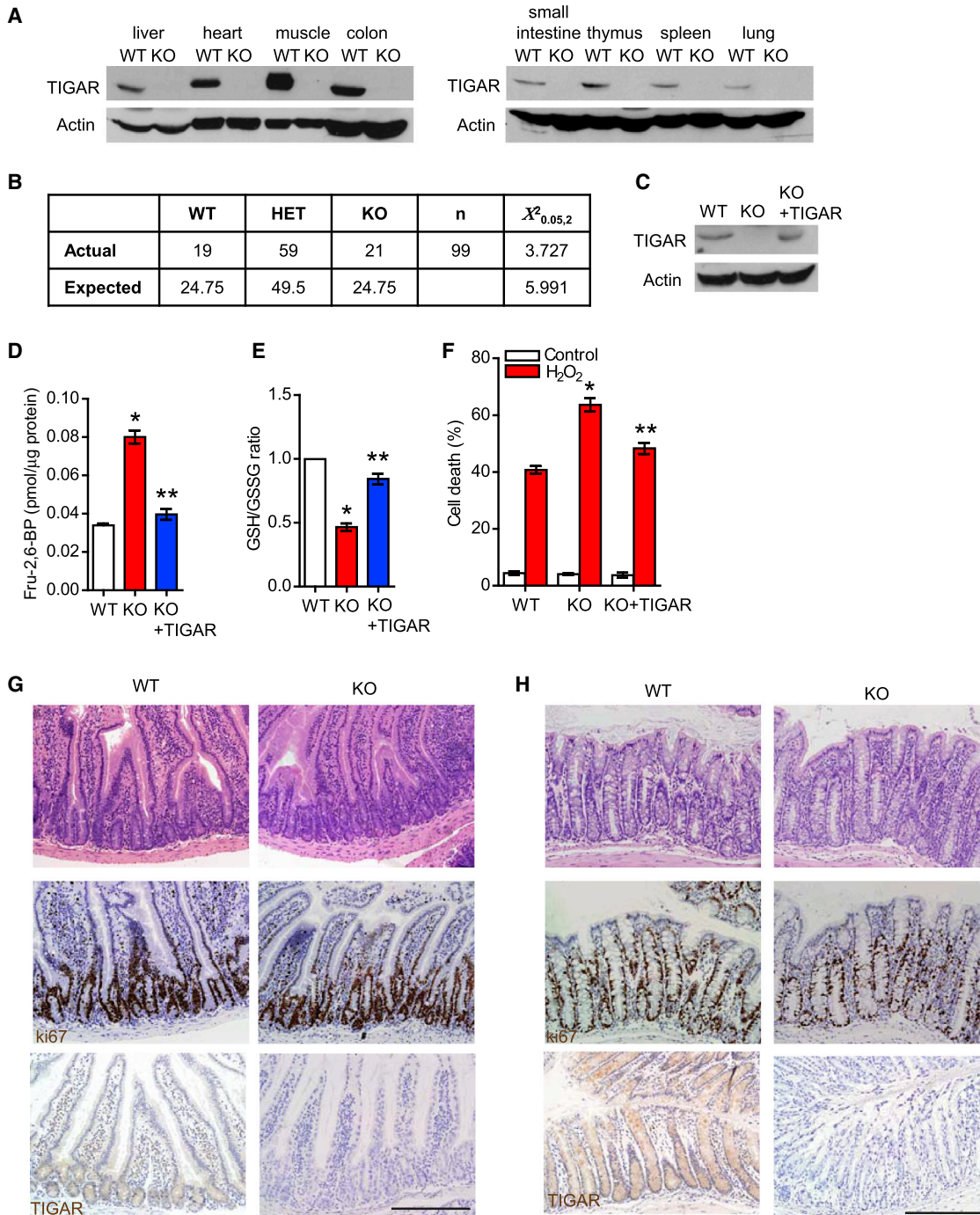


Figure 1. TIGAR-Deficient Mice

(A) Western blot analysis of the indicated tissues from WT and TIGAR-deficient animals.

(B) Mendelian ratio from *TIGAR*^{+/-} matings.

(C) Western blot analysis of baby mouse kidney (BMK) cultures from wild-type (WT), *TIGAR*^{-/-} (KO), and KO cultures transfected with human TIGAR construct. (D) Level of fructose-2,6-bisphosphate in WT, KO, and KO BMK cell cultures transfected with TIGAR construct (KO + TIGAR). *p < 0.05 compared to WT; **p < 0.05 compared to KO.

(E) Ratio of oxidized and reduced glutathione (GSH/GSSG) of WT, KO, and KO + TIGAR BMK cells. *p < 0.05 compared to WT; **p < 0.05 compared to KO.

(F) Cell death as measured by PI exclusion of WT, KO, and KO + TIGAR BMK cells after hydrogen peroxide treatment. *p < 0.05 compared to WT; **p < 0.05 compared to KO.

(G and H) Untreated small intestine (G) and colon (H) from WT and KO animals. Top: hematoxylin and eosin staining (H&E); middle: Ki67; bottom: TIGAR staining. Scale bar, 200 μm. Data are represented as mean ± SEM (n = at least 3).

See also Figure S1.

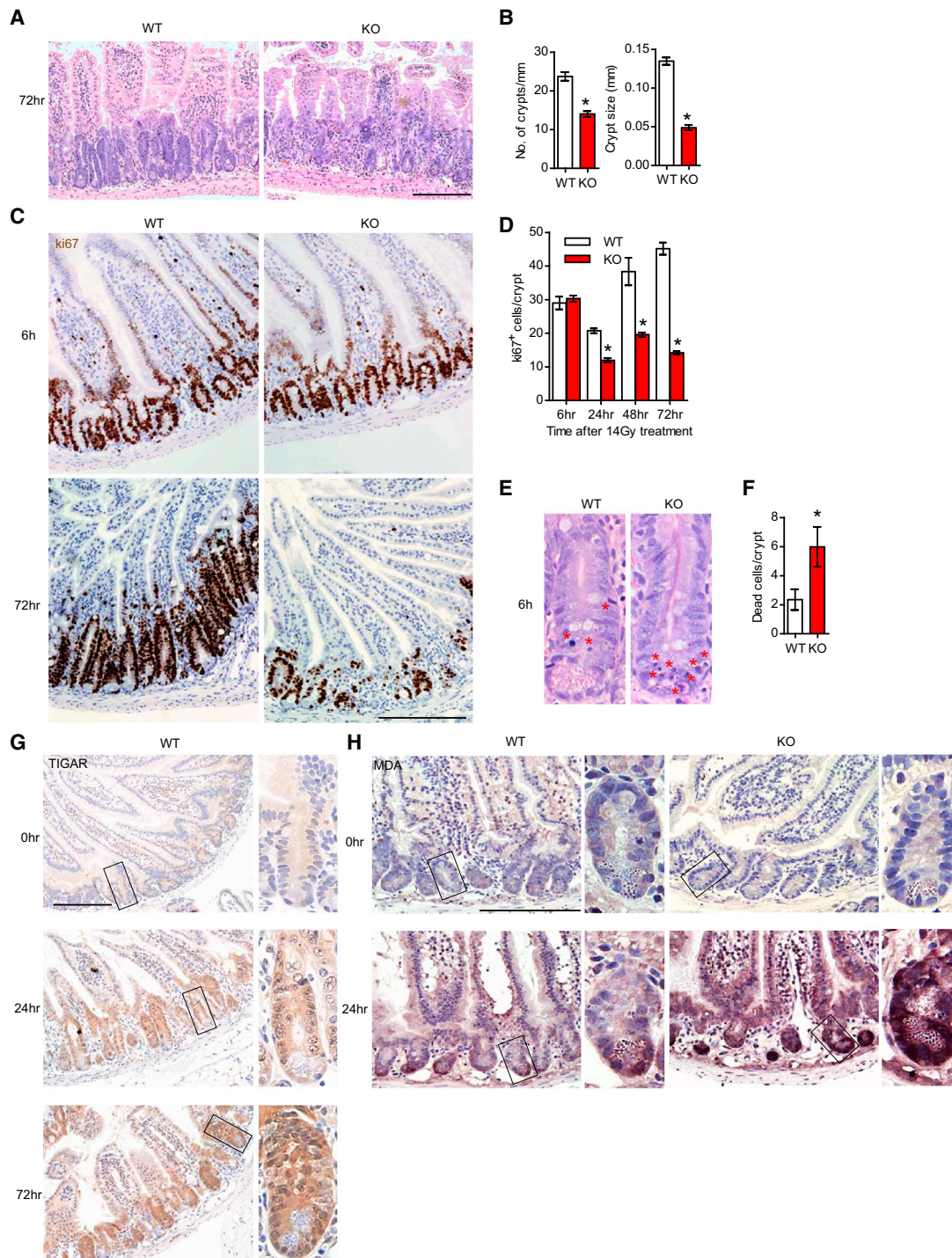


Figure 2. TIGAR-Deficient Mice Have Reduced Regenerative Capacity in the Intestinal Crypt after 14 Gy Whole-Body IR

(A) Small intestine from WT and *TIGAR*^{-/-} (KO) animals 72 hr after 14 Gy IR. Bar = 200 μ m.

(B) Number of crypts per millimeter (left) and size of crypts (right) 72 hr after 14 Gy IR. * $p < 0.05$ compared to WT.

(C) Ki67 staining of WT and KO intestines 6 and 72 hr after 14 Gy IR. Bar = 200 μ m.

(D) Quantification of Ki67⁺ cells at the indicated times after 14 Gy IR. * $p < 0.05$ compared to WT.

(E) Apoptosis in the small intestine 6 hr after 14 Gy IR. Asterisks denote cells with apoptotic nuclear morphology.

(F) Number of apoptotic cells in the crypts 6 hr after 14 Gy IR. * $p < 0.05$ compared to WT.

(G) TIGAR staining of WT animals before IR and 24 and 72 hr after 14 Gy IR. Scale bar, 200 μ m. Panels show details of crypt structures indicated in the box.

(H) Malondialdehyde (MDA) staining of WT and KO animals before and 24 hr after 14 Gy IR. Scale bar, 200 μ m. Data are represented as mean \pm SEM (n = at least 3). See also Figure S2.

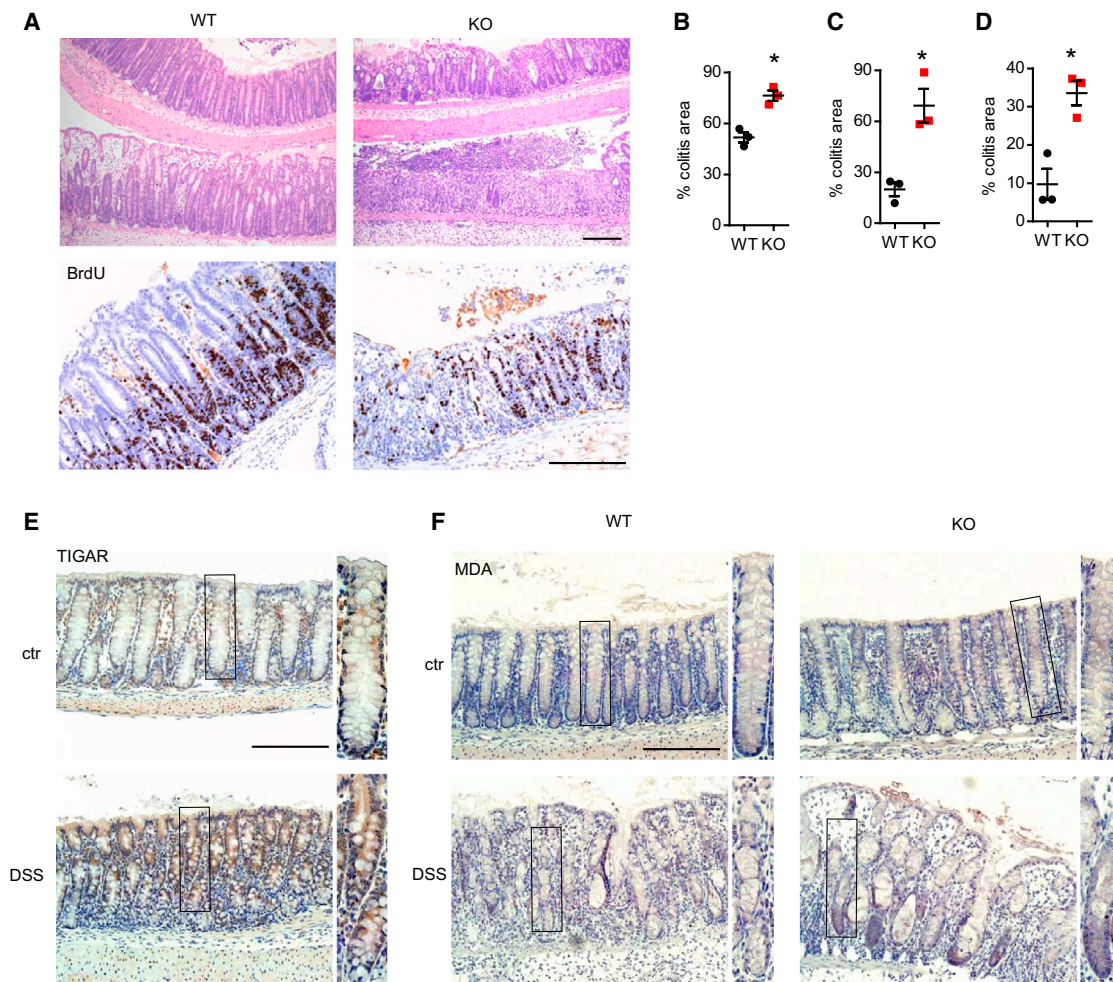


Figure 3. TIGAR-Deficient Mice Are More Sensitive to DSS-Induced Colitis

(A) Colon from WT and *TIGAR*^{-/-} (KO) animals 2 days after 2% DSS treatment. Top: H&E; bottom: BrdU staining. Bar = 200 μ m.

(B) Percentage of colitis area one day after 3.5% DSS in WT and KO animals. * $p < 0.05$ compared to WT.

(C) Percentage of colitis area one day after 2% DSS in WT and KO animals. * $p < 0.05$ compared to WT.

(D) Percentage of colitis area 2 days after 2% DSS in WT and KO animals. * $p < 0.05$ compared to WT.

(E) TIGAR staining in WT animals, untreated (ctr) or after 3.5% DSS treatment. Scale bar, 200 μ m. Panels show details of crypt structures indicated in the box.

(F) MDA staining of WT and KO animals before and after 2% DSS treatment. Scale bar, 200 μ m. Data are represented as mean \pm SEM ($n =$ at least 3).

See also Figure S3.

ROS levels in vivo. The importance of TIGAR in response to IR damage is underscored by similar effects observed following damage induced by cisplatin (Figure S2). After cisplatin treatment, *TIGAR*^{-/-} mice showed a reduced ability to regenerate crypts (Figures S2B and S2C), which was accompanied by a decrease in proliferation (Figures S2D and S2E) and an increase in apoptosis at early time point (Figures S2F and S2G).

TIGAR Is Required for Colon Regeneration in a Model of Ulcerative Colitis

The results described above revealed an interesting role for TIGAR in supporting tissue growth and survival under conditions of rapid regeneration in adult mice, consistent with the proposed metabolic function of TIGAR. To determine whether TIGAR can also play a role in recovery following damage in a different setting, we investigated a model of ulcerative colitis in the colon.

Treatment of mice with dextran sulfate sodium (DSS) over several days resulted in an ablation of colon epithelium, followed by inflammation and hyperproliferation of the crypts to allow for repair (Cooper et al., 1993). While the resting colons of WT and TIGAR-deficient mice were indistinguishable (Figure 1H), the extensive formation of new crypts seen in WT colons following DSS treatment and recovery was much less apparent in *TIGAR*^{-/-} animals (Figure 3A). Furthermore, compared to WT mice, there is a defect in proliferation in TIGAR-deficient animals after DSS treatment, as indicated by bromodeoxyuridine (BrdU) incorporation (Figure 3A). Consistently, *TIGAR*^{-/-} mice subjected to DSS treatment showed poorer recovery and succumbed approximately 1 day earlier than WT animals. The difference between WT and *TIGAR*^{-/-} mice was more obvious following exposure to milder damage (2% DSS) compared to a more damaging treatment (3.5% DSS) (Figures 3B and 3C),

and the difference was sustained days after treatment, although at this time point some recovery in *TIGAR*^{-/-} mice was also seen (Figures 3C and 3D; note difference in scale of y axis). TIGAR expression can therefore limit but not completely prevent damage, and even in the absence of TIGAR some recovery is possible.

Analysis of TIGAR protein levels in WT mice showed increased expression following DSS treatment (Figure 3E), similar to that seen in small intestine after IR damage (Figure 2G). TIGAR-deficient animals accumulated elevated ROS following DSS treatment, as indicated by an increase in MDA staining (Figure 3F), suggesting an important role of TIGAR in limiting ROS damage after DSS-induced colitis. These results indicated that, as seen in the regenerating small intestine after IR or treatment with cisplatin, efficient repair of damage to the colon was dependent on TIGAR expression.

The requirement for TIGAR in intestinal regeneration was confirmed using animals with conditional *TIGAR* allele (*TIGAR*^{fl/fl}) crossed with deleter cre *TIGAR*^{fl/fl;cre/+} animals (Figures S1B and S1C). Loss of TIGAR expression in these animals also resulted in increased sensitivity to DSS-induced colitis in the colon (Figure S3), recapitulating the phenotype seen with the *TIGAR*^{-/-} mouse. Taken together, these results show that lack of TIGAR compromises the ability of cells to limit ROS and undergo proliferation necessary to regenerate intestinal epithelium after ablation.

TIGAR Provides Antioxidants and Nucleosides for Growth

Our analysis of the recovering small intestine suggested that TIGAR might be important in both lowering apoptosis and allowing cell growth and proliferation. Previous work has indicated that TIGAR could contribute to these responses by limiting oxidative damage and may promote the generation of metabolic intermediates, such as nucleotides, that are necessary for tissue expansion. To examine directly the defect that underlies the failure of *TIGAR*^{-/-} intestinal crypts to regenerate properly, we turned to an in vitro intestinal crypt culture model (Sato et al., 2009). Compared to cells derived from WT mice, intestinal crypts from *TIGAR*^{-/-} mice were defective in their ability to proliferate in this three-dimensional tissue culture model (Figures 4A and 4B). *TIGAR*^{-/-} cells were less able to form crypt structures, and the culture of these cells produced fewer new crypt outgrowths over time (Figures 4A and 4B). Quantification of 100 individual crypt structures of each genotype clearly showed the defect in crypt formation in cultures from *TIGAR*^{-/-} cells (Figure 4C). Direct staining of the crypt structures with Ki67 also showed less proliferation in the *TIGAR*^{-/-} cultures, even when comparing crypt structures of similar size (Figure 4D), which is consistent with the regeneration failure seen in vivo in these mice. This defect could be rescued by the addition of *N*-acetyl L-cysteine (NAC; to control ROS) and nucleosides (to compensate for any lack of ribose phosphate production). Indeed, compared to the WT crypts, essentially complete rescue was observed following treatment with nucleosides or NAC alone (Figures 4A–4D). The effect of NAC indicates an importance of antioxidant function to the rescue, and interestingly we showed that treatment of cells with nucleosides also resulted in an increase in the GSH/GSSG ratio (Figure S4A), showing that nucleosides can also provide antioxidant function. To explore the contribution of the nonoxi-

dativ branch of the PPP, we treated cultures with oxythiamine (which inhibits transketolase in the nonoxidative PPP). Levels of oxythiamine that did not affect the growth of WT crypts exacerbated the growth defect of *TIGAR*^{-/-} crypts (Figure S4B), showing that loss of TIGAR makes cells more sensitive to inhibition of this branch of the PPP. Interestingly, oxythiamine also somewhat impeded, but did not completely inhibit, the ability of NAC to rescue the growth of TIGAR-null cells, again suggesting that the main defect in these cells is in antioxidant function.

TIGAR Is Critical for Tumor Development in an Intestinal Adenoma Model

Our results show that TIGAR plays an important role in allowing growth and proliferation required for the repair of damaged intestinal epithelium in adult mice. The modulation of metabolic pathways to allow anabolism and ROS limitation has been proposed to play an important role in tumorigenesis. We were therefore interested to determine whether TIGAR also contributes to the abnormal proliferation of tumor cells in the intestine. To address this question, we used a model in which the tumor suppressor APC is deleted in LGR5⁺ intestinal stem cells, leading to the development of intestinal adenoma (Barker et al., 2007, 2009). Using a protocol involving multiple doses of tamoxifen to maximize the incidence of adenoma development, TIGAR-deficient mice (knockout [KO]: *TIGAR*^{-/-} *Lgr5-EGFP-IRES-creER*^{T2}/*APC*^{fl/fl}) showed a reduced burden of abnormally proliferating adenoma in the small intestine compared to mice with WT TIGAR (WT: *TIGAR*^{+/+} *Lgr5-EGFP-IRES-creER*^{T2}/*APC*^{fl/fl}) (Figures 5A–5D). Specifically, TIGAR-deficient mice showed a significant reduction in total tumor burden and average tumor size compared to WT mice (Figures 5B–5D). Staining of TIGAR in WT tissues show a higher expression in the adenoma compared with surrounding normal tissue (Figure 5A), which is consistent with the role of TIGAR in supporting proliferation in tumor tissues. Similarly, the TIGAR-deficient mice showed a reduction in size of colon adenomas compared to WT mice (Figures 5E–5H). Interestingly, when examining the colon, there were no significant differences in the number of tumors in the colon (Figure 5F), indicating that TIGAR may be more important for tumor growth than for tumor initiation in this tissue. These results indicated that the absence of TIGAR limited tumor development, and so to determine the effect of TIGAR depletion on the survival of mice, we turned to a protocol of a single tamoxifen induction, which allows a slower onset of adenoma. As seen previously, fewer and smaller tumors developed in the small intestine of the TIGAR-deficient mice (Figures 5I–5L). In addition, there was less proliferation (less Ki67 staining) and more ROS damage (more MDA staining) in TIGAR-null compared to WT animals (Figure 5I), indicating a contribution of TIGAR to proliferation and ROS limitation that is similar to that seen following acute intestinal damage. Staining of GFP as a marker of LGR5-positive stem cells in these models (Barker et al., 2007, 2009) revealed that the absence of TIGAR does not deplete the tumors of stem cells (Figure S5). Overall, there appeared to be a slight decrease in the number of crypts with positive GFP staining, although as with the damage model this was difficult to interpret in view of the defects in proliferation in TIGAR-null animals. Importantly, the reduction in tumor burden correlated with an increased survival of mice lacking TIGAR (Figure 5M).

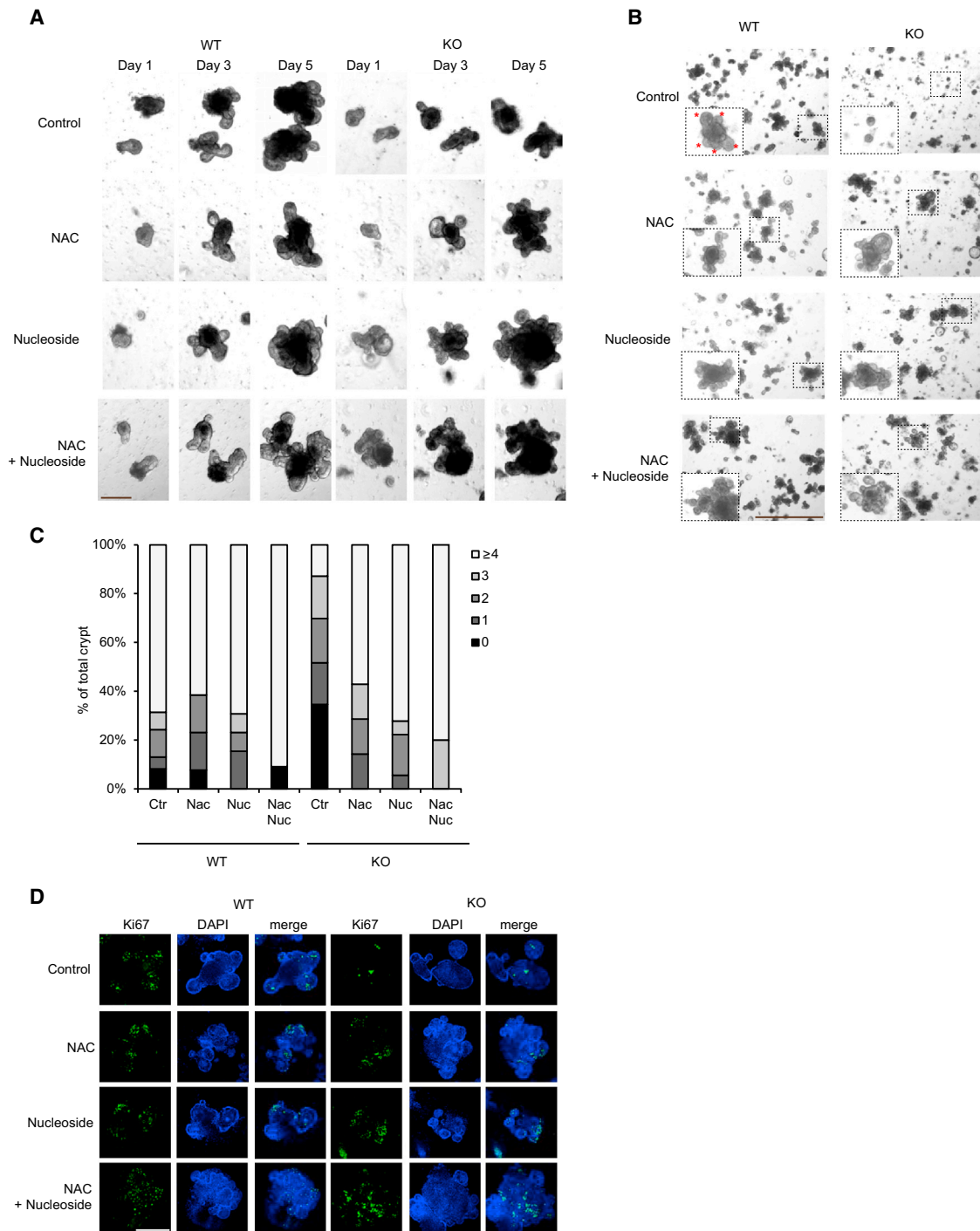


Figure 4. Reduction of Proliferation in TIGAR-Deficient Intestinal Crypt Can Be Rescued by the Addition of ROS Scavengers and Nucleoside

(A) Crypt cultures from WT and *TIGAR*^{-/-} (KO) small intestines after the indicated treatment. The same crypts were followed on days 1, 3, and 5. Scale bar, 100 μ m.

(B) Crypt cultures from WT and KO small intestines 5 days after the indicated treatment. Asterisks indicate growing buds from the crypt. Scale bar, 300 μ m.

(C) Quantification of the number of buds (0 to ≥ 4) from the crypts from WT and KO small intestinal crypt cultures.

(D) Ki67 staining of the crypt cultures from WT and KO small intestine treated with the indicated drugs for 5 days. Scale bar, 100 μ m.

See also Figure S4.

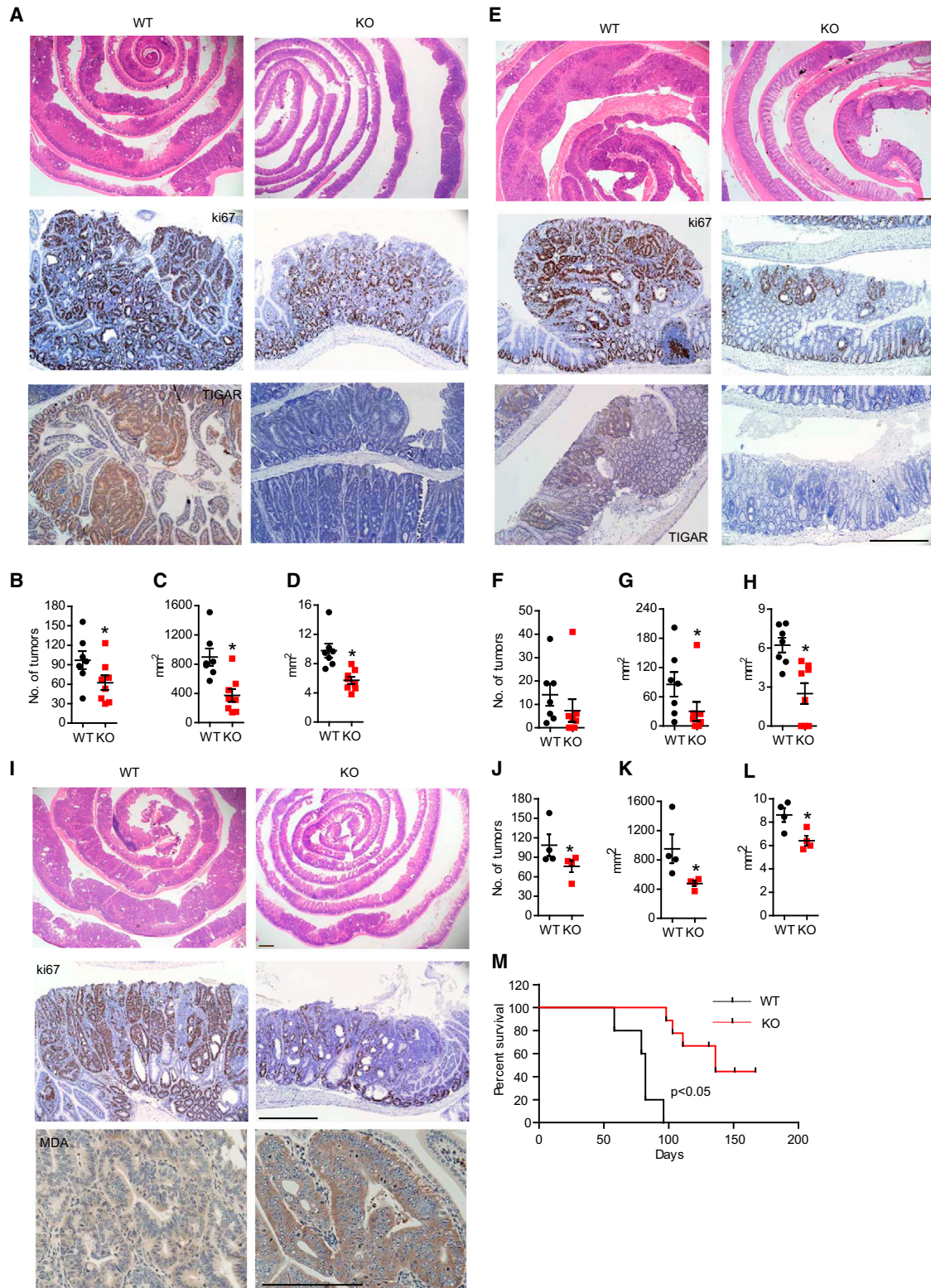


Figure 5. TIGAR Deficiency Reduced the Tumor Burden in a Mouse Model of Intestinal Adenoma

(A) H&E staining (top), Ki67 staining (middle), and TIGAR staining (bottom) of the small intestines from *TIGAR*^{+/+} *Lgr5-EGFP-IRES-creER*^{T2}/*APC*^{fl/fl} (WT) mice and *TIGAR*^{-/-} *Lgr5-EGFP-IRES-creER*^{T2}/*APC*^{fl/fl} (KO) mice after multiple rounds of tamoxifen induction.

(B) Number of tumors from WT and KO mice. *p < 0.05 compared to WT.

(C) Total tumor burden in the small intestine of WT and KO mice. *p < 0.05 compared to WT.

(legend continued on next page)

TIGAR Provides Nucleosides, NADPH, and Antioxidants for the Development of Intestinal Adenomas

The reduction of tumor progression in TIGAR-null mice was also reflected in an *in vitro* tumor crypt culture model (Sato et al., 2011). These cultures grow as large cystic organoids, which do not show the differentiation or structural organization of similar cultures derived from normal intestine (compare Figures 4A and 6A). The tumor crypt cultures from TIGAR-deficient mice showed a significant impairment of growth, as revealed by the reduction of the crypt size (Figures 6A and 6B) and decreased proliferation (Figures 6C and S6A) compared to those from WT animals. To determine the underlying cause of the failure of TIGAR-null tumor cells to grow, we examined the effect of exogenous addition of either methyl-malate, which can provide additional NADPH by a non-PPP mechanism via malic enzyme (Frenkel, 1975; Schafer et al., 2009; Yang et al., 2010a), nucleosides, or NAC to decrease ROS damage. Each of these treatments partially rescued the defect in growth (Figures 6A and 6B) and proliferation (Figures 6C and S6A), while the addition of NAC and malate also prevented the accumulation of ROS, as measured by MDA staining (Figure 6D). Interestingly, treatment of these tumor crypts with nucleosides also partially inhibited ROS damage (Figure 6D), consistent with our earlier observation that nucleosides can help maintain GSH/GSSG ratios (Figure S4A). However, in this system, complete rescue of crypt size (Figures 6A and 6B) and proliferation (Figures 6C and S6A) was only achieved when both malate and nucleosides or NAC and nucleosides were provided. These results therefore support an importance of TIGAR in generating both NADPH and ribose phosphate to allow the growth of these highly proliferative tumor cells. Although there are several mechanisms for NADPH production, the PPP has been shown to be critical for redox balance in hypoxia (Anastasiou et al., 2011). Consistently, we found that TIGAR-deficient crypts are more sensitive to hypoxia than WT crypts (Figure 6E).

To confirm that the defects seen in these crypts were the result of loss of TIGAR, we re-expressed human TIGAR in these cells (Figure 6F). Interestingly, while WT TIGAR completely rescued crypt growth, a partial rescue was also seen following expression of a catalytic inactive TIGAR construct (TIGAR-TM) (Bensaad et al., 2006) (Figure 6F). These results suggest that a catalytically independent role of TIGAR, such as a recently described ability to enhance HK2 activity (Cheung et al., 2012), can contribute to the maintenance of crypt growth.

Taken together, our results indicate that the defect in growth shown by TIGAR-deficient tumor crypts reflects increased

ROS and decreased nucleotide synthesis. Intriguingly, the *TIGAR*^{-/-} crypts also showed an increased sensitivity to chemotherapeutic drugs compared to WT tumor crypts (Figure S6B).

The human *TIGAR* gene is p53 responsive, and cells containing WT p53 show elevation of TIGAR levels in response to various forms of stress (Bensaad et al., 2006). The function of TIGAR under these conditions contributes to cell survival and is likely to allow for repair or adaptation of normal tissue to mild, transient, or nongenotoxic damage. However, our results in mice suggest that TIGAR expression may also be advantageous to tumor cells, and so we examined tumor cell lines to determine whether the expression of TIGAR was strictly dependent on the presence of WT p53. A survey of a number of *p53*^{-/-} or mutant-p53-expressing tumor cell lines showed that TIGAR expression was not dependent on the retention of WT p53 (Figure 7A). Therefore, the expression of TIGAR can become decoupled from p53 and there may be a selection for expression of TIGAR during malignant progression.

To establish whether TIGAR expression is also associated with the development of human cancers, we examined a series of colon tissue microarrays (TMAs) comparing normal, tumor, and metastatic tissue from the same patient. Staining for TIGAR expression by IHC showed an increase in TIGAR protein in both the primary colon cancer and associated metastases compared to normal tissue (Figures 7B and 7C). These results are consistent with the suggestion that TIGAR expression can help to support malignant development, potentially by allowing rapid proliferation and expansion of the abnormal lesion.

DISCUSSION

We have generated TIGAR-deficient mice to investigate the contribution of TIGAR to normal development and in rapidly proliferating cells after acute tissue damage and during tumor growth. *TIGAR*^{-/-} mice did not show a clear developmental defect, suggesting either that TIGAR function is not required during embryogenesis or that there is compensatory adaptation to the constitutive lack of TIGAR during these stages of development. However, we found a clear need for TIGAR in supporting rapid proliferation of adult tissue, in particular the ability of the adult intestinal epithelium to regenerate following damage. The requirement for TIGAR under these conditions is also highlighted by the increase in TIGAR expression seen in crypts during the recovery of proliferation in WT mice and by the corresponding increase in oxidative damage in the TIGAR-deficient animals. Whether there is a similar requirement for TIGAR in other

(D) Average size of tumor from WT and KO mice. **p* < 0.05 compared to WT.

(E) H&E staining (top), Ki67 staining (middle), and TIGAR staining (bottom) of the colon from WT and KO mice after multiple dosage of tamoxifen induction. Scale bar, 200 μ m.

(F) Number of tumors from the colon of WT and KO mice.

(G) Total colon tumor burden of WT and KO mice. **p* < 0.05 compared to WT.

(H) Average colon tumor size of WT and KO mice. **p* < 0.05 compared to WT.

(I) H&E staining (top), Ki67 staining (middle), and MDA staining (bottom) of the small intestines from *TIGAR*^{+/+} *Lgr5-EGFP-IRES-creER*^{T2}/*APC*^{fl/fl} (WT) and *TIGAR*^{-/-} *Lgr5-EGFP-IRES-creER*^{T2}/*APC*^{fl/fl} (KO) after a single dosage of tamoxifen induction. Scale bar, 200 μ m.

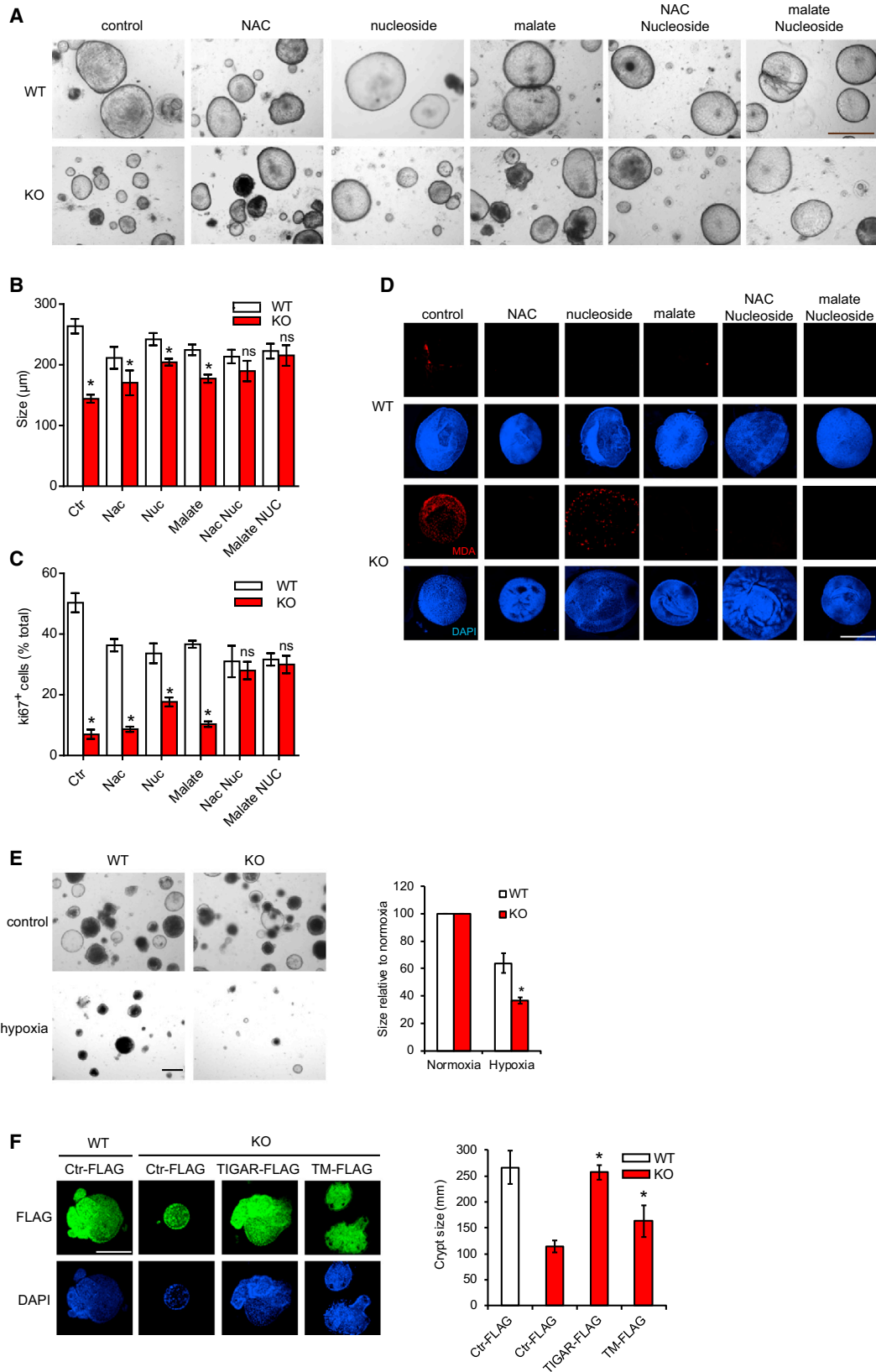
(J) Number of tumors from WT and KO animals. **p* < 0.05 compared to WT.

(K) Total tumor burden in the small intestine of WT and KO animals. **p* < 0.05 compared to WT.

(L) Average size of tumor from WT and KO animals. **p* < 0.05 compared to WT.

(M) Kaplan-Meier survival curves showing adenoma-free survival of WT (n = 5) and KO (n = 7) mice. Data are represented as mean \pm SEM (n = at least 3).

See also Figure S5.



(legend on next page)

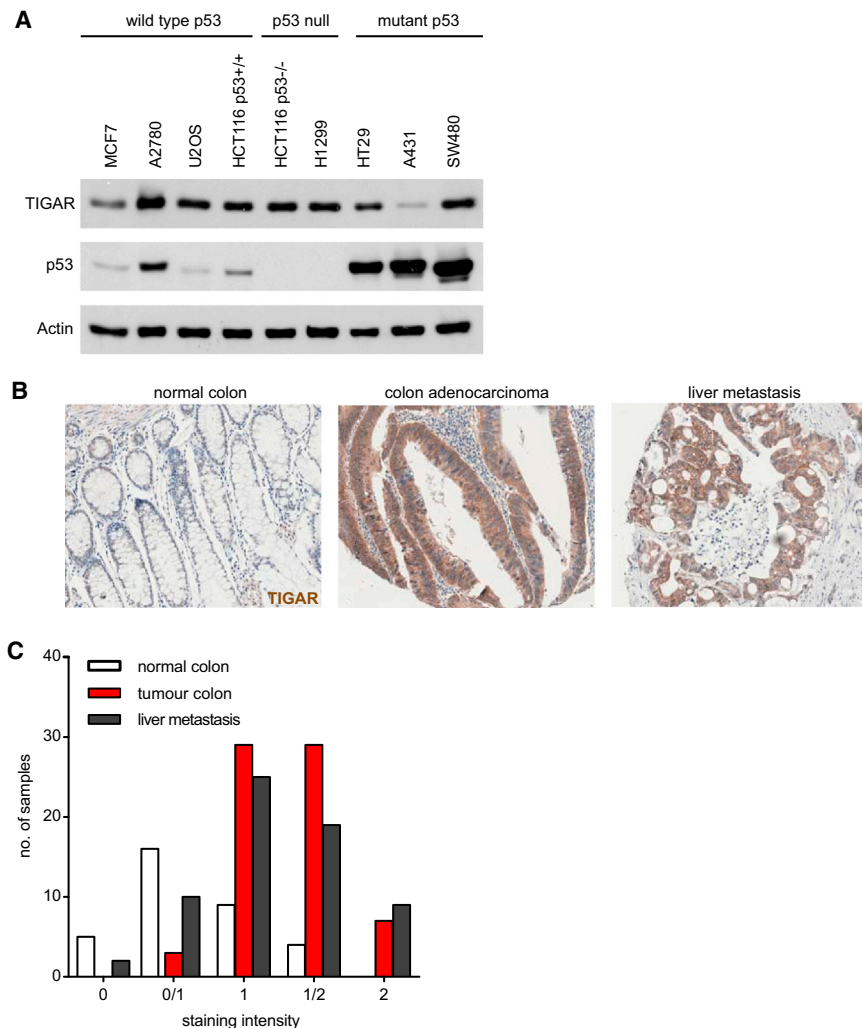


Figure 7. Increased TIGAR Expression in Primary Human Colon Cancer and Associated Metastases

(A) Expression of TIGAR in various human cancer cell lines with different p53 status. (B) Example of TIGAR staining in matched samples of human normal colon, colon adenocarcinoma, and liver metastasis from the same patient. (C) Quantification of the staining intensity in normal human colon, primary adenocarcinoma (tumor), and liver metastases.

ating tissue also suggested a possible contribution of TIGAR to the development or progression of malignancies. In a mouse model of intestinal tumor induced by deletion of APC in the intestinal stem cells, TIGAR expression was increased and we detected a reduction in tumor development and enhanced survival in *TIGAR*^{-/-} mice.

There has been much interest recently in the revival of the suggestion that altered metabolism can contribute to, as well as respond to, oncogenic transformation. Several elegant studies have illustrated the importance of metabolic transformation in cancer development (Freed-Pastor et al., 2012; Locasale et al., 2011; Schafer et al., 2009; Ying et al., 2012), although there is limited information about how these metabolic changes may impact on tumorigenicity in vivo. The regulation of glucose metabolism by TIGAR may have several important consequences; while the

proliferative tissues remains to be determined, and a role for TIGAR in recovery from partial hepatectomy or in mounting an immune response will be extremely interesting to examine. Our studies show that TIGAR plays an important role in tissue regeneration and that lack of TIGAR results in a failure to repair damaged intestinal epithelium, with an associated increased morbidity in a model of ulcerative colitis. In these systems, therefore, TIGAR expression is necessary to maintain normal healthy tissues following stress or damage. The ability of TIGAR to contribute to the growth and survival of cells in rapidly prolifer-

contribution of TIGAR to antioxidant activity has been shown in several cell systems (Bensaad et al., 2006; Li and Jøgl, 2009; Wanka et al., 2012), the potential promotion of the pentose phosphate pathway would also help to support anabolic pathways for the production of lipids and nucleic acids, and so contribute directly to cell growth (Tong et al., 2009). Although an inability to properly regulate ROS may account for enhanced apoptosis and so an indirect failure in cell proliferation, analysis of the regenerating epithelium suggested that a transient increase in apoptosis in the *TIGAR*^{-/-} mice (although this did not result in

Figure 6. Reduction of Proliferation in TIGAR-Deficient Tumor Crypt Can Be Rescued by the Addition of Malate and Nucleoside

(A) Tumor cystic organoid cultures from *TIGAR*^{+/+} *Lgr5-EGFP-IRES-creER*^{T2}/*APC*^{fl/m} (WT) and *TIGAR*^{-/-} *Lgr5-EGFP-IRES-creER*^{T2}/*APC*^{fl/m} (KO) small intestines after the indicated treatment for 5 days. Bar = 100 μm. (B) Quantification (average diameter of the organoids) of (A). *p < 0.05 compared to WT. ns, no significant difference. (C) Quantification of the percentage of Ki67-positive cells in the tumor crypt cultures from WT and KO animals treated with the indicated treatments for 5 days. *p < 0.05 compared to WT. ns, no significant difference. (D) MDA staining of the tumor crypt cultures from WT and KO animals with the indicated treatments for 5 days. Scale bar, 100 μm. (E) Size of TIGAR-deficient and control crypts following exposure to 1% oxygen (hypoxia) for 5 days. *p < 0.05 compared to WT. (F) TIGAR-deficient and control crypts were electroporated with the indicated constructs and then cultured for 5 days. Crypts expressing comparable levels of each protein, as visualized by FLAG staining, were measured for size. *p < 0.05 compared to KO with Ctr-FLAG. Data are represented as mean ± SEM (n = 3). See also Figure S6.

complete loss of stem cells) was accompanied by a failure to recover proliferation. The importance of TIGAR in limiting ROS was supported by the analysis of normal crypt cultures in vitro, where the defect in *TIGAR*^{-/-} crypts was efficiently rescued by treatment of the cells with antioxidant or nucleosides, with the observation that nucleoside treatment also provided antioxidant function. However, in the tumor crypt cultures, a full rescue of growth defects in TIGAR-null cells required the addition of both antioxidants (or NADPH generating capacity) and nucleosides, suggesting that in these cells TIGAR is important in supporting both antioxidant activity and nucleotide synthesis.

ROS has been suggested to both limit and promote tumor progression, reflecting the observation that different species of ROS have different functions. While elevated ROS can both induce potentially oncogenic mutations and function as a signaling molecule to drive proliferation, excess mitochondrial ROS can induce cell death and activation of pathways that block proliferation (Hamanaka and Chandel, 2010). These different ROS species can be differentially controlled; for example, the glutathione pool regulates oxidative stress while the peroxiredoxin pool regulates ROS signaling (Murphy, 2012). Therefore, it is possible that TIGAR mainly lowers oxidative stress via managing the glutathione level and has less of an impact on the regulation of redox signaling (which would drive proliferation).

In humans, TIGAR is p53 inducible and has been suggested to play a role under conditions of mild or transient stress to help promote the repair and survival of damaged cells (Bensaad et al., 2006; Li and Jogle, 2009; Wanka et al., 2012). These metabolic functions of p53 can play a role in tumor suppression (Li et al., 2012), and the activation of the pentose phosphate pathway by ATM has been shown to enhance NADPH production and increase nucleotide synthesis, so controlling ROS and contributing to DNA repair. These responses were shown to be important in allowing ATM to limit cancer development (Cosenz et al., 2011). However, there is also a clear potential that TIGAR activity, by limiting ROS and providing precursors for nucleotide synthesis, could be advantageous to tumor cells (Trachotham et al., 2006). Neoplastic cells generally produce more ROS than normal cells (Szatrowski and Nathan, 1991); therefore, they are more vulnerable to oxidative stress because they function with a higher basal level of ROS. On one hand, these higher levels of ROS could promote tumor progression by stimulating cell growth and proliferation (Hu et al., 2005), genetic instability (Radisky et al., 2005), and anchorage-independent growth (Weinberg et al., 2010). However, increased ROS also render tumor cells more vulnerable to cell death and it is therefore essential for the tumor cells to dynamically regulate ROS level to avoid prolonged oxidative damage. For example, oncogenes such as K-Ras, B-Raf, and Myc all increase the activity of NRF2, a transcriptional factor that increases ROS detoxification and tumorigenesis at the early stages of tumor development (DeNicola et al., 2011). Deletion of NRF2 in vivo reduces the ability of K-Ras to induce proliferation and tumorigenesis (DeNicola et al., 2011), supporting the importance of ROS limitation in tumor outgrowth. One response to increased ROS is a decrease in the activity of PKM2 through oxidation at cysteine in PKM2. This diverts glycolytic intermediates into the PPP and, as we describe for TIGAR, generates reducing potential for ROS detoxification. Importantly, this activity has been shown to be essential

for tumor formation in a xenograft model (Anastasiou et al., 2011; Tong et al., 2009).

Taken together, therefore, it would appear that TIGAR can help to support tumorigenesis, both by limiting ROS and by providing precursors for nucleotide synthesis. Both of these activities can be provided by promotion of the PPP, although we also provide evidence that the recently described catalytically independent function of TIGAR in ROS regulation under hypoxia (Cheung et al., 2012) also contributes to its overall ability to support tumor cell growth.

It was therefore very interesting to determine that TIGAR was highly expressed in many human colon cancers, consistent with a contribution to the tumorigenic phenotype. Increased expression of TIGAR has recently also been described in other tumor types, including glioblastomas and breast cancers (Wanka et al., 2012; Won et al., 2012). Importantly, p53 is mutated in the majority of colon cancers, suggesting that, as seen in the cancer cell lines, selection for TIGAR overexpression is uncoupled from the activity of WT p53. This potential oncogenic activity of a p53 target gene has also recently been described for carnitine palmitoyltransferase 1c (Cpt1c), a p53-inducible gene that contributes to fatty acid oxidation. Cpt1c is upregulated in many cancer cell types and can protect against metabolic stress and contribute to growth of the tumor (Zaugg et al., 2011). Our observations indicate that the inappropriate or sustained activation of proteins like TIGAR, uncoupled from the dependence on p53, may help to support the growth and survival of cancer cells.

Our studies show that the regulation of metabolism by TIGAR is not required for normal tissue growth and development but becomes important in supporting rapid proliferation in adult intestinal epithelium. This specific requirement under conditions of tissue regeneration has also been described for FAK (Ashton et al., 2010), which is not needed in normal adult tissue but is required for intestinal regeneration and tumorigenesis. Therefore, while loss of TIGAR is deleterious to the recovery from intestinal damage, lack of TIGAR becomes advantageous under conditions where enhanced proliferation occurs in the context of tumor development. These data clearly predict that inhibition of TIGAR expression may carry some therapeutic advantage, although TIGAR inhibition would also be predicted to enhance the deleterious effects of genotoxic cancer therapies that damage normal gut and other proliferating cells. Indeed, an increase in the TIGAR level in the intestine may provide protection from acute intestinal damage such as ulcerative colitis and intestinal radiosensitivity. We are presently generating tumor models with our conditional TIGAR allele to allow us to determine the effect of targeted deletion of TIGAR in premalignant or malignant lesions.

EXPERIMENTAL PROCEDURES

Transgenic Mouse Models

Details of the creation of *TIGAR*^{-/-} and *TIGAR*^{fl/fl} mice are provided in the [Supplemental Experimental Procedures](#). All animal work was carried out in line with the Animals (Scientific Procedures) Act 1986 and the EU Directive 2010 and sanctioned by local ethical review process (University of Glasgow).

Creation of the Intestinal Adenoma Model with *TIGAR*^{-/-}

To investigate the role of TIGAR in the development of intestinal adenoma due to deletion of *Apc* in LGR5⁺ intestinal crypt cells (Barker et al., 2007, 2009),

TIGAR^{-/-} mice were interbred with *Lgr5-EGFP-IRES-creER^{T2}/APC^{fl/fl}* mice to generate *TIGAR^{+/+} Lgr5-EGFP-IRES-creER^{T2}/APC^{fl/fl}* (WT) and *TIGAR^{-/-} Lgr5-EGFP-IRES-creER^{T2}/APC^{fl/fl}* (KO). To induce recombination of APC in LGR5-expressing cells, mice aged 6–8 weeks were injected intraperitoneally with single dosage of tamoxifen (3 mg tamoxifen) or multiple dosages of tamoxifen (3 mg of tamoxifen for 1 day followed by 2 mg of tamoxifen for 3 days). Mice were monitored until showing signs of intestinal illness, and tissues were collected for histology, immunohistochemistry, and intestinal crypt culture.

Cell Culture and Protein Analysis

BMK cells were cultured and used as previously described (Mathew et al., 2008). Western blot analysis, transfection of the BMK cells with TIGAR constructs, measurement of Fru-2,6-BP, and GSH/GSSG were performed as previously described (Bensaad et al., 2006).

IR, Cisplatin Treatment, and DSS-Induced Colitis

Gamma IR-induced intestinal damage was performed as previously described (Ashton et al., 2010). For cisplatin-induced intestinal damage, cisplatin (10 mg/kg) was intraperitoneally injected into 8- to 10-week-old mice. Saline was used as control. For DSS-induced colitis, mice received 2% or 3.5% of DSS in drinking water for 5 days. Then DSS was omitted and mice received tap water for 2 days. Tap water was used as control. Intestinal tissue was isolated and processed as described previously (Jamieson et al., 2012).

Histology and Immunohistochemistry

Histology and immunohistochemistry was performed as described previously (Sansom et al., 2004). Primary antibodies used were anti-Ki67 (Lab Vision), anti-TIGAR (Millipore), anti-MDA (Abcam), anti-BrdU (Sigma), anti-Olfm4 (Abcam), anti-LGR5/GPR49 (Abcam), anti-GFP (Abcam), and anti-FLAG (Sigma).

Small Intestinal Crypt Culture and Immunofluorescence

Small intestinal crypt culture and tumor crypt culture were performed as described previously (Sato et al., 2009, 2011). Briefly, small intestine was washed in cold PBS and villi were scraped using a glass coverslip. Then the small intestine was cut into small pieces and the pieces were further washed with cold PBS. The pieces were transferred into PBS with 2 mM EDTA and incubated for 30 min, after which crypts were collected by pipetting mechanically and supernatant enriched with crypts were collected. The crypts were then pelleted by centrifugation (1,200 rpm, 5 min), suspended in ADF media (advanced DMEM F12 [Invitrogen], 1% glutamine, 1% penicillin/streptomycin, 0.1% BSA, 10 mM HEPES), and passed through 70 μ m cell strainer. The fraction was then centrifuged at lower speed (600 rpm, 2 min) to avoid single cells being spun down. The final pellet with crypt was resuspended with growth factor reduced Matrigel (356231, BD) in ADF that contained 0.05 μ g/ml EGF (Peprotech), 0.1 μ g/ml NOGGIN (Peprotech), and 0.5 μ g/ml mR-Spondin (R&D Systems). For tumor crypts, adenomas were cut into small pieces, washed, and then dissociated with trypsin for 30 min in 37°C. After several washes the cells were pelleted and were suspended with Matrigel in ADF that contained EGF and NOGGIN. The cultures were passaged every 7–10 days. For the rescue experiments, 200 μ M NAC (Sigma), 1 \times nucleoside (Millipore), 2.5 mM methyl-malate (Sigma), and 10 μ M oxythiamine (Sigma) were added to the culture on the first day. Hypoxia was performed as described previously (Cheung et al., 2012). For Amaxa nucleofection into cancer crypt organoids, 1 μ g (per well) control, WT TIGAR, or catalytically TIGAR mutant (TIGAR-TM) (Bensaad et al., 2006) constructs was transfected into cancer crypt organoids using solution T and program X-001 (Lonza). The rate of growth of the intestinal crypt was measured by the number of buds present in at least 100 crypt structures as previously described (Mustata et al., 2011). The rate of growth of the tumor crypt was measured by the average size (diameter) of at least 150 crypts in each treatment from tumors from three individual animals (WT and KO). For nucleofected cancer crypt measurements, the average size (diameter) of at least 100 crypts that were stained positive with FLAG was measured from cultures of three individual animals (WT and KO).

Immunofluorescence of Crypt Cultures

Crypts were fixed with 2% paraformaldehyde (PFA) in PBS for 20 min at room temperature and then permeabilized with 0.5% Triton X-100 in PBS for 10 min at 4°C. After three 10 min washes of 1 \times PBS-glycine (7.5 mg/ml) to quench PFA, crypts were incubated with 10% BSA primary block in immunofluorescence wash (0.13 M NaCl, 13 mM Na₂HPO₄, 3.5 mM NaH₂PO₄, 0.2% Triton X-100, 0.04% \times Tween-20) for 1 hr, followed by incubation with secondary block (10% BSA and 1:100 Fab immunoglobulin G [Jackson ImmunoResearch] in immunofluorescence wash) for 30 min. The primary antibody (prepared in secondary block) was incubated overnight at 4°C and washed three times in immunofluorescence wash before incubation with the appropriate fluorescent dye coupled secondary antibody (Alexa Fluor, Molecular Probes) for 1.5 hr. DAPI (1 μ g/ml) in 1 \times PBS was used to visualize nuclei.

Human TMA analysis

TMA of human cancer patients was obtained from AccuMax Array (A203(II)-colon cancer tissues liver metastasis) and was stained with anti-human TIGAR antibody (ProSci). The scoring of the TMAs was carried out by two independent scorers.

Quantifications and Statistical Analysis

For crypt number counting in the small intestine, the intestinal length corresponding to a minimum of 100 crypts per animal per treatment was measured and was expressed as number of crypts per millimeter of intestinal length. For crypt size measurements in the intestine, a minimum of 50 crypts were measured for the height of the crypt. For cell death measurement in the crypts, the number of cells exhibiting apoptotic morphology (Li et al., 1992; Merritt et al., 1997) from at least 50 crypts per animal per treatment was scored and was expressed as the average number per crypt. The number of Ki67-positive cells was measured in at least 50 crypts per animal per treatment. The survival data were analyzed by log-rank test using GraphPad Prism 5 software. The data represent mean values \pm SEM from at least three independent experiments (n = 3) unless otherwise noted. All p values were obtained using two-way ANOVA and Fisher's post hoc tests.

SUPPLEMENTAL INFORMATION

Supplemental Information includes Supplemental Experimental Procedures and six figures and can be found with this article online at <http://dx.doi.org/10.1016/j.devcel.2013.05.001>.

LICENSING INFORMATION

This is an open-access article distributed under the terms of the Creative Commons Attribution-NonCommercial-No Derivative Works License, which permits non-commercial use, distribution, and reproduction in any medium, provided the original author and source are credited.

ACKNOWLEDGMENTS

Work in the K.H.V., K.B., D.S., and O.J.S. laboratories is funded by CR-UK. E.C.C. is supported by a fellowship from the Canadian Institutes of Health Research, and P.L. is in receipt of an MRC studentship. The authors thank Eyal Gottlieb for advice and critical reading of the manuscript and the Biological Services at the Beatson Institute for Cancer Research for technical assistance.

Received: December 12, 2012

Revised: April 23, 2013

Accepted: May 1, 2013

Published: May 30, 2013

REFERENCES

Anastasiou, D., Poulgiannis, G., Asara, J.M., Boxer, M.B., Jiang, J.K., Shen, M., Bellingier, G., Sasaki, A.T., Locasale, J.W., Auld, D.S., et al. (2011). Inhibition of pyruvate kinase M2 by reactive oxygen species contributes to cellular antioxidant responses. *Science* 334, 1278–1283.

- Ashton, G.H., Morton, J.P., Myant, K., Pheese, T.J., Ridgway, R.A., Marsh, V., Wilkins, J.A., Athineos, D., Muncan, V., Kemp, R., et al. (2010). Focal adhesion kinase is required for intestinal regeneration and tumorigenesis downstream of Wnt/c-Myc signaling. *Dev. Cell* **19**, 259–269.
- Barker, N., van Es, J.H., Kuipers, J., Kujala, P., van den Born, M., Cozijnsen, M., Haegerbarth, A., Korving, J., Begthel, H., Peters, P.J., and Clevers, H. (2007). Identification of stem cells in small intestine and colon by marker gene *Lgr5*. *Nature* **449**, 1003–1007.
- Barker, N., Ridgway, R.A., van Es, J.H., van de Wetering, M., Begthel, H., van den Born, M., Danenberg, E., Clarke, A.R., Sansom, O.J., and Clevers, H. (2009). Crypt stem cells as the cells-of-origin of intestinal cancer. *Nature* **457**, 608–611.
- Bensaad, K., and Vousden, K.H. (2007). p53: new roles in metabolism. *Trends Cell Biol.* **17**, 286–291.
- Bensaad, K., Tsuruta, A., Selak, M.A., Vidal, M.N., Nakano, K., Bartrons, R., Gottlieb, E., and Vousden, K.H. (2006). TIGAR, a p53-inducible regulator of glycolysis and apoptosis. *Cell* **126**, 107–120.
- Bensaad, K., Cheung, E.C., and Vousden, K.H. (2009). Modulation of intracellular ROS levels by TIGAR controls autophagy. *EMBO J.* **28**, 3015–3026.
- Borodovsky, A., Seltzer, M.J., and Riggins, G.J. (2012). Altered cancer cell metabolism in gliomas with mutant IDH1 or IDH2. *Curr. Opin. Oncol.* **24**, 83–89.
- Budanov, A.V., Sablina, A.A., Feinstein, E., Koonin, E.V., and Chumakov, P.M. (2004). Regeneration of peroxiredoxins by p53-regulated sestrins, homologs of bacterial AhpD. *Science* **304**, 596–600.
- Cairns, R.A., Harris, I.S., and Mak, T.W. (2011). Regulation of cancer cell metabolism. *Nat. Rev. Cancer* **11**, 85–95.
- Cheung, E.C., Ludwig, R.L., and Vousden, K.H. (2012). Mitochondrial localization of TIGAR under hypoxia stimulates HK2 and lowers ROS and cell death. *Proc. Natl. Acad. Sci. USA* **109**, 20491–20496.
- Cooper, H.S., Murthy, S.N., Shah, R.S., and Sedergran, D.J. (1993). Clinicopathologic study of dextran sulfate sodium experimental murine colitis. *Lab. Invest.* **69**, 238–249.
- Cosentino, C., Grieco, D., and Costanzo, V. (2011). ATM activates the pentose phosphate pathway promoting anti-oxidant defence and DNA repair. *EMBO J.* **30**, 546–555.
- Dang, C.V. (2012). Links between metabolism and cancer. *Genes Dev.* **26**, 877–890.
- Deberardinis, R.J., Sayed, N., Ditsworth, D., and Thompson, C.B. (2008). Brick by brick: metabolism and tumor cell growth. *Curr. Opin. Genet. Dev.* **18**, 54–61.
- DeNicola, G.M., Karreth, F.A., Humpston, T.J., Gopinathan, A., Wei, C., Frese, K., Mangal, D., Yu, K.H., Yeo, C.J., Calhoun, E.S., et al. (2011). Oncogene-induced Nrf2 transcription promotes ROS detoxification and tumorigenesis. *Nature* **475**, 106–109.
- Freed-Pastor, W.A., Mizuno, H., Zhao, X., Langerød, A., Moon, S.H., Rodriguez-Barrueco, R., Barsotti, A., Chicas, A., Li, W., Polotskaia, A., et al. (2012). Mutant p53 disrupts mammary tissue architecture via the mevalonate pathway. *Cell* **148**, 244–258.
- Frenkel, R. (1975). Regulation and physiological functions of malic enzymes. *Curr. Top. Cell. Regul.* **9**, 157–181.
- Goidts, V., Bageritz, J., Puccio, L., Nakata, S., Zapatka, M., Barbus, S., Toedt, G., Campos, B., Korshunov, A., Momma, S., et al. (2012). RNAi screening in glioma stem-like cells identifies PFKFB4 as a key molecule important for cancer cell survival. *Oncogene* **31**, 3235–3243.
- Hamanaka, R.B., and Chandel, N.S. (2010). Mitochondrial reactive oxygen species regulate cellular signaling and dictate biological outcomes. *Trends Biochem. Sci.* **35**, 505–513.
- Hu, Y., Rosen, D.G., Zhou, Y., Feng, L., Yang, G., Liu, J., and Huang, P. (2005). Mitochondrial manganese-superoxide dismutase expression in ovarian cancer: role in cell proliferation and response to oxidative stress. *J. Biol. Chem.* **280**, 39485–39492.
- Jamieson, T., Clarke, M., Steele, C.W., Samuel, M.S., Neumann, J., Jung, A., Huels, D., Olson, M.F., Das, S., Nibbs, R.J., and Sansom, O.J. (2012). Inhibition of CXCR2 profoundly suppresses inflammation-driven and spontaneous tumorigenesis. *J. Clin. Invest.* **122**, 3127–3144.
- Kroemer, G., and Pouyssegur, J. (2008). Tumor cell metabolism: cancer's Achilles' heel. *Cancer Cell* **13**, 472–482.
- Li, H., and Jögl, G. (2009). Structural and biochemical studies of TIGAR (TP53-induced glycolysis and apoptosis regulator). *J. Biol. Chem.* **284**, 1748–1754.
- Li, Y.Q., Fan, C.Y., O'Connor, P.J., Winton, D.J., and Potten, C.S. (1992). Target cells for the cytotoxic effects of carcinogens in the murine small bowel. *Carcinogenesis* **13**, 361–368.
- Li, T., Kon, N., Jiang, L., Tan, M., Ludwig, T., Zhao, Y., Baer, R., and Gu, W. (2012). Tumor suppression in the absence of p53-mediated cell-cycle arrest, apoptosis, and senescence. *Cell* **149**, 1269–1283.
- Locasale, J.W., Grassian, A.R., Melman, T., Lysyiotis, C.A., Mattaini, K.R., Bass, A.J., Heffron, G., Metallo, C.M., Muranen, T., Sharfi, H., et al. (2011). Phosphoglycerate dehydrogenase diverts glycolytic flux and contributes to oncogenesis. *Nat. Genet.* **43**, 869–874.
- Mathew, R., Degenhardt, K., Haramaty, L., Karp, C.M., and White, E. (2008). Immortalized mouse epithelial cell models to study the role of apoptosis in cancer. *Methods Enzymol.* **446**, 77–106.
- Merritt, A.J., Allen, T.D., Potten, C.S., and Hickman, J.A. (1997). Apoptosis in small intestinal epithelial from p53-null mice: evidence for a delayed, p53-independent G2/M-associated cell death after gamma-irradiation. *Oncogene* **14**, 2759–2766.
- Murphy, M.P. (2012). Mitochondrial thiols in antioxidant protection and redox signaling: distinct roles for glutathionylation and other thiol modifications. *Antioxid. Redox Signal.* **16**, 476–495.
- Mustata, R.C., Van Loy, T., Lefort, A., Libert, F., Strollo, S., Vassart, G., and Garcia, M.I. (2011). *Lgr4* is required for Paneth cell differentiation and maintenance of intestinal stem cells *ex vivo*. *EMBO Rep.* **12**, 558–564.
- Piruat, J.I., Pintado, C.O., Ortega-Sáenz, P., Roche, M., and López-Barneo, J. (2004). The mitochondrial SDHD gene is required for early embryogenesis, and its partial deficiency results in persistent carotid body glomus cell activation with full responsiveness to hypoxia. *Mol. Cell. Biol.* **24**, 10933–10940.
- Pollard, P.J., Spencer-Dene, B., Shukla, D., Howarth, K., Nye, E., El-Bahrawy, M., Deheragoda, M., Joannou, M., McDonald, S., Martin, A., et al. (2007). Targeted inactivation of *fnh1* causes proliferative renal cyst development and activation of the hypoxia pathway. *Cancer Cell* **11**, 311–319.
- Radisky, D.C., Levy, D.D., Littlepage, L.E., Liu, H., Nelson, C.M., Fata, J.E., Leake, D., Godden, E.L., Albertson, D.G., Nieto, M.A., et al. (2005). Rac1b and reactive oxygen species mediate MMP-3-induced EMT and genomic instability. *Nature* **436**, 123–127.
- Ros, S., Santos, C.R., Moco, S., Baenke, F., Kelly, G., Howell, M., Zamboni, N., and Schulze, A. (2012). Functional metabolic screen identifies 6-phosphofructo-2-kinase/fructose-2,6-bisphosphatase 4 as an important regulator of prostate cancer cell survival. *Cancer Discov.* **2**, 328–343.
- Sansom, O.J., Reed, K.R., Hayes, A.J., Ireland, H., Brinkmann, H., Newton, I.P., Battle, E., Simon-Assmann, P., Clevers, H., Nathke, I.S., et al. (2004). Loss of *Apc* in vivo immediately perturbs Wnt signaling, differentiation, and migration. *Genes Dev.* **18**, 1385–1390.
- Sato, T., Vries, R.G., Snippert, H.J., van de Wetering, M., Barker, N., Stange, D.E., van Es, J.H., Abo, A., Kujala, P., Peters, P.J., and Clevers, H. (2009). Single *Lgr5* stem cells build crypt-villus structures in vitro without a mesenchymal niche. *Nature* **459**, 262–265.
- Sato, T., Stange, D.E., Ferrante, M., Vries, R.G., Van Es, J.H., Van den Brink, S., Van Houdt, W.J., Pronk, A., Van Gorp, J., Siersema, P.D., and Clevers, H. (2011). Long-term expansion of epithelial organoids from human colon, adenoma, adenocarcinoma, and Barrett's epithelium. *Gastroenterology* **141**, 1762–1772.
- Schafer, Z.T., Grassian, A.R., Song, L., Jiang, Z., Gerhart-Hines, Z., Irie, H.Y., Gao, S., Puigserver, P., and Brugge, J.S. (2009). Antioxidant and oncogene rescue of metabolic defects caused by loss of matrix attachment. *Nature* **461**, 109–113.
- Szatrowski, T.P., and Nathan, C.F. (1991). Production of large amounts of hydrogen peroxide by human tumor cells. *Cancer Res.* **51**, 794–798.

- Tong, X., Zhao, F., and Thompson, C.B. (2009). The molecular determinants of de novo nucleotide biosynthesis in cancer cells. *Curr. Opin. Genet. Dev.* **19**, 32–37.
- Trachootham, D., Zhou, Y., Zhang, H., Demizu, Y., Chen, Z., Pelicano, H., Chiao, P.J., Achanta, G., Arlinghaus, R.B., Liu, J., and Huang, P. (2006). Selective killing of oncogenically transformed cells through a ROS-mediated mechanism by beta-phenylethyl isothiocyanate. *Cancer Cell* **10**, 241–252.
- van der Flier, L.G., Haegebarth, A., Stange, D.E., van de Wetering, M., and Clevers, H. (2009). OLFM4 is a robust marker for stem cells in human intestine and marks a subset of colorectal cancer cells. *Gastroenterology* **137**, 15–17.
- Vander Heiden, M.G., Cantley, L.C., and Thompson, C.B. (2009). Understanding the Warburg effect: the metabolic requirements of cell proliferation. *Science* **324**, 1029–1033.
- Vousden, K.H., and Ryan, K.M. (2009). p53 and metabolism. *Nat. Rev. Cancer* **9**, 691–700.
- Wanka, C., Steinbach, J.P., and Rieger, J. (2012). Tp53-induced glycolysis and apoptosis regulator (TIGAR) protects glioma cells from starvation-induced cell death by up-regulating respiration and improving cellular redox homeostasis. *J. Biol. Chem.* **287**, 33436–33446.
- Weinberg, F., Hamanaka, R., Wheaton, W.W., Weinberg, S., Joseph, J., Lopez, M., Kalyanaraman, B., Mutlu, G.M., Budinger, G.R., and Chandel, N.S. (2010). Mitochondrial metabolism and ROS generation are essential for Kras-mediated tumorigenicity. *Proc. Natl. Acad. Sci. USA* **107**, 8788–8793.
- Wise, D.R., and Thompson, C.B. (2010). Glutamine addiction: a new therapeutic target in cancer. *Trends Biochem. Sci.* **35**, 427–433.
- Won, K.Y., Lim, S.J., Kim, G.Y., Kim, Y.W., Han, S.A., Song, J.Y., and Lee, D.K. (2012). Regulatory role of p53 in cancer metabolism via SCO2 and TIGAR in human breast cancer. *Hum. Pathol.* **43**, 221–228.
- Yang, C.S., Thomenius, M.J., Gan, E.C., Tang, W., Freel, C.D., Merritt, T.J., Nutt, L.K., and Kornbluth, S. (2010a). Metabolic regulation of Drosophila apoptosis through inhibitory phosphorylation of Dronc. *EMBO J.* **29**, 3196–3207.
- Yang, H., Brose, S., Acin-Perez, R., Slavkovich, V., Nishino, I., Khan, R., Goldberg, I.J., Graziano, J., Manfredi, G., and Schon, E.A. (2010b). Analysis of mouse models of cytochrome c oxidase deficiency owing to mutations in Sco2. *Hum. Mol. Genet.* **19**, 170–180.
- Ye, J., Mancuso, A., Tong, X., Ward, P.S., Fan, J., Rabinowitz, J.D., and Thompson, C.B. (2012). Pyruvate kinase M2 promotes de novo serine synthesis to sustain mTORC1 activity and cell proliferation. *Proc. Natl. Acad. Sci. USA* **109**, 6904–6909.
- Yin, L., Kosugi, M., and Kufe, D. (2012). Inhibition of the MUC1-C oncoprotein induces multiple myeloma cell death by down-regulating TIGAR expression and depleting NADPH. *Blood* **119**, 810–816.
- Ying, H., Kimmelman, A.C., Lyssiotis, C.A., Hua, S., Chu, G.C., Fletcher-Sananikone, E., Locasale, J.W., Son, J., Zhang, H., Coloff, J.L., et al. (2012). Oncogenic Kras maintains pancreatic tumors through regulation of anabolic glucose metabolism. *Cell* **149**, 656–670.
- Zaugg, K., Yao, Y., Reilly, P.T., Kannan, K., Kiarash, R., Mason, J., Huang, P., Sawyer, S.K., Fuerth, B., Faubert, B., et al. (2011). Carnitine palmitoyltransferase 1C promotes cell survival and tumor growth under conditions of metabolic stress. *Genes Dev.* **25**, 1041–1051.